GOVERNMENT OF BANGLADESH
FLOOD PLAN COORDINATION ORGANIZATION

FAP 24 RIVER SURVEY PROJECT

SEDIMENT TRANSPORT
&
HYDRAULIC ROUGHNESS.

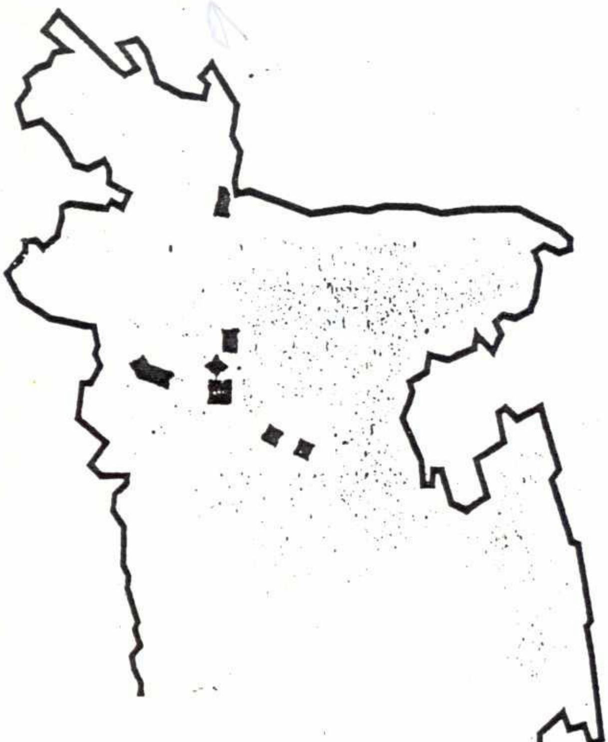

DELFT HYDRAULICS
DANISH HYDRAULIC INSTITUTE
OSIRIS
HYDROLAND
APPROTECH

Project ALA/90/04 — Commission of the European Communities

GOVERNMENT OF BANGLADESH
FLOOD PLAN COORDINATION ORGANIZATION

FAP 24 RIVER SURVEY PROJECT

SEDIMENT TRANSPORT
&
HYDRAULIC ROUGHNESS.

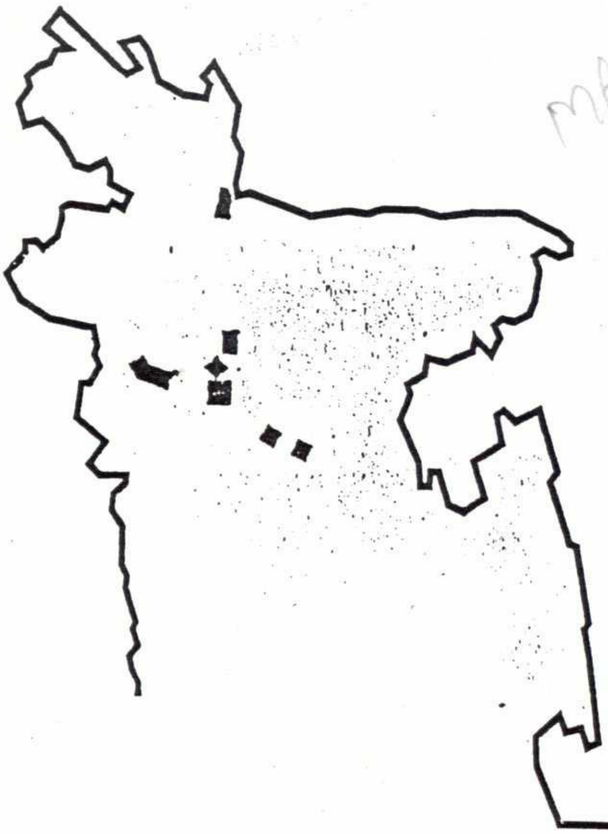

DELFT HYDRAULICS
DANISH HYDRAULIC INSTITUTE
OSIRIS
HYDROLAND
APPROTECH

Project ALA/90/04 — Commission of the European Communities

6

SEDIMENT TRANSPORT
&
HYDRAULIC ROUGHNESS.

Lecturer : G. J. Klaassen

Lecture notes : H.N.C. Breusers :
(River Hydraulics, Chapter 9 - 13)

8

SEDIMENT TRANSPORT
&
HYDRAULIC ROUGHNESS.

Lecturer : G. J. Klaassen

Lecture notes : H.N.C. Breusers :
(River Hydraulics, Chapter 9 - 13)

These lecture notes should be considered as an introduction to the subject. The following general references may be used for further studies:

S. LELIAVSKY	1955	An introduction to fluvial hydraulics. Constable, London.
T. BLENCH	1957	Regime behaviour of canals and rivers. Butterworths, London.
F.M. HENDERSON	1966	Open channel flow (Ch. 4 - Sediment transport) MacMillan, New York.
F. ENGELUND	1967	A monograph on sediment transport in alluvial streams. Teknisk Forlag, Copenhagen.
W.H. GRAF	1971	Hydraulics of sediment transport. Mc Graw Hill, New York (very complete treatment
H.W. SHEN (ed.)	1971	River Mechanics I. Ft. Collins, Colorado.
J.L. BOGARDI	1974	Sediment transport in alluvial streams. Akadémiai Kiadó, Budapest.
V.A. VANONI	1975	River Dynamics, Advances in applied mechanics Vol. 15, pp. 1 - 87. (C.S. Yih, ed.) Academic Press, New York.
V.A. VANONI (ed.)	1975	Sedimentation Engineering. A.S.C.E. New York.
A.J. RAUDKIVI	1976	Loose boundary hydraulics (2nd ed.). Pergamon Press Oxford.
D.B. SIMONS, F. SENTÜRK	1977	Sediment Transport Technology. Water Res. Publ., Ft. Collins, Colorado
R.J. GARDE, K.G. RANGA RAJU	1977	Mechanics of Sediment Transportation and Alluvial Stream Problems. Wiley Eastern Limited, New Delhi.
P.Ph. JANSEN (ed.)	1979	Principles of river engineering. Pitman, London.
H.W. SHEN, H. KIKKAWA (eds.)	1980	Application of stochastic processes in sediment transport (Proc. U.S.-Japan Seminar Hawai 1978). Water Resources Publ., Littleton, Colorado.

PART 2. SEDIMENT TRANSPORT

9. INTRODUCTION

A study of the sediment transport by water is of importance in several aspects of hydraulic engineering:

- fluvial hydraulics: knowledge of sediment transport forms the basis for the design of river-training works, navigation improvement, flood control.
- irrigation: design of stable channels, intakes, settling bassins.
- coastal engineering: prediction of littoral drift, design of coastal protection works and harbours.
- dredging: the suction, transport and deposition of material has many aspects related to the transport of sediments.

The main objective of sediment transport hydraulics is to predict whether an equilibrium condition, erosion (scour) or deposition (silting) will occur and to determine the quantities involved. The rate of sediment transport, expressed as mass, weight or volume per unit time can be determined from measurements or from calculations. Both methods only have a low degree of accuracy so that the sensitivity of the design to possible variations in the calculated transport rates has to be considered.

The main reason for the empirical character of sediment transport knowledge is the complexity of the transport process. The interaction of a turbulent flow, the characteristics of which are only known by empirism, and a boundary consisting of loose sediments cannot be described by simple equations. Most of our knowledge is based therefore on experiments and measurements both in the field and in laboratories.

The following subjects will be discussed:

- the characteristics of the sediments
- their mutual interaction:
  - initiation of motion,
  - transport mechanisms,
  - bed forms, roughness,
  - bed material transport - bed load,
    - suspended load.

10. PROPERTIES OF THE TRANSPORT MATERIAL

Some of the properties of sediment which are often used are:

size
shape
density
fall velocity
porosity

10.1 Size

A classification of particles according to size is given in table 10.1. This table gives the classification by the American Geophysical Union for clay, silt, sand, gravel, cobbles and boulders.

Various definitions of "diameter" are possible:

sieve diameter D = diameter of square mesh sieve which will just pass the particle.

sedimentation diameter D_s = diameter of sphere with same density and same settling velocity in same fluid at same temperature.

nominal diameter D_n = diameter of sphere with equal volume.

triaxial dimensions a, b, c (a = largest, c = smallest axis)

Size determination

boulders, cobbles and gravel: direct measurement
gravel, sand : sieving
fine sand, silt : sedimentation or microscope analysis

10.1.1. Sieving

Sieving can be applied for particles down to 44 μm but gives good results down to 74 μm. Sieve sizes (openings) are made in a geometric series with every sieve being $\sqrt[4]{2}$ larger in size than the preceding. Taking every other size gives a $\sqrt{2}$ series. For most sands a $\sqrt{2}$ series gives sufficient results but a $\sqrt[4]{2}$ series may be necessary for very uniform sands. Some general rules for sieving can be given:

1. Do not overload sieves to avoid clogging. The following maximum residues on individual 8-inch sieves are recommended (after Shergold 1946).

Table 10.1

Major classification of sediment size according to H.A. Einstein

Size	Designation	Remark
$D < 0.5\mu$	Colloids	Always flocculated
$0.5\mu < D < 5\mu$	Clay	Sometimes or partially flocculated
$5\mu < D < 64\mu$	Silt	Nonflocculating-individual crystals
$64\mu < D < 2$ mm	Sand	Rock fragments
2 mm $< D$	Gravel, boulders	Rock fragments

American Geophysical Union (AGU) grade scale for particle sizes

Size			Class
Millimeters	Microns	Inches	
4,000-2,000		160-80	Very large boulders
2,000-1,000		80-40	Large boulders
1,000-500		40-20	Medium boulders
500-250		20-10	Small boulders
250-130		10-5	Large cobbles
130-64		5-2.5	Small cobbles
64-32		2.5-1.3	Very coarse gravel
32-16		1.3-0.6	Coarse gravel
16-8		0.6-0.3	Medium gravel
8-4		0.3-0.16	Fine gravel
4-2		0.16-0.08	Very fine gravel
2.00-1.00	2,000-1,000		Very coarse sand
1.00-0.50	1,000-500		Coarse sand
0.50-0.25	500-250		Medium sand
0.25-0.125	250-125		Fine sand
0.125-0.062	125-62		Very fine sand
0.062-0.031	62-31		Coarse silt
0.031-0.016	31-16		Medium silt
0.016-0.008	16-8		Fine silt
0.008-0.004	8-4		Very fine silt
0.004-0.002	4-2		Coarse clay
0.0020-0.0010	2-1		Medium clay
0.0010-0.0005	1-0.5		Fine clay
0.0005-0.00025	0.5-0.24		Very fine clay

Sieve opening mm.	U.S. Sieve nr.	Maximum residue in grams		
		2-series	$\sqrt{2}$-series	$\sqrt[4]{2}$-series
2.4	8	150	75	38
1.2	16	100	50	25
0.6	30	70	35	18
0.295	50	50	25	12
0.15	100	35	18	9
0.076	200	25	12	6

The total sample size should be about 20 - 50 grams for 8"-inch sieves and fine sand.

2. A sieving time of 10 minutes with a mechanical sieving apparatus should be used
3. For coarse sands and gravel the following minimum size is recommended to obtain a sufficient number of grains in each fraction (see De Vries 1971).

   Sample size (gram) > $20.D_{85}{}^3$ D_{85} in mm.

Sieve types and series are different in various countries, but are generally based on a $\sqrt[4]{2}$-series.

10.1.2 Sedimentation

For fine sand and silt a size distribution can be determined by sedimentation. For particles < 50 µm the Stokes law for the settling velocity is valid; for coarser particles empirical relations have to be used. Various principles are used: sedimentation balances, pipette analysis, visual accumulation tube (fig. 10.1) (for a review see ASCE 1969). Sedimentation gives of course no independent size and shape determination.

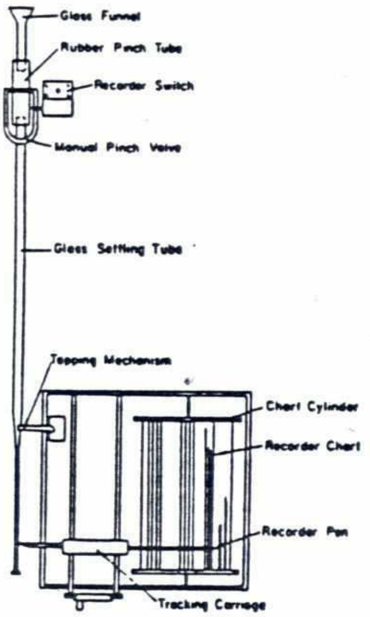

Fig. 10.1 .—SKETCH OF VISUAL ACCUMULATION TUBE AND RECORDING MECHANISM

10.1.3. Size distribution

By sieving or sedimentation a size distribution can be obtained which is generally expressed as a "percent by weight" vs "grain size" distribution. The cumulative size distribution of most sediments can be approximated by a log-normal distribution. A log-normal distribution will give a straight line if logarithmic probability paper is used (figure 10.2).

From the cumulative size distribution the mean diameter can be defined:

$\bar{D}$ or $D_m = \overset{i}{\Sigma}\, p_i D_i / \overset{i}{\Sigma}\, p_i$

in which p_i : fraction with diameter D_i.
D_i is the geometric mean of the size fraction limits.
Also the notation D_p is used which denotes the diameter in a mixture of which p% is smaller than D_p. D_{50} is also called the median diameter

For a given distribution we can define the geometric mean diameter

$D_g = (D_{84} \cdot D_{16})^{\frac{1}{2}}$ (which is equal to D_{50} for a log-normal distribution) and the geometric standard deviation:

$\sigma_g = [D_{84}/D_{16}]^{\frac{1}{2}}$

In geological literature also Ø-units are used:

$\text{Ø} = -{}^{2}\log D$ (D in mm)

Ø (1 mm) = 0, Ø (0.5 mm) = 1 etc.

σ_g becomes in Ø-units: $\sigma_{\text{Ø}} = \frac{1}{2}(\text{Ø}16 - \text{Ø}84)$.

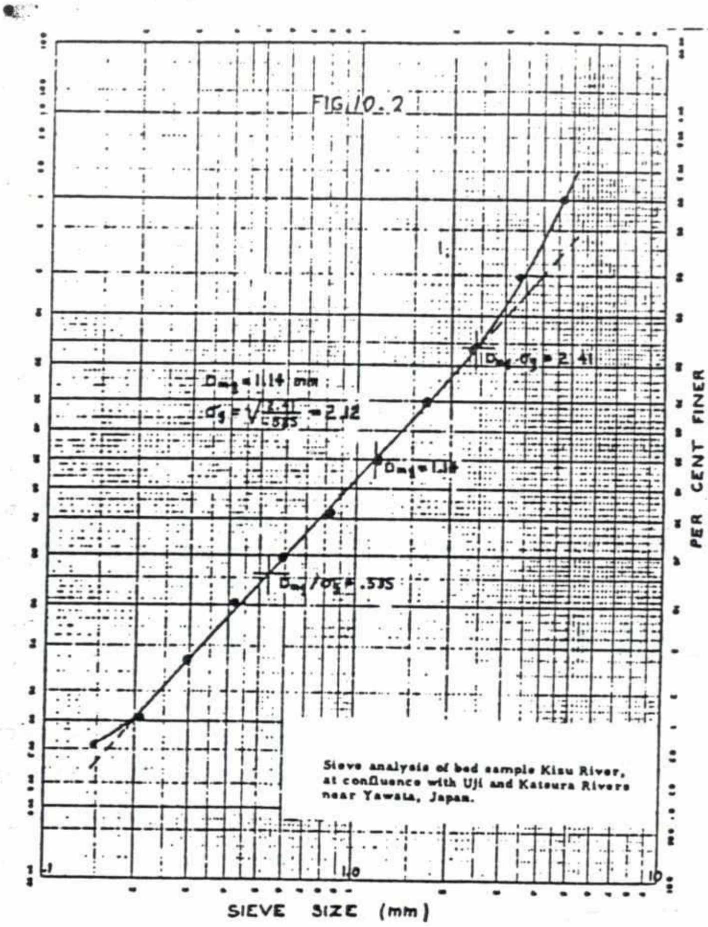

Fig. 10.2 Example of cumulative distribution of sieve diameter on logarithmic probability paper

10.2. Shape

Beside of the grain-diameter also the shape is of importance. A flat particle will have a smaller fall velocity and will be more difficult to transport as a rounded particle as bed load.

Several definitions may be used to characterise the shape:

Sphericity = ratio of the surface area of a sphere and surface area of the particle at equal volume

Roundness = ratio of the average radius of curvature of the edges and the radius of circle inscribed in the maximum projected area of the particle

Shape factor = s.f = $c/\sqrt{ab}$ in which a, b and c are three mutually perpendicular axes, from which a is major, b is intermediate and c is minor axis.

For spheres s.f = 1, for natural sands s.f ≈ 0.7

Roundness and sphericity are not suited for practice whereas the shape factor gives sufficient results for practical application.

10.3. Density

Most sediments originate from disintegration or decomposition of rock.

clay : fragments of feldspars and micas
silt : silicas
sand : quartz
gravel and boulders: fragments of original rock

The density of most sediment particles (< 4 mm) varies between narrow limits. Since quartz is predominant in natural sediments the average density can be assumed to be 2650 kg/m³ (specific gravity 2.65). Sometimes heavy minerals are present which can be segregrated during ripple formation or other modes of transport. Clay minerals range from 2500 - 2700 kg/m³.

10.4. Fall velocity

The fall velocity of a sediment is an important parameter in studies on suspension and sedimentation of sediments. The fall velocity is defined by the equation giving equilibrium between gravity force and flow resistance:

$$\underbrace{\frac{\pi}{6} \cdot D^3 (\rho_s - \rho_w)\, g}_{\text{gravity}} = \underbrace{C_D \cdot \tfrac{1}{2}\rho_w W^2 \cdot \frac{\pi}{4} D^2}_{\text{resistance}}$$

in which C_D = drag coefficient
W = fall velocity

From this relation follows:

$$W = \left(\frac{4}{3} \cdot \frac{gD}{C_D} \cdot \Delta \right)^{\frac{1}{2}}$$

in which $\Delta = (\rho_s - \rho_w)/\rho_w$

Values of C_D depend on a Reynold's number $W.D/\nu$ and the shape of the particle (expressed by $s.f = c/\sqrt{ab}$)

For spherical particles and low Reynolds number (Re < 1), C_D can be given by $C_D = 24/Re$ so that:

$$W = \frac{\rho_s - \rho_w}{18\eta}\, gD^2 = \frac{\Delta g\, D^2}{18\nu} \quad \text{(Stokes law)}$$

For large Reynolds numbers C_D becomes a constant so that W varies as:

$(\Delta g D)^{\frac{1}{2}}$

Therefore W varies with $D^{\frac{1}{2} \text{ to } 2}$.

Relations between C_D, Re and s.f are given by Albertson (1953) (see Figure 10.3). For natural sands s.f $\approx$ 0.7. From these relations graphs for W as a function of grain size, shape and temperature can be obtained (see Figure 10.4).

(1,24)

$C_D = \frac{24}{Re} = 24$

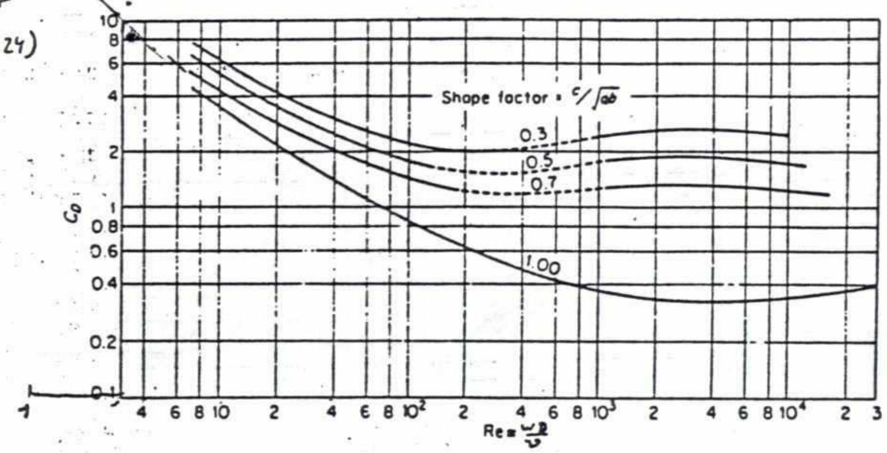

Fig. 10.3. Drag coefficient vs. Reynolds number for different shape factors. [*After* ALBERTSON (*1953*).]

The presence of large number of other particles will decrease the fall velocity of a single particle. A cluster of particles will have a greater velocity however. Therefore care must be taken with experiments on the fall velocity to avoid currents in the fluid that will influence the fall velocity of the particle <u>and</u> the influence of concentration should be considered.

There are many expressions giving the influence of concentration on the fall velocity. Based on systematic experiments, Richardson and Zaki (1954) give a useful expression:

$W(c)/W(o) = (1 - c)^{\alpha} \qquad 0 \leq c < 0.3$

W(c) is the fall velocity of a grain in a suspension with concentration by volume c

W(o) is the fall velocity for a single grain

α is a function of Reynolds number $W.D/\nu$

Re < 0.2	$\alpha = 4.65$
0.2 < Re < 1	$\alpha = 4.35.Re^{-0.03}$
1 < Re < 200	$\alpha = 4.45.Re^{-0.1}$
Re > 500	$\alpha = 2.39$

The coefficient is slightly dependent on particle shape but this can be neglected. For fine sediments this means that a concentration of 1% gives a reduction in fall velocity of 5%.

The fall velocity of a particle in a turbulent fluid can be different from that in a quiescent fluid (see chapter 13.2).

Example: D = 0.4 mm s.f = 0.7 T = 10° C

This gives W = 5.3 cm/s

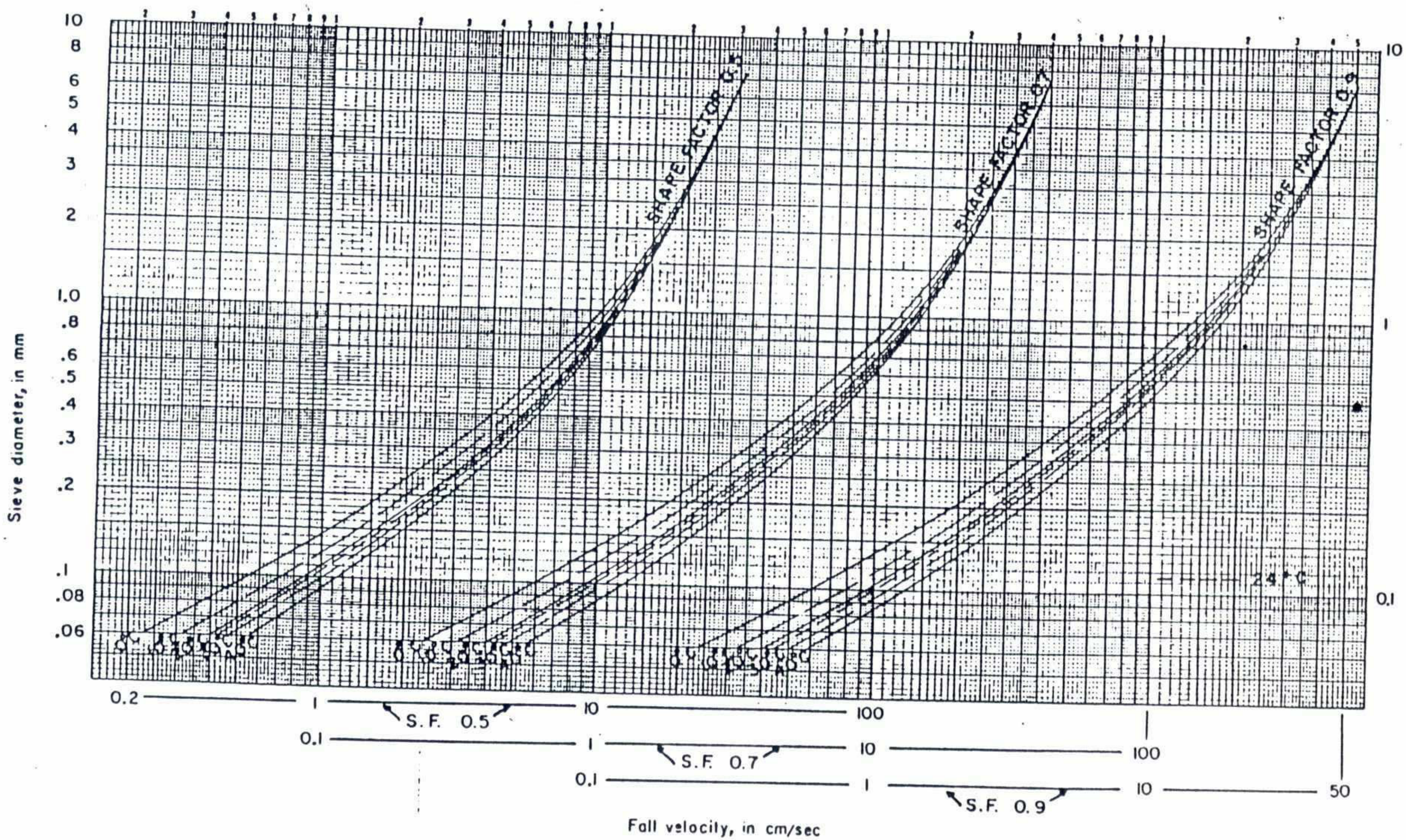

FIG.10.4 RELATION OF SIEVE DIAMETER AND FALL VELOCITY FOR NATURALLY WORN QUARTZ PARTICLES FALLING ALONE IN QUIESCENT DISTILLED WATER OF INFINITE EXTENT

10.5. Bulk density and porosity

In estimating the life of a reservoir and similar cases the calculated weight of the sediment transported to the reservoir has to be converted into volume. For this the dry mass per unit volume of sediment in place, bulk density, ρ_b, has to be estimated.

For instance for air-dried fine sediments 1200-2000 kg/m³ applies. The same material deposited under continuously submerged conditions may range from 300 - 1000 kg/m³. The density will also depend on the grainsize and silt content.

Bulk density, ρ_b = the mass of dry sedimentary material within a unit of volume (kg/m³). The volume taken by the sediment depends on the conditions of settling and may be a function of time due to consolidation. An empirical relation is presented by Lane and Koelzer (1953) for estimating the bulk density of deposits in reservoirs:

$$\rho_{b_T} = \rho_{b_1} + B \log T \qquad \rho_b = (1 - \varepsilon)\rho_s$$

ε = relative pore volume (porosity)

T = time in years

ρ_{b_1} = initial bulk density taken to be the value after one year of consolidation

B = consolidation coefficient

Reservoir operations	sand		silt		clay	
	ρ_{b_1}	B	ρ_{b_1}	B	ρ_{b_1}	B
sediment always submerged or nearly submerged	1500	0	1050	90	500	250
normally a moderate reservoir drawdown	1500	0	1185	45	750	170
normally considerable reservoir drawdown	1500	0	1275	15	950	100
reservoir normally empty	1500	0	1320	0	1250	0

Lane and Koelzer also gave the simple relation $\rho_{b_1} = 817(P + 2)^{0.13}$ in which P = percentage of sand.

Lara and Pemberton (1963) analysed 1316 samples and gave somewhat different values of ρ_{b_1} (in kg /m³). The following size classification was used

clay: material < 4μm

silt: material 4 to 62.5 μm

sand: material > 62.5 μm

Type	Reservoir operation	ρ_{b_1}		
		clay	silt	sand
I	Sediment always submerged or nearly submerged	420	1120	1550
II	Normally moderate to considerable reservoir drawdown	560	1135	1550
III	Reservoir normally empty	640	1150	1550
IV	River-bed sediments	960	1170	1550

The r.m.s. deviation for the correlation was 200 kg/m³ which means that considerable deviations are possible.

Example: A sediment in a type I reservoir contains 20% clay, 45% silt and 35% sand. The density of the sediment will then be

$$\rho_{b_1} = 0.20 \times 420 + 0.45 \times 1120 + 0.35 \times 1550 = 1130 \text{ kg/m}^3$$

Murthy and Banerjee (1976) analysed 832 samples from Indian reservoirs with type II operation. The following values of ρ_{b_1} were obtained:

sand:1506 kg/m³ silt: 866 kg/m³ clay: 561 kg/m³

The results cannot be compared directly with Lara and Pemberton because the division between sand and silt was taken at 20 μm.

10.6. Literature

F.A. Shergold, 1946 — The effect of sieve loading on the results of sieve analysis of natural sands. J. Soc. of Chem. Ind. London, 65, p. 245 - 249

M.L. Albertson, 1953 — Effect of shape on the fall velocity of gravel particles. Proc. 5th Hydr. Conf. Univ. of Iowa, Bull. no. 34.

E.W. Lane, 1953
V.A. Koelzer

Density of sediments deposited in reservoirs. Rep. no. 9 of a study of methods used in measurements and analysis of sediment loads in streams. Univ. of Iowa, Iowa.

J.F. Richardson, 1954
W. Zaki

Sedimentation and fluidisation. Trans. Inst. Chem. Eng. 32, p. 35 - 53

W. Batel, 1960

Korngrössen Messtechnik. Springer Verlag, Berlin

V.A. Vanoni, 1961

Lecture notes on sediment transport and channel stability. Calif. Inst. of Technology, Rep. KH-R.I.

J.M. Lara, 1963
E.L. Pemberton

Initial Unit weight of deposited sediments. Proc. Federal Interagency Sedimentation Conf. p. 818 - 845, Misc. Publ. no. 970, US Dept. of Agriculture.

N.A. Fuchs, 1964

The mechanics of aerosols. Pergamon Oxford.

T. Allen, 1968

Particle size measurement. Chapman and Hall London.

H.P. Guy, 1969

Laboratory theory and methods for sediment analysis. US Geol.Survey. Techniques of Water Research Investigations, Book 5, Chapter Cl.

ASCE, 1969

Task Comm. on Preparation of Sedimentation Manual Sediment measurement techniques. Proc. ASCE 95 (HY5), pp. 1515 - 1543.

M. de Vries, 1970
On the accuracy of bed-material sampling.
J. of Hydr. Research 8 (4), pp. 523 - 533.

R.J. Gibbs, 1972
The accuracy of particle-size analysis utilizing settling tubes.
J. Sed. Petr. 42 (1) pp. 141 - 145.

B.N. Murthy, 1976
B.K. Banerjee
Initial unit weight of deposited sediments in reservoirs with considerable draw-down.
Proc. Symp. on Modeling Techniques in Hydraulic Engineering, Poona, Nov. 1976 1, paper A 6.

11. INITIATION OF PARTICLE MOTION

11.1 Introduction

The equilibrium of a particle on the bed of a stream is disturbed if the resultant effect of the disturbing forces (drag force, lift force, viscous forces on the particle surface) becomes greater than the stabilising forces as gravity and cohesion. Cohesion is only important for sediments in the clay and silt range or fine sands with an appreciable silt content. The acting forces have to be expressed in known quantities such as velocities or bottom shear stress. They will have a strongly fluctuating character so-that the initiation of motion also has a statistical aspect.

Theoretical work on the initiation of a motion has started with work by Brahms (1753) who gave a sixth power relation between flow velocity and the necessary weight of a stone and by Dubuat (1779, 1786) who introduced the concept of bottom shear stress and did some experiments on particle movement. Most of the older relations have the form:

$$U_{bottom,\ crit} = (4 - 5)\sqrt{D} \qquad (D \text{ in m, } U \text{ in m/s})$$

As the "bottom" is not well defined the use of this type of formula is limited.

11.2 Theory

White (1940) gave a thorough discussion on the equilibrium of a grain on the bed of a stream.

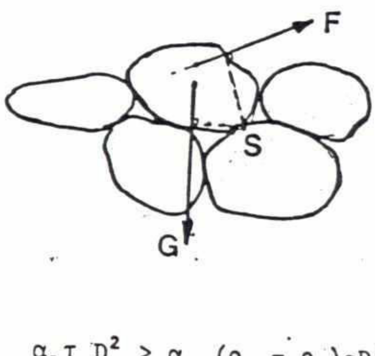

The disturbing force F (resultant of drag and lift forces) will be proportional to the bottom shear stress τ_o and the particle surface area (D^2).
The stabilizing gravity force is proportional to $(\rho_s - \rho_w)gD^3$. Taking the moment with respect to the turning point S gives the equation:

$$\alpha_1 \tau_o D^2 \geq \alpha_2 (\rho_s - \rho_w) g D^3$$

or: $\tau_o \geq C(\rho_s - \rho_w)gD$

The factor C will depend on the flow condition near the bed, particle shape, the position of the particle relative to other particles etc. The flow condition near the bed can be described by the ratio of grainsize to thickness of the viscous sublayer which ratio is proportional to $U^{x} D/\nu = Re^{x}$, a Reynoldsnumber based on grainsize and shear velocity.

All other theoretical considerations based for example on drag force due to velocity will give the same result that:

$$\psi_{cr} = U^{x2}_{cr}/\Delta gD = f(Re^{x})$$

11.3. Experiments

The relation:

$$\psi_{cr} = \frac{\tau_{cr}}{(\rho_s - \rho_w)gD} = \frac{U^{x2}_{cr}}{\Delta gD} = f\frac{(U^{x}_{cr}D)}{\nu} = f\ (Re^{x})$$

has been investigated by many authors especially by Shields (1936) who did systematic tests and compared his results with results from other investigations (see figure 11.1). The difficulty in all tests is the definition of "initiation" of motion. It is the movement of the first particle or of a large number of grains? Shields correlated the rate of sediment transport with τ_o and defined τ_{cr} by extrapolating to zero material transport.

For large Re^{x} (rough bed) it can be seen that U^{x}_{cr} varies with $\sqrt{D}$ (figure 11.2). For equal values of h/D and therefore equal values of $\bar{U}/U^{x}$ it follows that $\bar{U}_{cr} \sim \sqrt{D}$ and that the critical velocity of a stone is proportional to the 1/6 power of the weight of the stone (or stone weight proportional to $\bar{U}^6$).

11.4. Influence of various factors

11.4.1 Effect of criterion

It is clear that the critical value of τ_o will depend on the criterion for initiation of motion. To get an objective criterion Neill (1968, 1969) proposed the dimensionless parameter :

$$N = nD^3/U^{x}$$

in which n is the number of grains displaced per unit area and unit time. Shields graph corresponds roughly with a N-value of 15.10^{-6} for coarse material. For designs of bottom protections etc. a much lower criterion

20

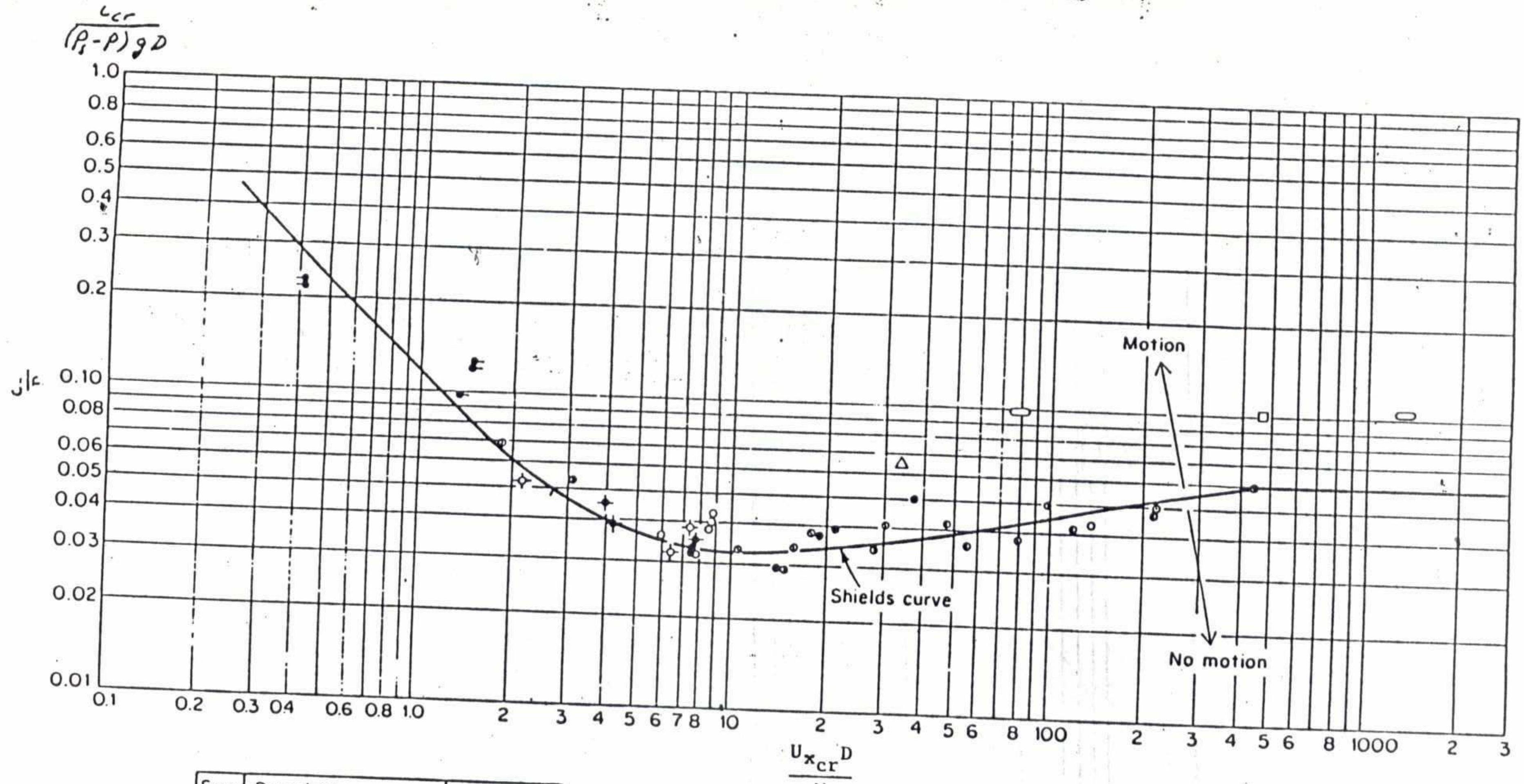

Fully developed turbulent velocity profile

Sym	Description	γ_s, g/cm³
○	Amber (Shields)	1.06
●	Lignite (Shields)	1.27
◉	Granite (Shields)	2.7
◉	Barite (Shields)	4.25
◉	Sand (Casey)	2.65
✧	Sand (Kramer)	2.65
✦	Sand (U.S.W.E.S)	2.65
⊙	Sand (Gilbert)	2.65

Turbulent boundary layer

●–	Sand (Vanoni)	2.65
–●	Glass beads (Vanoni)	2.49
□	Sand (White)	2.61
⬭	Sand in air (White)	2.10
△	Steel shot (White)	7.9

Fig.11.1 Shields' diagram; dimensionless critical shear stress vs. shear Reynolds number. [*After* VANONI (*1964*).]

22

Curves are derived from Shield's curve, Fig.11.1 for ρ_s = 2650 $^{kg}/_{m^3}$ and $\nu = 10^{-6}$ m^2/s (20°C)

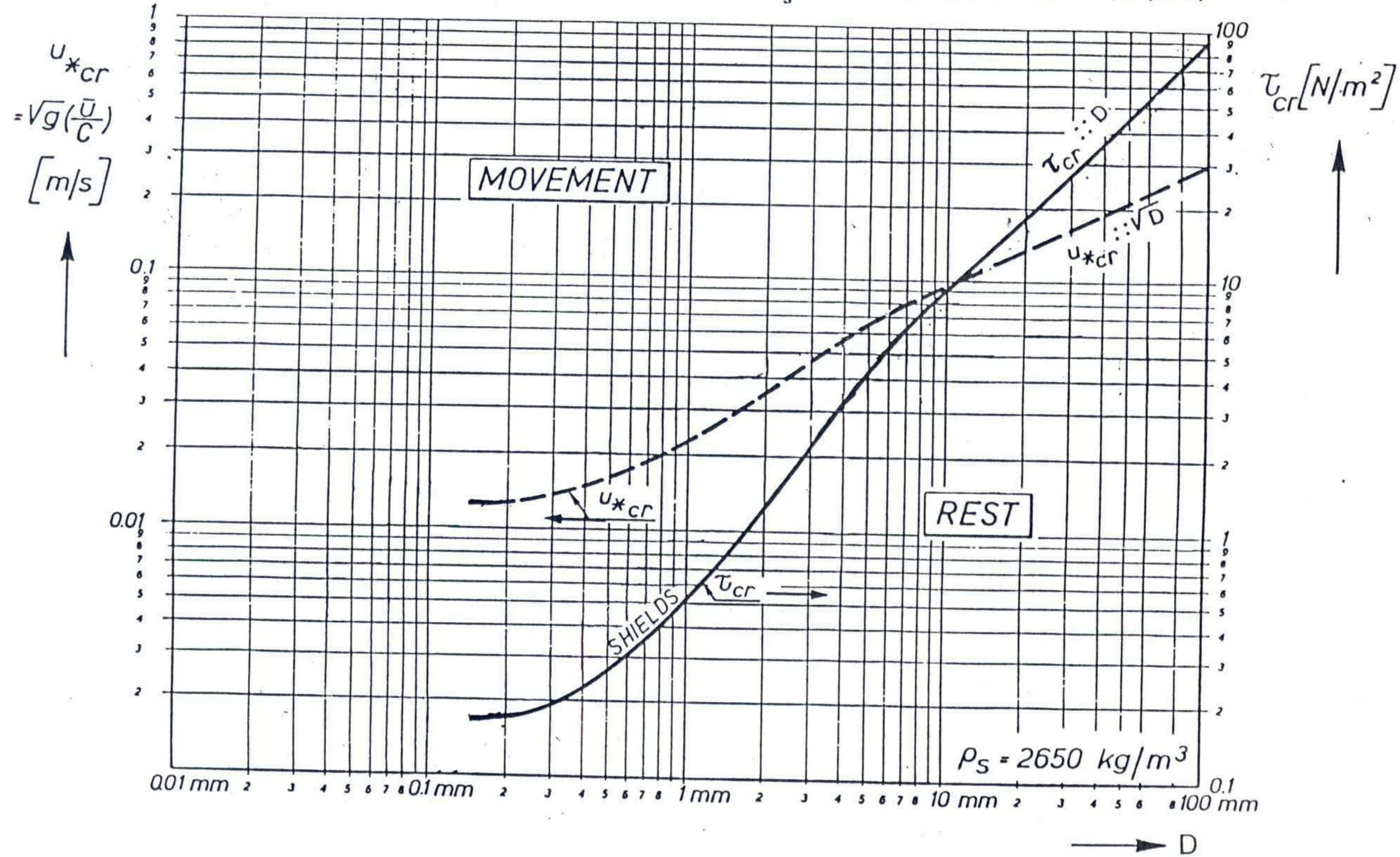

CRITICAL SHEAR STRESS AND CRITICAL SHEAR VELOCITY
AS FUNCTION OF GRAIN SIZE FOR ρ_s = 2650 kg/m³ (SAND)

FIGURE 11.2

should be used (for instance $N = 10^{-6}$). Also Paintal (1971) has measured very low rates of transport with coarse material down to $\psi = 0.02$, thus well below the Shields value (see Figure 11.3).

11.4.2 Effect of particle shape

Shields experiments were done with several types of material and systematic influence of shape could not be observed. Tests at the Delft Hydraulics Laboratory with coarse material showed that the critical value of ψ is the same for various shapes (spheres, cubes, broken stones etc.) if the nominal diameter D_n is used for comparison.

11.4.3 Effect of gradation

It will be clear that a wide gradation will have an influence on τ_{cr}. In practice however the gradation has an influence for $D_{95}/D_5 > 5$ only (Knoroz, 1971), because the larger grains are more exposed and smaller grains are shielded by the larger ones. Therefore D_{50} is a good measure for most samples. For the effect of a gradation also see Eguisaroff (1965).

For a wide particle gradation the effect of armoring will occur which means that fine particles are eroded and an armor layer of coarse particles is formed, which prevents the bed from further scour. This effect is very important in degradation downstream of dams (Livesey, 1963, Gessler 1970). In that case D_{85} to D_{95} can be taken as a representative value for the mixture.

11.4.4 Effect of h/D

For small values of h/D (waterdepth/particle diameter) a deviation from Shields graph is possible because τ_o is not representative in that case for the turbulent flow structure. The turbulence structure near the bed in an infinite fluid is completely defined by bed shear stress (τ_o) and roughness (k_s) but for small values of h/D also the waterdepth gives a limitation on size and frequency of the large eddies. Also the ratio of eddy duration and the time necessary to accelerate a particle becomes small sothat an influence of h/D may be expected (more stability with smaller h/D). Experiments have indeed shown that ψ_{cr} increases with decreasing h/D (Ashida 1973).

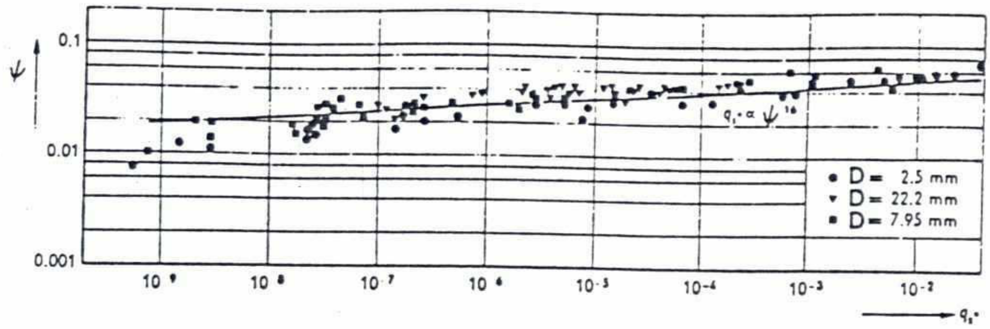

Variation of bed load transport at low shear values.

Débit de charriage à tension de frottement faible.

$$q_s^{x} = \frac{q_s}{(\Delta g D^3)^{\frac{1}{2}}} \qquad q_s = \text{sed.tr.}/\text{m.s}$$

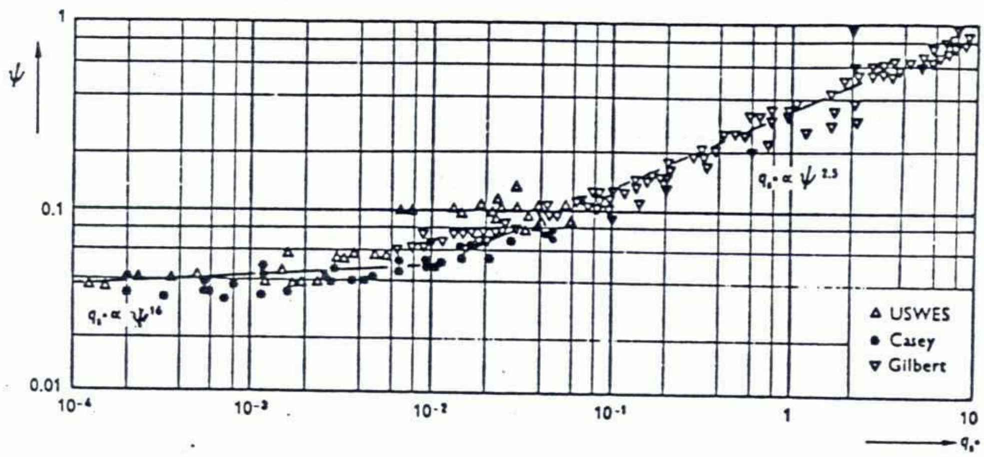

Variation of bed load transport at high shear values.

Débit de charriage à tension de frottement élevée.

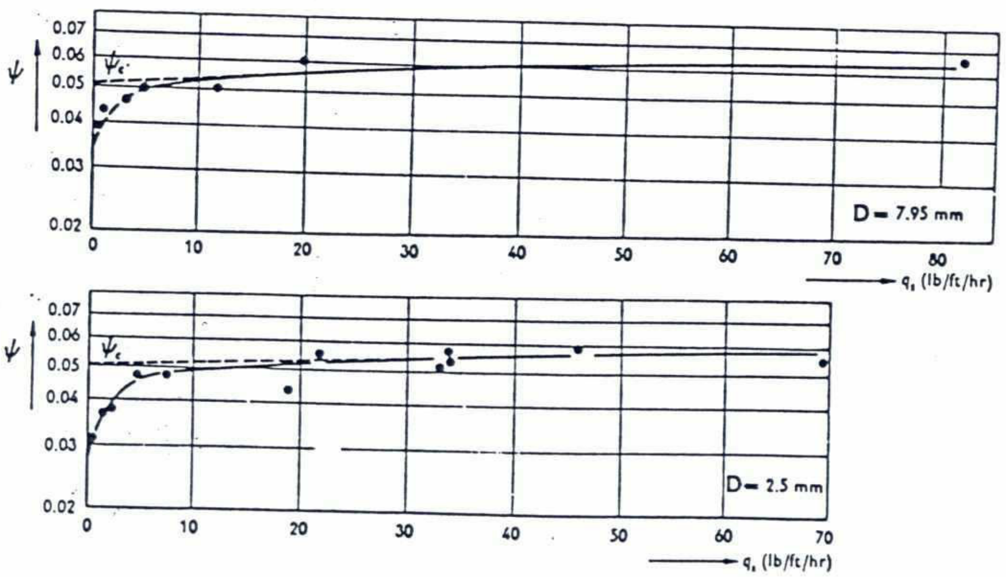

Determination of critical shear stress.

Détermination de la tension de frottement critique.

Figure 11.3 Measurements by Paintal.

11.4.5 Influence of bed slope

For a particle on a slope the value of τ_{cr} will be reduced. For a horizontal bed the relation

$$F(o) = G \tan\phi$$

is valid, in which ϕ is an angle characteristic for the particle stability.

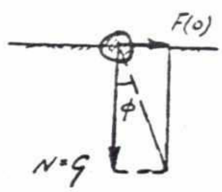

For a bed slope in the flow direction with angle α the following stability condition holds:

$$F(\alpha) + G \sin\alpha = N \tan\phi =$$

$$G \cos\alpha \tan\phi$$

$$F(\alpha) = G \cos\alpha \tan\phi - G \sin\alpha$$

$$\frac{F(\alpha)}{F(o)} = \frac{G \cos\alpha \tan\phi - G \sin\alpha}{G \tan\phi}$$

$$= \frac{\cos\alpha \sin\phi - \sin\alpha \cos\phi}{\sin\phi}$$

$$k(\alpha) = \frac{F(\alpha)}{F(o)} = \frac{\sin(\phi - \alpha)}{\sin\phi}$$ (given by Schoklitsch in 1914!)

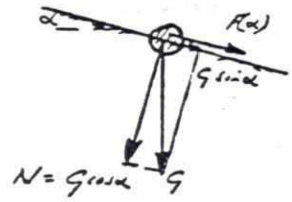

For a side slope with angle β

Stability condition

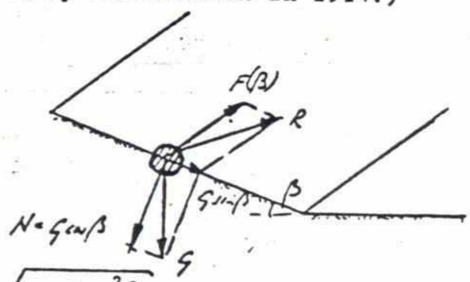

$$R = \sqrt{F(\beta)^2 + G^2\sin^2\beta} = G \cos\beta \tan\phi$$

$$F(\beta) = \sqrt{G^2\cos^2\beta \tan^2\phi - G^2\sin^2\beta}$$

$$k(\beta) = \frac{F(\beta)}{F(o)} = \sqrt{\frac{\cos^2\beta \tan^2\phi - \sin^2\beta}{\tan^2\phi}} = \cos\beta \sqrt{1 - \frac{\tan^2\beta}{\tan^2\phi}}$$ (given by Leiner in 1912!

For a combination of longitudinal and side slope the reduction factor $k(\alpha,\beta)$ becomes $k(\alpha,\beta) = k(\alpha).k(\beta)$.

11.4.6 Influence of pore water-flow

It might be expected that an inflow or outflow of water from a sand bed has an influence on the stability of the sand particles. The pore-water flow may be caused by a ground-water table lower or higher than the river water level. It has been shown by Oldenziel and Brink (1974) however, that the influence is very limited. For hydraulic gradients up to $\pm$ 0.3 only a factor of 2 in the transport rate was observed. In view of the strong variation of transport rate with ψ near incipient motion this means only a few percent variation in ψ_{cr} and can be neglected.

There is one exception however. Harrison and Clayton (1970) have shown that seepage into the bed for a flow carrying fine silt particles, gives an enormous increase in stability due to the formation of a plastered bed layer.

11.5 Cohesive sediments

11.5.1. Consolidated sediments

If a soil has a certain cohesion it will have an increased resistance against erosion. Empirical data on critical mean velocities are given by Lane (1953).

material	loose	moderately compact	compact
sandy clay	0.45 m/s	0.9 m/s	1.25 m/s
clay	0.35 m/s	0.8 m/s	1.20 m/s
lean clayey soil	0.30 m/s	0.7 m/s	1.05 m/s

Several authors have tried to correlate critical shear stress with mechanical properites of the soil (siltcontent, plasticity index, vane shear strength) (see Smerdon and Beasly (1959), Carlson and Enger (1960), Raudkivi and Tan (1984)). Paaswell (1973) concludes that generally used soil classification parameters can not be used as erosion predictors. For a certain soil type it can be shown that erosion resistance increases with the plasticity index (difference between liquid limit and plastic limit).

Kamphuis and Hall (1983) did tests on samples consolidated at very high pressures (50-200 kPa). Critical shear stresses increased slightly with consolidation pressure but were mainly influenced by clay content. Critical shear stresses were measured in a water tunnel and were in the range of τ_{cr} = 1 to 10 N/m^2. (U^*_{cr} = 3 to 10 cm/s).

Raudkivi and Tan (1985) studied the erosion rates of artificial clay samples and found a strong influence of pH-value and salt concentration of the eroding fluid on erosion rates.

For practical application it can be stated that the majority of data for cohesive soils with D_{50} = 10 to 100 μm show that critical shear velocities U^*_{cr} in the range of 3 to 4.5 cm/s will be possible. There is some tendency for an increase of U^*_{cr} with vane shear strength and plasticity index.

11.5.2 Recent sediments

For recently deposited sediments (mud in estuaries) various authors (Migniot 1968, 1977, Courmault 1971, Thorn and Parsons (1980), Partheniades (1970) and others) give relations between U^*_{cr}, vane strength, yield stress or the dry weight of the sediments. Minimum values are in the order of U^*_{cr} = 1.0 cm/s (consolidation period of some days) to 3.0 cm/s for consolidation periods of several weeks. For an example see Fig 11.4., taken from Terwindt and Breusers (1972).

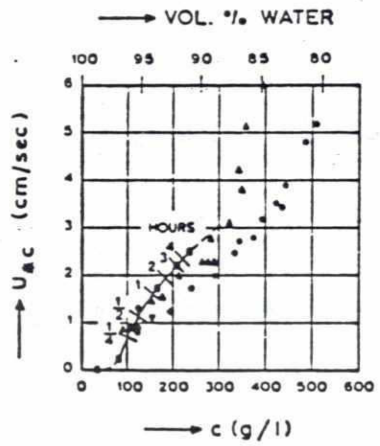

MUD:		SAND IN %	THICKNESS OF MUDLAYER IN cm
Δ "LA VILLAINE"	(MIGNIOT, 1968)	8	12
• "MAHURY"	(MIGNIOT, 1968)	2	12
—+—	I	37	2
▼	II	7	20
o	III	2	2

Fig.11.4 Critical shear velocity in relation to mud concentration.

Courmault (1971) found for Gironde mud (D_{50} = 2 μm)

$$U^*_{cr} = 0.0055\, C_s + 0.0000026\, C_s^{\,2}$$

C_s = dry weight in kg/m^3 $150 < C_s < 450$ kg/m^3.

The erosion rate was:

$$E = 2.10^{-4}\ (\tau/\tau_{cr}-1)$$

E = erosion rate in kg/m^2s.

Migniot (1968, 1977) analysed various mud types and found a relation between U^*_{cr} and the yield stress τ_y:

$$U^*_{cr} = 1.7\ \tau_y^{0.25} \qquad \tau_y < 1.5\ N/m2$$

U^*_{cr} in cm/s

$$U^*_{cr} = 1.4\ \tau_y^{0.5} \qquad \tau_y > 1.5\ N/m^2$$

Loire mud (N.N. 1984) showed the following properties.

C_s (kg/m^3):	115	175	200	250	285	345	470
τ_y (N/m^2) :	0.09	0.3	0.6	1.2	3.1	10	28
U^*_{cr} (cm/s):	0.9	1.25	1.5	1.8	2.5	4.4	7.4

Thorn and Parsons (1980) give for three estuaries: Forth (Scotland), Brisbane River (Australia) and Belawan (Indonesia):

$$U^*_{cr} = 7.4.\ 10^{-3} C_s^{\ 1.14}$$

U^*_{cr} in cm/s

$$80 < C_s < 200\ kg/m^3$$

For short erosion times (10 min) the erosion rate was

$$E = 0.0026\ (\tau-\tau_{cr})$$

E in kg/m^2s

The erosion rate decreased for longer erosion times.

Parchure and Trimbak (1985) found that in a consolidating mud bed (kaoline and a lake mud) sediment density increased with distance in the bed and that corresponding U^*_{cr} values also increased. Values of U^*_{cr} at the surface were in the order of 1.0 cm/s and in the order of 2 to 2.5 cm/s at a depth of 1 cm. In conclusion it can be said that critical shear velocities and erosion rates are greatly variable, depending upon type of mud and consolidation time. Tests with the actual sediment are necessary to obtain accurate values.

11.6 Stability of stones

The stability of stones on dams or in revetments is discussed by several authors. Taking a "safe" value for the Shields parameter $\psi = 0.03$ and $k_s = 2\ D$ (in view of the large roughness of stones) the following relation is obtained:

$$\frac{\overline{U}_{cr}}{\sqrt{\Delta g D}} = 1.0 \log \frac{6h}{D}$$

Isbash (1935) neglects the influence of h/D and gives an empirical relation for the stability of a stone in a bed:

$$\overline{U}_{cr} = 1.2 \sqrt{2\Delta g D} = 1.7 \sqrt{\Delta g D}$$

For a stone on the top of a dam the critical velocity is reduced:

$$\overline{U}_{cr} = 0.86 \sqrt{2g\Delta D} = 1.2 \sqrt{\Delta g D}$$

Goncharov (see Shamov 1959) gives the following relations:

$$\frac{\overline{U}_{cr}}{\sqrt{\Delta g D}} = 0.75 \log \frac{8.8h}{D} \quad \text{for absolute rest of a stone}$$

and

$$\frac{\overline{U}_{cr}}{\sqrt{\Delta g D}} = 1.07 \log \frac{8.8h}{D} \quad \text{for the critical condition.}$$

Levi (see Shamov 1959) gives the empirical relation:

$$\frac{\overline{U}_{cr}}{\sqrt{\Delta g D}} = 1.4 \left(\frac{h}{D}\right)^{0,2}$$

Maynord (1978) gives the empirical expression:

$$\frac{D_{50}}{h} = 0.22\ Fr^3 \qquad Fr = \frac{\overline{U}}{\sqrt{gh}}$$

This can be converted into (taking $\Delta = 1.65$):

$$\frac{\overline{U}_{cr}}{\sqrt{\Delta g D}} = 1.28 \left(\frac{h}{D}\right)^{1/6}$$

All relations are compared in Fig. 11.5

The formulas given do not take into account the influence of turbulence generated by constructions for example dams.
In that case the critical velocity has to be reduced with a factor

$$\alpha = \frac{1.45}{1 + 3r}$$

in which r is the relative turbulence intensity and a value $r = 0.15$ has been assumed in uniform flow over a rough bed.
Just downstream of a hydraulic jump (stilling basin) values of r in the order of 0.3 to 0.35 can be expected. This gives a value for α of about

$$\alpha = 0.7$$

This agrees with the design graphs given by Cox (1958).

62

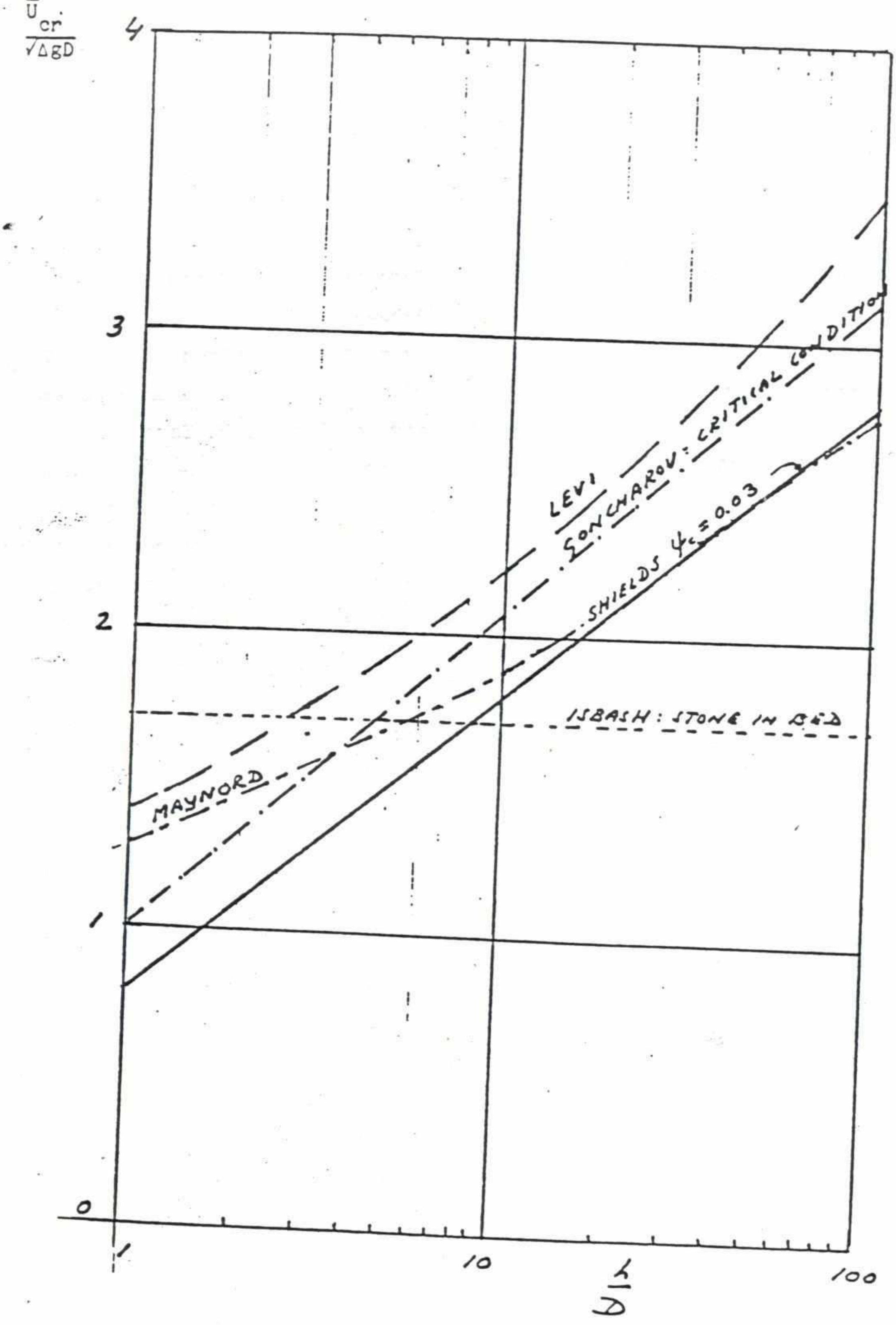

Fig. 115 Critical velocities for stones

92

11.7 Literature

A. Brahms, 1753 — Anfangsgründe der Deich- und Wasserbaukunst, Aurich

L.G. Dubuat, 1779 — Principes d'Hydraulique, Paris

L.G. Dubuat, 1786 — Principes d'Hydraulique et de Pyrodynamique, Paris

O. Leiner, 1912 — Zur Erforschung der Geschiebe- und Sinkstoff-bewegung, Zeitschrift für Bauwesen 62, p. 490 - 515

A. Schoklitsch, 1914 — Über Schleppkraft und Geschiebebewegung, Leipzig und Berlin, W. Engelman

A. Shields, 1936 — Anwendung der Aehnlichkeitsmechanik und der Turbulenzforschung auf die Geschiebebewegung Mitt. Der Preuss. Versuchsanstalt für Wasserbau und Schiffbau Berlin, Heft 26

C.M. White, 1940 — The equilibrium of grains on the bed of a stream, Proc. Royal Society London A 174, no. 958, p. 332

E.W. Lane, 1953 — Progress report on studies on the design of stable channels, Proc. ASCE 79, sep. 280

E.W. Lane, 1954; E.J. Carlson — Some observations on the effect op particle shape and the movement of coarse sediment. T. Am. Geoph. Un. 35 (3), p. 453-462

R.T. Smerdon, 1959; R.P. Beasley — The tractive force theory applied to stability of open channels in cohesive soils. Coll. of Agric. Exp. Station. Res. Bull 715

E.J. Carlson, 1962; P.F. Enger — Tractive force studies of cohesive soils for design of earth canals. U.S. Bur. of Recl. Denver, Colorado.

R.H. Livesey, 1963 — Channel armoring below Fort Randall Dam Proc. Fed. Interagency Sed. Conf. U.S. Dept. of Agric. Misc. publ. 970, p. 461-470

E. Partheniades, 1965 — Erosion and deposition of cohesive soils. Proc. ASCE 91 (HY1), p. 105-139

66

I.V. Eguisaroff, 1965 — Calculations of non-uniform sediment concentration. Proc. ASCE 91 (HY4), p. 225-247

ASCE, 1966 — Initiation of motion. Proc. ASCE 92, pp. 291-314.

C.M. Migniot, 1968 — Etude des propriétés physiques de different sédiments tres fins et de leur comportement sous des actions hydrodynamiques. La Houille Blanche 23 (7), p. 591-620.

C.R. Neill, 1968 — A re-examination of the begining of movement for coarse granular-bed materials, H.R.S. Wallingford.

C.R. Neill, 1969 — Quantitative definition of beginning of bed movement, Proc. ASCE 95 (HY1), p. 585-588

E. Partheniades, 1970 — Erodibility of channels with cohesive boundary, Proc. ASCE 96 (HY3), p. 755-771

J. Gessler, 1970 — Self-stabilizing tendencies of alluvial channels, Proc. ASCE 96 (WW2), May, p. 225-249

R. Paaswell, 1970 — Causes and mechanisms of cohesive soil erosion: The state of the art. Highway Res. Board Washington USA. 135 no. 52 p. 52-72

S.S. Harrison, 1970
L. Clayton — Effects of ground-water seepage on fluvial processes. Bull. Geol. Soc. Am. no. 811, P. 1217-1225

A.S. Paintal, 1971 — Concept of critical shear stress in loose boundary open channels. J. Hydr. Res. 9 (1), p. 91-113

V.S. Knoroz, 1971 — Natural armouring and its effects on deformations of channel beds formed by materials non-uniform in size. Proc. 14th IAHR Congress, Paris, paper 3, p. 35-42.

P. Courmault, 1971 — Détermination expérimentale du débit solide d'érosion de sédiments fins cohesifs. Proc. 14th IAHR Congress Paris 4 p. 9-16.

J.H.J Terwindt, 1972 — Experiments on the origin of flaser, lenti-

08

H.N.C. Breusers — cular and sand-clay alternating bedding. Sedimentology 19, p. 85-98.

K. Ashida, 1973
M. Bayazit — Initiation of motion and roughness of flow in steep channels. Proc. IAHR Congress, Istanbul, paper A 58

D.M. Oldenziel, 1974
W.E. Brink — Influence of suction and blowing on entrainment of sand particles. Proc. ASCE 100 (HY7), p. 935-949

A.J. Raudkivi, 1974
D.L. Hutchinson — Erosion of kaolinite clay by flowing water. Proc. Royal Society London A 337, p. 437-454.

K. Arulanandan, 1975
P. Loganathan, R.B. Krone — Pore and eroding fluid influence on surface erosion of soils. Proc. ASCE 101 (GT1), p. 51-66.

C. Migniot, 1977 — Action des courants, de la houle et du vent sur les sédiments. La Houille Blanche, 32 (1) p. 9-47.

M.F.C. Thorn, 1980
J.G. Parsons — Erosion of cohesive sediments in estuaries. 3d Int. Symp. on Dredging Technology, Bordeaux. BHRA, Cranfield, p. 349-358

J.W. Kamphuis, 1983
K.R. Hall — Cohesive material erosion by unidirectional current. J. of Hydr. Eng. ASCE 109 (1) p. 49-61

A.J. Raudkivi, 1984
S.K. Tan — Erosion of cohesive soils. J. of Hydr. Res 22 (4) p. 217 - 233

N.N., 1984 — Rapport final de l'estuaire de la Loire. CNEXO, Le Havre, Rapp. no. 55.

T.M Parchure 1985
A.J. Mehta — Erosion of soft cohesive sediment deposits. J. of Hydr. Eng. (ASCE) 111 (10) p. 1308-1326

Stability of stones

S.V. Isbash, 1935	Construction of dams and other structures by dumping stones into flowing water. Trans. Res. Inst. Hydrot. Leningrad 17 p. 12-66.
See also:	
S.V. Isbash, Kh. Khaldre, 1970	Hydraulics of river channel closure. Butterworths, London.
R.G. Cox, 1958	Velocity forces on submerged rock. U.S.W.E.S. Vicksburg. Misc. Paper No. 2-265.
G.I. Shamov, 1959	River Sediments. Leningrad, Gidrometeorizdat.
S.T. Maynord, 1978	Practical riprap design. U.S.W.E.S. Vicksburg, Misc. Paper H-78-7.

11.8. Problems

Use Shields curve and $k_s = D$ unless otherwise specified. $\nu = 10^{-6}\ m^2/s$

11.1 Given: A wide open channel excavated in uniform material ($\rho_s = 2650\ kg/m^3$) with $D = 2$ mm has a slope $I = 0.5.10^{-3}$ and a depth of $h = 2$ m.

Question: Is the channel bed stable?

11.2 Given: A wide open channel has a depth of $h = 1.7$ m, a mean velocity $\bar{U} = 2.5\ m/s$.

Question: What is the minimum size of the bed material to obtain a stable bed? $\rho_s = 2650\ kg/m^3$

11.3 Given: A wide open channel has a slope $I = 10^{-5}$ and bed material $D = 0.2$ mm. No bedforms are present.

Question: What is the maximum discharge /m^1 without movement of bed material. ($\rho_s = 2650\ kg/m^3$)?

11.4 Given: A wide open channel is excavated in uniform material with ($\rho_s = 2650\ kg/m^3$) and $D = 3$ mm under a slope $I = 10^{-4}$.

Question: What is the permissible discharge/m^1 ?

11.5 Given: The bottom of a wide open channel with a depth of 4 m is protected with stones with a mass of 30 kg. $\rho_s = 2800\ kg/m^3$.

Question: What is the critical mean velocity for this bottom protection, using $\psi_{cr} = 0.03$ and the nominal diameter as the representative size.

11.6 Given: Experiments are designed to check Shields curve, using a wide flume (neglect side-wall effects). The waterdepth for the experiments is 0.6 m.

Question: If uniform flow is required (water surface slope = bed slope), what is the required slope of the channel bed and discharge/m^1 for: a) an experiment with uniform sand $k_s = D = 200\ \mu m$;

b) an experiment with uniform gravel $k_s = D = 4$ mm.

$\rho_s = 2650\ kg/m^3$

12 TRANSPORT MECHANISM, BED FORMS, ALLUVIAL ROUGHNESS

12.1 Introduction

For turbulent flow over a rigid bed a description of the flow structure could be given only by empirical methods. Bottom shear stress, waterdepth and bed roughness were the most important parameters. Description of particle motion under the action of the flow is also largely empirical sothat it is not difficult to understand why there is only a limited theoretical basis for the relation between flow and sediment transport.

Most of the existing knowledge is obtained from experiments and general physical arguments. For the initiation of motion a reasonable picture was obtained in this way. At greater values of the bed-shear stress sediment transport will increase and deformation of the bed will occur. As the deformation is also time-dependent and nature is always unsteady, an equilibrium situation will be hardly found in practice.

12.1 Transport mechanism

According to the mechanism of transport two major modes may be distinguished:

1. Bed load - movement of particles in contact with the bed by rolling, sliding and jumping
2. Suspended load - movement of particles in the flow. The settling tendency of the particle is continuously compensated by the diffusive action of the turbulent flow field.

A sharp distinction is not possible. A general criterion for the beginning of suspended load is a ratio of shear velocity and fall velocity $U^x/W \sim 1.5$. Sometimes also saltation load is mentioned. This is the mode where particles bounce from one position to another. This is only important for particle movement in air. The maximum particle elevation of a particle moving in water is in the order of 2-3 times the diameter sothat this mode of transport can be considered as bed load.

According to the origin of the transported material a distinction is made as follows:

A. Bed-material transport — This transport has its origin in the bed, which means that the transport is determined by the bed and flow conditions (can consist of bed load and suspended load).

B. Wash load

Transport of particles not or in small quantities in the bed. The material is supplied by external sources (erosion) and no direct relationship with the local conditions exists (can only be transported as suspended load, generally fine material < 50 μm). It can have influence on turbulence and viscosity and therefore have some influence on the flow.

Wash load is not important for changes in the bed of a river but only for sedimentation in reservoirs etc.

12.3 Bed Forms

Much literature exists on the classification and dimensions of bedforms, mainly in the form of empirical relations. Bed forms are of interest in practice for several reasons.

- Bed forms determine the roughness of a stream. A change in bed form can give changes in friction factor of 4 and more.
- Navigation is limited by the maximum bed level and depends therefore on the height of the bed deformation.
- Bed forms and sediment transport have a mutual influence.

A generally accepted classification is the following:

A. Lower flow regime (Froude number $Fr = \bar{U}/\sqrt{gh} < 0.6 \pm 0.2$; no sharp transition).

A.1 flat bed At values of the bed shear stress just above the critical, sediment transport without deformation of the bed is possible. Grains are transported by rolling and bouncing.

A.2 ripples For sediment sizes < 0.6 mm and and increasing bed shear stress small regular waves appear with wavelenghts in the order of 5-10 cm and heights in the order of 1 cm. They become gradually irregular and three-dimensional in character.

A.3 dunes For all sediment sizes and increasing shear stress dunes are developed. Dunes are more two-dimensional than ripples and have much greater wavelengths and heights. The crests of the waves are perpendicular to the flow, the form is more or less triangular with a gentle slope along which the particles are transported and a steep downstream slope where particles are deposited. The angle of this slope is roughly the angle of repose of the material.

B. Upperflow regime (Fr > 0.6 ± 0.2)

B.1 plane bed As the velocity is further increased, the dunes are flattened, gradually disappear and the bed becomes flat. Sediment transport rates are high.

B.2 antidunes A further increase in velocity to Froude numbers around 1.0 causes the water surface to become instable. Interaction of surface waves and the bed (sediment transport is maximum under the troughs of the surface waves) gives a bed form called antidunes.
They can travel upstream and occur in trains of 4 to 20. Antidunes and surface waves grow in amplitude and often break in a way similar to ocean waves.

B.3 chute and pools At still higher velocities chutes and pools are formed. For an illustration of the bed forms see figure 12.1 (Simons and Richardson 1968).

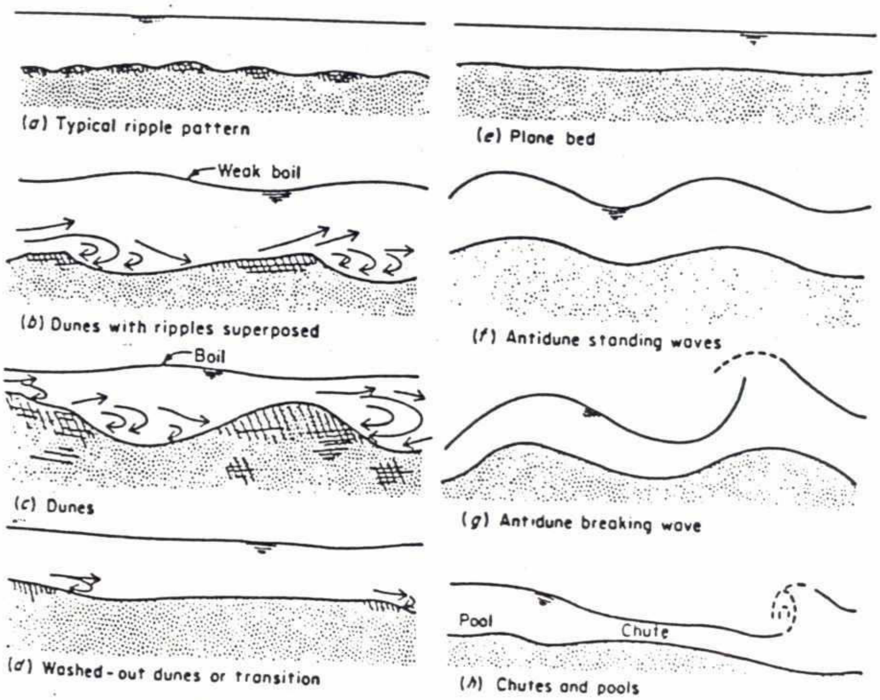

Fig. 12.1 Idealized bedforms in alluvial channels. [*After* SIMONS *et al.* (1961).]

12.4 Classification criteria

Several authors have tried to develop theoretical explanations for the origin of ripples and dunes (see for example Exner (1925) who discusses the growth of an initial instability on a sand bed.)

Other authors have assumed potential flow to predict the reaction of the main-flow on variations in bed level (Kennedy, 1963). The result of Kennedy's work is a relation between the wavelength L of the bed deformation and the Froude number (see figure 12.2). $Fr = \frac{\overline{U}}{\sqrt{gh}}$

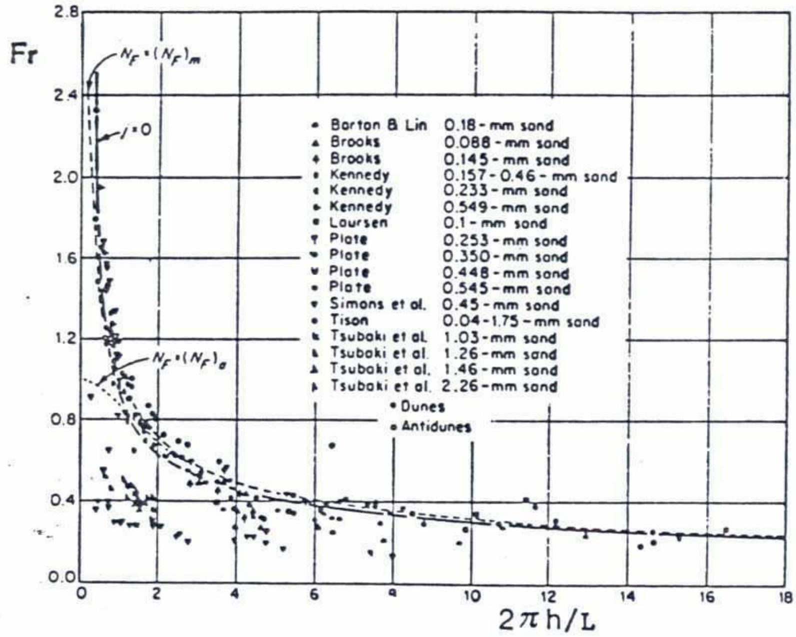

Fig. 12.2 Comparison of predicted and observed bedform regions. [*After* KENNEDY (*1963*).]

Results of the theoretical models are not very convincing sothat we have to rely again on empirical correlations. The first classification was given by Liu (1957) who proposed U^{*}/W vs $U^{*}D/\nu$ as a criterion for ripple formation. This diagram was extended by Simons (1966) for other bed forms (see fig. 12.3).

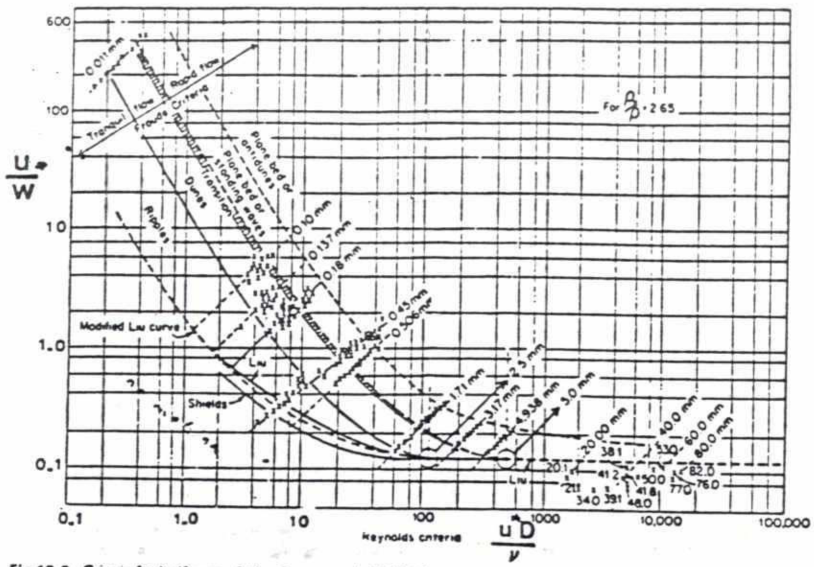

Fig.12.3 Criteria for bedforms. [*After* SIMONS *et al.* (1961*a*).]

Simons et al 1963 gave a diagram based on grainsize and streampower ($\tau_o . \bar{U}$), see figure 12.4.

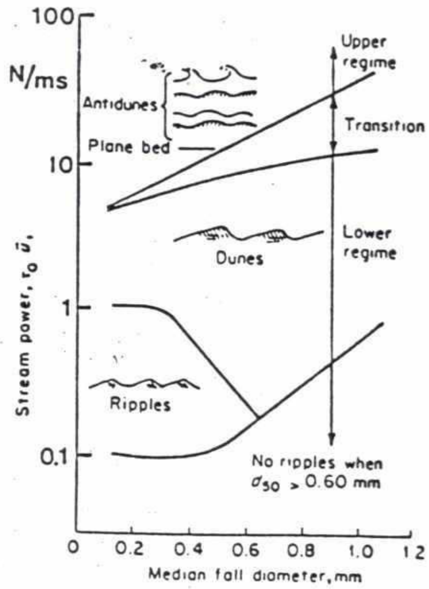

Fig. 12.4 Relation of bedforms to stream power and grain diameter. [*After* SIMONS *et al.* (1963*a*).]

The Froude number will be an important parameter in the upper-flow regime. It was used by Garde-Albertson (figure 12.5) and by Engelund and Hansen.

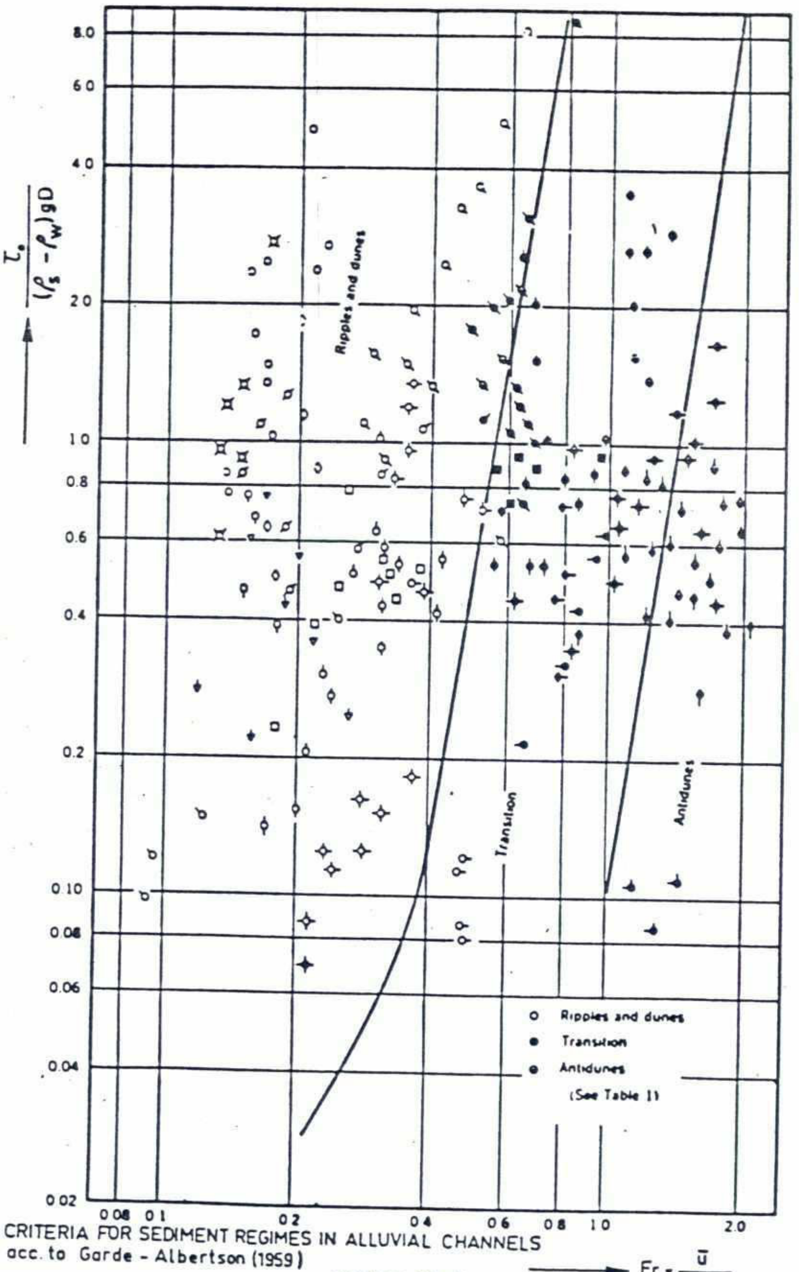

CRITERIA FOR SEDIMENT REGIMES IN ALLUVIAL CHANNELS
acc. to Garde - Albertson (1959)

FIGURE 12.5

Van Rijn uses the parameters D and T to classify the bed forms.

$$D_* = D_{50}\left[\frac{\Delta g}{\nu^2}\right]^{1/3} \qquad T = \left(\frac{U'_*}{U_{*cr}}\right)^2 - 1$$

Where T is computed using U'_* computed for a plane-bed situation, using $k_s = 3\ D_{90}$ as roughness, so

from: $\frac{\overline{U}}{U'_x} = 5.75 \log\left(\frac{12h}{3D_{90}}\right)$

A very large data set, both from flumes and the field has beed used to establish the relations. (see figure 12.6).

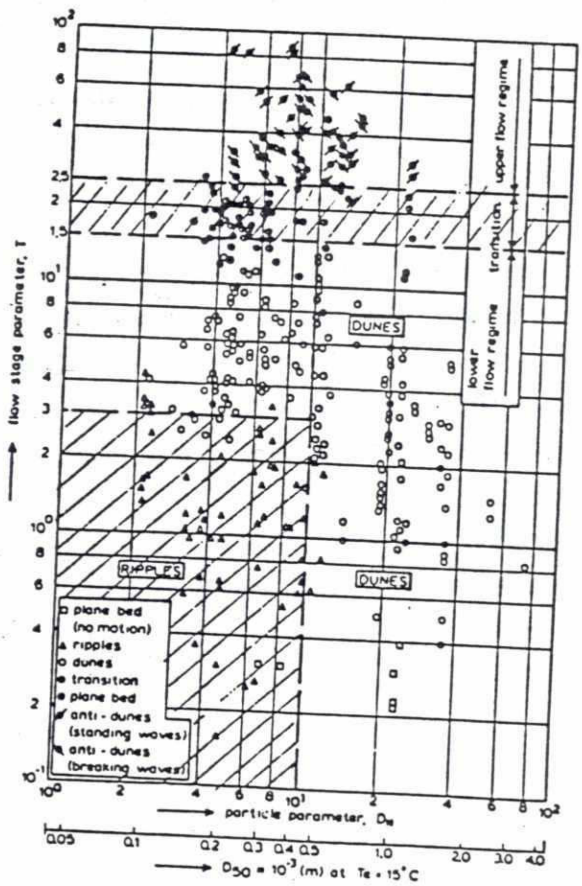

Fig. 12.6 Diagram for bed-form classification

48

It must be borne in mind that the transition in practical conditions from one bed form to another may show an important phase lag with changes in flow condition.

Raudkivi (1967) has measured the shear stress distribution on a dune profile. The maximum shear stress on the upper part of the dune had about the same value as for a horizontal bed with the same mean velocity and grain roughness. Behind the steep downstream face of the dune an eddy develops. Around the reattachment point the flow is very turbulent sothat particles are transported in bursts.

12.5 Alluvial roughness

The bed forms discussed in par.12.3 all have their specific roughness. For a flat bed without transport it can be assumed that the roughness is in the order of the grainsize (for example D_{65} or D_{90}). For flows over ripples and dunes the total resistance consists of two parts:
the roughness of the grains and the form drag of the bed forms. The roughness of a dune bed is much greater than that of a flat bed and the corresponding friction factor is also much larger. Dunes generally give the maximum roughness of a flow.

A flat bed with sediment transport (B.1) can have a friction factor slightly different from that of a flat bed without transport. The presence of antidunes does not appreciably change the magnitude of the effective roughness of the bed if compared with a flat bed. If the waves break however, the friction factor will be increased due to the energy dissipation in wave breaking.

It cannot be expected in general that the friction factor of an alluvial channel is constant. Experiments have shown that the friction factor can vary by a factor 5 or more. This is demonstrated in figure 12.8 and 12.9 where changes in bed form give a great difference in bed roughness.

Figure 12.9 shows that the same value of τ_o can occur for different values of $\bar{U}$ (take for example $\tau_o = 0.1$ lbs/ft^2). Due to phase lags between bed form (and roughness) and flow condition rivers very often exhibit hysteresis effects in discharge-stage relations (not to be confused with the hysteresis during a flood wave).

Prediction methods for the roughness of an alluvial stream generally divide the total shear τ_o or friction factor (C or λ) into two parts, one for the grain roughness (surface drag) denoted by τ_o' or C' or λ' and one for the form drag (τ_o'', C'' or λ'').

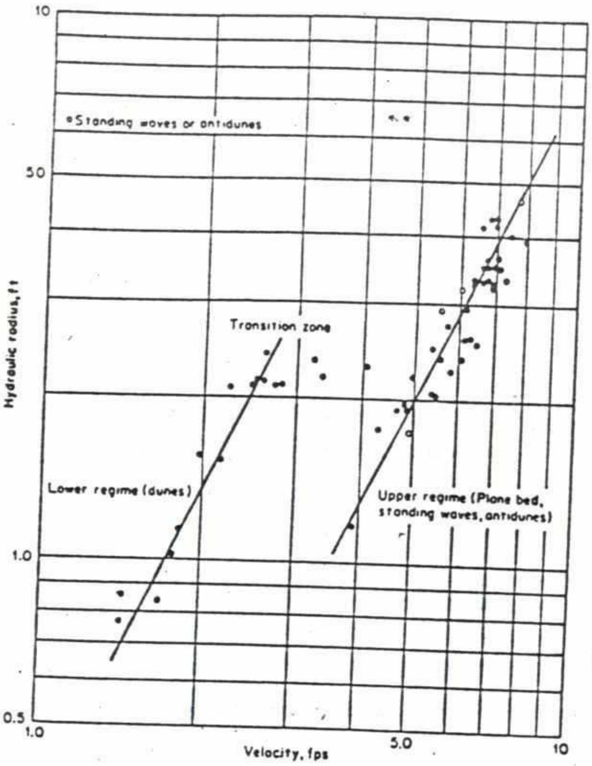

Fig. 12.8 Relation of hydraulic radius to velocity for Rio Grande near Bernalillo. [*After* NORDIN (1964).]

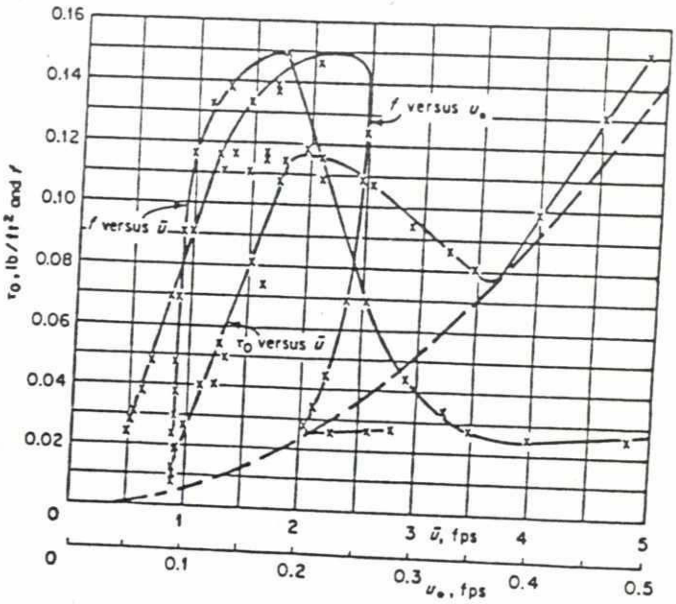

Fig. 12.9 Flow resistance due to bedforms. [*After* RAUDKIVI (1967).]

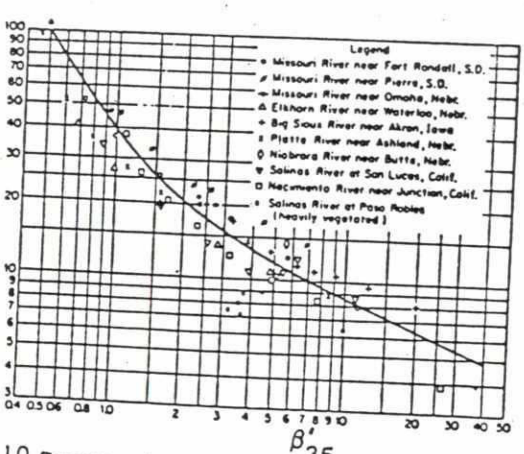

Fig. 12.10 Flow resistance due to bedforms. [*After* EINSTEIN *et al.* (1952).]

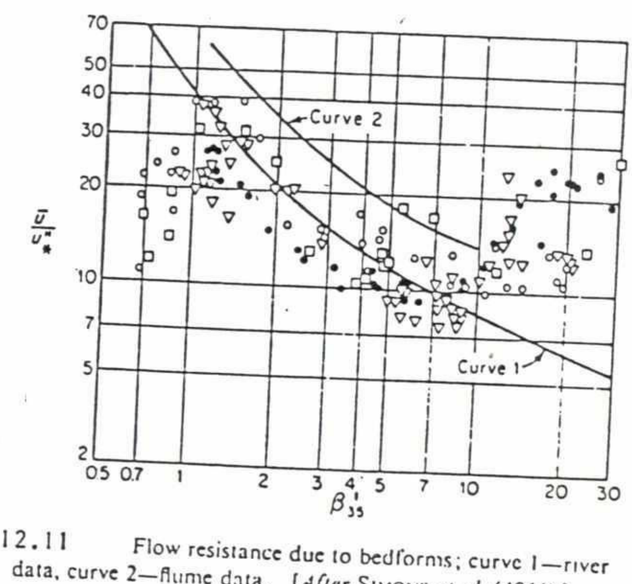

Fig. 12.11 Flow resistance due to bedforms; curve 1—river data, curve 2—flume data. [*After* SIMONS *et al.* (1966).]

267

By definition:

$$\tau_o = \tau_o' + \tau_o'' \qquad C^{-2} = C'^{-2} + C''^{-2} \qquad \lambda = \lambda' + \lambda''$$

λ is defined by $I = \text{slope} = \lambda \cdot \frac{1}{4R} \cdot \frac{U^2}{2g} \qquad \lambda = \frac{8g}{C^2}$

Several procedures are given in literature.

1. Einstein-Barbarossa (1952)

E.B. divide the hydraulic radius R in two parts: R' and R", where $R' + R'' = R$ and $R'/R'' = \tau_o'/\tau_o''$. $U^{*'}$ is computed by taking $k_s = D_{65}$ in the Chézy relation and β'_{35} is computed from:

$$\beta'_{35} = \frac{\Delta g D_{35}}{(U^{*'})^2} = \frac{\Delta D_{35}}{h'I} \qquad \text{and} \qquad \frac{\overline{U}}{U'_*} = 5.75 \log \frac{12h'}{D_{65}}$$

With the diagram given in figure 12.10 the value of $\overline{U}/U^{*''}$ is found by trial and error. For larger values of β'_{35} (> 7) deviations are observed for river data (see figure 12.11).

Procedure

a) If I and h are given and $\overline{U}$ has to be known: guess h', compute β'_{35}, U_x' and $\overline{U}$ and with fig. 12.10: $\overline{U}/U_*''$. Compute h" from U_*'' and $h = h' + h''$. If h is not correct, estimate a new value for h' and repeat untill $h = h' + h''$. Then use the last value of $\overline{U}$.

b) If q and h are given and I or C has to be computed: estimate h' and compute β_{35}' and $\overline{U}/U_x''$. From U_x' and U_x'' a new value of h' can be obtained. Repeat untill U_*' remains constant. Then compute

$$U_* = (U_x'^2 + U_x''^2)^{\frac{1}{2}}, \quad I \text{ and } C.$$

2. Engelund and Hansen (1967)

E. and H. give an expression for f" of the form:

$f'' = \alpha H^2/h.L \qquad H = \text{dune height} \qquad L = \text{dune length} \qquad h = \text{water depth}$

where $f = \tau/(\frac{1}{2}\rho U^2) = 2g/C^2 = \frac{1}{4}\lambda$

and introduce the dimensionless parameters:

12h'/2.5 D50

$$\psi = \tau/\rho g \Delta D_{50} \qquad \psi' = \tau'/\rho g \Delta D_{50} \qquad \tau' = \rho U^{*'2} \qquad \overline{U}/U^{*'} = 5.75 \log \cancel{4.8h'/D}_{50}$$

Engelund concludes that ψ is a function of ψ' only (see figure 12.12).

... & parallels for rising curve

← transition zone: 2 solutions possible (instability)

due to bedforms (not to diff. slope in wave)

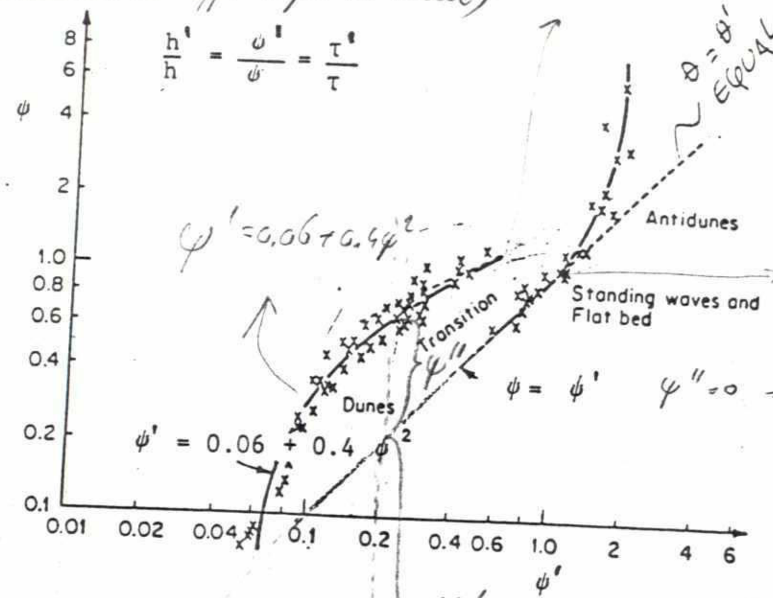

Fig. 12.12 Flow resistance [After ENGELUND] et al. (1967).]

Procedure

a) If I and h are known and $\overline{U}$ has to be computed:
Compute τ, ψ and with fig. 12.12 ψ'. This gives τ', U_*' and h'.
Then compute $\overline{U}$.

b) If h and q are given and I or C has to be computed:
Guess h', compute U_*', ψ' and with fig. 12.12 ψ and then τ. Compute h' from $h'/h = \tau'/\tau$; if different from first value, repeat calculation untill h' is constant. Then compute U_*, I and C.

3. White, Paris, Bettess (1980)

WPB give an empirical relation between:

$$F_{fg} = \frac{U_*}{(\Delta g D)^{\frac{1}{2}}} \quad , \qquad D_{gr} = D \cdot \left(\frac{\Delta g}{\nu^2}\right)^{1/3} = D_*$$

and
$$F_{gr} = \frac{U_*^{\,n}}{(\Delta g D)^{\frac{1}{2}}} \left\{\frac{\overline{U}}{5.64 \log (10h/D)}\right\}^{1-n} = \frac{U_*^n (U_*')^{1-n}}{(\Delta g D)^{\frac{1}{2}}} \tag{a}$$

where the characteristic diameter is $D = D_{35}$.

The relation is given by (see Fig. 12.13):

$$\frac{F_{gr} - A}{F_{fg} - A} = 1.0 - 0.76 \left\{1.0 - \exp\left[-(\log D_{gr})^{1.7}\right]\right\} \tag{b}$$

where A and n are functions of D_{gr}:

$n = 0$ and $A = 0.17$ for $D_{gr} \geq 60$

68

$$\left.\begin{aligned} n &= 1.0 - 0.56 \log D_{gr} \\ A &= 0.23\, D_{gr}^{-\frac{1}{2}} + 0.14 \end{aligned}\right\} \qquad 1 \leq D_{gr} < 60$$

(see also Fig. 13.8)

Procedure:

a) If h and I are given and $\overline{U}$ has to be computed:
Compute U_*, D_{gr}, n, A and F_{fg}. Compute F_{gr} using Fig. 12.13 or formula (b).
Compute $\overline{U}$ from expression (a).

b) If $\overline{U}$ and h are given and I or C has to be known:
Compute U'_* and estimate U_* by trial and error.

4. van Rijn (1984)

van Rijn has analysed a large number of data on bed-form dimension and roughness, mainly for dunes as bed forms. The relations are:

$T = \left(\dfrac{u'_*}{u_{*c}}\right)^2 - 1$

kind of Shields parameter

$$\left.\begin{aligned} &\text{dune height } H: \quad \frac{H}{h} = 0.11 \left(\frac{D_{50}}{h}\right)^{0.3} (1 - e^{-0.5T})(25 - T) \\ &\text{dune steepness } \frac{H}{\lambda}: \quad \frac{H}{\lambda} = 0.015 \left(\frac{D_{50}}{h}\right)^{0.3} (1 - e^{-0.5T})(25 - T) \end{aligned}\right\} \quad L = 7.3\,h$$

also not according to [illegible] dunes.

This means that the dune length λ is equal to 7.3 h. (Yalin says $\frac{L}{h} = 2\pi$)
T was defined on page 12.7.

The equivalent roughness for this bedform (k_s) is then computed from the relation:

$$k_s = 3\, D_{90} + 1.1\, H\, (1 - e^{-25\, H/\lambda}).$$

$\overline{U}$ is computed using this value of k_s and U_*.

Comparison of various prediction methods

van Rijn has used 786 field data and 758 flume data (h > 0.1 m, D in the range 100 to 2500 μm) to compare the predictive ability of various methods. The results were for relative errors in the value of Chézy-coefficient C of ± 10%, 20% and 30%:

	± 10% in C			± 20%			± 30%		
	R	E-H	W	R	E-H	W	R	E-H	W
786 field data	43%	25%	33%	74%	47%	58%	89%	62%	79%
758 flume data	34%	37%	33%	56%	65%	54%	71%	75%	66%
Total set	39%	31%	33%	65%	56%	56%	80	68%	73%

R = van Rijn   E-H = Engelund Hansen   W = White, Paris and Bettess

It appears that van Rijn is somewhat better for the field data and gives comparable results for flume data.

$$\frac{H}{h}\cdot\left(\frac{D_{50}}{h}\right)^{-0.3} = f(T)$$

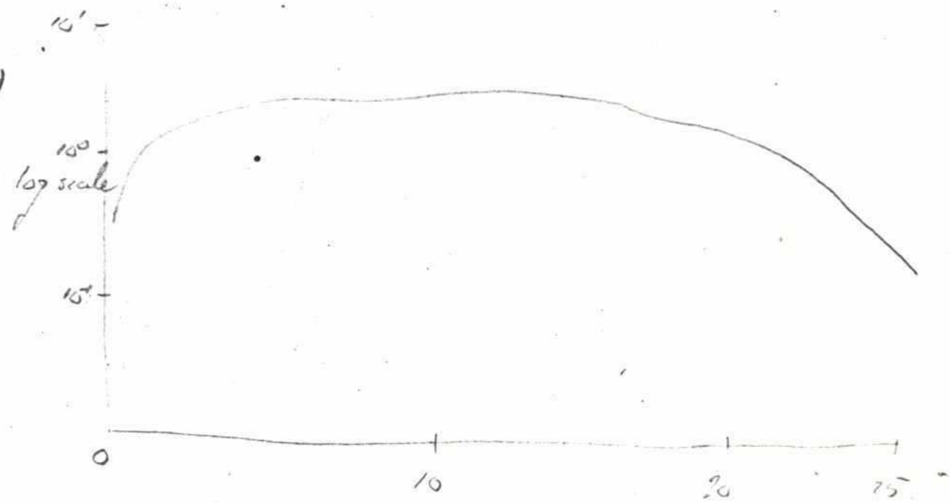

does not hold for dune case ($L \approx 200 \cdot h$)

$$\frac{u}{u_f'} = 5.75 \log \frac{12h}{3D_{90}}$$ → differs from E.H. assumptions. So take care, different methods use diff. [illegible] here.

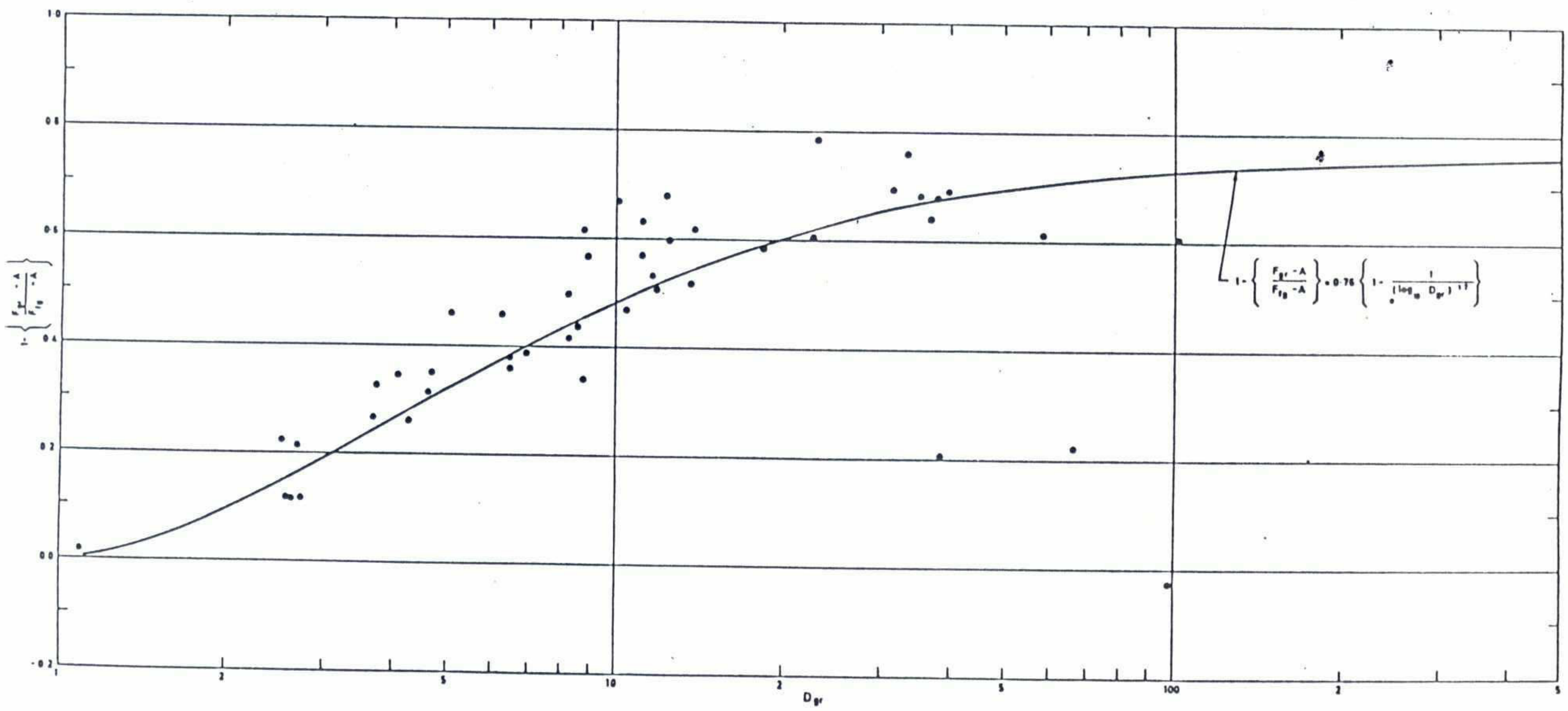

Fig. 12.13 Shear relationship based on D_{35} of the parent material, (New method)

12.6 Literature

F.M. Exner, 1925 — Über die Wechselwirkung zwischen Wasser und Geschiebe in Flüssen. Sitzber. Akad. Wiss. Wien pt Ia Bd 134.

H.A. Einstein, 1952; N.L. Barbarossa — River channel roughness. Trans. ASCE, 117, p. 1121-1132.

H.K. Liu, 1957 — Mechanics of sediment - ripple formation, Proc. ASCE, 83 (HY2), p. 1-21

R.J. Garde, 1959; M.L. Albertson — Sand waves and regimes of flow in alluvial channels. Proc. IAHR, Montreal 4, paper 28.

D.B. Simons, 1961; E.V. Richardson — Forms of bed roughness in alluvial channels. Proc. ASCE, 87 (HY3), p. 87-105.

D.B. Simons, 1963; M.L. Albertson — Uniform water conveyance in alluvial material. Trans. ASCE, 128 (1)

J.F. Kennedy, 1963 — The mechanics of dunes and anti-dunes in erodible bed channels. J. Fluid Mech., 16 (4), p. 521-544.

C.F. Nordin, 1964 — Aspects of flow resistance and sediment transport. Rio Grande near Bernalillo, New Mexico. U.S. Geol. Survey Water Supply, paper 1498-H.

D.B. Simons, 1966; E.V. Richardson — Resistance to flow in alluvial channels. U.S. Geol. Survey-Prof. paper 422-J.

F. Engelund, 1967; E. Hansen — A monograph on sediment transport in alluvial stream. Teknisk Forlag Copenhagen.

A.J. Raudkivi, 1967 — Loose boundary hydraulics. Pergamon, Oxford.

E.V. Richardson, 1967; D.B. Simons — Resistance to flow in sand channels. IAHR Ft. Collins paper.

W.R. White, 1980; E. Paris, R. Bettess — The frictional characteristics of alluvial streams: a new approach. Proc. Inst. Civ. Eng. 69, Sept. p. 737-750.

E. Paris, 1980 — Un metodo per il calcolo del coefficiente di scabrezza in alvei mobili. l'Energia Elettrica (no. 12) p. 577-581.

E. Paris, 1980 — New criteria for predicting the frictional characteristics in alluvial streams. Proc. Int. Symp. River Eng., Belgrade, paper D5.

• L.C. van Rijn, 1984 The prediction of sediment transport and alluvial roughness. To be published in Proc. ASCE (HY).

12.7 Problems $\nu = 10^{-6}\ m^2/s$ s.f. = 0.7 T=20°

12.1 Given: depth h = 2 m grainsize D = 150 μm (uniform)
T = 20° C chezy C = 63 $m^{\frac{1}{2}}/s$
mean vel. $\bar{U}$ = 0.6 m/s

Question: What bedform can be expected according to:

a) Simons - Liu (Fig. 12.3)
b) Simons - stream power (Fig. 12.4)
c) Garde - Albertson (Fig. 12.5)
d) van Rijn (Fig. 12.6)

12.2 Same questions as in 12.1
for h = 0.5 m D = 1 mm C = 42 $m^{\frac{1}{2}}/s$
$\bar{U}$ = 1.5 m/s T = 20° C

12.3 Given: depth h = 2 m, grainsize D = 0.5 mm (uniform)
Slope $I = 2.10^{-4}$ T = 20° C

Question: Compute $\bar{U}$ using the methods of Engelund-Hansen, White c.s. and van Rijn.
For the Engelund-Hansen method assume that dunes are present.

12.4 Same question for slope $I = 10^{-4}$.

12.5 Given: depth h = 2 m, grainsize D = 0.2 mm (uniform)
$\bar{U}$ = 0.7 m/s T = 20° C

Question: Compute C using the methods of Engelund-Hansen and van Rijn.

13. BED MATERIAL TRANSPORT

Bed material transport can be divided in bed load and suspended load. Both modes of transport have an influence on processes of erosion and deposition. Many relations between sediment transport and flow conditions are based on the bed shear stress. It has been shown that the bed-shear stress may be divided in a form drag and a grain roughness. It will be clear that the form drag does not contribute to the transport but that only the grain roughness will be of importance. Measurements of water depth and slope give the total bed shear stress, so that most transport relations require a reduction of the total bed shear stress to a value which is relevant for the transport.

This reduction factor is called the ripple factor μ. Theoretically one should expect: $\mu = \frac{\lambda'}{\lambda} = (\frac{C}{C'})^2$.

Many authors use μ as a closing term, however, so that various expressions are given. This manipulation with the bed shear stress has led several authors to use the mean velocity $\bar{U}$ instead of τ_o as the important factor for the sediment transport. The problem then is that the same value of $\bar{U}$ in different water depths will give different sediment transport rates, so that again some correction is necessary.

13.1 Bed load

Because several authors use some type of a physical model to predict a sediment transport relation it is not surprising that most formulas may be expressed as relations between dimensionless groups. The most common are a group related to the transport:

$$\Phi = S/\left[D^{3/2}(g\Delta)^{1/2}\right]$$

S = transport in m^3/ms transport = volume of grains

For conversion to total volume, S has to be divided by $(1 - \varepsilon)$ in which ε = porosity. As a first estimate, take $\varepsilon = 0.4$

$\Delta = (\rho_s - \rho_w)/\rho_w$

D = grainsize

and a group related to the flow:

$\psi = U^{*2}/\Delta g D$ $\psi' = \psi.\mu$ = effective value of ψ

(the parameter used by Shields for the initiation of motion).

Some of the relations given in literature are the following:

1. Du Bois (1879)

Du Boys gave a simple model in which layers of sediment move relative to each other. The number of layers was proportional to τ_o/τ_{cr}.
The resulting expression is of the form:

$$S = \text{const. } \tau_o(\tau_o - \tau_{cr})$$

Although the physical model is not very convincing, it has been found that the form of the relation can be used to describe experiments in a reasonable way.

2. Kalinske (1947)

Kalinske assumed that grains are transported in a layer with thickness D with an instantaneous grain velocity U_g equal to:

$$U_g = b(U_o - U_{cr})$$

U_o = instantaneous fluid velocity at grain level

U_{cr} = critical fluid velocity to start grain movement.

For U_o a normal distribution is assumed:

$$f(U_o) = \frac{1}{\sigma\sqrt{2\pi}} \text{ exp. } \left[-\frac{(U_o - \bar{U}_o)^2}{2\sigma^2}\right]$$

σ = r.m.s. value of velocity fluctuations.

Taking the number of grains per unit area $p/(\pi/4D^2)$ and using $\bar{U}_g$ then the mean rate of particle movement, by dry weight per unit width and time is:

$$T_b = \frac{2}{3}\rho_s gD.\bar{U}_g.p \qquad p = 0.35$$

$$\text{where } \bar{U}_g = b\int_{U_{cr}}^{\infty}(U_o - U_{cr})f(U_o)dU_o \qquad b = 1.0$$

The resulting expression may be made dimensionless with the parameters Φ and ψ with the result:

$$\Phi = 2.5\psi^{\frac{1}{2}}\left\{\frac{r}{\sqrt{2\pi}} \text{ exp. } \left[-\frac{1}{2r^2}\left(\sqrt{\frac{0.12}{\psi}} - 1\right)^2\right] - \left(\sqrt{\frac{0.12}{\psi}} - 1\right)\frac{1}{2\sqrt{\pi}} \text{ erf } \left[\left[\frac{1}{r\sqrt{2}}\left(\sqrt{\frac{0.12}{\psi}} - 1\right)\right]\right\}$$

(see figure 13.1)

in which $r = \sigma/\bar{U}_o$ $\qquad$ r= 0.17

Kalinske did not reduce the bed shear stress, so the relation is valid for plane beds only, so $\psi = \psi'$

$$\Phi = \frac{S}{D^{3/2}(g\Delta)^{1/2}}$$

$$\psi' = \frac{\mu h_I}{\Delta D} = \frac{U_x'^2}{\Delta g D}$$

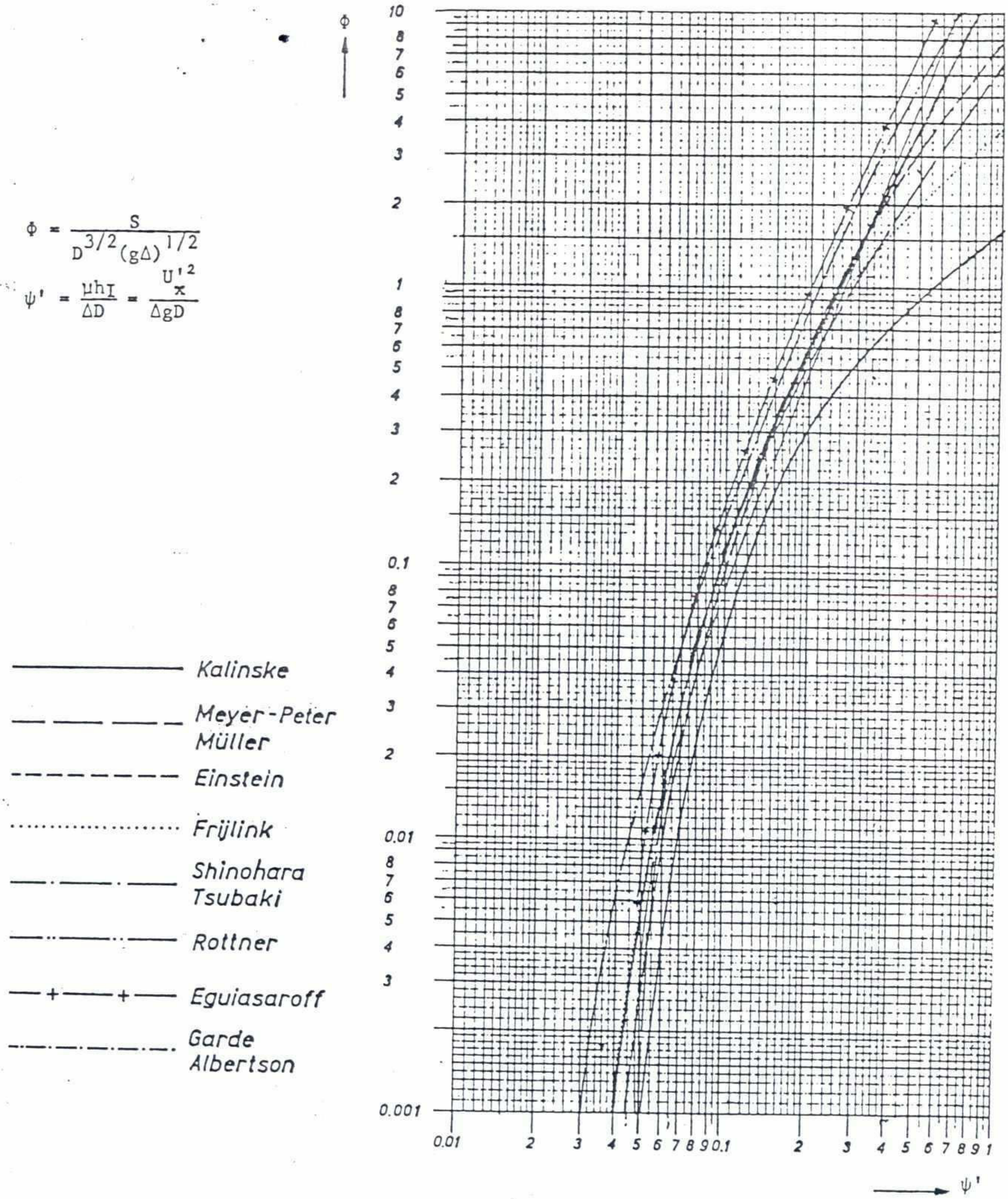

COMPARISON OF BED-LOAD TRANSPORT EQUATIONS

FIGURE 13.1

3. Meyer - Peter and Müller

M.P.M. have performed a large number of experiments in a wide flume with coarse sands. The resulting empirical expression may be written in Φ and ψ' units as:

$$\Phi = (4\psi' - 0.188)^{3/2} \quad \text{(figure 13.1)}.$$

By comparison of results with flat beds and dune beds the ripple factor is found:

$$\mu = (C/C')^{3/2} \quad \text{(theoretical exponent 2)}. \quad C' = 18 \log \frac{12h}{D_{90}}$$

For a mixture M.P.M. take:

$D_m = \bar{D} = \Sigma\, p.D/\Sigma p$ as the relevant parameter for the value of ψ' and Φ ; $D = D_{90}$ for the grain roughness.

4. Einstein (1950)

Einstein gave a complicated statistical description of the grain transport process in which the exchange probability of a grain is related to flow conditions. The resulting expression is given in figure 13.1 in a graphical form.

For the determination of the ripple factor μ a graphical procedure is given by Einstein.x) He used $D = D_{35}$ as the relevant parameter for the transport and $D = D_{65}$ for the roughness. The correlation is not valid for large rates of transport because there the transport varies with the first power of velocity $\bar{U}$ only.

x) See par. 12.5

The relations given were for bed-load. In most conditions a predominant contribution of suspended load will be present. The final accuracy of the bed-material discharge will depend therefore mostly on the accuracy of the suspended load determination.

13.2 Suspended load

Suspended load can be determined from measurements of $U(z)$ and $C(z)$ and integration of:

$$S = \int_0^h C(z)\, U(z)\, dz$$

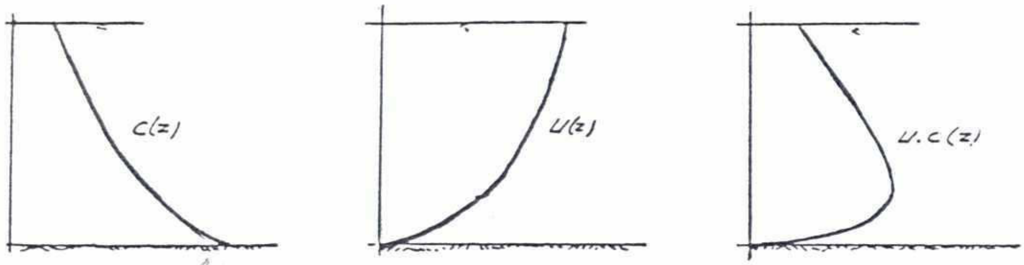

Concentration profile

In most cases estimates based on theoretical expressions will be necessary. The basic equation describing the concentration distribution in uniform steady flow is:

$$W \cdot C + \varepsilon_s \cdot \frac{\partial C}{\partial z} = 0$$

The first term W . C (W = fall velocity; C = volume concentration of sediments) represents the settling tendency of the flow. The second term represents the diffusive action of the turbulence. ε_s is the turbulent diffusion coëfficient. An explanation for this term is the following. Water packets moving upward carry a larger amount of grains than packets moving downward because there is a concentration gradient. Although there is no net transport of water there will be a net vertical transport due to this exchange of water packets, which will be proportional to the local value of the concentration gradient.

If it is assumed that the diffusion coëfficient for sediment is equal to the coëfficient to the exchange of momentum, then:

$$\varepsilon_s = \varepsilon_m = \kappa . U^* z \ (1 - z/h)$$

The resulting equation may be integrated and gives:

$$\frac{C(z)}{C(a)} = \left(\frac{h - z}{z} \ \frac{a}{h - a} \right)^{\alpha}$$

with $\alpha = W/\kappa U^*$. a is a reference level where C = C(a).
For a graphical presentation see figure 13.2

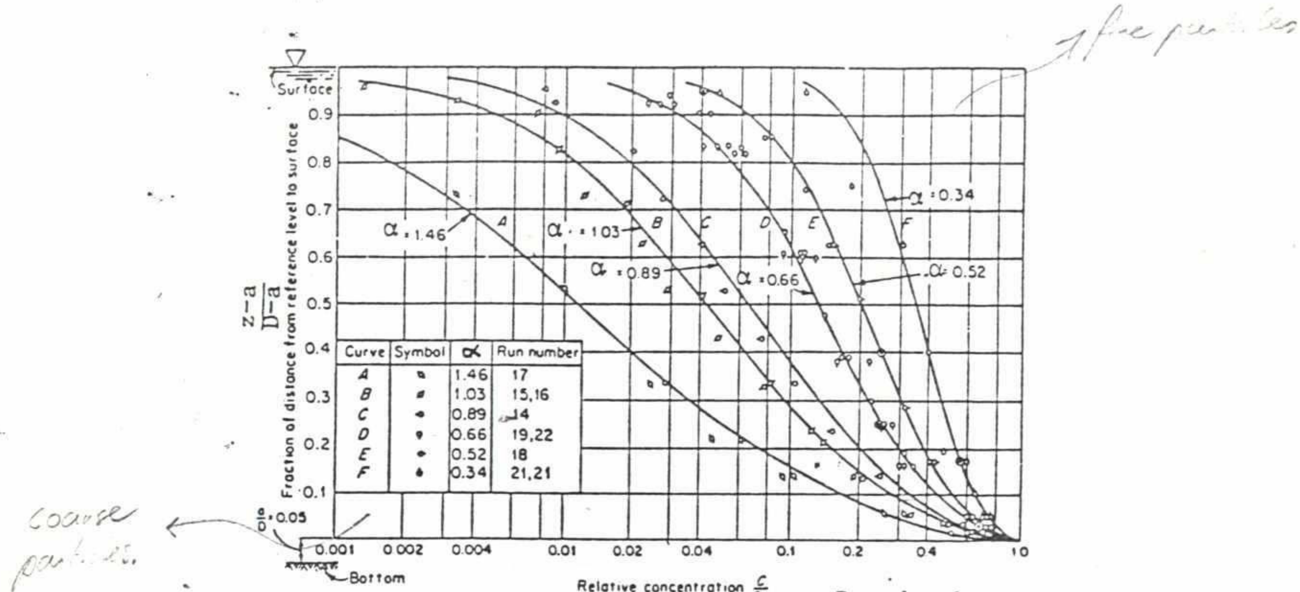

D = depth

Fig. 13.2 Distribution of suspended sediment; comparison of experimental data with Eq. (8.35). [*After* VANONI (1946).]

From this figure and the analytical expression the following rough criteria may be given:

$W/\kappa U^{*} = \alpha$	U^{*}/W	description
1.6	1.5	some suspension
0.8	3	concentration at surface > 0
0.25	10	fully developed suspension
0.06	40	almost uniform concentration

The last criterion shows that particles < 50 μm ($W < 0.2$ cm/s) are uniformly distributed for $U^{*} > 8$ cm/s or $\bar{U} > 1 - 1.5$ m/s.

Although the basic equation is very simple, some critical remarks have to be made:

1. The term W.C. should be (1 - C).C.W to account for the presence of the particles (see Hunt 1954). This correction is not important for $C \ll 1$.
2. The fall velocity is changed by the presence of other particles (see chapter 10 and by the turbulent movements of the water. Symmetric vertical velocity fluctuations give a-symmetrical drag force for non-Stokes particles. Therefore, although the mean value of the vertical velocity is zero, there will be a resultant vertical force which will reduce the settling velocity.

y0

3. The expression for ε_s gives $\varepsilon_s = 0$ for $z = 0$ or $\partial C/\partial z = \infty$ at $z = 0$ which is not very real.
4. The value of $C = C(a)$ is not given. Several assumptions are made in the literature. Einstein (1950) divides the computed bed-load by a layer with thickness 2 D and by the velocity in this layer. ($11.6\ U_*'$) The value of C(a) is one of the problems to be solved in sediment transport.
5. The velocity distribution is influenced by the presence of particles. The weight of the particles suppresses the vertical velocity fluctuations and gives a decrease in the momentum diffusion coëfficient. This is similar to a decrease in the value of κ. In fact several expressions have been given in which κ decreases with the power to keep the sediment in suspension: C.W.Δ/U.I (see figure 13.3).
   Velocity profiles become less "full" by this effect. Care should be taken in the application of this correlation because the determination of κ from velocity profiles or concentration profiles is not very accurate. For literature see Einstein and Ning Chien (1954) and Ippen (1971).

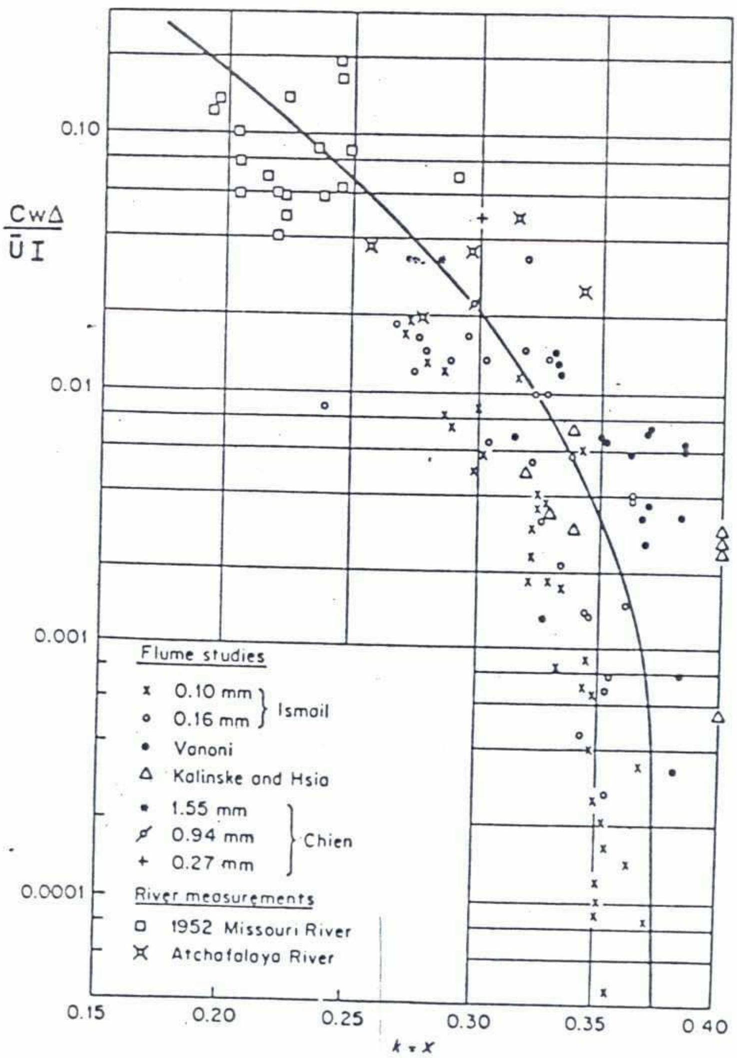

Fig. 13.3 Effect of suspended load on the k value. [*After* EINSTEIN et al. (*1954*).]

6. The assumption $\varepsilon_s = \varepsilon_m$ has also some objections. It is not necessary that the diffusion of particles is equal to that of momentum. Measurements by Coleman (1970) show indeed that ε_s-values derived from concentration profiles give some differences with values of ε_s obtained from:

   $$\varepsilon_s = \varepsilon_m = \kappa U^* z(1 - z/h).$$

   It is a reasonable assumption, however. Differences between ε_s and ε_m are generally put in κ which is often used as a closing factor. If $U(z)$ and $C(z)$ are known, integration will give the suspended load. The integration cannot be performed analytically. Graphs are presented by Einstein (see Graf 1971, p. 189-195).

13.3 Total bed-material load

The total bed-material load of a stream can be determined by adding the bed-load and the suspended load. This is done in the Einstein (1950) procedure. This procedure was modified by Colby (1955, 1961). Also Toffaletti (1969) gives a procedure which is especially adapted for computer programming.

Besides these "adding" procedures several direct empirical relations are proposed in literature:

1. Shinohara and Tsubaki (1959) gave an empirical relation:
   $\Phi = 25(\psi')^{1.3}\ (\psi' - 0.038)$ (see figure 13.1).
   The corresponding ripple factor $\mu = (C/C')$.
2. Garde and Albertson (1961) gave a graphical relation of $\Phi/\sqrt{\psi}$ with $\bar{U}/U^*$ as the third variable. The resulting $\Phi - \psi$ relation is almost identical with Shinohara (figure 13.1).
3. Colby (1964) has given a graphical relation between total load, mean velocity $\bar{U}$, flow depth and grain-size with correction factors for temperature and silt content (see figures 13.4 and 13.5).
4. Engelund and Hansen (1967) gave an empirical relation of the form:
   $\Phi = 0.1 f^{-1} \psi^{2.5}$ with $f = \tau/(\frac{1}{2}\rho\bar{U}^2) = 2g/C^2$
   The formula is based on measurements with $D_{50} < 1$ mm and gave good results in comparison with sediment transport measurements in rivers. At all values of ψ, the sediment rate increases with the fifth power of the velocity.

5. Ackers and White (1973) define the parameters:

$$F_{gr} = \frac{U^{*n} \cdot (U^{*'})^{1-n}}{(\Delta g D)^{\frac{1}{2}}} \qquad U^{*'} = \frac{\bar{U}}{5.64 \log(10\ h/D)}$$

$$D_{gr} = D \cdot \left(\frac{\Delta g}{\nu^2}\right)^{1/3} \qquad \text{(dimensionless grain size)}$$

$$G_{gr} = \frac{S}{\bar{U}D} \cdot \left(\frac{U^*}{\bar{U}}\right)^n \qquad \text{(transport parameters)}$$

The relation between the transport parameter G_{gr} and the sediment mobility number F_{gr} is given as:

$$G_{gr} = C\left(\frac{F_{gr}}{A} - 1\right)^m$$

in which C, A, m and n are functions of the dimensionless grain size D_{gr} (see figure 13.8).

For coarse materials ($D_{gr} > 60$) $n = 0$ and $U^* = U^{*'}$ sothat the parameters F_{gr} and G_{gr} are reduced to a more simple form.

For a modest range of particle sizes ($D_{84}/D_{16} < 5$) Ackers and White suggest to take $D = D_{35}$. For a wider gradation a fraction by fraction computation is suggested, using a corrected value for A:

$$A' = A \cdot \left(\frac{Di}{D_{50}}\right)^{-0.2} \qquad \text{in which}$$

Di = average size of the fraction (Ackers and White, 1980)

NOTE

It must be noted that due to the strong variation of sediment transport with velocity, predictions of total sediment load will not be very accurate. Differences of a factor 10 between various formulas or between computations and measurements are no exception (see figure 13.6 and 13.7).

13.4 Comparison of relations

White, Milli and Crabbe (1975) have made a comparison of 8 of the most widely used transport relations (a.o. Meyer-Peter Müller, Einstein, Engelund and Hansen and Ackers and White) with 840 flume data and 260 field experiments in natural water courses. If the percentage of all data with a ratio R of calculated to observed transport in the range

$\frac{1}{2} < R < 2$ is taken then the following result is obtained:

Ackers and White	68%
Engelund and Hansen	63%
Einstein	46%

It is not surprising that Ackers and White give relatively good results in view of the large number of tuning parameters (C, A, m and n are all functions of grain size). It is surprising however that the far more simple formula of Engelund and Hansen gives such a good result.

Application of formulas remains a matter of experience. For each situation a comparison with field measurements and an adjustment of the formulas remains necessary for reliable results.

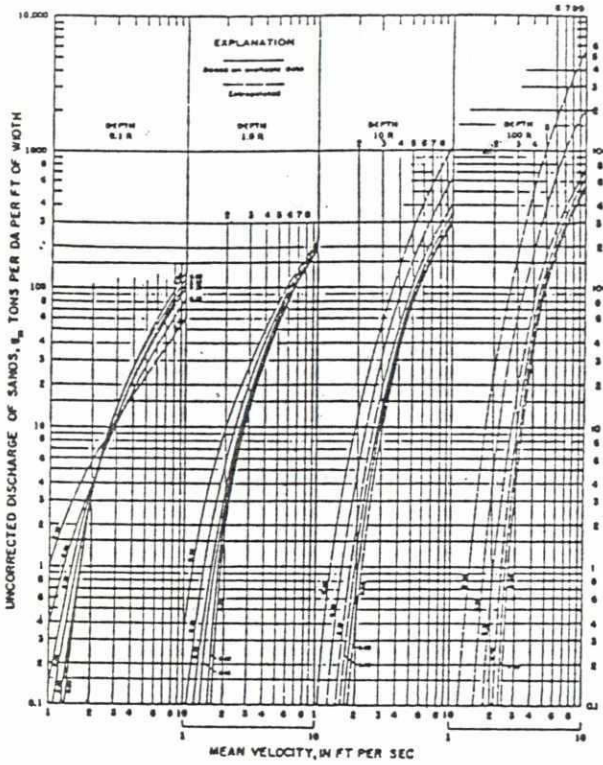

FIG. 13.4 —COLBY'S (2-H.14) RELATIONSHIP FOR DISCHARGE OF SANDS IN TERMS OF MEAN VELOCITY FOR 6 MEDIAN SIZES OF BED SANDS, 4 DEPTHS OF FLOW, AND WATER TEMPERATURE OF 60° F

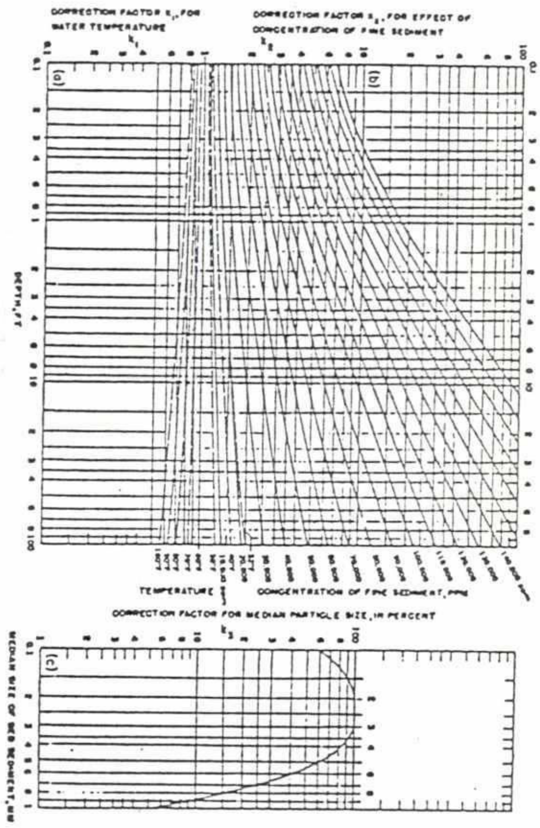

FIG. 13.5 -COLBY'S (2-H.14) CORRECTION FACTORS FOR EFFECT OF WATER TEMPERATURE, CONCENTRATION OF FINE SEDIMENT AND SEDIMENT SIZE TO BE APPLIED TO UNCORRECTED DISCHARGE OF SAND GIVEN BY FIG. 2-H.10

Colby correction factor $k = [1 + (k_1 k_2 - 1).0.01\ k_3]$

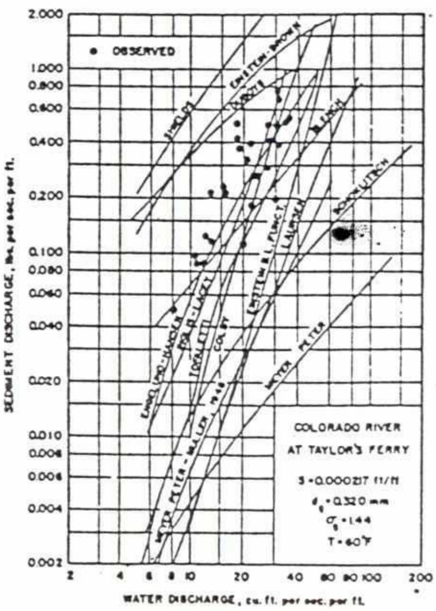

FIG. 13.6 .—SEDIMENT DISCHARGE AS FUNCTION OF WATER DISCHARGE FOR COLORADO RIVER AT TAYLOR'S FERRY OBTAINED FROM OBSERVATIONS AND CALCULATIONS BY SEVERAL FORMULAS

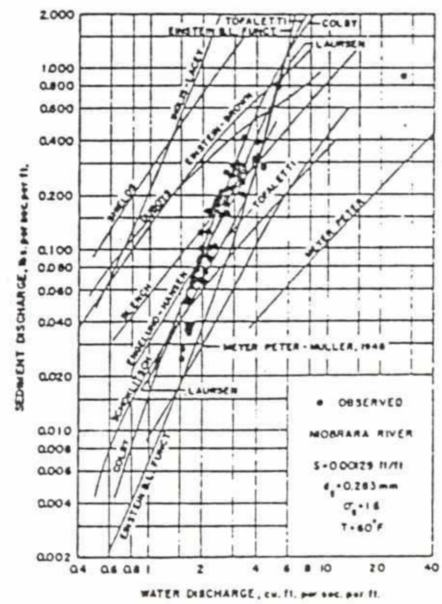

FIG. 13.7 —SEDIMENT DISCHARGE AS FUNCTION OF WATER DISCHARGE FOR NIOBRARA RIVER NEAR CODY, NEB. OBTAINED FROM OBSERVATIONS AND CALCULATIONS BY SEVERAL FORMULAS

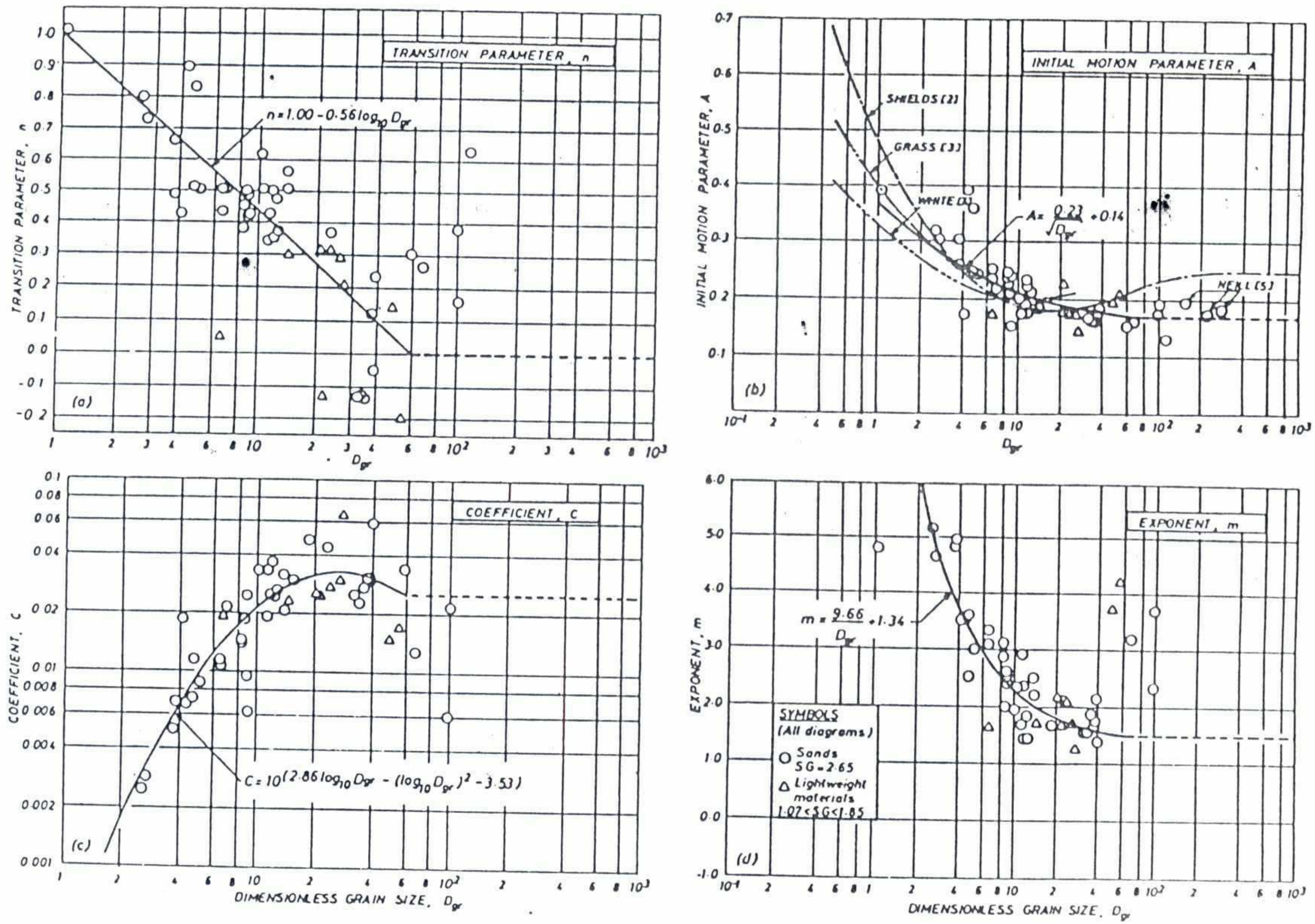

FIG. 13.8

Coefficients in General Sediment Tra port Function (Ackers and White)

13.4 Literature

M.P. Duboys, 1879 — Le Rhone et les Rivières a lit affouillable. Mem. Doc. Ann. Ponts et Chaussées, ser. 5, vol. 18

A.A. Kalinske, 1947 — Movement of sediment as bed-load in rivers. Trans. Am. Geoph. Un., 28 (4), p. 615 - 620

E. Meyer-Peter, R. Müller, 1948 — Formulas for bed-load transport. Int. Ass. Hydr. Res. 2nd Meeting, Stockholm

H.A. Einstein, 1950 — The bed-load function for sediment transportation in open channel flows. U.S. Dept. of Agric. Soil Cons. Service, TB no. 1026

J.N. Hunt, 1954 — The turbulent transport of suspended sediments in open channels. Proc. Roy. Soc. London 224 A, p. 322-335

H.A. Einstein, Ning Chien, 1954 — Second approximation to the solution of the suspended load theory. Unif. of Calif. Inst. Eng. Res., Publ. no. 3

H.A. Einstein, Ning Chien, 1955 — Effects of heavy sediment concentration near the bed on velocity and sediment distribution. Unif. Calif. Inst. Eng. Res., Publ. no. 8

B.R. Colby, C.H. Hembree, 1955 — Computations of total sediment discharge. U.S. Geol. Survey. Water Supply Paper 1357.

K. Shinohara, T. Tsubaki, 1959 — On the characteristics of sand waves formed upon the beds of the open channels and rivers. Rep. Res. Inst. Appl. Mech., Kuyushu Univ. (25), p. 15-45

B.R. Colby, D.W. Hubbell, 1961 — Simplified method for computing total sediment discharge with the modified Einstein procedure. U.S. Geol. Survey Water Supply paper 1593.

R.J. Garde, M.L. Albertson, 1961 — Bed-load transportation in alluvial channels. La Houille Blanche 16 (3), p. 274-286

ASCE, 1963 — Suspension of sediment. Proc. ASCE 89 HY5, p. p. 45-76.

B.R. Colby, 1964 — Practical computations of bed-material discharge. Proc. ASCE 90 HY2, p. 217.

77

F. Engelund, 1967 E. Hansen	A monograph on sediment transport. Teknisk Forlag Copenhagen.
F.B. Toffaletti, 1969	Definitive computations on sand discharge in rivers. Proc. ASCE <u>95</u> HY1, p. 225-248
N.L. Coleman, 1970	Flume studies of the sediment transfer coefficient. Water Res. R <u>6</u> (3), p. 801-809.
W.H.Graf, 1971	Hydraulics of sediment transport. McGraw Hill, New York.
ASCE, 1971	Fundamentals of sediment transportation. Proc. ASCE <u>97</u>, HY12, p. 1979-2023.
ASCE, 1971	Sediment discharge formulas. Proc. ASCE, <u>97</u> HY4, p. 523-567.
A.T. Ippen, 1971	A new look at sedimentation in turbulent streams. Journ. of the Boston Soc. of Civ. Eng. <u>58</u> (3), p. 131-163.
P. Ackers, 1973 W.R. White	Sediment transport: New approach and analysis. Proc. ASCE <u>99</u> HY11, p. 2041-2060
W.R. White, 1975, H. Milli, A.D. Crabbe	Sediment transport theories: a review. Proc. Inst. Civ. Eng. (London), part 2, June, <u>59</u>, p. 265 - 292.
P. Ackers, 1980, W.R. White.	Bed-material transport: A theory for total load and its verification. Int. Symp. on River Sedimentation, Beijing, March. Paper B 10.

13.5 Problems

13.1 Given: A wide river with $h = 3$ m, $\bar{U} = 1.2$ m/s, $I = 1/6000$
$T = 20^0$ C $D_m = 2$ mm $D_{90} = 3$ mm.
Question: Compute the bed load with the Meyer-Peter-Müller method.

13.2 Given: A wide river with depth $h = 2$ m, width $B = 80$ m, $\bar{U} = 1.4$ m/s,
$I = 8.10^{-4}$, $D_m = 0.6$ mm, $D_{90} = 1.5$ mm, $\varepsilon = 0.4$.
Question: Compute the annual bulk transport using the M.P.M. method.

13.3 Given: A wide river has the following characteristics:
depth $h = 3.2$ m
Slope $I = 0.5.10^{-4}$
bed mat.: $D_m = 0.5$ mm $D_{90} = 1$ mm $D_{50} = 0.4$ mm
Temp.: $T = 20^0$ C
Questions:
1) Determine the critical shear stress τ_{cr} of the bed material and the bottom shear stress τ_o. Is there transport?
2) Which type of bottom configuration is present according to Simons-Liu (Fig.12.3)? Use D_m to obtain the fall velocity.
3) If the mean velocity $\bar{U} = 0.66$ m/s, what is the bed roughness k_s?
Is the bed hydraulically smooth or rough?
4) Compute the ripple factor μ according to M.P.M.
5) Compute $\tau' = \mu\tau_o$ and the bed load/m' according to M.P.M.
6) Will there be transport in suspension?

13.4 Given: In a wide river a trench is made for a pipe line crossing. The depth of the trench is 3 m. Because it takes some time to lay the pipe and the river transports bed load, some storage has to be provided.

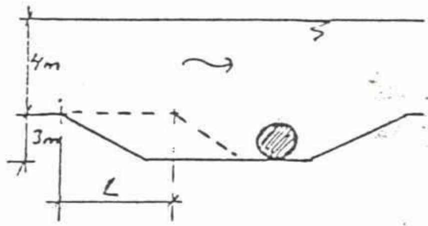

River data: $\bar{U} = 1.2$ m/s $h = 4$ m $C = 45$ m$^{\frac{1}{2}}$/s
$D_m = 1$ mm $D_{90} = 2$ mm $\varepsilon = 0.4$.
The relation of M.P.M. is valid.
Question: How large should L be to provide sufficient storage for 2 days?

13.5 Given: A wide open channel, $h = 3$ m, $\bar{U} = 1.2$ m/s, $I = 10^{-4}$.
Transported material $D = 150$ μm (uniform)
The concentration at $z = 0.5$ m is 250 mg/l.
Question: Compute the concentration at $z = 0.25$ m and $z = 2$ m.

13.6 Given: A wide river with $h = 2$ m $I = 1.5.10^{-4}$ $\bar{U} = 0.9$ m/s
sediment uniform $D = 0.2$ mm $\varepsilon = 0.4$.
Question: What is the bulk transport/m'.day using the Engelund-Hansen method.

13.7 Same question for:

$h = 3$ m $I = 10^{-4}$ $\bar{U} = 0.8$ m/s $D = 0.15$ mm (uniform)

13.8 Use the data of 13.6 and compute the total-load with the method of Ackers-White (as bulk load/m.day).

13.9 Use the data of 6.1 and the method of Ackers-White to compute the transport. $D_{35} = 1.5$ mm.

13.10 Given: Sediment size $D = 150$ µm (uniform) and shear velocity $U^* = 0.05$ m/s.
Question: Compute fall velocity (Fig.10.4), critical shear stress (Fig.11.2) bedform according to Simons (Fig.12.3) and the degree of suspension (table page 13.6).

13.11 Same question for $D = 2$ mm. and $U^* = 0.05$ m/s.

GOVERNMENT OF THE PEOPLE'S REPUBLIC OF BANGLADESH
JAMUNA MULTIPURPOSE BRIDGE AUTHORITY

WORLD BANK
UNITED NATIONS DEVELOPMENT PROGRAMME

Jamuna Bridge Appraisal Study

PHASE I: CHARACTERISTICS AND CONFIGURATION

FINAL REPORT

February 1987

APPENDIX C – HYDROLOGY, MORPHOLOGY AND RIVER ENGINEERING

RENDEL PALMER & TRITTON
NEDECO
BANGLADESH CONSULTANTS LTD

APPENDIX C.3
RIVER MORPHOLOGY

From: RPT/Nedeco/BCL (1987), Jamuna Bridge Appraisal Study, Phase I, Final Report, Appendix C: Hydrology, Morphology and River Engineering

APPENDIX C.3 MORPHOLOGICAL FEATURES OF THE JAMUNA AND PADMA RIVERS

CONTENTS

72

LIST OF TABLES

LIST OF FIGURES

C.3.1 INTRODUCTION

This Appendix deals with the morphological features of the Jamuna and Padma rivers as relevant for the present study.

The morphology of the river is important for a number of reasons. Migration of the main channels or channel avulsions may jeopardise the functioning of the bridge, meanders encroaching on the bridge approaches may cause a serious threat, and the safety of the bridge may be endangered by scour of the bed level underneath the bridge. Migration of the main channels and associated bank line changes are mainly dealt with in Appendix C.4; here the available morphological data is analysed to address the above indicated problems.

Because a number of corridors are considered between Bahadurabad along the Jamuna River and Mawa along the Padma River, the emphasis is put on these stretches of the rivers. Whenever appropriate supplementary information is used of other river stretches, i.e. the Ganges River in Bangladesh and the Brahmaputra River in India.

The approach followed is to use existing data only. Th available time did not allow additional data to b collected in the field, apart from some hydrographi surveys (see sections C.3.2.6 and Appendix C.1).

The structure of this Appendix is as follows. A overview of the available data on planfor characteristics, bed and bank levels, bed material sediment transport and bedforms is given in sectio C.3.2. The results of the preliminary processing of part of the data is presented in section C.3.3, i which water depths, river and channel widths, slopes are discussed. In section C.3.4 a more detaile analysis of resistance to flow and sediment transpor of the Jamuna and Padma Rivers is presented, giving du attention to the essential role that bedforms play Section C.3.5 deals with planform characteristics while in section C.3.6 maximum (natural) scour depth in the river stretches of interest are discussed i more detail.

27

C.3.2.1 General

Data are available from various Government agencies and existing literature. The Consultants have collected original or processed data mainly from the following agencies:

- BWDB (Bangladesh Water Development Board)
- Survey of Bangladesh
- BIWTA (Bangladesh Inland Water Transport Authority)
- SPARRSO (Space Research and Remote Sensing Organisation).

Existing literature, including consultancy reports on the Jamuna and Padma River, is listed at the end of this Appendix. Data on the Ganges River used here mainly originate from NEDECO (1983). Data on the Bahmaputra River in India have been found in Goswami (1984).

The information and data collected by the Consultants do not pretend to be complete but are sufficiently representative. Preference was given to more recent information that might be more appropriate for studying present conditions.

C.3.2.2 Water levels and discharges

Water levels, discharges, rating curves and other relevant hydrological information was obtained from BWDB. For details, reference is made to Appendix C.2.

C.3.2.3 Planform Characteristics

Planform characteristics of the Jamuna and Padma were studied from maps, aerial photographs and satellite imageries. Satellite imageries are available for recent years and enable the study of gradual changes in the planform pattern.

The Consultants have obtained copies of the imageries covering the period 1972-1985 (see Table C-3.1). The stretch of the Jamuna River of interest to the present study is covered by the imagery 138-043, and the Padma River by imagery 137-044. The scale of most imageries is 1:1million and some were enlarged to approximately scale 1:250000.

C.3.2.4 Bed and Bank levels

Cross sections across the Jamuna and Padma rivers have been measured by BWDB during low water since 1966. The measurements extend over the whole cross section, including channels and chars. The locations of the cross sections are indicated in Figure C-3.1. In total, 19 cross sections across the Jamuna River and 8 across the Padma River are related to the river stretches of interest. Copies of the cross sections measured in the period 1977-1984 were obtained for the present study.

The BWDB cross section measurements have been carrie out during low flow conditions only. According t Coleman (1969), however, the channel depths ar 2
decreasing during receding discharges. Therefore th BWDB measurements may not be representative for floo conditions. In order to obtain bed level data durin flood stages the Consultants have studied discharg measurements covering the hydrological year 1985-86 fo two stations (Bahadurabad and Mawa). During thes discharge measurements, carried out throughout th year, a sounding of the bed level in the sampled cros section is also obtained, and the changes in the be level can be analysed.

Another constraint is that the BWDB soundings are a 2
intervals of several km. Consequently importan information, e.g. the largest scour depths, may not b identified. A more complete coverage of the deepe channels is carried out by BIWTA, who produce rive survey charts for navigation purposes. The surveys ar carried out with echosounding equipment and a Decc main chain positioning system. Survey charts ar normally plotted on scale 1:25000 or 1:50000 and lane are plotted at 250m intervals. Table C-3.2, shows th BIWTA soundings used in the present study. Only thre full coverages of the Jamuna River over the stretche of interest are available. More frequent soundings ar only available for the Aricha-Nagarbari area .

Bank level data have not been collected on a larg scale within the present project. A topographical ma was obtained from BWDB-Master Planning Organisation showing levels on a 4 km grid. The map provided onl approximate insight in bank levels, but is quite usefu for a general understanding of the flood plain area Levels of embankments along the Jamuna River wer obtained from consultancy reports.

C.3.2.5 Bed Material

Reports of the River Research Institute (RRI) are th main source of information on bed material of th Jamuna River. The information consists of:

- date of sampling;
- location of sample in the vertical;
- depth of sampling (and thus of local water depth);
- D_{35} and D_{65}

A sieve curve is available for most of the samples.

Apart from these RRI reports, limited data are given in consultancy reports, e.g. Nedeco (1969), JICA (1976), etc. This information partly overlaps with the RRI reports. Hardly any data are available on the Padma River.

.6 Resistance to Flow

Resistance to flow can only be determined indirectly from discharge measurements since no separate measurements are carried out. Resistance to flow data have been analysed by Engineering Consultants/ACE (1971) as far as the Padma River is concerned [see also Stevens and Simons (1973)]. More recent Jamuna data were analysed by Nazim (1985). In both cases, the overall slope between two gauges was used locally, which may have resulted in considerable errors.

.7 Sediment Transport

Sediment transport in the Jamuna River has been measured since 1967 (FAO, 1969). Measurements are carried out at weekly intervals during the flood season and on a 2-weekly basis during the other parts of the year. Sediment transport is usually measured on the day following a discharge measurement. Sediment transport is measured at Goalundo, Baruria and Mawa. The measurements are done with a Bankway concentration meter at 0.2 and 0.8 of the local depth. The samples are divided in the field into a sand fraction and a finer fraction containing silt and clay particles. This is done by using a technique which is essentially based on the difference in fall velocity of the particles. It is claimed that the threshold is about 0.050mm. The observed concentrations of the sand fractions are related to the mean concentration in a vertical according to the following formula:

$$C_{m} = 0.375\, C_{0.8h} + .0625\, C_{0.2h}$$

Sediment transport is measured in a number of verticals. The average concentration thus obtained is multiplied by discharge, yielding the local sediment transport.

For more details on the measuring procedure, reference is made to BWDB (1972). A critical review of the methodology is given in Engineering Consultants/ACE (1971). In JICA (1976), part of these sediment transport data have been analysed.

Data given in BWDB (1972) have been used in the study in particular. In addition, some more data were obtained from BWDB and included analysis. The measurements relate to suspend only. Bed load measurements have not yet been out in Bangladesh. However, from Coleman (196 information on bed load transport can be derived the dune-tracking method in rudimentary form.

C.3.2.8 Bedforms

Only limited information is available on dimensions in the Jamuna . For the Padma, no d all could be found. Coleman (1969) provides info on the Jamuna River. His measurements are also to flood conditions. Bristow (1986) carri measurements more recently, but his data seem limited to low flow conditions only.

Within the framework of the present study two soundings were made to collect additional bedfor (see Appendix C.1).

C.3.3 MAIN CHARACTERISTICS

C.3.3.1 Introduction

In this chapter an overview is given of the main characteristics of the Jamuna and Padma rivers. This is done on the basis of a preliminary analysis of the available data. In sections C.3.4, C.3.5 and C.3.6, some aspects are discussed in more detail.

C.3.3.2 Primary Data

(a) Discharges, Water Levels and Slopes

Table C-3.3 shows the results of the analysis of the discharge and water levels at a number of stations for the yearly average and the once per 100 year flood. More details are reported in Appendix C.2.. The water level slopes along the Jamuna and Padma River can be determined from plotting the water levels at the appropriate distances between the various stations. In Table C-3.4 the resulting slopes are presented. The slope of the Jamuna is about 7.10^{-5}, whereas the Padma slopes are less. The figures relate to the direct slope along a straight line along the river. The actual slope will be larger, due to the curvature of the channels, epecially during low flow conditions. Considering the sinuosity of the channels (see also section C.3.5), it is probable that the water level slope along the Jamuna River decreases in the downstream direction, although the figures in Table C-3.4 suggest the opposite.

(b) Planform Characteristics

The Jamuna River is a braiding stream with chars and deeper channels in between. The braiding character is most prominent in the upstream reaches, as observed on a number of satellite imageries taken during low flow conditions (see Figure C-3.31). The channel pattern changes frequently, but main channels are present over a period covering quite a number of years. This holds especially for the reach downstream of Sirajganj.

From the satellite imageries, the radii of curvature of a number of bends have also been determined. The radii in the Jamuna River seem to vary between 1.5km and more than 10km. There is a clear tendency for the wider channels to have larger radii. This is what is to be expected from experience from other rivers, assuming that the wider channels also carry more water during floods.

From the planforms drawn in Figure C-3.31 it may be concluded that the Padma River is almost straight, with alternate bars passing through the river alo banks, although there may also be a tenden meander. The flow is mostly limited to one channe present bends do not have radii of curvature less about 6 km, although locally the flow may b curved due to the presence of alternate bars. Thi possibly also explain the very pronounced bend p present at Mawa. More details on pl characteristics are given in section C.3.5.

(c) Cross Section Characteristics

Characteristics of the cross sections of the Jamu Padma rivers were analysed from the BWDB sour Some cross sections are shown on the Figures through C-3.8, corresponding to the various co considered in this study. The mean annual floo is also indicated, corresponding to the average flood of 65000m³/s for the Jamuna and 88000m Padma River. Most cross-sections can be charac as a flat sand bed with an elevation some metre the annual flood level in which deep channe carved. These deep channels are clearly comp several smaller ones. Typical bend profiles seem present both in the Jamuna River and in th River.

The following characteristics were determined by section and year:

- total river width, defined as the width betw edges of the deeper channels;
- the number of main channels;
- the combined width of the channels;
- the total wet area of the main channels belo mean annual flood level,
- the maximum depth.

The average depths were computed from the t area and the combined widths of the main channe values for the different parameters were de averaging the data of the available years. Some are presented in the Figures C-3.9 through C- the following observations can be made:

(i) The total width of the Jamuna River between 4 and 15 km. The width of the Pad also varies considerably, and a decreasi in downstream directions cannot be ascert

(ii) The combined width of the deep channels in the Jamuna River varies between 4 and 6 km. These values however, are slightly biased by the fact that a number of cross-sections are no longer perpendicular to the channel axis (due to the changing of channel locations and direction due to braiding), and so in general may be too large.

(iii) The local wet cross section area of the Jamuna River varies by cross section and year. The wet area has varied between 25000 and 60000 m². This large variation was also observed in JICA (1976) and may be partly ascribed to the inaccuracy in measuring the cross section width (not perpendicular to main current direction) and from variations in the water slope along the river. In the Padma River the variation in wet area is also considerable, ranging between 30000 and 65000m².The smaller value applies to Mawa, where the small wet area is balanced by the great depths.

(iv) The average depth of the main channels varies between about 5m in Bahadurabad, 8m at Nagarbari, and 11-13m at Goalundo and Mawa. The maximum depth is discussed in more detail in section C.3.6.

(d) Bed Material

Data on bed material of the Jamuna River are available in a number of RRI reports. The Consultants have collected all available data and a preliminary review resulted in the following conclusions:

- there is only a small variation in grain size in one sample

- the variations in average grain size of the bed material are appreciable for various dates and depths.

Contrary to JICA (1976), the Consultants believe that the bed material size in the Jamuna does not vary in time. Vertical sorting is thought to be the major cause of differences in size. It may be concluded from Figure C-3.12 that during low flow conditions the more elevated parts of the river bed are not sampled. Because the bed material size decreases with bed level, JICA (1976) concluded that there is a seasonal fluctuation in bed material size.

To arrive at a fair estimate of the bed material si and its gradation, the Consultants have analysed D and D_{65} - values by stations and by year. Consideri the large variation in D_m (see Figure C-3.12), t standard deviation can be considered as an estimate the gradation of the bed material. The results a listed in Table C-3.5. The average bed material si were also computed and are presented in Figure C-3.1 together with the standard deviations and t approximate gradations. The following results obtained for the Jamuna River:

Station	D_{50}	(mm)
Chilmari	0.235	1.3
Bahadurabad	0.215	1.3
Sirajganj	0.190	1.3
Nagarbari	0.165	1.3

Hardly any information is available on the bed materi of the Padma River. The few samples of sieve curv presented in Nedeco(1969) show a wide scatter, but t average particle diameter is in the order of 0.13 while probably the geometric standard deviation slightly larger than for the Jamuna River. This also plausible because the Ganges bed material appe to be slightly finer than the Jamuna bed material.

C.3.3.3 C

In the bed samples of both the Jamuna and the Pad very fine sand (down to 0.0120 mm) was found. T would imply that the distinction between wash load bed material load would be slightly different from assumptions made during the analysis of the sedim transport (see section C.3.2.7).

(e) Resistance to flow

Resistance to flow data of the Jamuna River have b analysed by Nazim (1985) and indicate generally values. There are indications that during floo washed out dunes and possibly even flat bed conditi may occur. From the data it may also be concluded t there is a considerable lagging behind of resistance to flow.

Resistance to flow data for the Padma River are gi in Engineering Consultants/ACE (1971) and conditions seem to be comparable to the Jamuna Riv Flat bed conditions may also occur here during flood

For a more extensive analysis of data on resistance flow, reference is made to sections C.3.4.3 C.3.4.5.

(f) Sediment Transport

Measured monthly sediment transport rates in the Jamuna River vary between less than 1million tons/month(low flow) and more than 250million tons/month(floods). Concentrations of over 4000ppm have been observed, although the average sediment content is much lower. The average annual suspended sediment transport (period 1957-1975) is in the order of 600 million tons. Bed load may be considerable. Coleman (1971) estimates that the bed load may be up to 50 per cent of the suspended transport load. According to JICA (1976) the Engelund-Hansen formula provide a fair estimate of bed material transport, implying that the sediment transport would vary with the velocity to the fifth power. Goswami (1984) estimates the annual sediment transport in the Brahmaputra river to be about 400 million m^3, which corresponds well with the IECO(1980) figures - 600 million ton, when it is assumed that $1m^3$ sediment (pores included) corresponds to about 1.6 tons.

IECO (1980) figures for the Padma River yield average annual suspended sediment load (1967-1974) of about 660 million tons.

For more details on sediment transport rates reference is made to sections C.3.4.4 and C.3.4.5.

C.3.3.3 Characteristic Parameters

The preliminary analyses of the various available data on the morphological phenomena of the Jamuna and the Padma rivers can be described with characteristic parameters.

For an evaluation of the planform characteristics of the two rivers, Leopold, Wolman and Miller (1967) use a graph (see Figure C-3.14.) showing the relations between the channel slope and the discharge for various rivers. As can be seen from the figure, braiding occurs when

$$i_b > 1.16 \times 10^{-2} \times Q^{-0.44}$$

In the figure the Jamuna and Padma data have also been plotted. It appears that the Jamuna River plots are approximately on the dividing line, while the Padma river plots are below it. The implication may be that the Jamuna River is on a transition between braiding and meandering. However, small changes in river characteristics may cause an appreciable change in planform characteristics.

With the data given in section C.3.3.2 some insig into sediment transport processes in the Jamuna a 3.4
Padma River can also be obtained using the Shiel
parameter and the suspended load parameter, defined a 3.4.1

Shields parameter: $hi/\Delta.D_{50}$

Suspended load parameter: u_*/w

Where: h = water depth (m),
i = slope (-)
Δ = relative specidic density, = $(\rho_s/\rho_w)1$
ρ_s = density of sediment,
ρ_w = specific density of water,
D_{50} = size particle (m),
u_* = shear velocity (m/s), = $(ghi)^{0.5}$
g = acceleration of gravity (m/s^2),
w = fall velocity (m/s).

In Figure C-3.15 the two characteristic parameters given for the two rivers. The Shields parameters $hi/\Delta D_{50}$ varies between about 1 in the upstream reac of Jamuna River to 3 in the downstream sections of Padma. The figures relate to average flood conditio As a value of 0.03 to 0.05 for the Shields parame corresponds to initiations of movement, it can concluded that bed material transport will be qu large during average flood conditions. Even during flow conditions sediment transport will still present.

The suspended load parameter u_*/w indicates to w extent suspended load is a relatively important mod transport . For u_*/w values less than about 3.4.2
suspended load is negligible; only for u_*/w in exc of about 2, does suspended load become dominant (Rijn, 1984). For the Jamuna and Padma River, parameter u_*/w varies between 2 and 4, implying suspended transport becomes increasingly important the downstream direction. Especially in the u reaches of the Jamuna River, bed load and suspe load are approximately equally important (see section C.3.4.4 and C.3.4.5).

8M

BEDFORMS, RESISTANCE TO FLOW AND SEDIMENT TRANSPORT

Introduction

Bedforms, resistance to flow and sediment transport are closely related. Bedforms at the interface between river bed and water increase the resistance to flow considerably. They also have a considerable effect on sediment transport rates and consequently on the celerity of morphological processes like degradation and bank erosion. Bedforms are also of direct importance for bridge design, as the trough depth of bedforms has to be added to the maximum scour depth.

Only limited information is available on bedforms in the Jamuna River and there is essentially none for the Padma River. More information is available on resistance to scour and sediment transport in the two rivers, but processing of the available data has been done only on a limited scale. It will be necessary, especially during the actual design of the bridge and the river training works, to have an overall understanding of these processes. A first outline of such an overall understanding is presented here. More data, in particular on bedform dimensions in the Jamuna and Padma Rivers, are urgently needed to improve the understanding, which may eventually lead to better prediction methods for the evaluation of the effects and risks of bridge construction.

In the sections C.3.4.2 through C.3.4.4 available data on bedforms, resistance to flow and sediment transport are discussed in some detail. In section C.3.4.5 an integrated discussion of these three features is given.

2 Bedforms

Data on bedforms in the Jamuna River were first provided by Coleman (1969), who distinguished four different kinds of bedforms:

- ripples : not relevant for the present study;
- mega ripples: typical height 1.0 m, typical velocity 120 m/day;
- dunes: typical height 5 m, typical celerity 60 m/day;
- Sandwaves: Typical height 10 m, typical celerity 200 m/day.

More recently Bristow (1985) also presented some data on bedform heights, but these are of limited relevance because they were collected during low flow conditions only.

Within the framework of the present study data also collected by the Consultants on the Jamuna near the E-W Interconnector (see Figure C-3.16) addition, thalweg soundings were made between A and Sirajganj. Data was processed and plotted ag average local water depth to obtain average be heights (see Figure C-3.17); the predicted be heights using various prediction methods have also indicated. The observed bedform heights are reaso well predicted by the method of Yalin (1964) or (1960), but the predictions of van Rijn (1984) consistently too low. As a first estimate o bedform height, a value of 0.20 times the water de can be used, with a standard deviation of 0.05xh.

The obtained bed level data were also analysed more detailed way. The probability distributions o dune heights were first determined for some soun carried out near the E-W Interconnector; the re are given in Figure C-3.18. It follows that patterns become more irregular when the average height increases. This may, however, at least pa be due to the difficulties in determining the heig relatively small bedforms. Even more interesting i variation in relative bed level height (see F C-3.19). It appears that the lowest relative bed heights correspond roughly with the average be height.

C.3.4.3 Resistance to Flow

Primary data presented by Nazim (1985) on the hyd conditions at Bahadurabad, Sirajganj and Naga were processed within the present study. Two para were computed:

(i) Chezy coefficient : $C = Q/B.(h)^{3/2}$.(

(ii) Darcey-Weisbach coefficient :

$f = (8.g.B^2.C^2.h^3.i$

The results for the above three stations are giv Figures C-3.20 to - 3.22. From the analysis data it follows that for low flow conditions C is 40 to $50m^{1/2}/s$. For Nagarbari station (Figure C some extremely low figures for the Chezy coeff were found. This is probably due to the fact tha overall parameters (e.g. slope) were combined local data (e.g. water velocity). The most imp aspect, however, is the very considerable reducti resistance to flow which occurs during conditions. The Chezy coefficient then reaches between 80 and $100m^{1/2}/s$. This holds for all stations.

Data on resistance to flow were analysed by ECI/ACE (1971) and the results are summarised by Stevens and Simons (1973) (see Figure C-3.23). They also observe considerable reductions of resistance to flow during floods.

Data for the Jamuna River resistance to flow were compared with the predictor of Engelund-Hansen (1967), essentially providing a relationship between θ and θ', where θ is the Shields parameter $h'i/\Delta D$ (see Jansen, 1979). The parameter h', (the water depth related to the skin roughness) is derived from the following equation:

$$u/g\ h'i = 9.45\ (h'/k)^{1/8}$$

For the equivalent roughness parameter k, a value of 2.5 D_{50} was taken here. Because of the power 1/8 the choice of expression to be used for k is less important. Engelund/Hansen (1970) found that for values of about one (see Figure C-3.24a), implying that the contribution of the form roughness vanishes. This is usually explained by the occurrence of washed-out dunes or transition to flat-bed conditions (see Figure C-3.24b). For lower values of θ the approximate relationship:

$$\theta' = 0.06 + 0.4.\theta^2$$

holds for some laboratory flumes.

In Figures C-3.25 through C-3.27, the Jamuna data are plotted in the resistance graph of Engelund-Hansen (1967). It may be concluded that there are deviations from the Engelund/Hansen graph. In particular the form roughness has a larger contribution during low flows than predicted, especially at Sirajganj. This may, however, also be due to the combination of local and overall data. It can be also concluded from this graph that for higher values of θ, $\theta' \cong \theta$, which corresponds to vanishing form roughness (see also section C.3.4.5).

82

C.3.4.4 Sediment Transport

The sediment transport can be classified according origin and mechanism as follows:

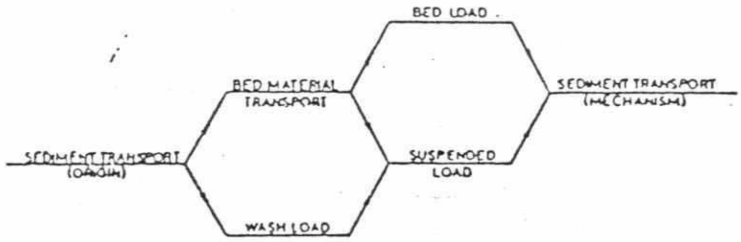

Bed load (transport) is defined as the transport of material by rolling and sliding. In water, saltat can be neglected (Kalinske, 1942) due to the sm difference in density between water and sedime Suspended load (transport) is defined as the transp of sediment which is suspended in the fluid for s time.

According to the mechanism of suspension the suspen sediment may belong to the bed material load and wash load. Wash load is defined as the transport material finer than the bed material. It has relation to the transporting capacity of the stre the rate is determined by the amount which bec available by erosion in the catchment area upstr Usually a diameter D with 0.050 < D <0.070mm is t as a practical distinction between wash load and material load. For most rivers, sediment of this (and smaller) is uniformly distributed over vertical. The distinction between bed load suspended load cannot be defined sharply. Both grain size and the flow conditions characterise distinction. Usually $u_*/w=2$ is used as a pract limit for the beginning of suspension (see Jans 1979, van Rijn,1984).

In the Jamuna and Padma rivers suspended load measured regularly. In the analysis a distinctio made between the coarse and the fine parts of transported mixture, whereby a separating metho used which is not completely clear (ECI/ACE, 1971) which is probably yielding results such that the co part corresponds to the suspended bed material and

90

fine part to the wash load. The IECO (1980) figures (see subsection C.3.3.2) relate to the total suspended load.

Results of sediment transport measurements in the Jamuna and the Padma Rivers, at Bahadurabad and at Mawa, were obtained by the Consultants. The sediment transport of the coarse fractions (bed material load) is plotted as a function of the discharge (see Figure C-3.28 and 3.29). A wide scatter is found, which is normal for this type of relationship when sediment transport and discharge are plotted on a linear scale. The scatter may even be larger than shown on the graph because the rivers are near transition during floods (see section C.3.4.3), which may cause a large variation in the contribution of the form roughness to the total roughness.

No bed load measurements have been carried out in either river until now. Considering the value of u_*/w (see section C.3.3.3), it can be assumed that bed load constitutes a considerable part of the total bed material load. An estimate of the bed load transport in the Jamuna River can be obtained from the bedform heights and celerities as given by Coleman (1969). This is done in Table C-3.6, for Coleman's megaripples, dunes and sandwaves, using the so-called dune-tracking method (Jansen, 1979), from which it follows that:

$$S_{bed\ load} = 0.6\ Hxc$$

Where: $S_{bed\ load}$ = bed load transport ($m^3/m/day$)

H = bedform height

c = celerity of bedforms (m/day).

From Table C-3.6 it can be concluded that the estimate obtained for bed load varies considerably, depending on the type of bedform considered. It may be reasoned, however, that the resulting figures should be approximately similar, as the various bedforms are superimposed. This casts some doubts on the figures given by Coleman (1969). Assuming a local width of the deeper channels of about 5km, the daily bed load transport is estimated to be 0.35 mn m^3/day for sand waves. From the dune dimensions, a total of 0.9 mn m^3/day is found, comparable to the coarse suspended transport during flood (see Figure C-3.28). In interpreting the echograms it should be realised that the various bedforms do not extend over the full width of the channels. The above analyses are therefore only approximate.

A comparison was also made between measured predicted sediment loads in the Jamuna River (Figure C-3.30). Three total bed material l predictors have been used, but in the figure only suspended load is used for the comparison. It foll that the measured coarse suspended load is in excess the predicted rates by a factor varying between 1.5 van Rijn (1984), 3 for Ackers and White (1973) and m than 5 for Engelund/Hansen (1967). The differen would have been even more if the bed load had also b taken into account. A similar comparison was made the Mawa transport data, resulting in simi conclusions . Thus, for the time being the van R (1984) sediment transport predictor is preferable the Jamuna and Padma rivers, possibly with a sligh adapted coefficient to improve the agreement.

C.3.4.5 Discussion

The most important aspect of bedform characteristic their height during extreme flood events. According Coleman (1969), sand waves with a height of up to 1 may occur. The data on resistance to flow, howe suggest that washed out dunes may occur during flo which would suggest that a considerable reductio bedform height may occur:

(i) If Coleman's suggestion is correct, a bed height/water depth ratio of about 0.5 would o in the Jamuna river. This value is far in ex of the values presented in Figure C-3 Furthermore, the Consultants have never obse such high values in large rivers. It is there believed that Coleman has erroneously interpr bars which are part of the braiding network sand waves. The small waterdepth shown on crest of the feature, as presented in one of echograms, supports this suggestion. Thu smaller bedform height than the 15m used in Inception Report may be appropriate.

(ii) The Consultants have recently carried out a s into bedform dimensions during transitions. preliminary results are given in Klaassen et (1986). During experiments it was observed bedform heights remain essentially the same flood conditions, and only the lengths incr significantly. This would indeed cause substantial reduction in resistance to flow, the lowest bed level would in principle re the same. Until now no field data have been f to suggest that reduction of bedform he occurs during floods.

(iii) For the time being it is proposed to use (0.20 +/-0.05) times the water depth as average bedform height during extreme events. It is strongly advised that bedform dimensions and related aspects be studied in considerably more detail via field measurements during the next phase of the project.

DV

C.3.5 PLANFORM CHARACTERISTICS

C.3.5.1 Introduction

In this section planform characteristics of the Jamu[na] and Padma Rivers are discussed. The planfo[rm] characteristics could not be comprehensive, but [a] number of subjects were studied in some detail, i.e.:

- bank line changes;
- changes in planform over time;
- channel curvature.

Bank line changes are treated in detail in Append[ix] C.4. Planform changes and channel radii are discuss[ed] here in the sections C.3.5.2 and C.3.5.3 respectively.

C.3.5.2 Planform changes

Satellite imageries are available from 1972, allow[ing] the study of changes in planform of the Jamuna [and] Padma Rivers. Some of the planforms as observed fr[om] these imageries are presented in Figure C-3.31. [The] imageries were taken during the low flow seasons.

The momentary discharges and thus the stages w[ere] different for the various imageries, as were the flo[ods] during the various years. This also affected the wi[dth] of the channels. Therefore, it may not be conclud[ed] from a mutual comparison of imageries, that [the] importance of a particular channel increased beca[use] its width is larger than on the imagery of the previ[ous] years. Only from a comparison of different channels [on] one imagery can such a conclusion be drawn. A number [of] observations can be made:

(i) Although the relative importance of channels [may] vary over time, the overall planform, includ[ing] the bank lines (see Appendix C.4) and the patt[ern] of island and channels, has remained fai[rly] stable over the years 1973-1985.

(ii) The dynamics of a braiding channels pattern [is] nicely illustrated by the development over t[ime] of a river reach downstream of Sirajganj. [In] Figure C-3.32, the planform of this reach [is] plotted on a slightly larger scale for [...] years. It can be observed that the main chan[nel] changed its position over the period 1978-1[...] due to bank erosion in the outer bend, t[hus] increasing its length. In 1981 another chan[nel] was developing that was essentially a short[cut] of the original main channel. By 1984 [the] original main channel had become a minor chan[nel] only, and the short-cut had developed into the major channel. In the meantime a shift in the upper part of this new channel has already taken place in a similar way as described above.

Similar observations were made by Bristow (1985), who states (see Figure C-3.33) "The broad picture is one of gradual changes in position in the main channels by lateral migration with very few avulsions. It is also apparent that there is a very high degree of reworking of previous deposits and quite rapid second order channel migration (over 1km per annum) within the braided belt, while the overall first order migration of the braid belt is only 76m per annum".

To some extent this picture seems opposite to the observations of Coleman, who observed sudden shifts of the thalweg as large as 600-900 m.

Coleman, however, has considered thalweg locations only, and therefore these large changes may be explained by relatively minor scour in one channel and depositions in another. For the time being, the Consultants hold the opinion that future changes of the braiding channel can be predicted to some extent over a period of say one year. This has an important bearing on the planning and execution of maintenance of river works.

3.5.3 Channel Curvature

The curvature of the various channels can be determined from the satellite imageries in an approximate way. The curvature of channels is of importance for the design of the river works as it determines the scour in the outer bends, and affects the length of the guide bunds and the intermediate distances of groynes and their toe level. Two imageries of the Jamuna and Padma Rivers were analysed and the curvature of the channels which could be distinguished was plotted against their chainage (see Figure C-3.34). A number of observations can be made:

(i) Downstream of Sirajganj the radii of the channels in the Jamuna river is larger than upstream.

(ii) The Padma River is characterised by less pronounced curves than the Jamuna River.

(iii) The radii of the Jamuna channels, in particular upstream of Sirajganj, were smaller in 1977 than in 1984. In 1976 the flood was larger than in 1983, although both were above the average.

The width of the channels as observed from the satellite imageries is plotted against the channel curvature in Figure C-3.35, together with the relationship presented by Leopold, Wolman and Miller (1967). Although there is a considerable scatter, it may be concluded that the curvature increases with the channel width. The following approximate relationship was found:

$$R = 0.46\ B^{1.3}$$

Where R = channel curvature (m)
B = channel width (m).

Apparently the observed radii are consistently large than would result from Leopold et. al. (1967). Th width of the channels was determined from satellit imageries taken during the low flow season and ma therefore be biased. This bias does not, however explain the considerable difference. A possibl explanation may be the limited role played b vegetation in braided rivers, facilitating the cuttin off of the main channels.

C.3.6 MAXIMUM NATURAL DEPTHS

C.3.6.1 Introduction

In this section maximum natural depths occuring in the Jamuna and Padma Rivers are considered. These natural depths are used as a basis for the estimation of the maximum depths that may occur if a bridge is constructed over the Jamuna or Padma River (see Appendix C.8). Essentially two sources of information have been used, i.e. BWDB cross section soundings and BIWTA sounding charts (see section C.3.2.3). In section C.3.6.2 this material is analysed.

As mentioned in section C.3.2.3, the main disadvantage of the available material is that it has been collected during moderate to low flows only. Some attempts were made to extrapolate to flood conditions. In section C.3.6.3 this is described in some detail, together with some experimental data on changes in thalweg depths in cross sections, where BWDB is measuring the discharges regularly.

C.3.6.2 Maximum Observed Depths

In section C.3.3.2(c) some results of BWDB soundings were presented. Maximum observed depths are shown in Figure C-3.9. The maximum depth is approximately constant along the Jamuna River and varies between 10 and 17m, except for downstream of Sirajganj, where maximum depths of about 30m have been observed.

In JICA (1976) the ratio maximum water depth/average cross sectional depth was studied. This was also done in the present study, using a slightly adapted procedure. Main channels were identified on satellite imageries and on the BWDB soundings. For each main channels the wet area was divided by the width (assuming flood conditions) to obtain the average depth. The maximum depth was also measured with respect to the flood stage, and the ratio h_{max}/h_{av} was computed. The results for the Jamuna river are plotted in Figure C-3.36. The ratio of h_{max}/h_{av} is less than 3.5, with a few exceptions only. In one cross section even a ratio of 6.1 was found. In JICA (1976), where no values exceeding 4 were given, the ratic h_{max}/h_{av} was plotted versus the eccentricity of the thalweg. This procedure has not been followed here because it is felt that in the case of a braiding river the eccentricity as defined for meandering channels has little meaning. Maximum depths were also identified on the BIWTA sounding charts (see section C.3.2.4 and Table C-3.2). It was observed that large depths occurred under three different circumstances:

- in outer bends of main channels;

- downstreams of confluences, either of a tributary (Teesta, Ganges or Meghna Rivers) or downstream of islands and chars, where two channels join;

- in reaches where bank protection is present, notably the railway ferry terminal near Bahadurabad, and the town protections of Sirajganj and Chandpur.

The observations are summarised in Figure C-3.37, where the minimum observed bed levels were plotted against the chainage along the Jamuna and Padma Rivers. The following remarks can be made:

(i) The largest depths were found in reaches where bank protection has been applied. This is probably due to unnatural flow patterns and turbulence generated here, and the absence of supply of material from eroding banks.

(ii) The depths in outer bends are usually smaller than the erosion holes downstream of confluences. This implies that the deepest scour holes may not be located near the banks but also midstream at the downstream end of islands/chars.

In Figure C-3.38, a comparison is made between the maximum depths resulting from BWDB cross sections and BIWTA-sounding charts. Apparently a too optimistic picture is obtained when only the BWDB-cross sections are considered. A good correspondence is observed for the Jamuna River apart from Sirajganj (effect of the protuding bank protection works). Near Mawa, the observed maximum depths are smaller than assumed in the Inception Report. If comparing the Inception Report figure with the actual observations, it should be realised that bed level fluctuations due to bedforms are to some extent incorporated in the observations. Finally the observations near bank protection works stress the need for special attention to the effect of structures on maximum scour depths in the river.

C.3.6.3 Extrapolations to Extreme Floods

The observations presented in Figure C-3.37 were al made during moderate or low flow conditions. The maximu depth during extreme flood conditions, however, is th major design parameter to be determined. No field dat are available for these conditions.

Experience in other rivers and experimental data from models indicate that the slope in the bend profile becomes steeper during floods and that deeper scour occurs along the outer bend. Recently the insight into the physical processes in curved channels has increased considerably. The Consultants have played and are playing an important role in the further development of, e.g. mathematical modelling of these processes (Struiksma et al, 1985). Based on this experience, the Consultants have attempted to make predictions for bend profiles in the Jamuna and Padma Rivers assuming fully-developed bend flow in symmetric channels. Taking into account the influence of the spiral motion on the main flow, the flow field is approximately described by:

$$u(z)/u_c = r/R_c\ (h/h_c)^{0.5}$$

where
- $u(z)$ = average velocity over the depth,
- u_c = depth-averaged velocity in the centre line,
- r = transverse coordinate,
- R_c = radius of curvature of centerline,
- h = water depth and
- h_c = water depth at the centerline.

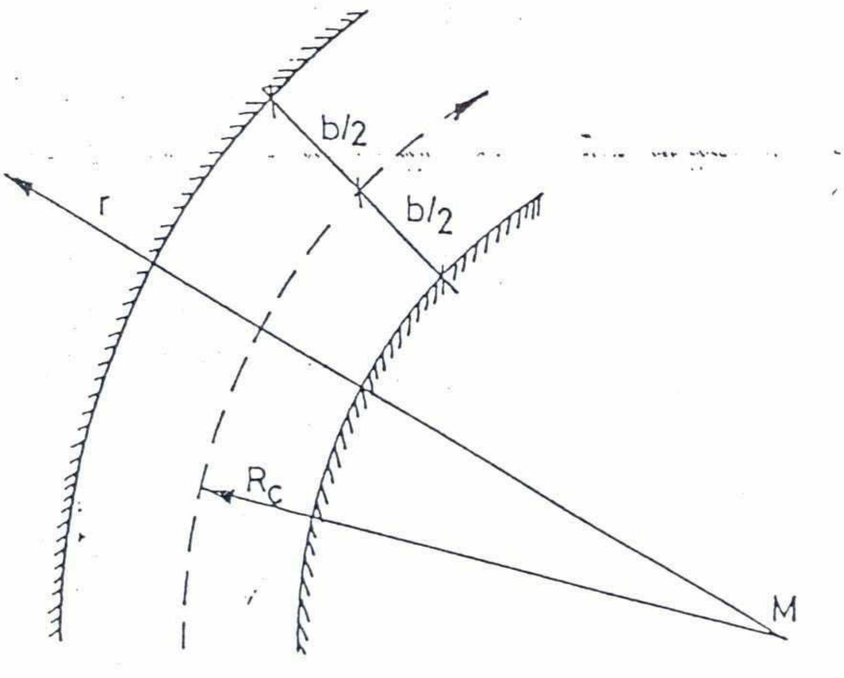

DD

The transferred depth distribution is assumed tc according to:

$$dh/dr = A \times 0.85\ (hi/\Delta D)^{0.5} \times h/r$$

where, $A = 2k^{-2}\ [1-2(g)^{0.5}/kc]$ = coefficient related to spiral motion.

f_s = slope factor (≈ 1.5)
i = water surface slope
Δ = submerged relative density
D = characteristic grain size
K = Von Karman constant (=0.4)
C = Chezy coefficient.

Combination of these two equations yields an expı for the transversal depth distribution:

$$h/h_c = [1+(0.5 \times A \times 0.85\ (\theta_c)^{0.5}(1-r/R_c$$

where: θ_c = center line value of $hi/\Delta D$.

This equation has been applied to some bends Jamuna and Padma Rivers. Two typical results application for the Jamuna conditions are gi Figure C-3.39. A number of remarks have to be mad

(i) Many cross sections, although locat pronounced bends, show profiles similar upper part of Figure C-3.39. Even if developed axi-symmetric flow would exist flood conditions, braiding becomes apparent pronounced during lower flow conditions hampers the appreciation of the equation ii cases.

(ii) The theoretical value for A varies between C = $40m^{0.5}/s$) to 11.5 (for C = $100m^{0.5}/s$). the observed bend profile in the lower p Figure C-3.39, a very low value of A = 5 ha accepted.

(iii) The effect of bank erosion, resulti reduction of the largest scour depth, included in the equation.

(iv) The values of R/B are less than 5 in many b the Jamuna river (see sections C.3.5.3 and C-3.35), which is well outside the range fo the equation was developed.

200

Consequently, the equation was not assumed to provide reasonable results for flood conditions. Some increase in scour depth in outer bends, however, has to be taken into account.

For confluences downstream of island/bars the possibilities of extrapolating to flood conditions are even worse, because the actual cause of this deep scour is not known. Possible explantions can be:

(i) An imbalance of water and sediment distribution downstream of the confluence (similar to the cause of point bar development, (see Struiksma et al, 1985),

(ii) Increased local pick-up of sediment due to increased turbulence levels.

For the time being it is assumed that scour depth will not increase for increased flows, but extensive field and possible laboratory measurements are needed to provide a better answer to this question.

The Consultants have also attempted to use results from discharge measurements of BWDB to get more insight into bed level variations over the year. During these measurements local depths in the sampled verticals are also noted. The bed level changes of several main channels near Bahadurabad are plotted in Figure C-3.40. In particular, at Bahadurabad the bed level seems to lower during the flood. However, the discharge measuring sites are usually not located at sections where the largest changes in bed level elevation are to be expected.

REFERENCES

ACKERS, P. and WHITE, W.R. (1972); Sediment Transport: New Approach and Analysis, Proc. ASCE, Vol. 99, HY11, pp. 2041-2060.

ALLEN, J.R.L. (1960); Current Ripples, Amsterdam, North Holl. Publ. Cy.

BRISTOW, C. (1985); Brahmaputra River: Channel Migration and Deposition (paper prepared for Conferenc Fluvial Sedimentology, preprint sent as pr communication to W.K. Cross).

BWDB(1978); Morphological features of major rivers in Bangla Dhaka, Bangladesh Water Development Board.

BWDB (1972); Sediment investigations in main rivers of Bangl 1968 and 1969, BWDB Water Supply paper no. 35

CHARLTON, F.G. (1969); Sediment Investigations 1967 and 1968 FAO-SF second Hydrological Survey in Pakistan, UNDP/FAO.

COLEMAN, J.M. (1969); Brahmaputra River: Channel Processes a Sedimentation, Journal of Sedimentary Geo Vol. 3, pp. 132-239.

ECI/ACE (1971); Dhaka South West Projects, Definite Project Report (East Pakistan Water and Power Develo Authority).

ENGELUND, F. and HANSEN, E. (1967); A monograph on sediment transport, Copenhagen, Teknisk Verlag.

FREEMAN, FOX and PARTNERS (1971); Brahmaputra (Jamuna) River Crossing Feasibility Study.

GOSWAMI, D.C. (1985); Brahmaputra River, Assam, India, Physiography, basin denudation and ch aggradation, Water Resources Research, Vol no. 7, pp. 959-978.

GALAY, V.J. (1980); River channel shifting on large rivers i Bangladesh, Proc. Intern. Symp. on Sedimentation, Beijing, China.

IECO (1980); South-West Regional Plan (BWDB), Suppl. III : Hydrology, IECO/BWDB Special Studies Director

SIR WILLIAM HALCROW AND PARTNERS (1984); Engineering Apprais the Brahmaputra Multipurpose Development Pro BWDB.

202

IECO (1968); Bank line movement of the Brahmaputra Jamuna River, IECO/EPWAPDA.

JANSEN, P. PH. (1979); Principles of river engineering; The non-tidal alluvial river, London, etc., Pitman Publ. Cy.

JICA (1976); Jamuna Bridge Construction Project, Feasibility Study Report, Vol. II: River Control.

KLAASSEN, G.J. OGINK, H.J.M. and RIJN, L.C. VAN (1984); DHL - research on bed forms, resistance to flow and sediment transport, Proc. 3rd Intern. Symp. on River Sedimentation, Jackson, Miss (USA).

LATIF, A. (1969); Investigations of Brahmaputra River, Proc. Hydraulics Division ASCE, Vol. 95, no. HY5, pp. 1687-1690.

MORGAN and MCINTIRE (1959); Quartenary Geology of the Bengal Basin, East Pakistan and India, Bull. Geol. Soc. America, Vol. 70, pp. 319-342.

NAZIM, U. (1985); Hydraulic parameters of the flow and riverbed routing of the Lower Brahmaputra/Jamuna River, Moscow Hydrotechnical Engineering Institute, Ph.D. Thesis (in Russian).

NEDECO (1967); East Pakistan Inland Water Transport Authority, Surveys of Inland Waterways and Ports, Vol.III: Hydrology and morphology, NEDECO/EPWAPDA.

NEDECO (1977); Brahmaputra Right Flood Embankment, Feasibility Study Report, NEDECO/BWDB.

RIJN, L.C. van (1984); Sediment transport, part I, II and III, Journal of Hydraulic Engineering ASCE, Vol. 110, pp. 1431-1456 + 1613-1641 + 1733-1754.

SESOREN, A. (1984); Geological interpretation of LANDSAT imageries of the Bangladesh Ganges Delta, ITC Journal, no. 3, pp. 229-232.

STEVENS, M.A. and SIMONS, D.B. (1973); Manning's roughness coefficient for the Padma River, Proc. 15 IAHR Congress, Istanbul, Turkey, paper A.2.

YALIN, M.S. (1964); Geometrical properties of sand waves, Proc. ASCE, Vol. 90, no. HY5, pp. 105-169.

MORPHOLOGY

LIST OF SYMBOLS

A	cross section area; area (m^2)
A_s	conveying cross section area (m^2)
B	storage width; width (m)
B_s	stream width (m)
C	Chezy coefficient($m^{0.5}/s$)
C	concentration
C_F, C_D	drag coefficient
c	celerity(m/s)
c_b	celerity of bedform(m/s)
D	particle diameter
D_n	diameter of particle such that n% of sample is finer(m)
D_{50}	median particle diameter(m)
F	Froude number
$F(...)$	function of
$f(...)$	function of
f	Darcy-Weisbach friction factor
g	gravity acceleration (m/s^2)
H	energy head; height of bedform(m)
$\overline{h}$	depth of flow; mean depth of flow (m)
h	mean depth of flow(m)
i	mean slope of energy line
i_b	mean slope of bottom
i_w	mean slope of water surface

208

U	flow velocity component(m/s)in x-direction; cross-sectional mean flow velocity in x (Q/A_s)
u_*	shear flow velocity in x-direction defin $u_* = (ghi)^{1/2}$(m/s)
w	settling velocity of particle (fall velocity)
X	dimensionless transport parameter [$s_b/D^{3/2}$(g.
x	coordinate in flow direction(m)
Y	dimensionless flow parameter ($\Delta D/\mu hi$)
y	coordinate in lateral direction(m)
z	vertical coordinate; level(m)
z_b	bed level(m)
z_w	water level(m)
β	angle
γ	angle
Δ	relative density $(\rho_s-\rho)/\rho$; increment
ε	porosity
θ	dimensionless shear stress, defined via
κ	Von Karman's constant
μ	ripple factor
ν	kinematic viscosity (m^2/s)
ρ	density of water (kg/m^3)
ρ_m	density of material (kg/m^3)
ρ_s	density of sediment (kg/m^3)
σ	standard deviation
τ	shear stress ($kg/m/s^2$)
τ_b	bottom shear stress ($kg/m/s^2$)
τ_c	critical shear stress ($kg/m/s^2$)

Years	Padma 47-042	Jamuna-S 48-043	Jamuna-N 48-042
1972	22-11-73	11-12-72	11-12-72
1973	5-12-73	21- 2-73	
1974			
1975	27- 3-75	12-10-75	
1976	27- 1-76	10- 1-76	10- 1-76
1977	8- 2-77	9- 2-77 28- 5-77	
1978	4- 5-78	22- 2-78	
1979	6-3-79		
1980	2-2-80		
1981	9-4-81	10-4-81 27-12-81	27-12-81
1982			
1983			
1984		23-2-84	
1985	10-2-85		

* Underlined dates enlarged to 1:250.000

Table C-3.1 SATELLITE IMAGERIES USED IN THE PRESENT STUDY.

287

Table C-3.2 BIWTA SOUNDINGS USED IN THE PRESENT STUDY

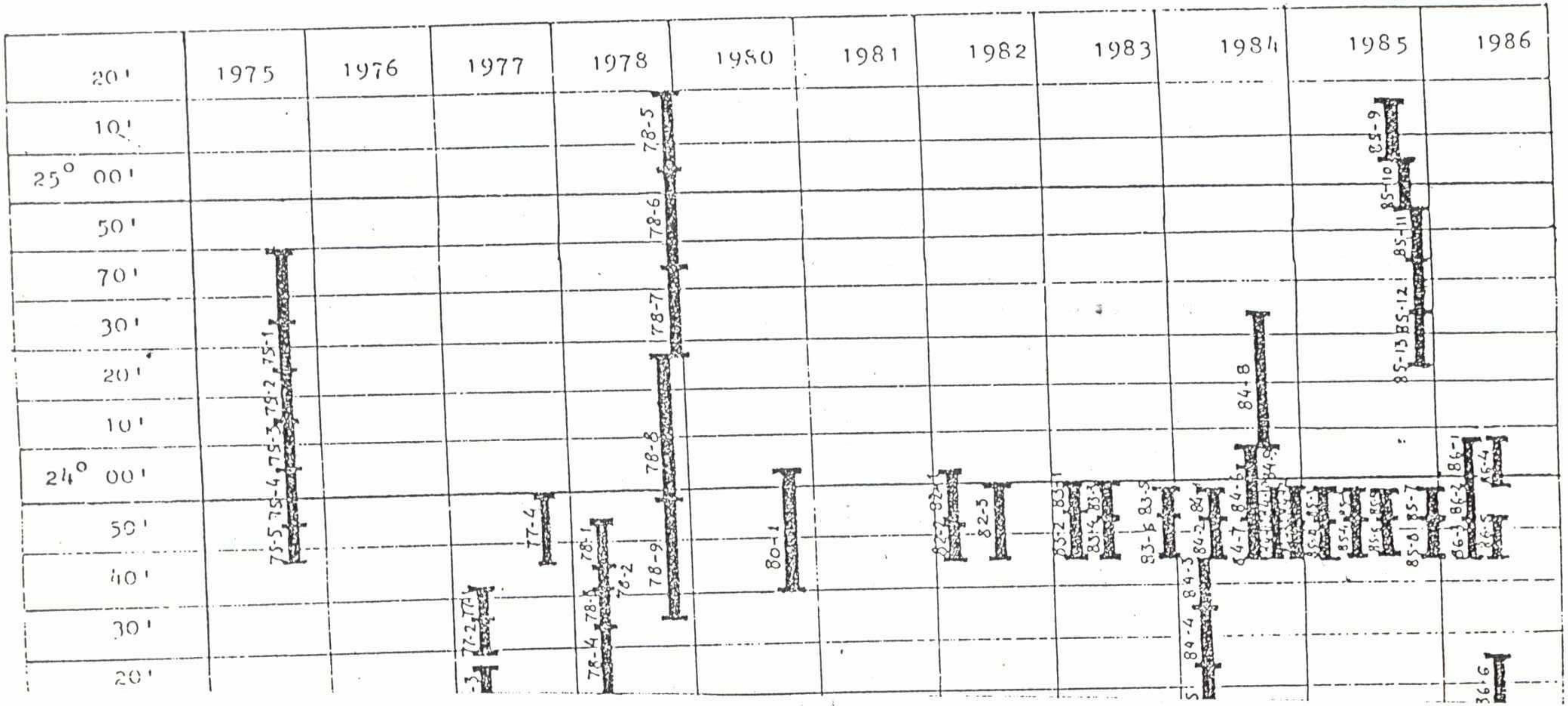

TABLE C-3.3 FLOOD DISCHARGES AND SLOPES ALONG THE JAMUNA AND PADMA RIVERS

Station	Average yearly flood		1:100 year	
	Q (m³/s)	h (m) + PWD	Q (m³/s)	h (m) + PWD
Bahadurabad	65.000	19.7	91.000	20.2
Gabargáon	65.000	16.8	91.000	17.4
Sirajganj	65.000	13.7	88.000	14.4
Nagarpur	65.000		81.000	
Goalundo	88.000	8.2	134.000	9.1
Mawa	88.000	6.0	134.000	7.1

Source : BWDB data, Constultants analysis (see Appendix C.2)

TABLE C-3.4 VALLEY SLOPES ALONG THE JAMUNA AND PADMA RIVERS

Station	Chainage (km)	Valley slope (x 10⁻⁵ = cm/km) Average Yearly flood	1:100 year flood
Bahadurabad	- 156.4		
		6.8	7.3
Sirajganj	- 76.8		
		7.1	7.4
Nagarbari	- 13		
Baruria	0		
		3.7	3.3
Mawa	60		

Table C-3.6 MEDIAN PARTICLE DIAMETER AND STANDARD DEVIATION BED MATERIAL JAMUNA RIVER

	Chilmari Ch.1A		Chilmari Ch 1B Thakurchar		Sirajganj Mainchannel		Sirajganj West Channel		Nagarbari Main channel		Nagarbari West channel Saturia		Mawa	
	D_{50} mm	S mm	D_{50} mm	S mm	D_{50} mm	S mm	D_{50} mm	S mm	D_{50} mm	S mm	D_{50} mm	S mm	D_{50} mm	S mm
1965					226	053								
1966					183	066								
1967													0,136	0,087
1968	0.261	0.110			0.163	0.066			0.170	0.068				
1969	0.211	0.074	0.225	.066	0.163	0.048			0.150	0.057				
1970	.240	0.073	.230	.078	.155	.078			.160	.063				
1971														
1972									.177	.059				
1973									.178	.052				
1974									.182	.043	.160	0.033		
1975	0.201	0.091	.209	.073					.198	.067	.170	0.047		
1976	0.241	0.066	.240	.062	.225	.062			.158	.083	.143	0.065		
1977	.247	.077	.238	.047	.204	.064					.149	0.057		
1978														
1979														
1980														
$\bar{X}$	0.234	0.082	0.228	0.065	0.188	0.062			0.172	0.062	.156	0.051		
–									[illegible]	[illegible]	[illegible]	.008		

ɟɒᵽ

able C-3.6 ESTIMATE OF THE BED LOAD TRANSPORT IN THE JAMUNA RIVER

	mega ripples	dunes	sand waves
edform height (ft)	3	15	35
(m)	1	5	~10
elerity (ft/day)	400	200	670
(m/day)	120	60	~200
iver width (m)	3000	3000	3000
ediment transport ton/day)	$0.3*10^6$	$0.8*10^6$	$5*10^6$
uration of flood (days)	90	90	90
otal sediment ransport (tons)	$25*10^6$	$70*10^6$	$450*10^6$

22D

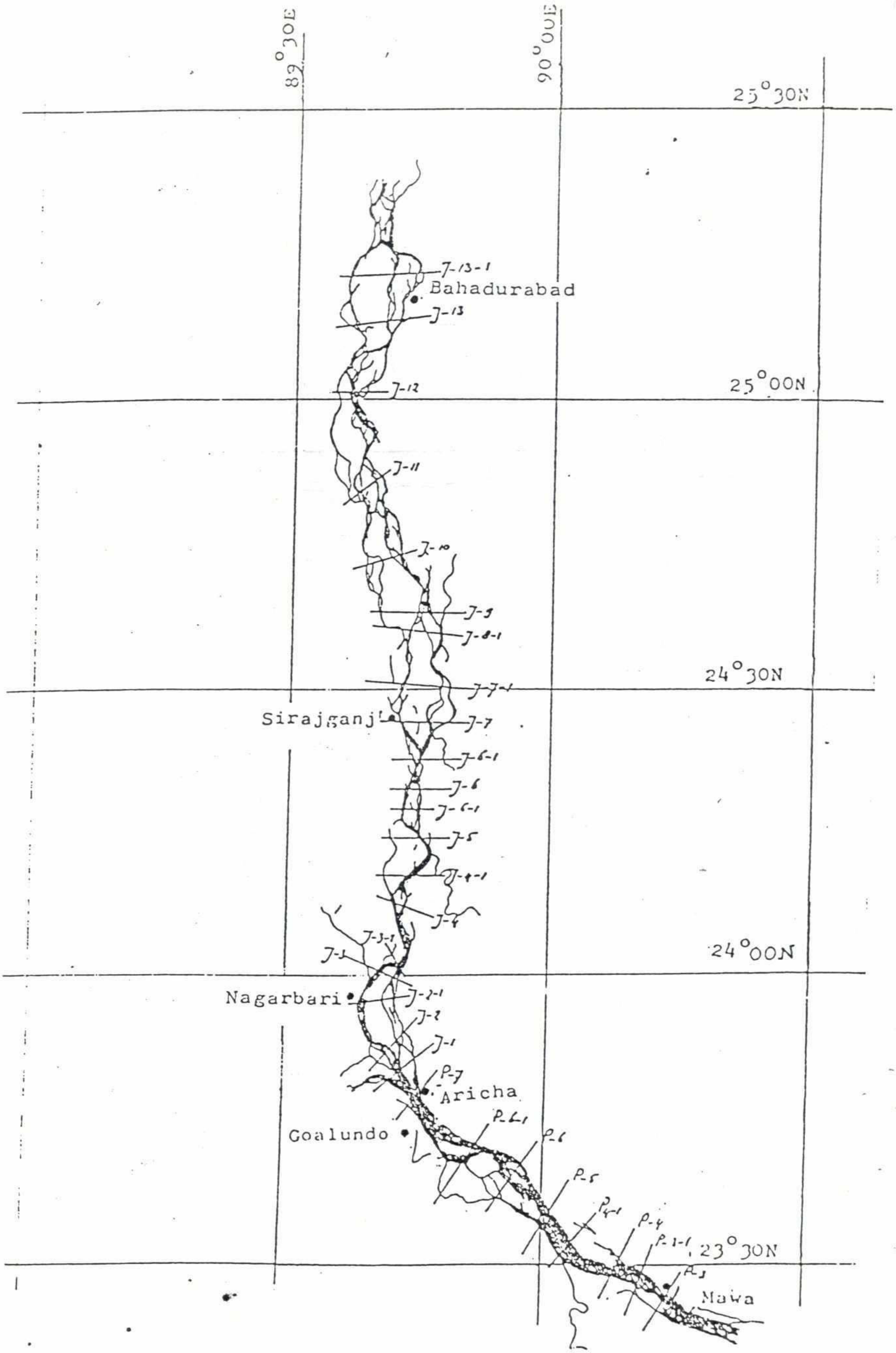

FIGURE C-3.1 BWDB CROSS-SECTIONS USED IN THE PRESENT ST

222

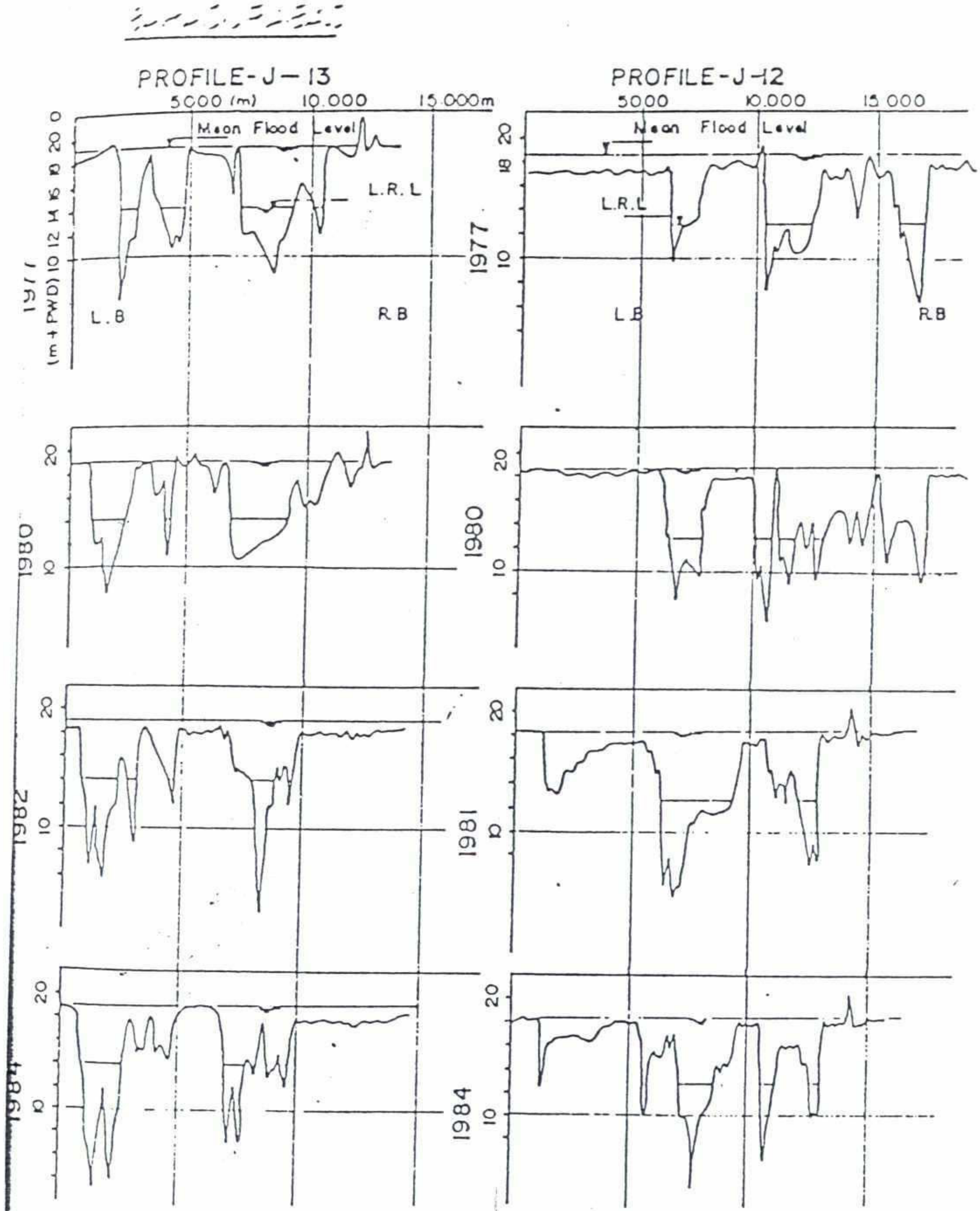

FIGURE C-3.2 MEASURED CROSS-SECTIONS AT BAHADURAPAD- JAMUNA RIVER

022

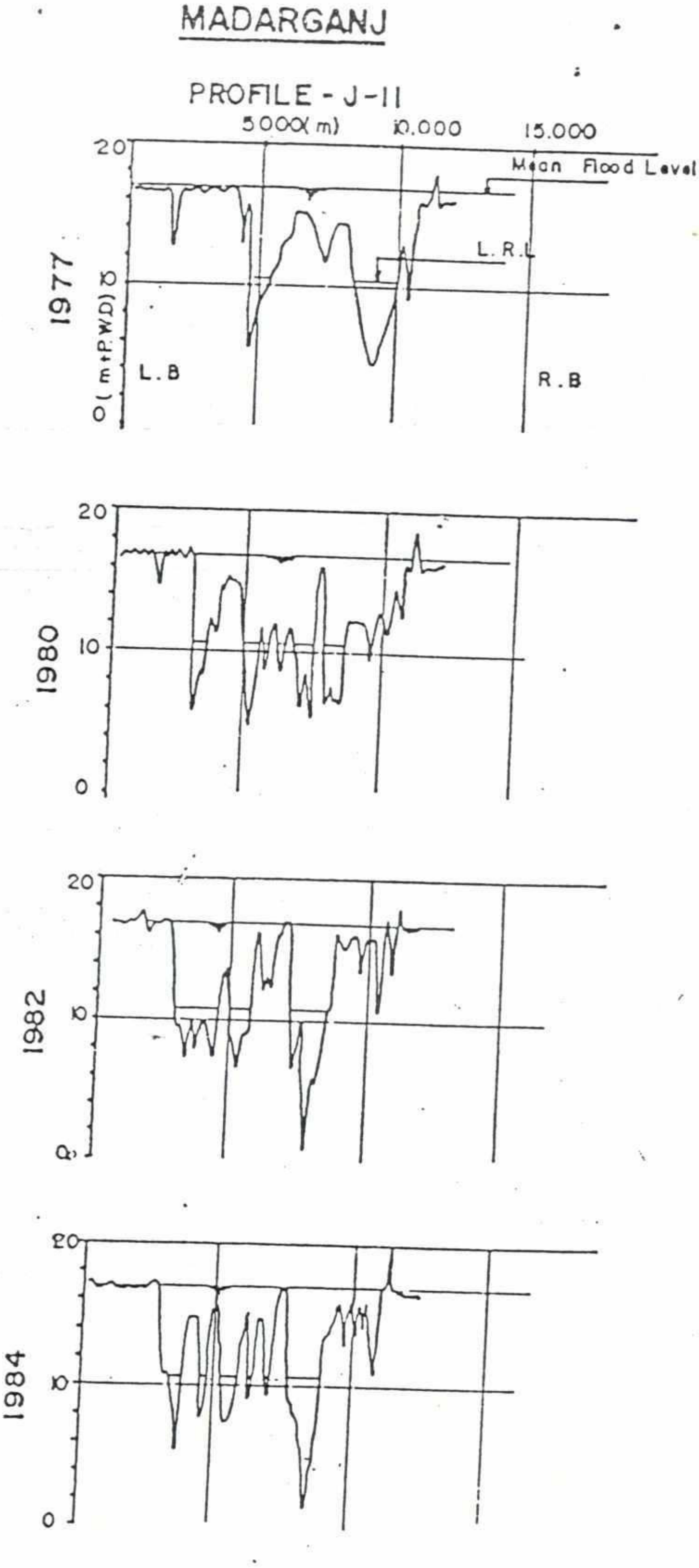

FIGURE C-3.3 MEASURED CROSS SECTIONS
AT MADARGANJ, JAMUNA RIVER

22

SIRAJGANJ

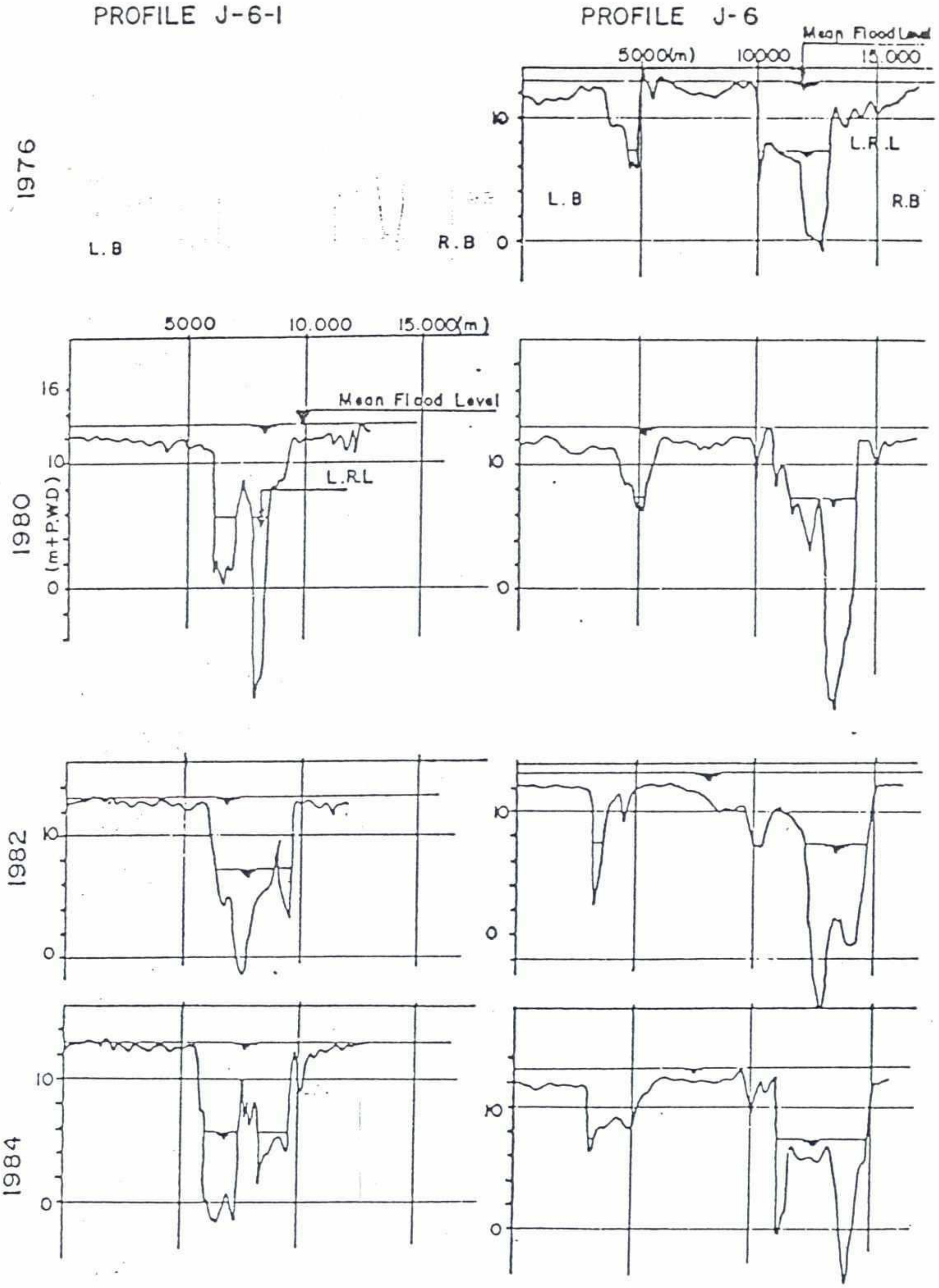

FIGURE C-3.4 MEASURED CROSS SECTIONS
SIRAJGANJ, JAMUNA RIVER

NAGARPUR

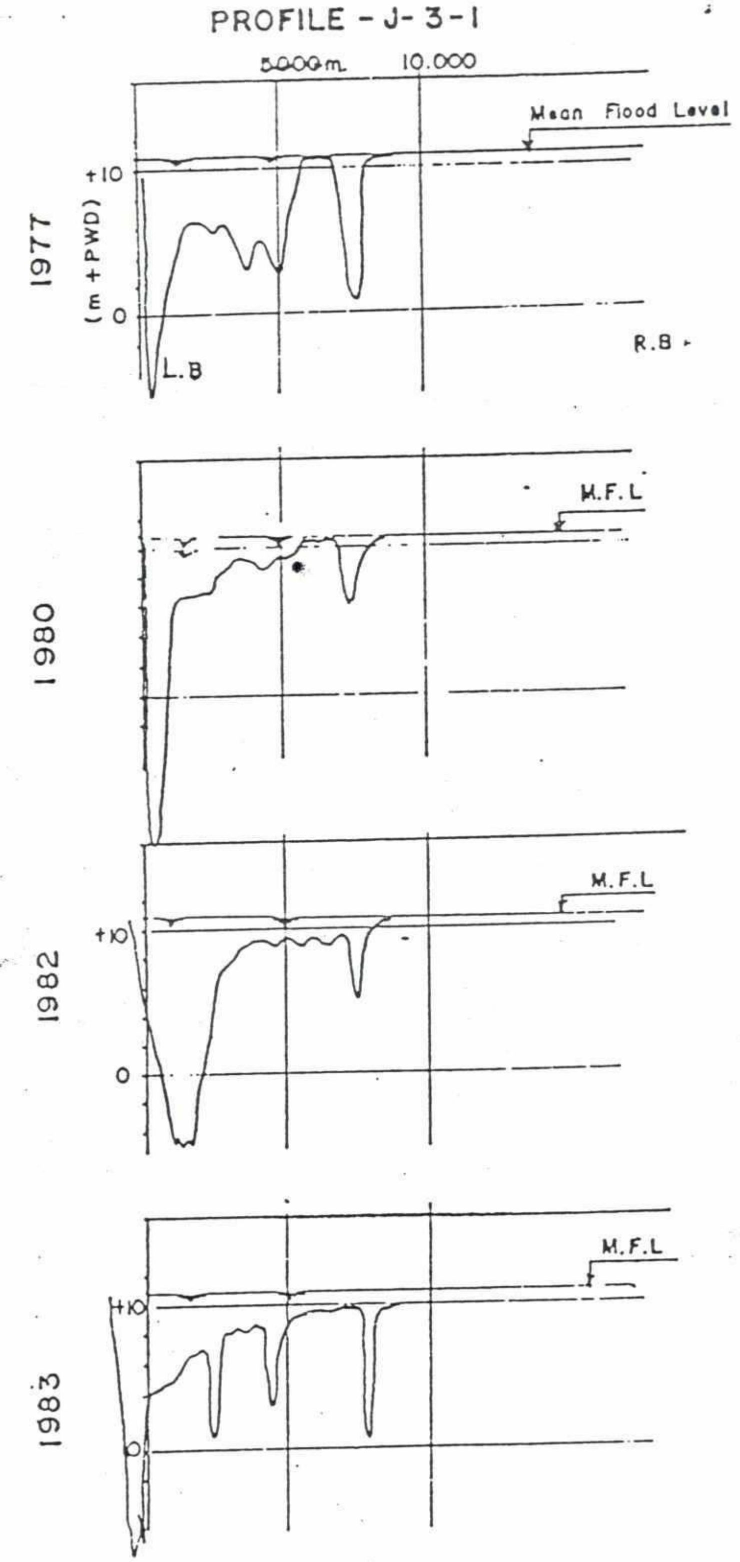

FIGURE C-3.5 MEASURED CROSS SECTIONS AT NAGARPUR, JAMUNA RIVER

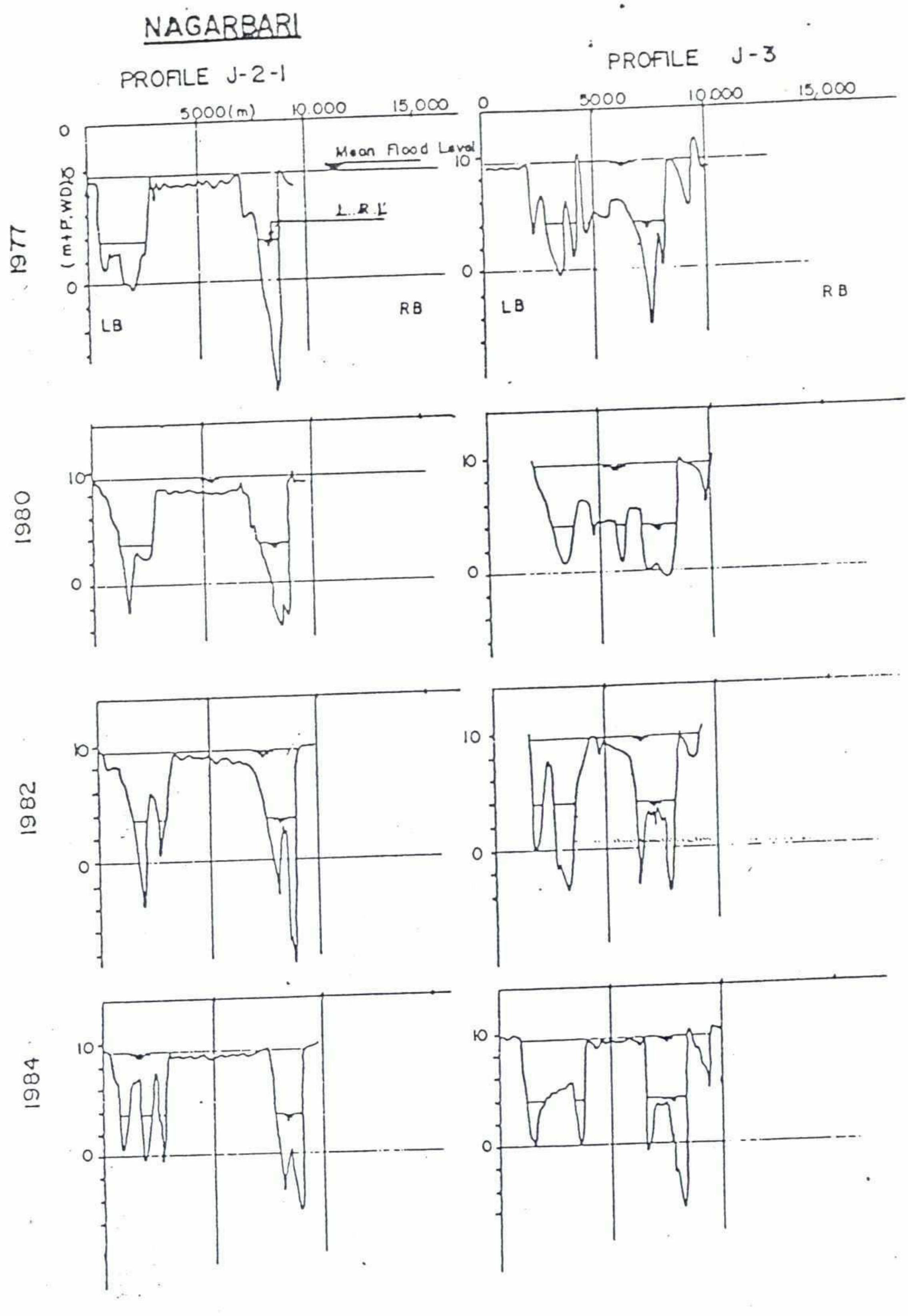

FIGURE C-3.6 MEASURED CROSS SECTIONS AT NAGARBARI, JAMUNA RIVER

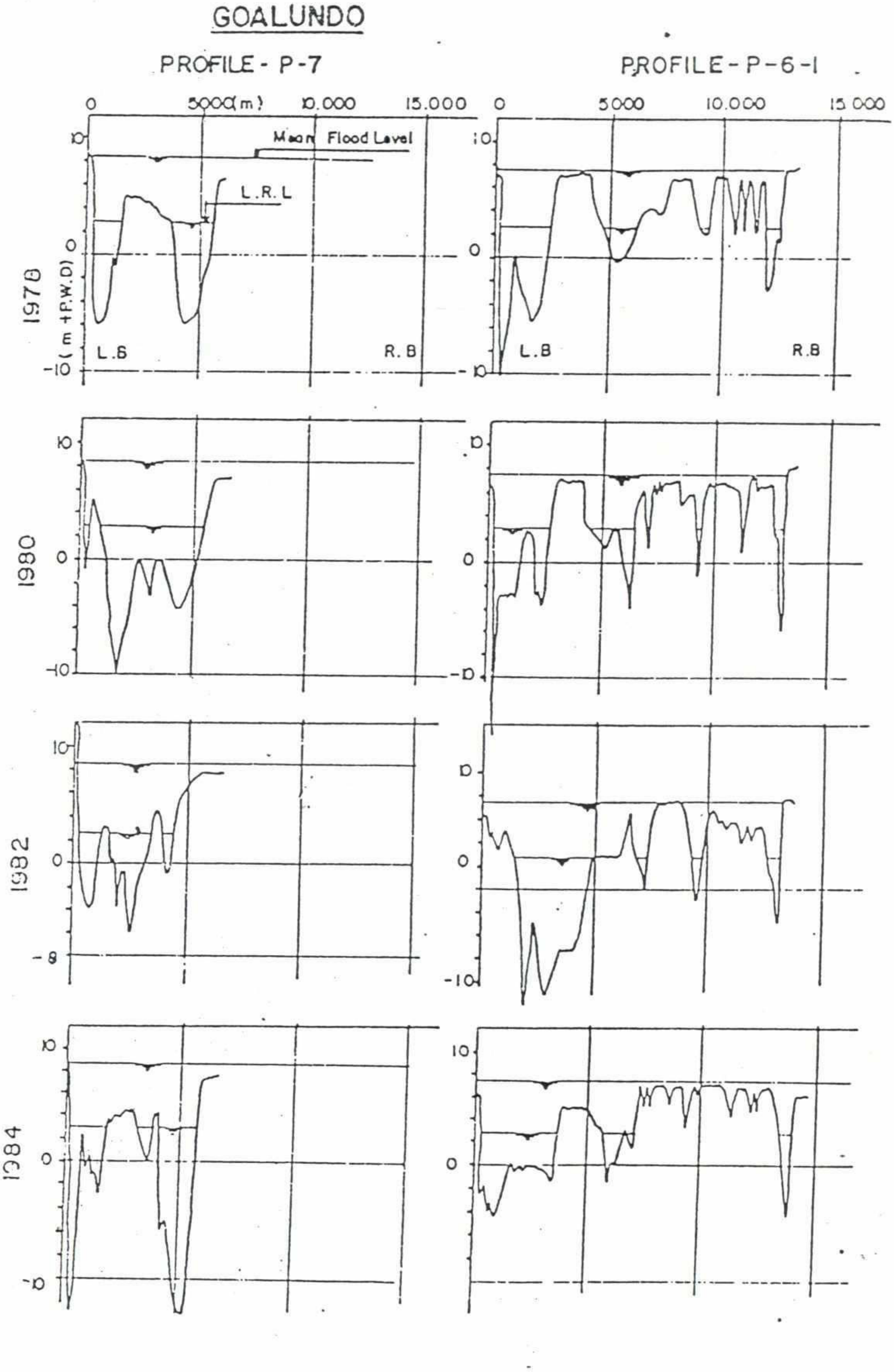

FIGURE C-3.7 MEASURED CROSS SECTIONS AT GOALUNDO, PADMA RIVER

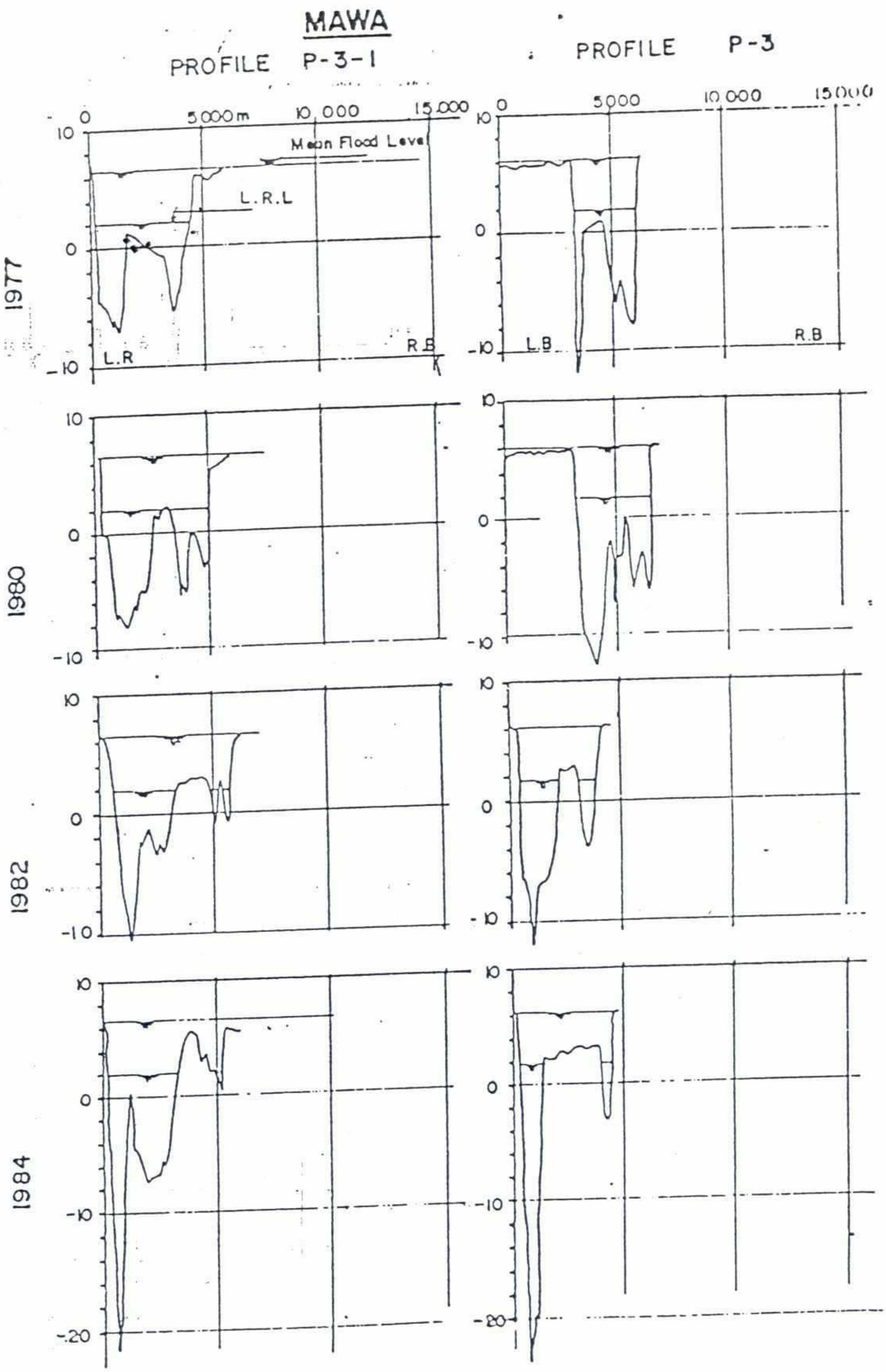

FIGURE C-3.8 MEASURED CROSS SECTIONS AT MAWA, PADMA RIVER

220

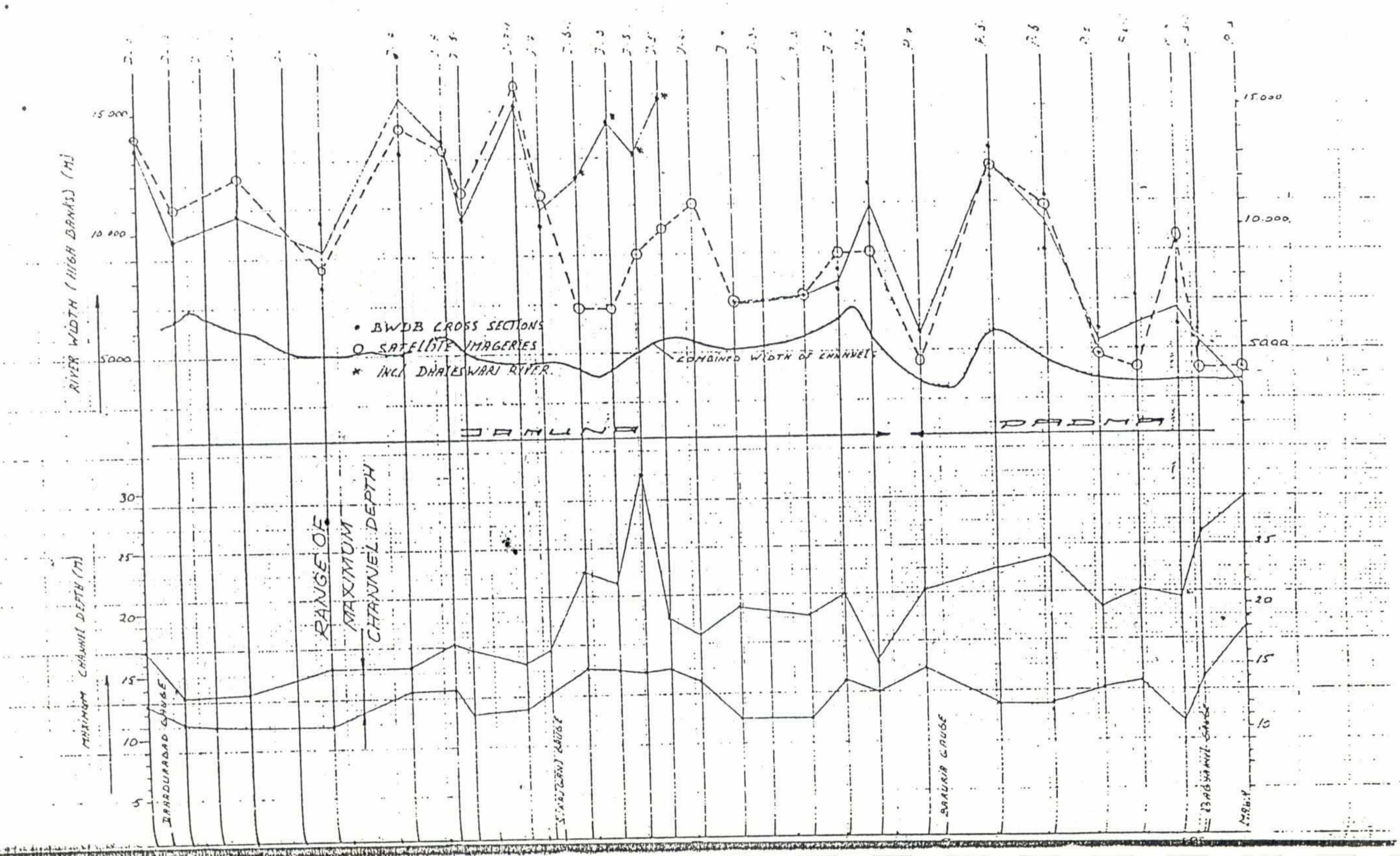

RIVER WIDTH (HIGH BANKS) (M)
MAXIMUM CHANNEL DEPTH (M)
15.000
10.000
5000
30
25
20
15
10
5
• BWDB CROSS SECTIONS
O SATELLITE IMAGERIES
* INCL DHALESWARI RIVER.
COMBINED WIDTH OF CHANNELS
JAMUNA
PADMA
RANGE OF MAXIMUM CHANNEL DEPTH
BAHADURABAD GAUGE
SIRAJGANJ GAUGE
BARURIA GAUGE
BAGYAKUL GAUGE

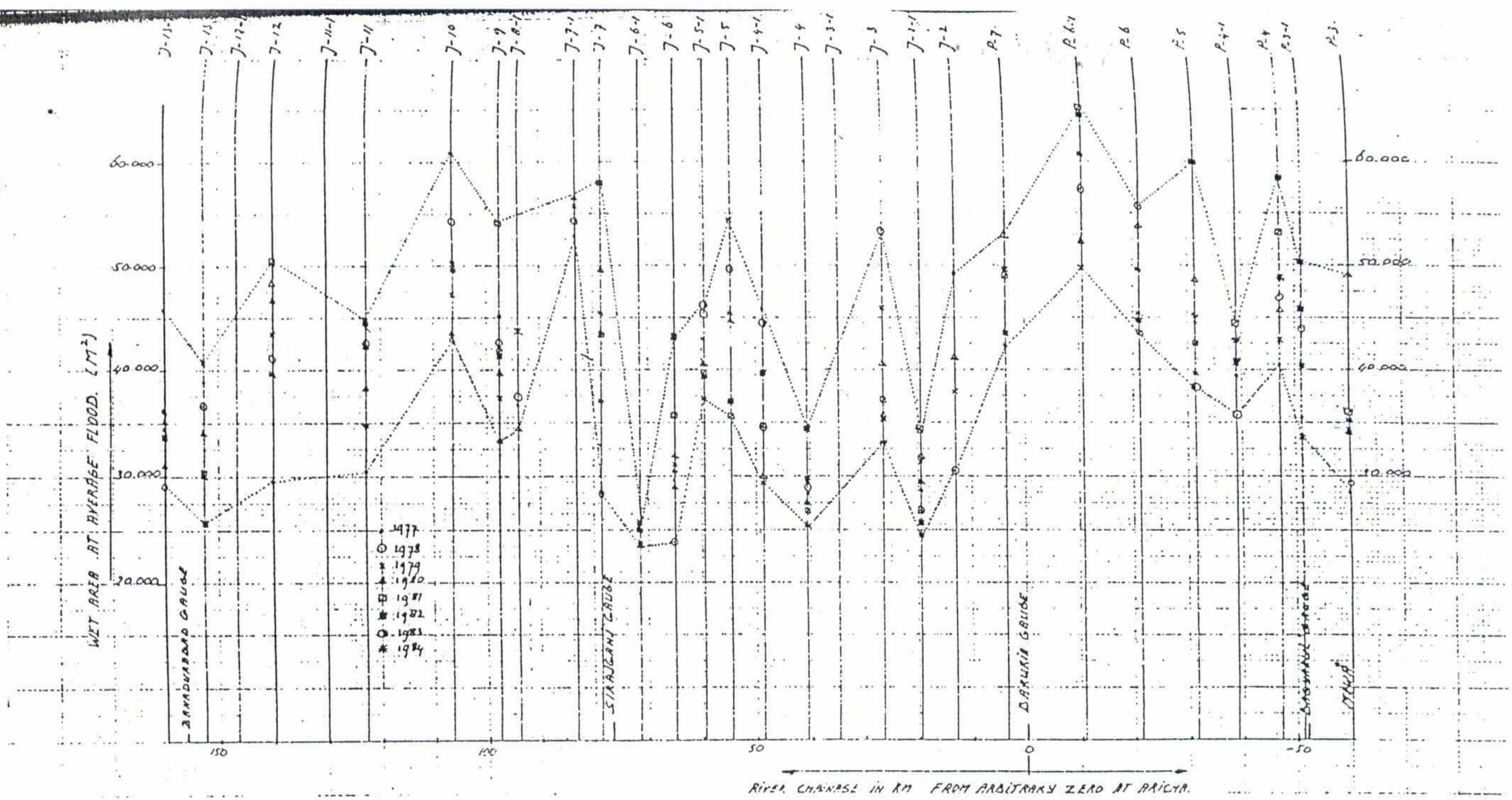

FIGURE C-3.10 WET AREA OF BWDB CROSS SECTIONS 1977 - 1984

Gec

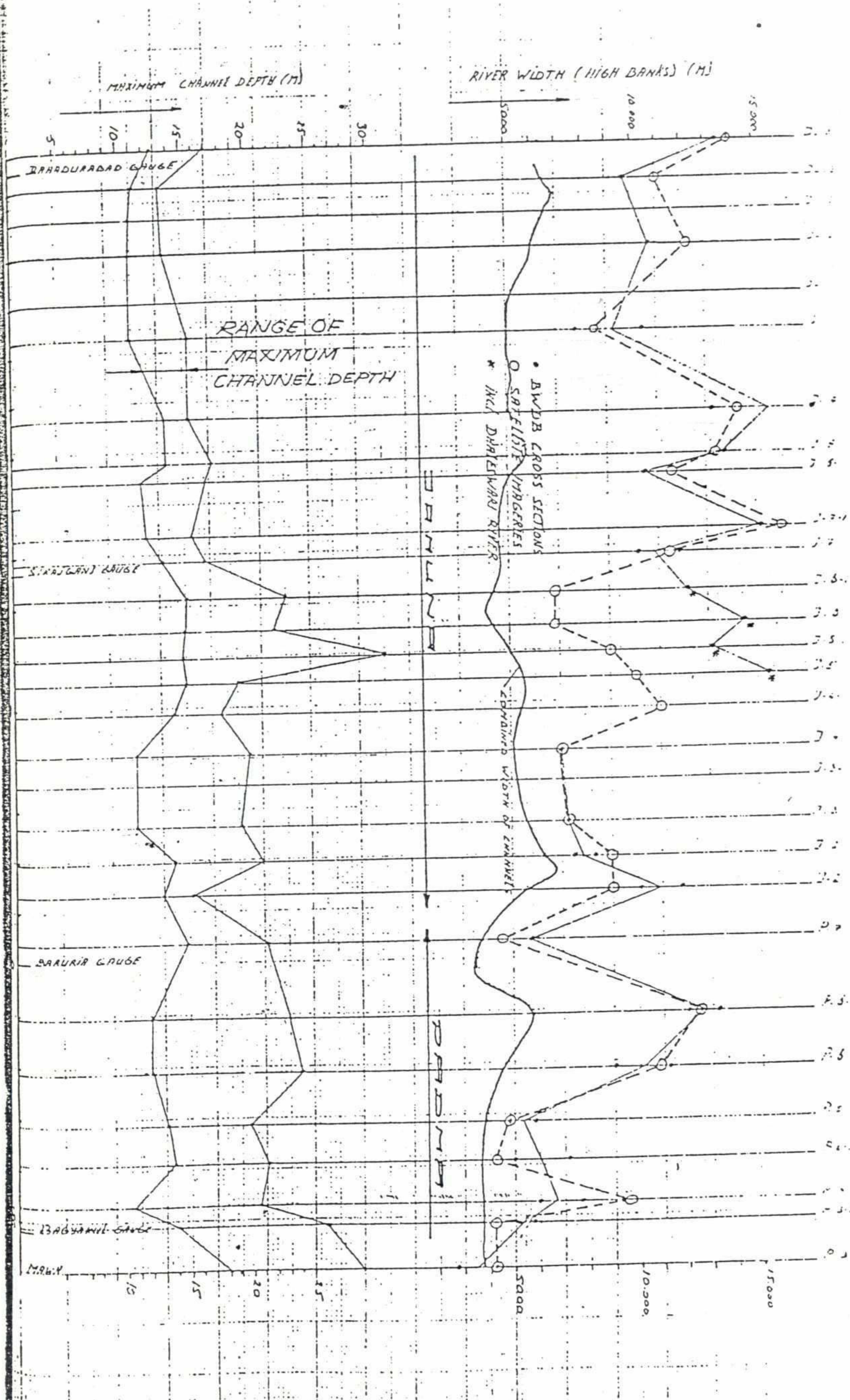
MAXIMUM CHANNEL DEPTH (M)
RIVER WIDTH (HIGH BANKS) (M)
5
10
15
20
25
30
5000
10 000
15 000
BAHADURABAD GAUGE
RANGE OF MAXIMUM CHANNEL DEPTH
• BWDB CROSS SECTIONS
O SATELLITE IMAGERIES
* INCL DHALESWARI RIVER
COMBINED WIDTH OF CHANNELS
SIRAJGANJ GAUGE
JAMUNA
BARURIA GAUGE
PADMA
BAGYAKUL GAUGE
10.000
15.000

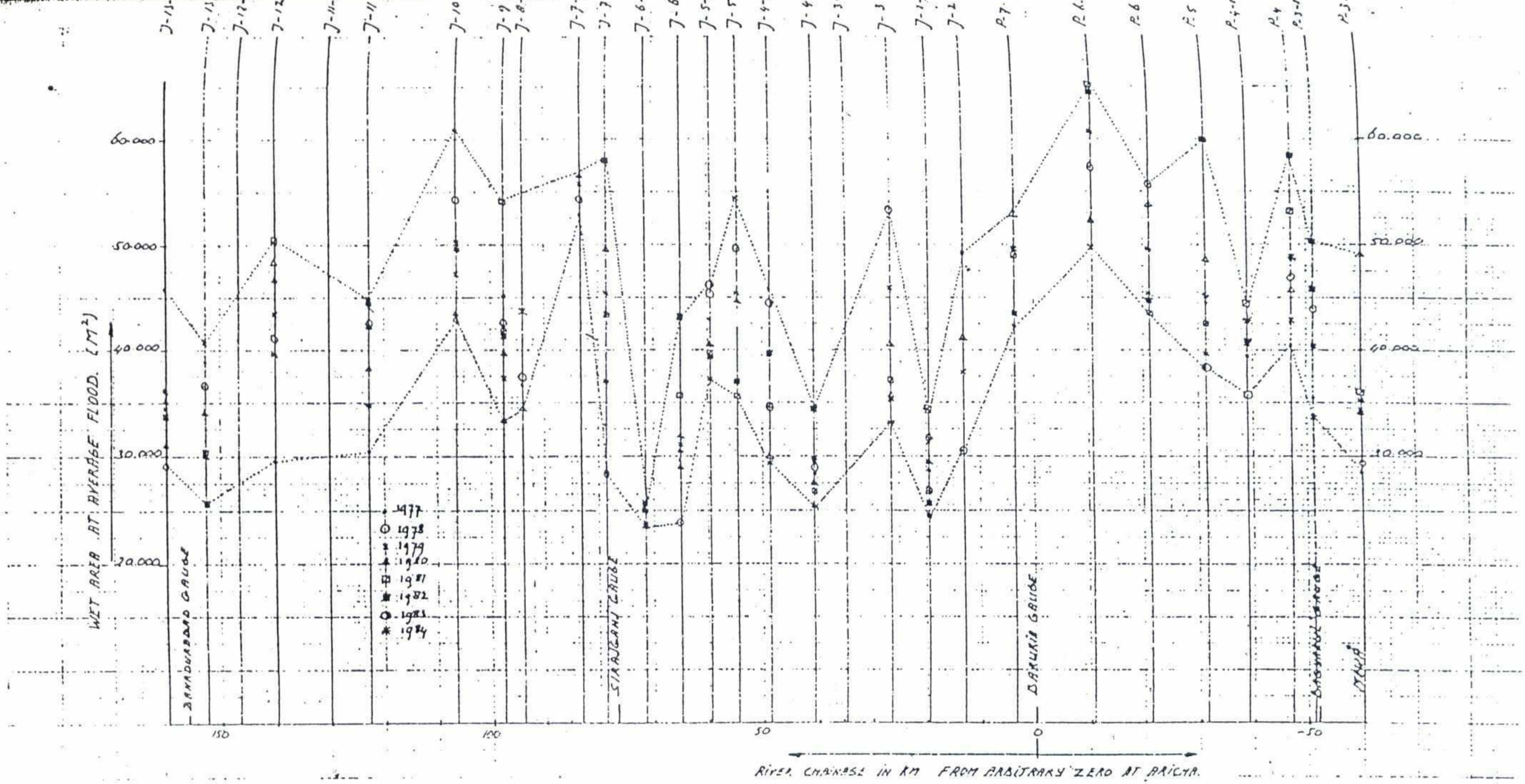

FIGURE C-3.10 WET AREA OF BWDB CROSS SECTIONS 1977 - 1984

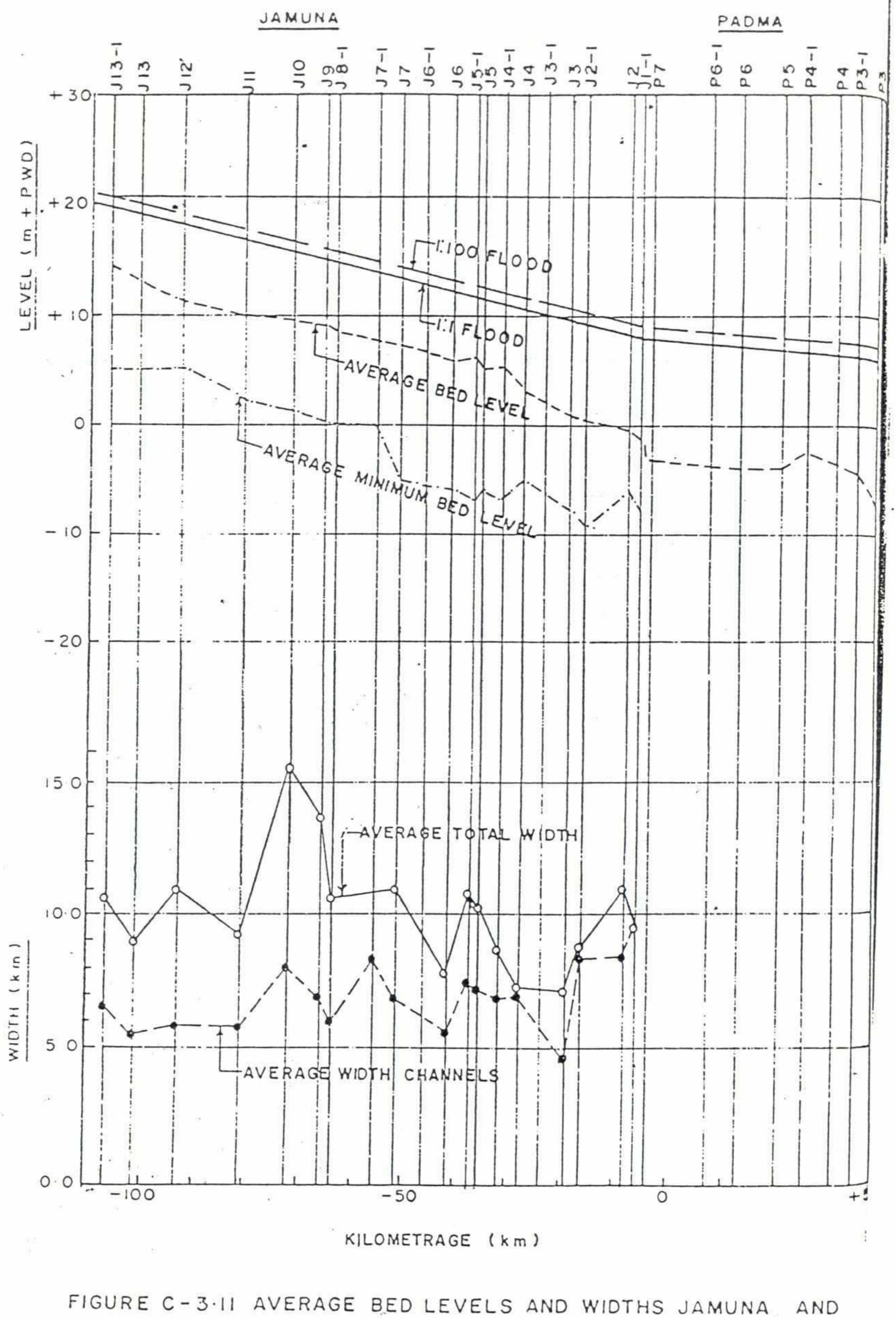

FIGURE C-3·11 AVERAGE BED LEVELS AND WIDTHS JAMUNA AND PADMA RIVERS FROM BWDB SOUNDINGS 1977-1984

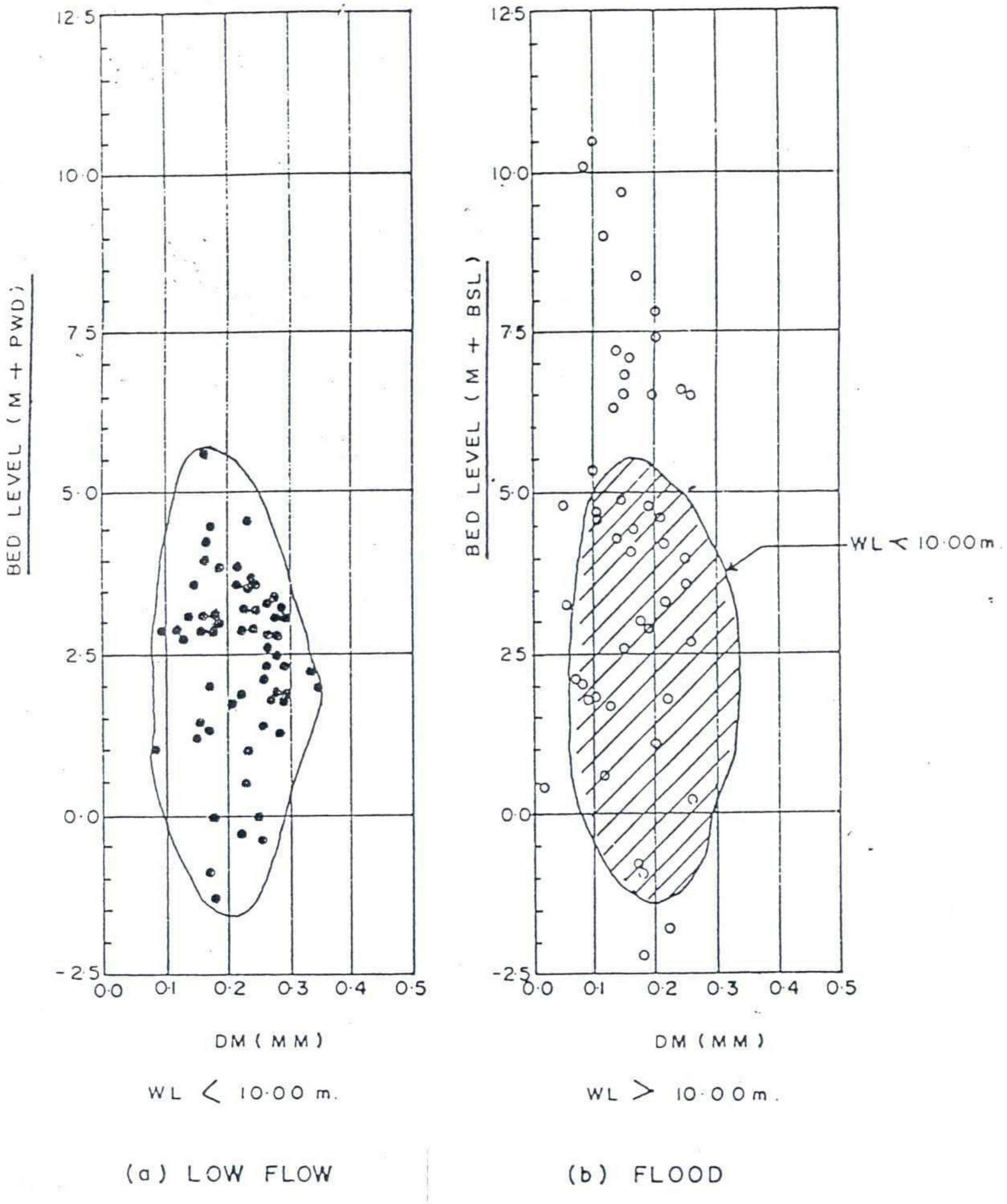

FIGURE C-3.12 PARTICLE SIZE VERSUMS DEPTH AT SIRAJGANJ FOR LOW FLOW AND FLOOD CONDITIONS.

228

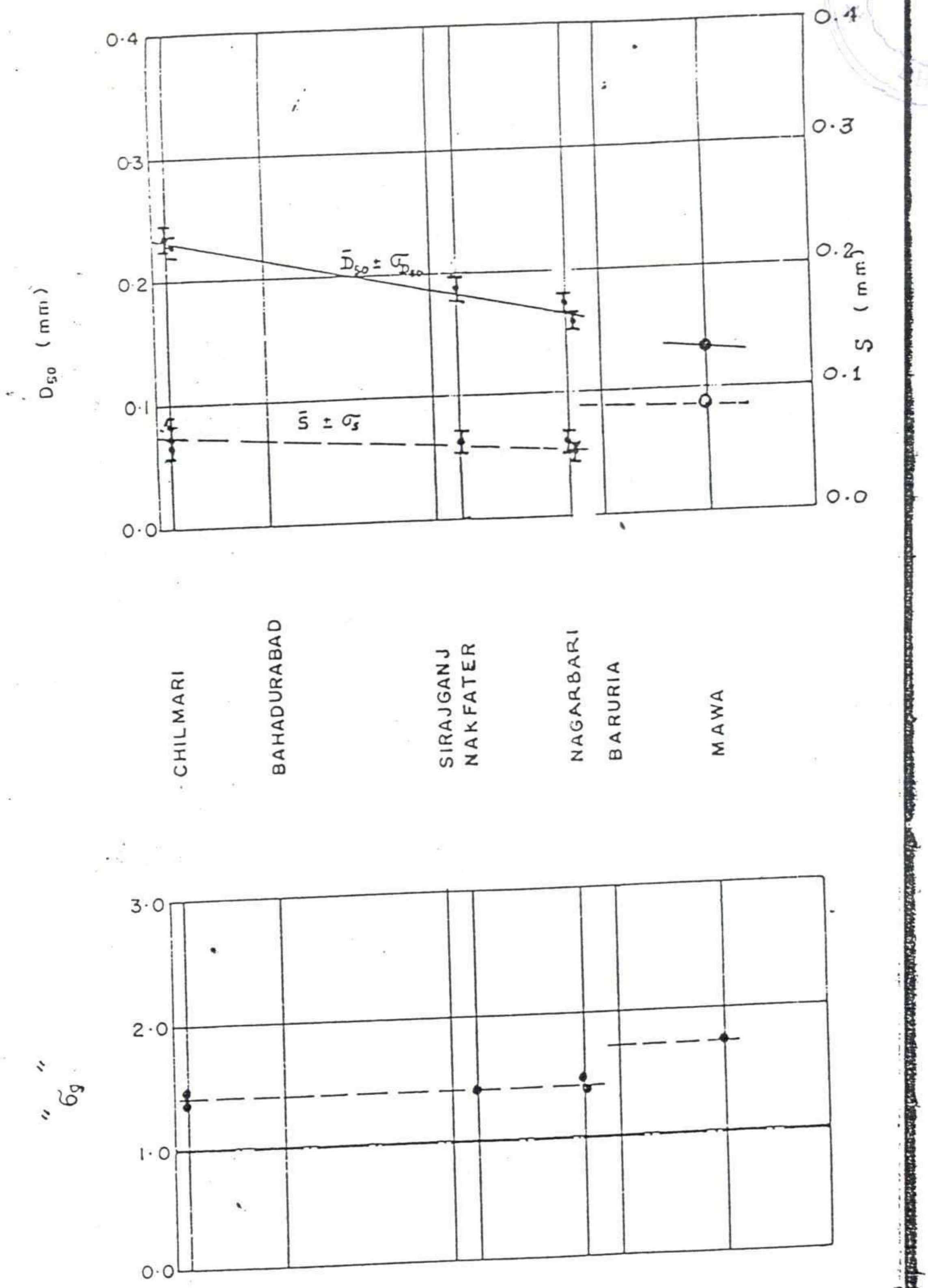

$D_{16} = D_{50} - \sigma$

$D_{84} = D_{50} + \sigma$

$\sigma = 1/2 \left(\frac{D_{84}}{D_{50}} + \frac{D_{50}}{D_{16}} \right)$

FIGURE C-3·13 AVERAGE BED MATERIAL SIZE AND GRADATION
JAMUNA AND PADMA RIVER

828

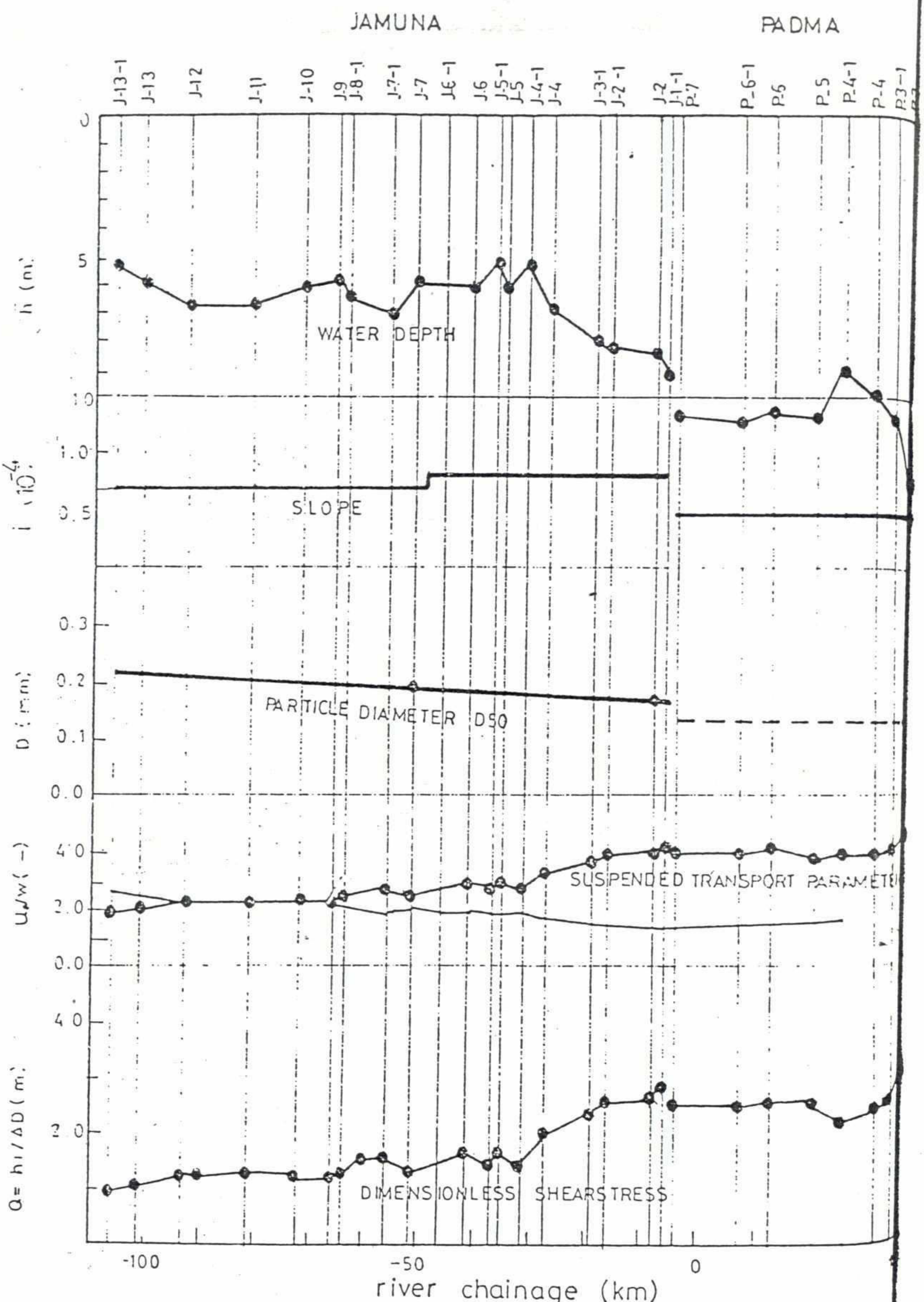

FIG. C-3.15 CHARACTERISTIC PARAMETERS OF THE JAMUNA AND THE PADMA RIVERS DURING FLOOD CONDITIONS

73

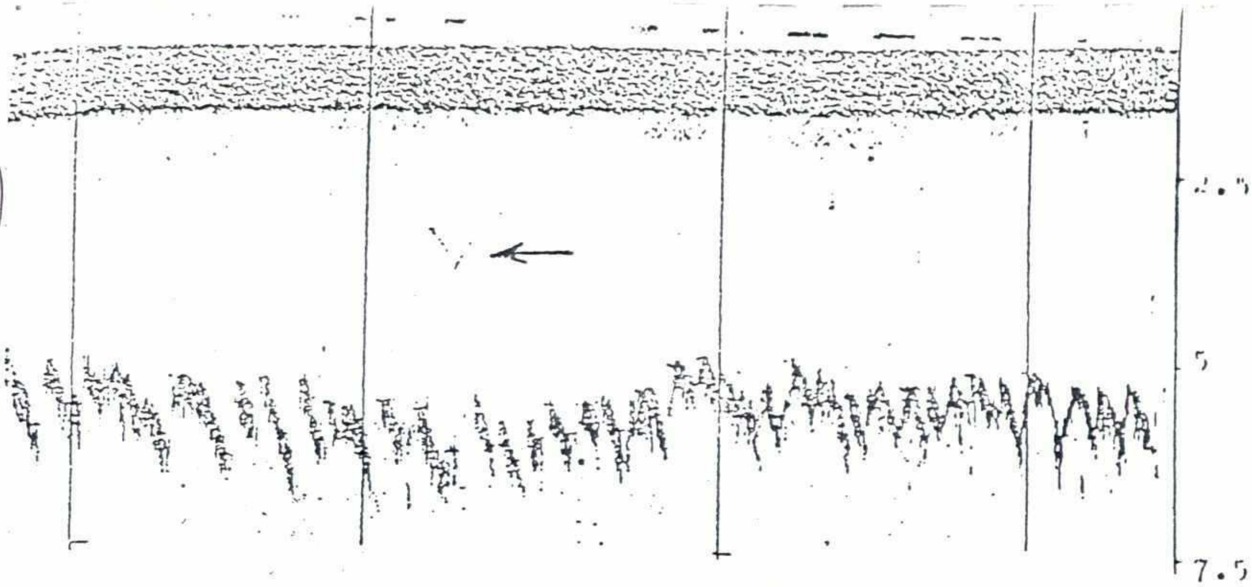

(b) Jamuna River near Aricha, 12-7-86

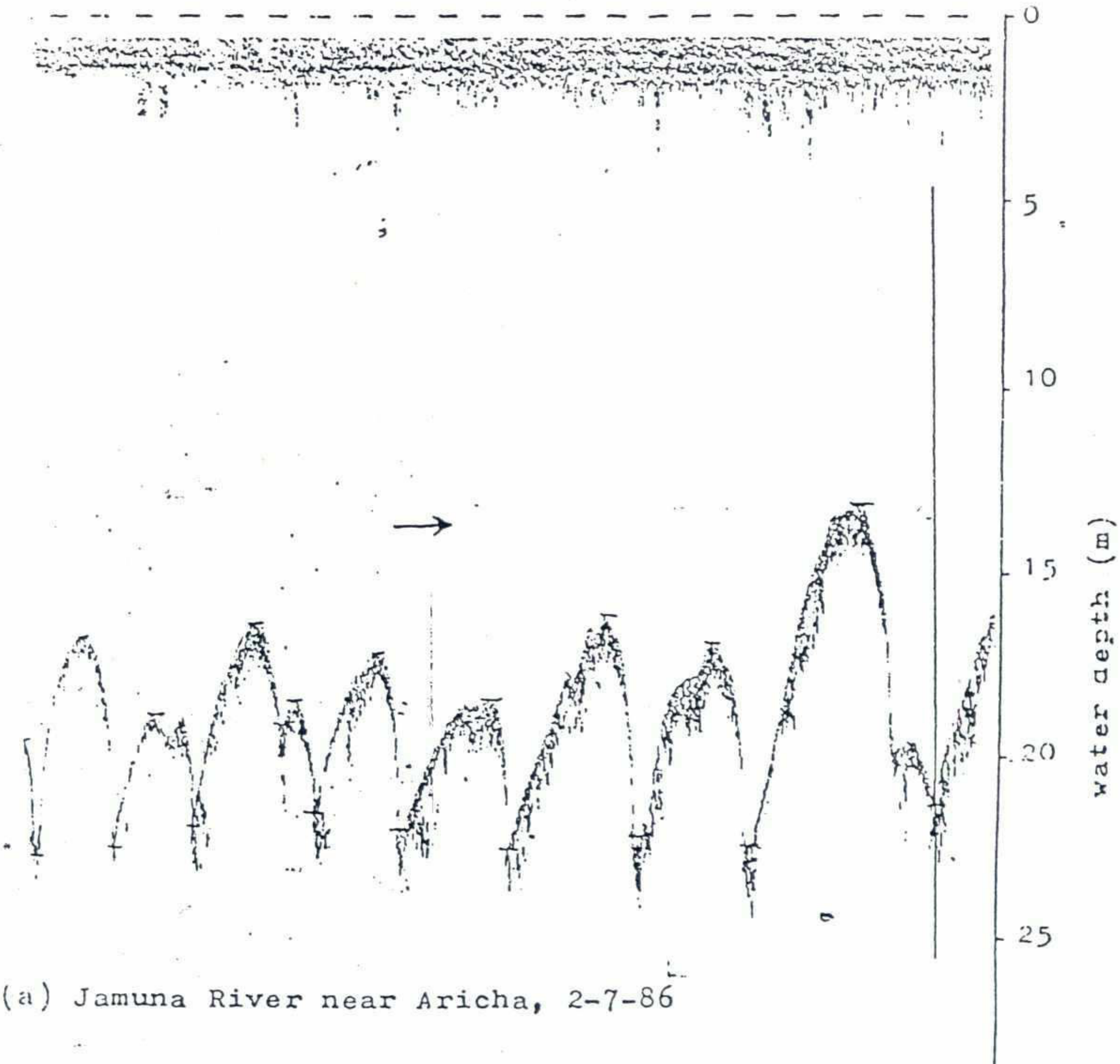

(a) Jamuna River near Aricha, 2-7-86

FIGURE C-3.16 BEDFORM DIMENSIONS JAMUNA RIVER

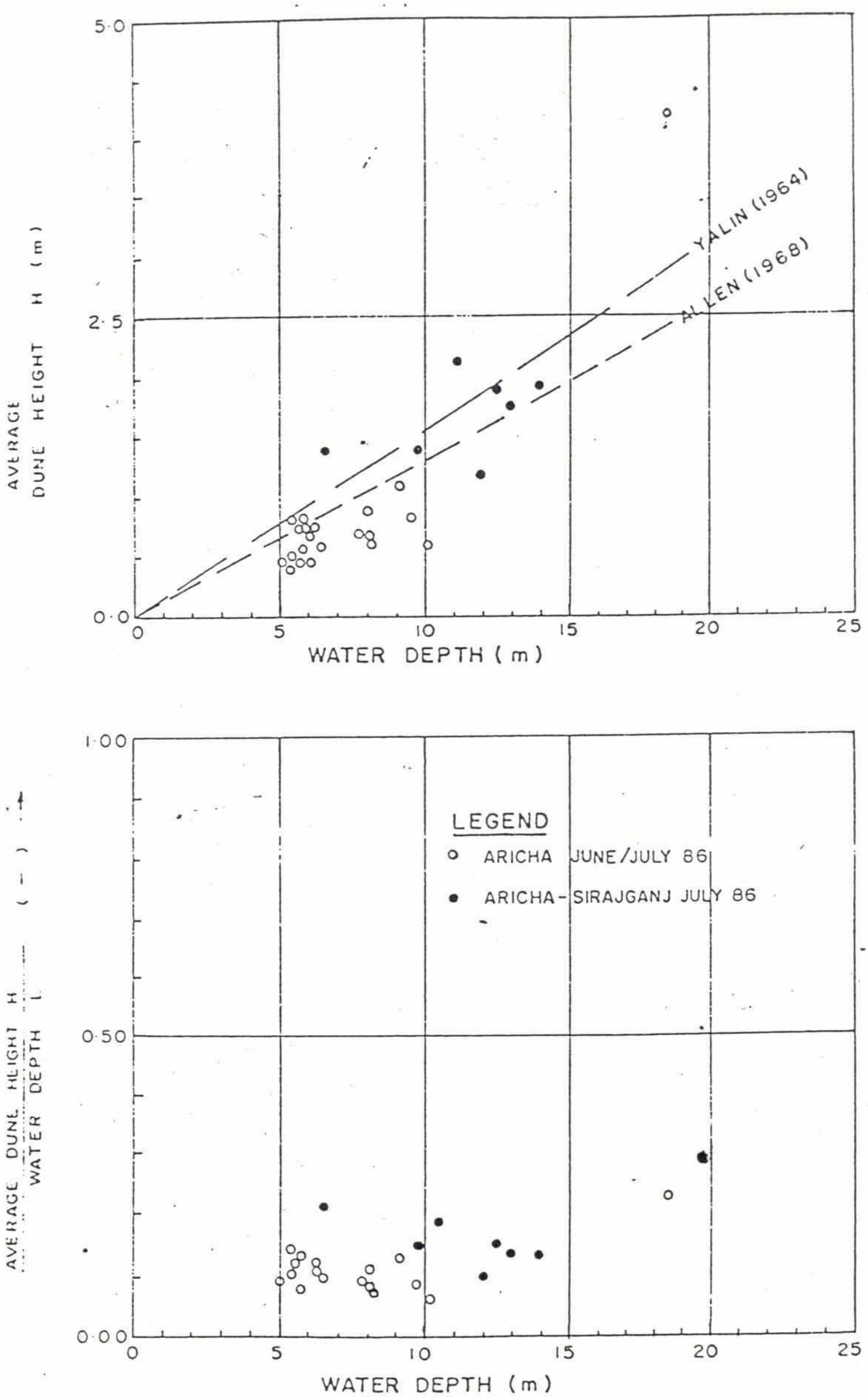

FIGURE C-3·17 MEASURED BEDFORM HEIGHT VERSUS WATER DEPT

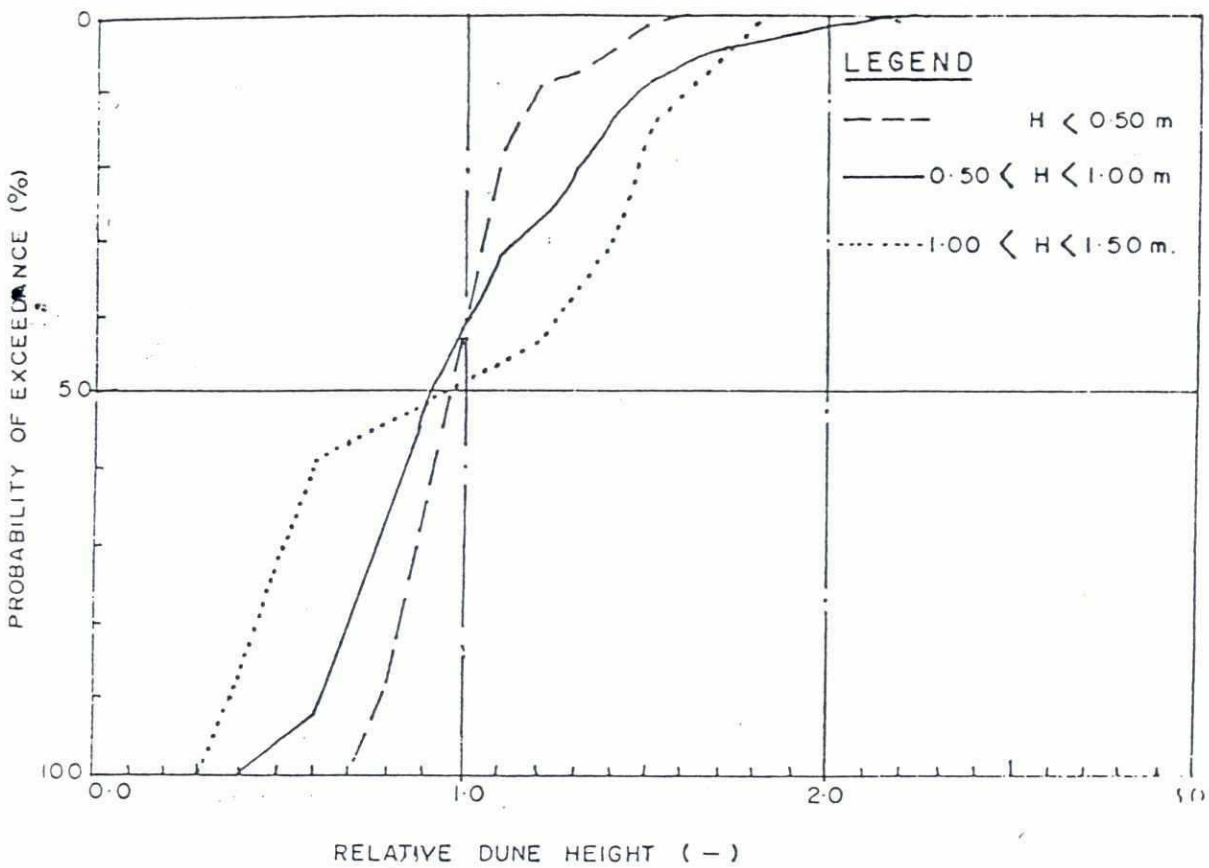

FIGURE C – 3·18 PROBABILITY RELATIVE DUNE HEIGHTS ECHO-SOUNDINGS ARICHA

TH

VRV

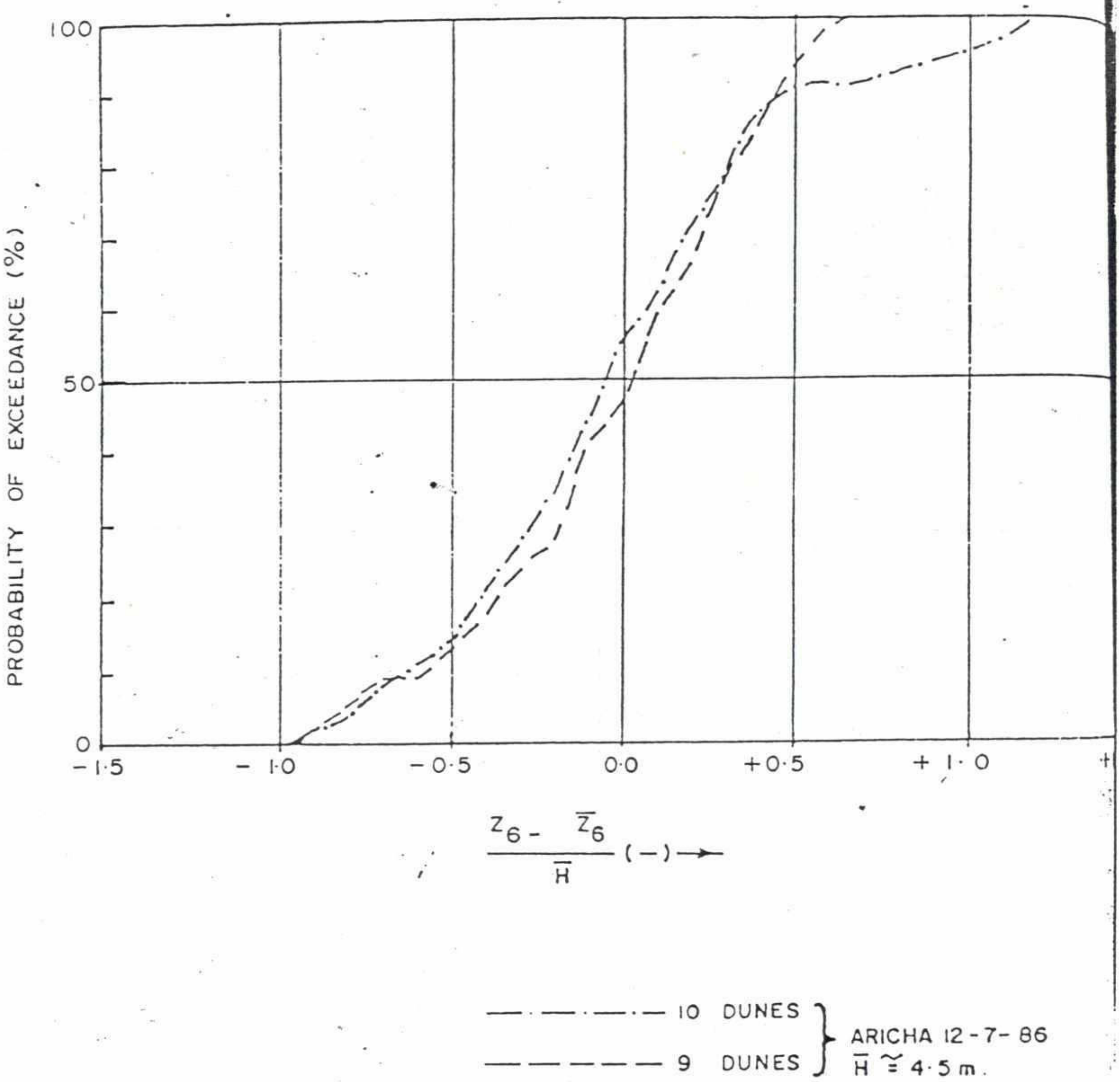

FIGURE C-3.19 PROBABILITY BED LEVEL HEIGHTS ECHO-SOUNDINGS AR

2Ø

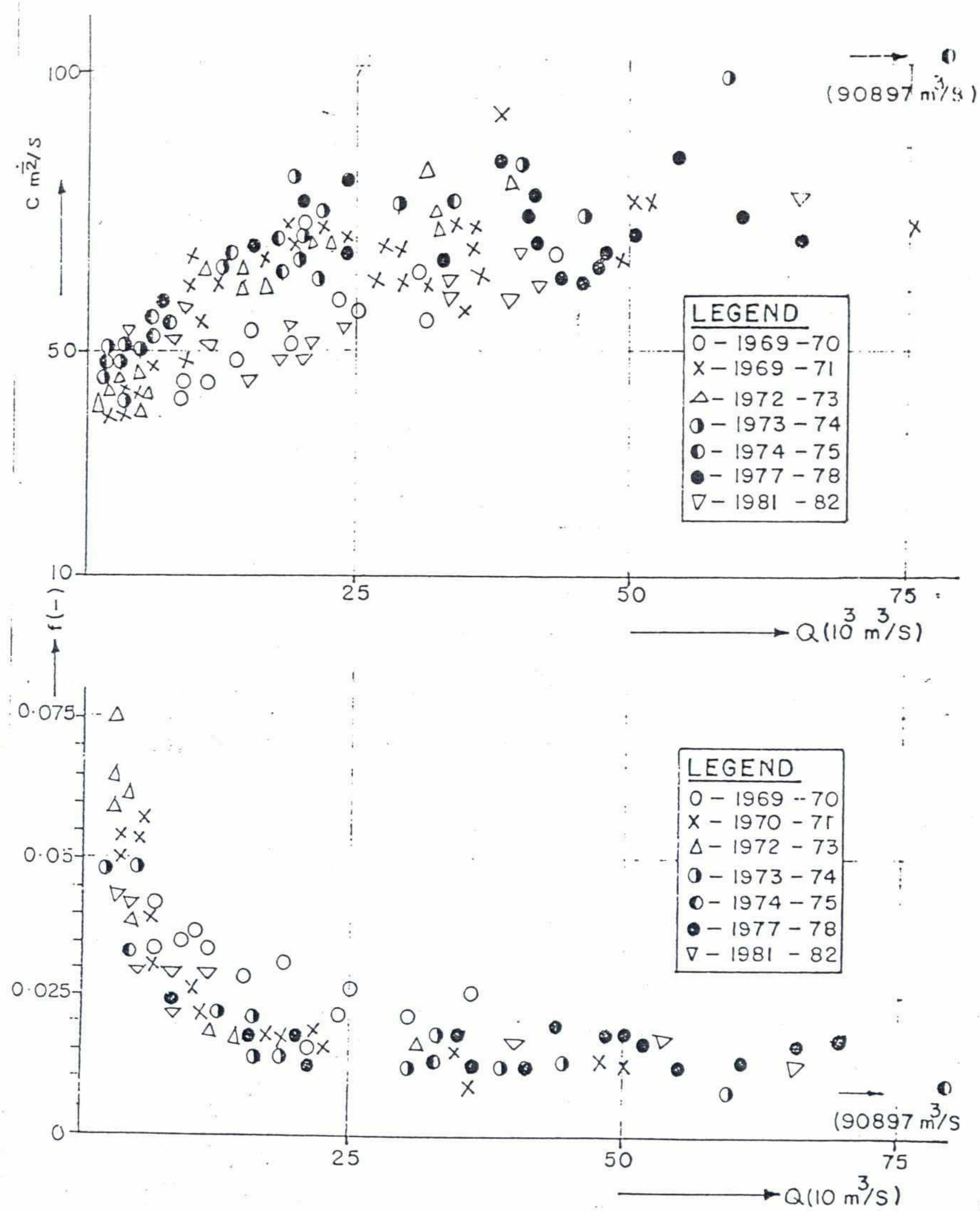

FIG. C-3.20 RESISTANCE TO FLOW JAMUNA RIVER AT BAHADURABAD

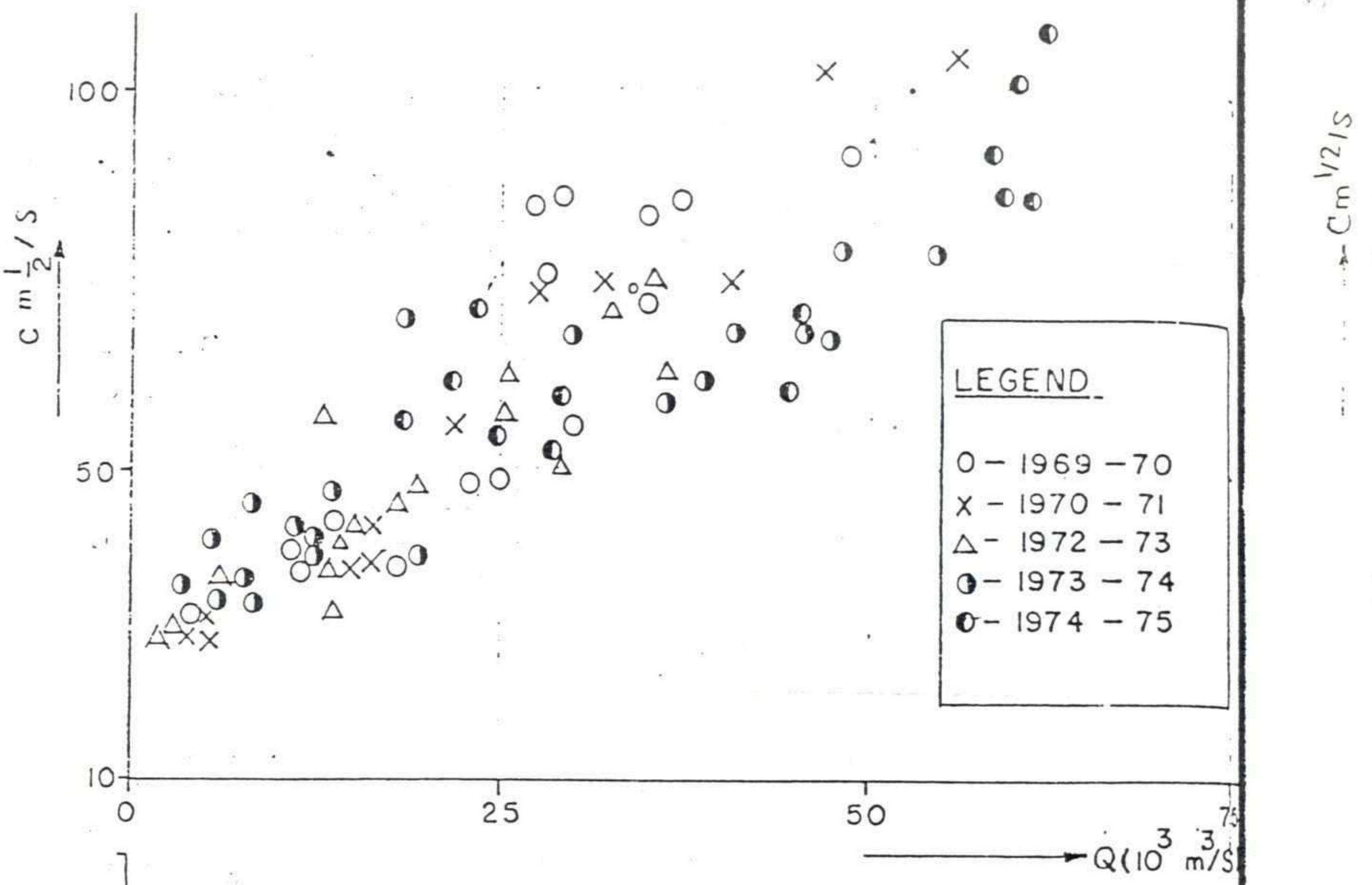

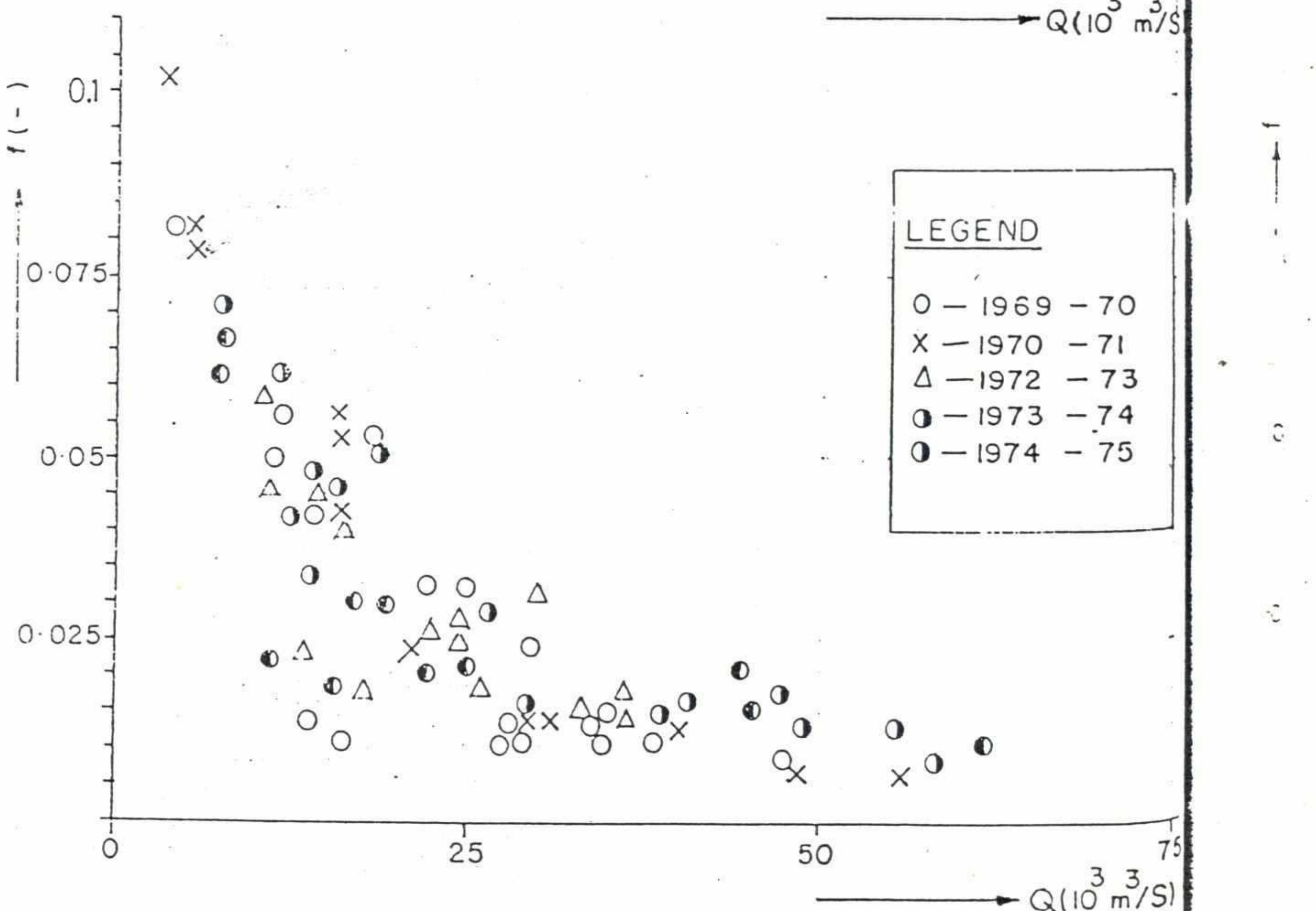

FIG. C - 3·21 RESISTANCE TO FLOW JAMUNA RIVER AT SIRAJGANJ

102

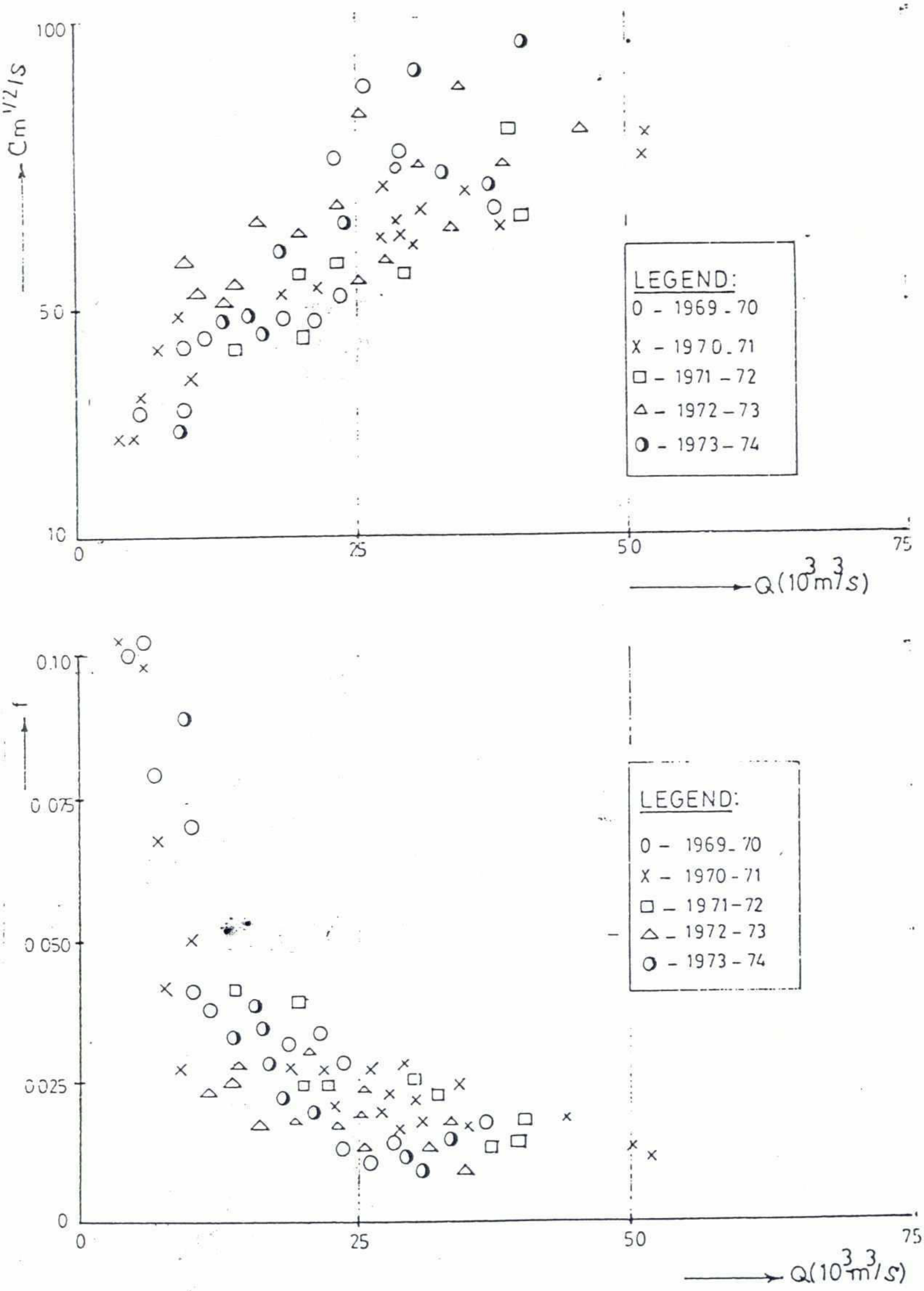

FIGURE C-3.22 Resistance to flow Jamuna river at Nagarbari

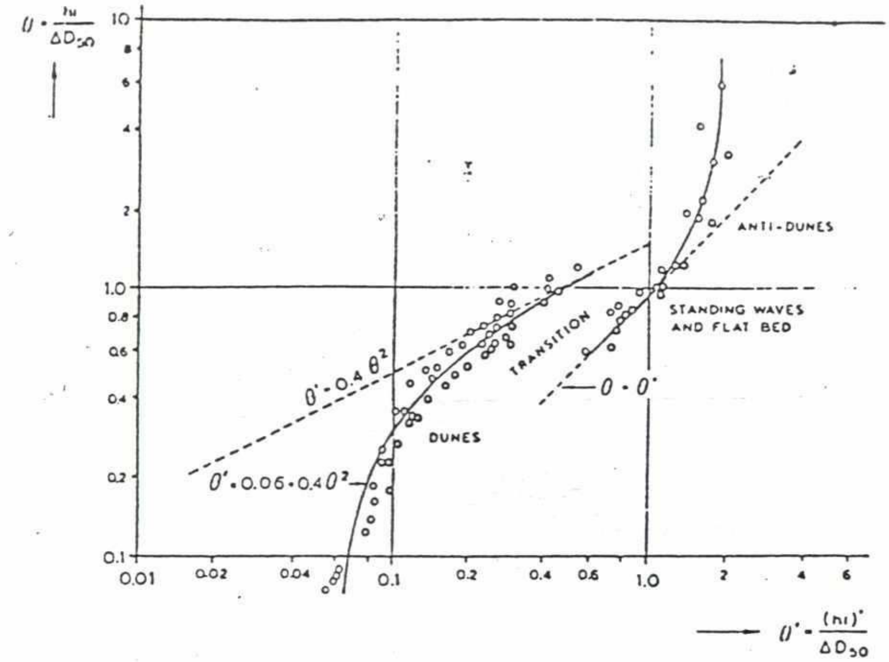

(a) Resistance graph after Englund/Hansen (1967)

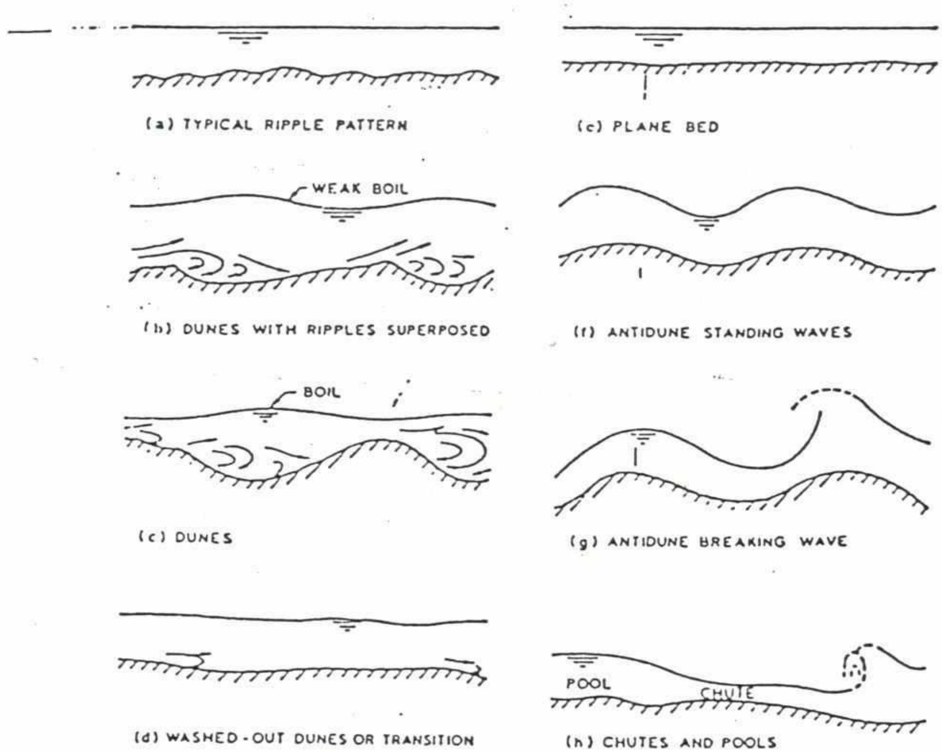

(b) Hierarchy of bedforms

FIGURE C-3.24 RESISTANCE TO FLOW AND BEDFORMS.

268

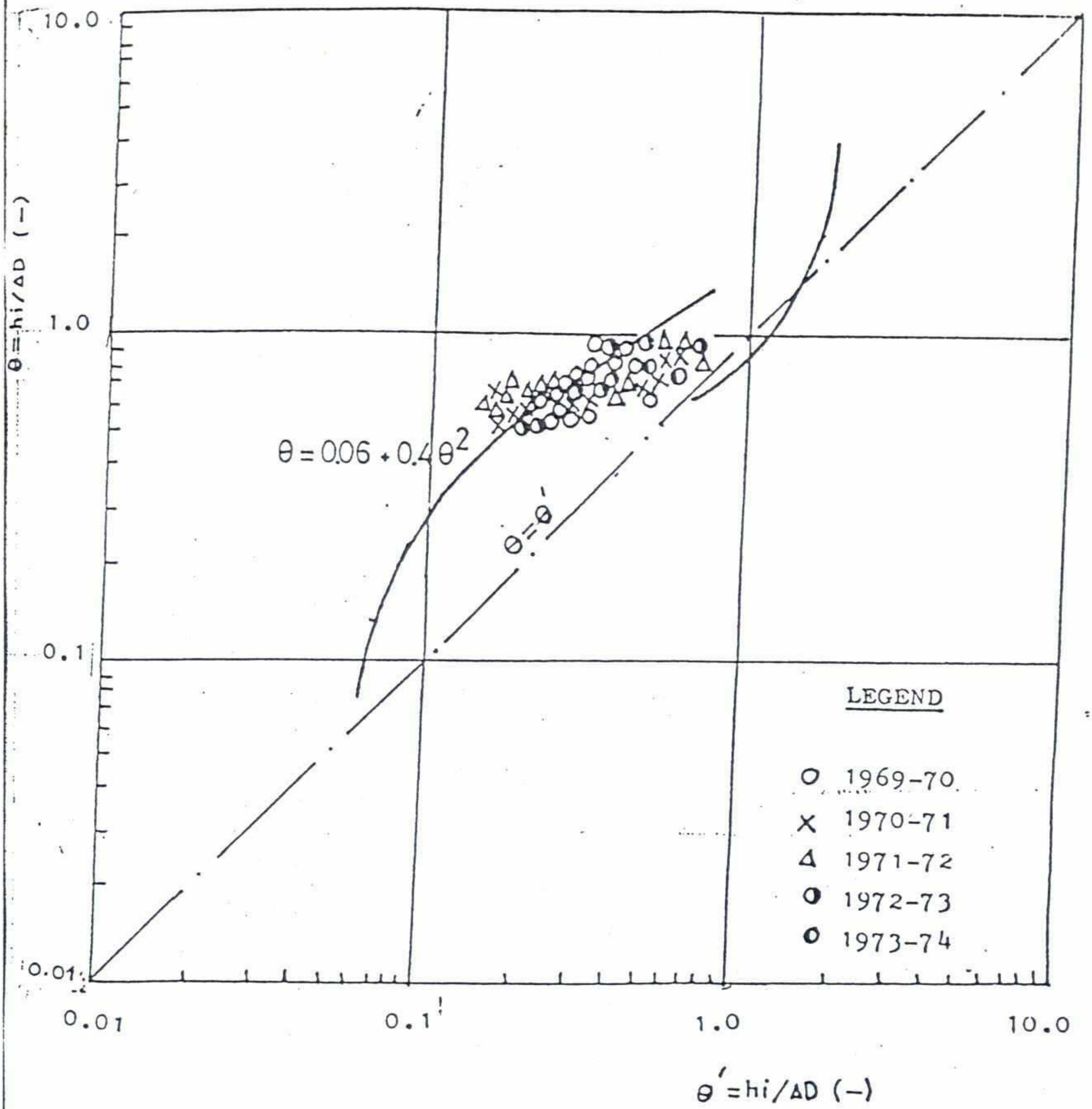

FIGURE C-3.25 COMPARISON OF BAHADURABAD DATA WITH THE ENGELUND/
HANSEN (1967) PREDICTOR.

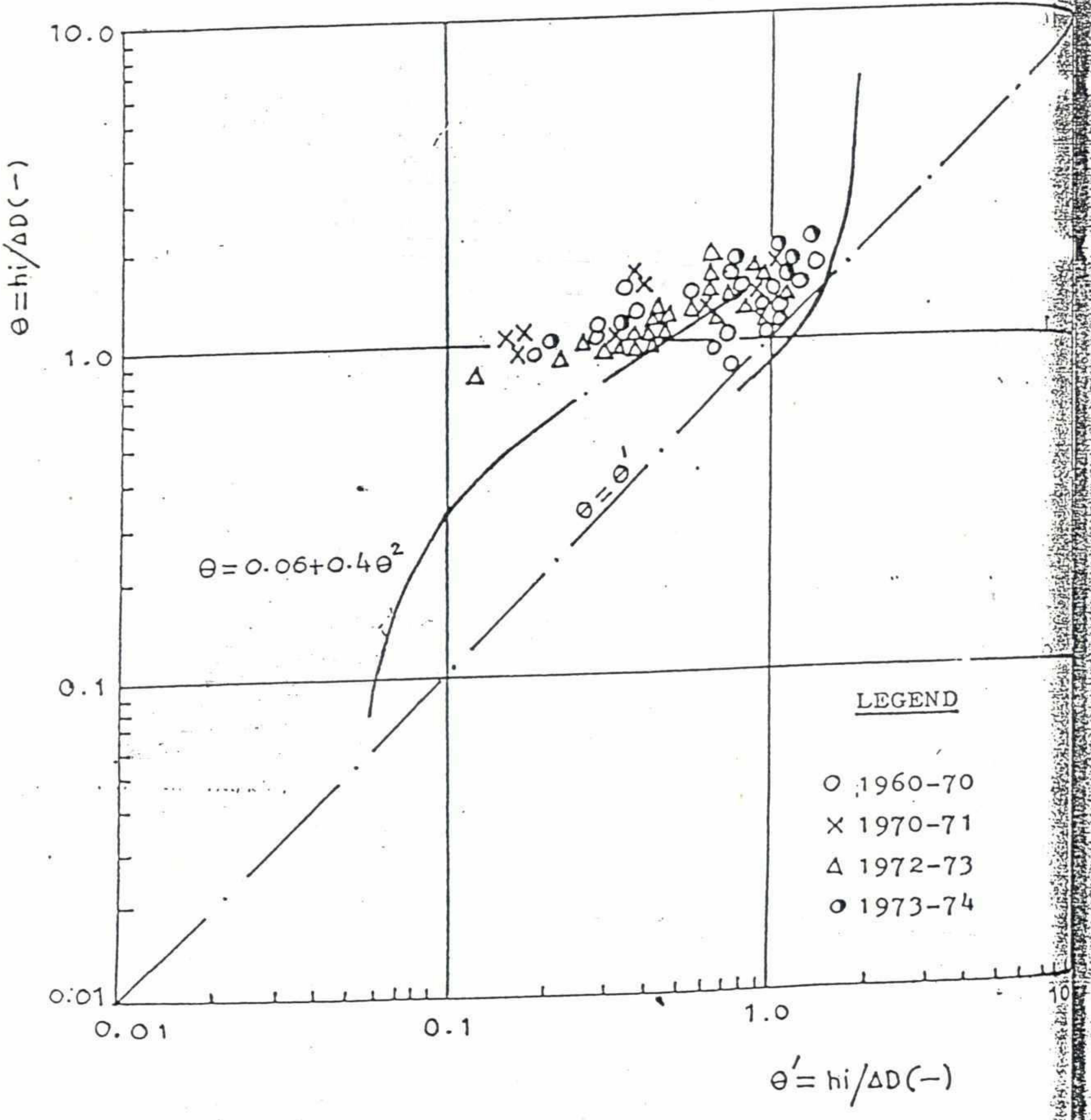

FIGURE C-3.26 COMPARISON OF SIRAJGANJ DATA WITH THE ENGELUND/ HANSEN (1967) PREDICTOR.

2G3

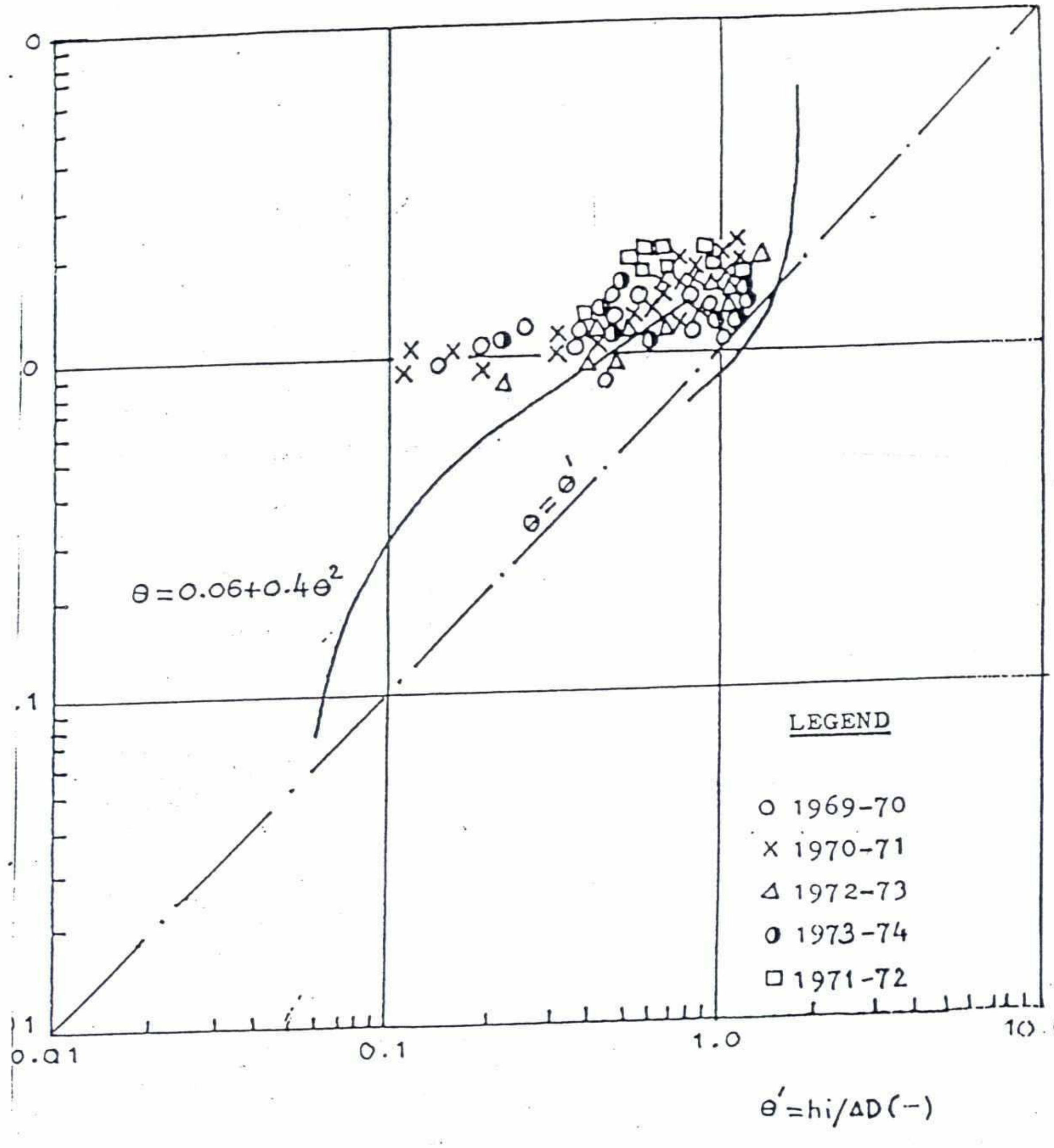

IGURE C-3.27 COMPARISON OF NAGARBARI DATA WITH THE ENGELUND/ HANSEN (1967) PREDICTOR.

209

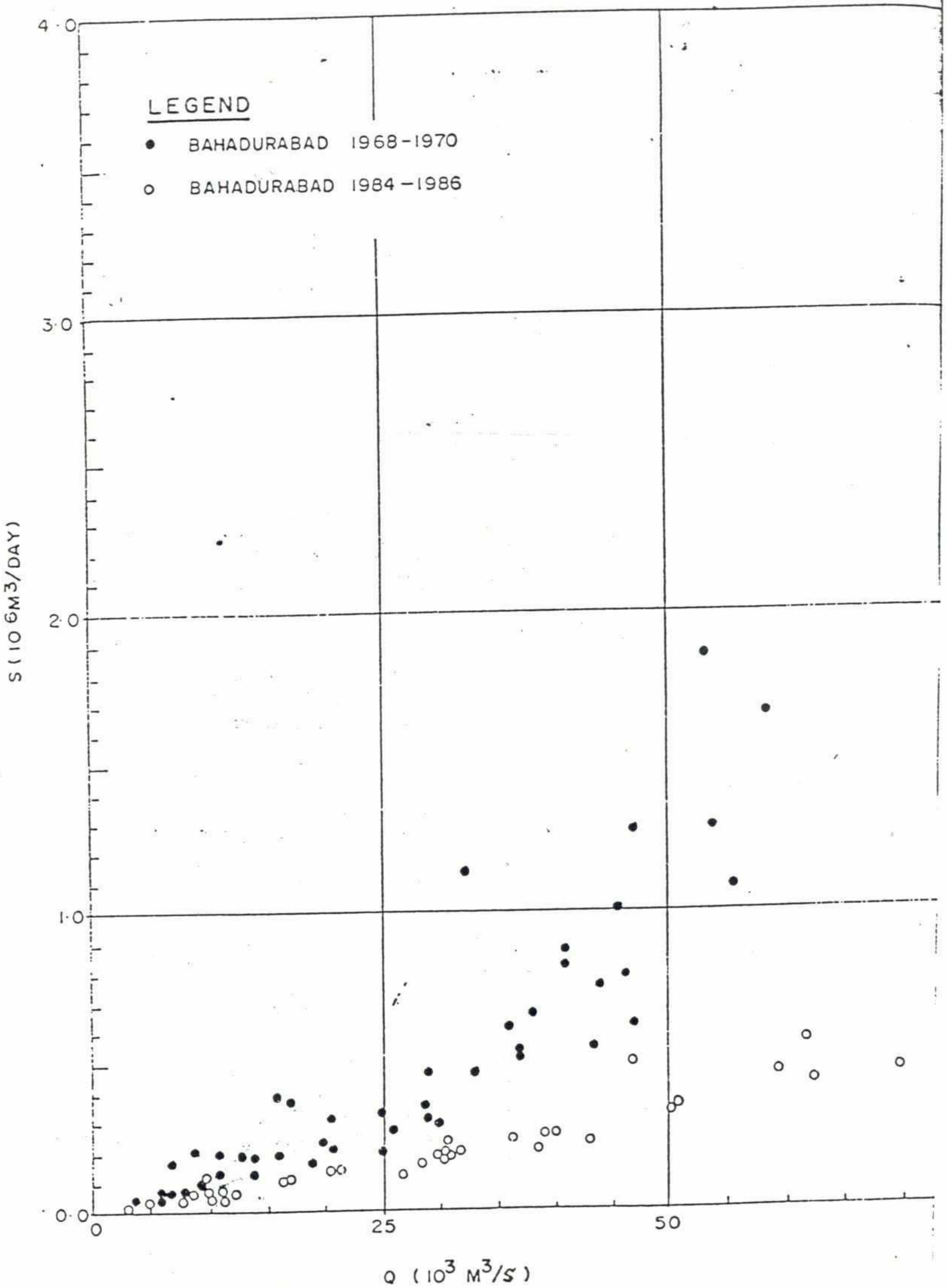

FIGURE C-3.28 COARSE SEDIMENT TRANSPORT IN JAMUNA RIVER AT BAHADI

26

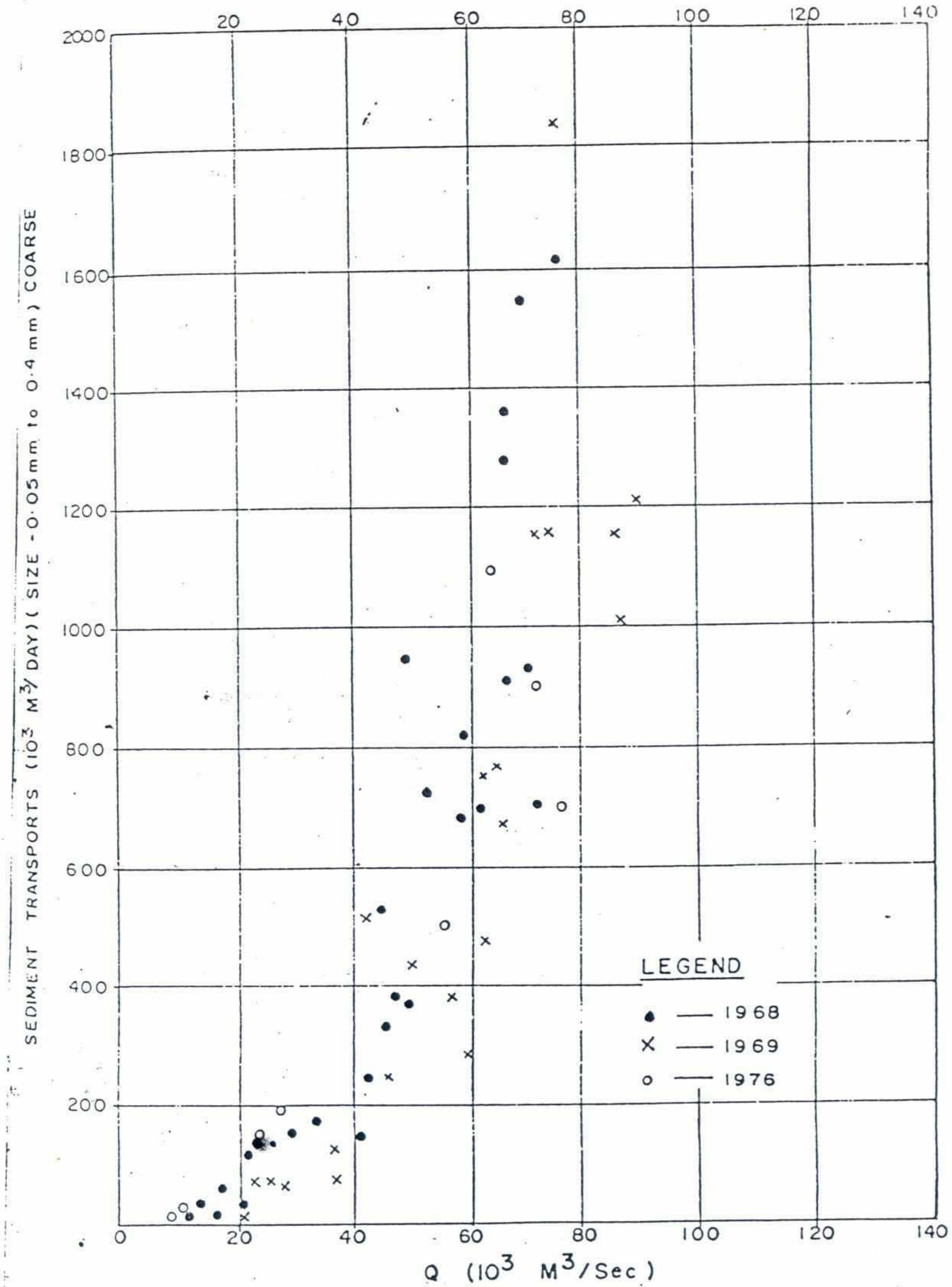

FIGURE C-3·29 COARSE SEDIMENT TRANSPORT PADMA RIVER AT MAWA

262

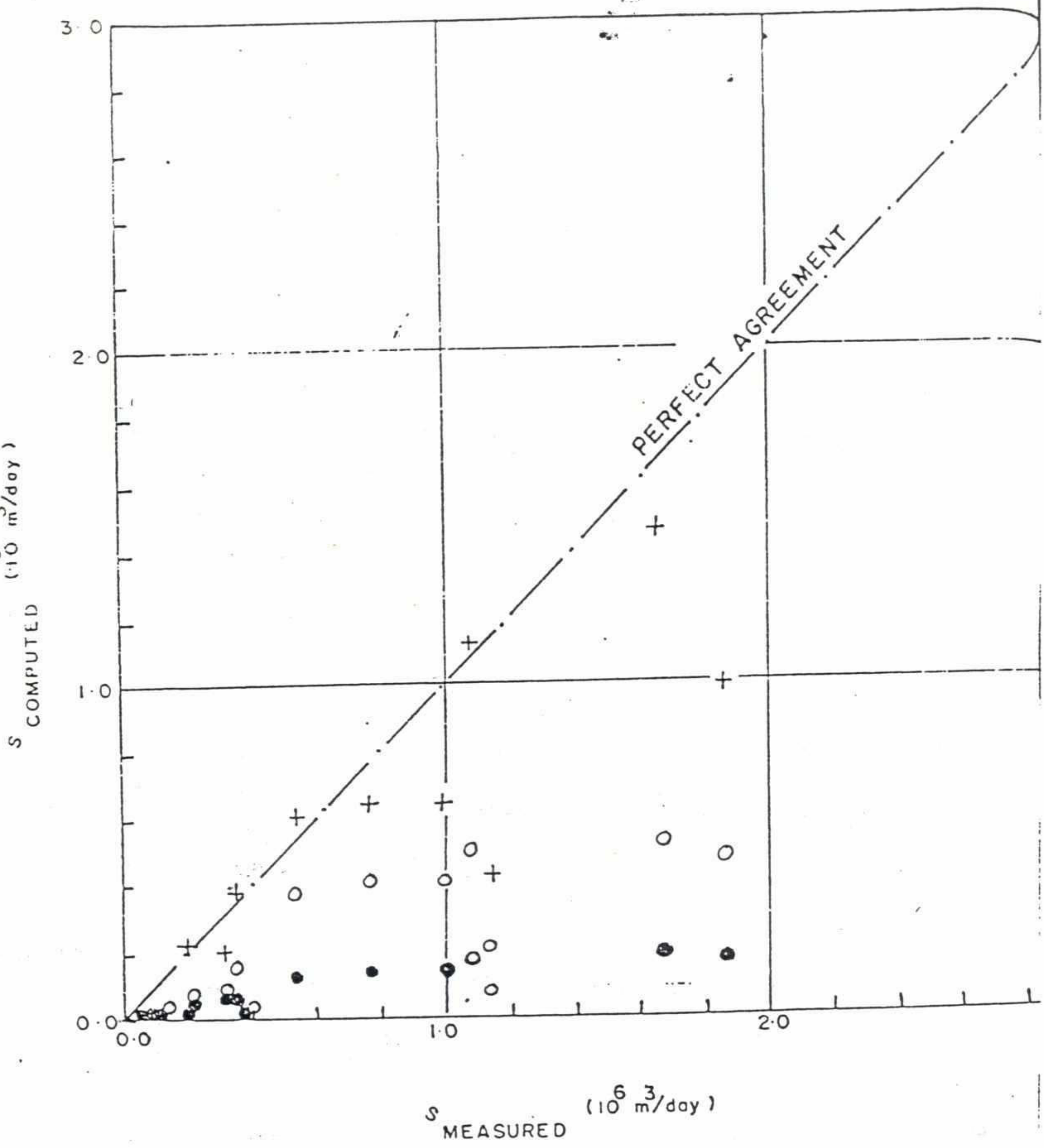

LEGEND

● ENGELUND/HANSEN (1967)

○ ACKERS/WHITE (1973)

+ VAN RIJN (1984)

BAHA[
19

FIGURE C-3·30

COMPARISON OF MEASURED AND COMPUTED SEDIMENT TRANSPORT IN JAMUNA RIVER AT BAHADURABAD.

FIGURE C-3.31 JAMUNA AND PADMA F
FROM SATELLITE IMAG

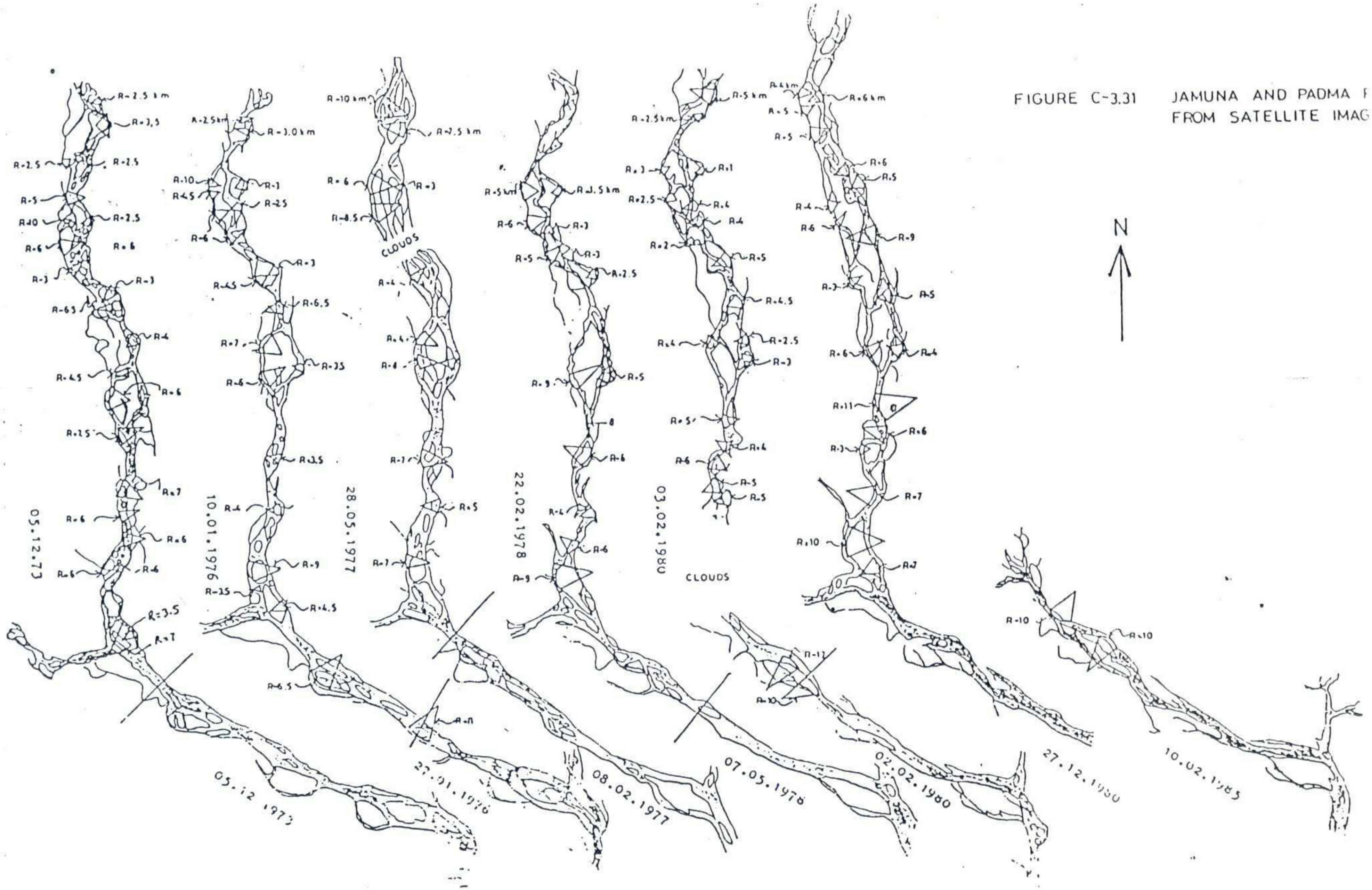

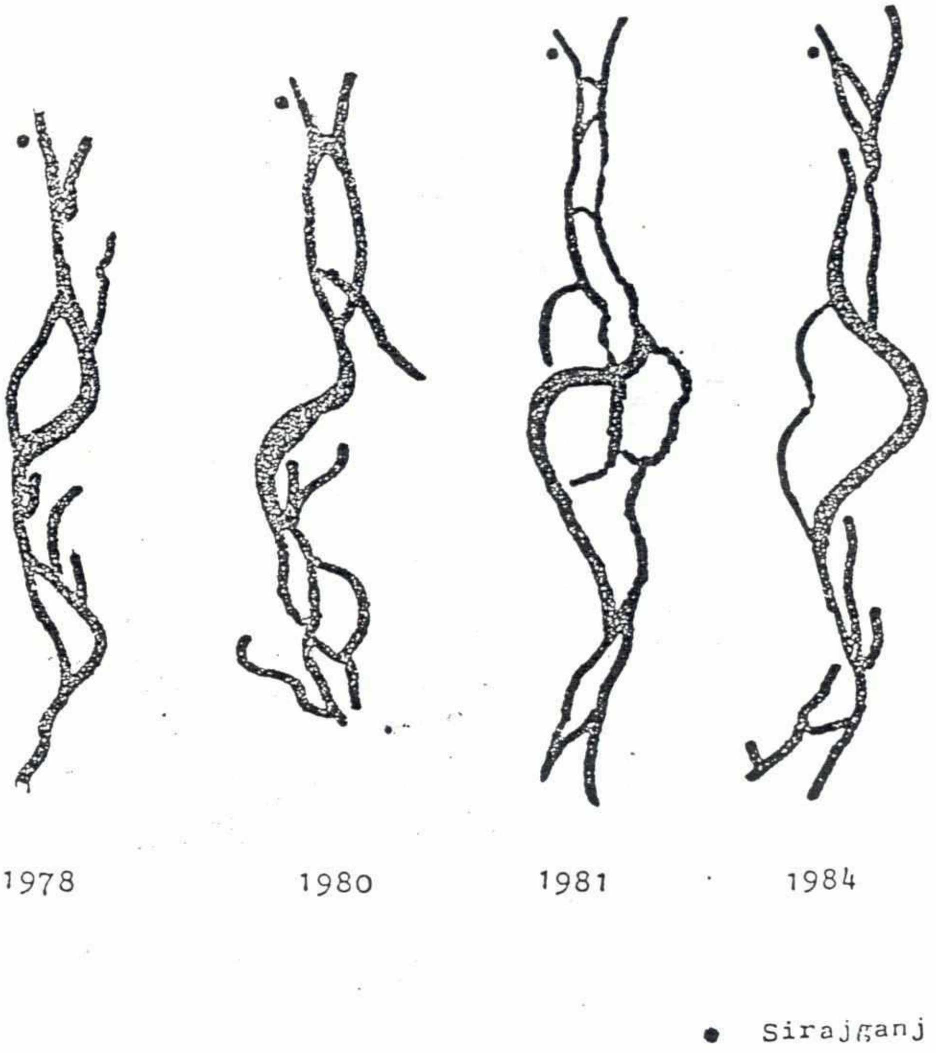

FIGURE C-3.32 PLANFORM CHANGES JAMUNA RIVER DOWNSTREAM OF SIRAJGANJ (Approximate Scale 1:500.000).

282

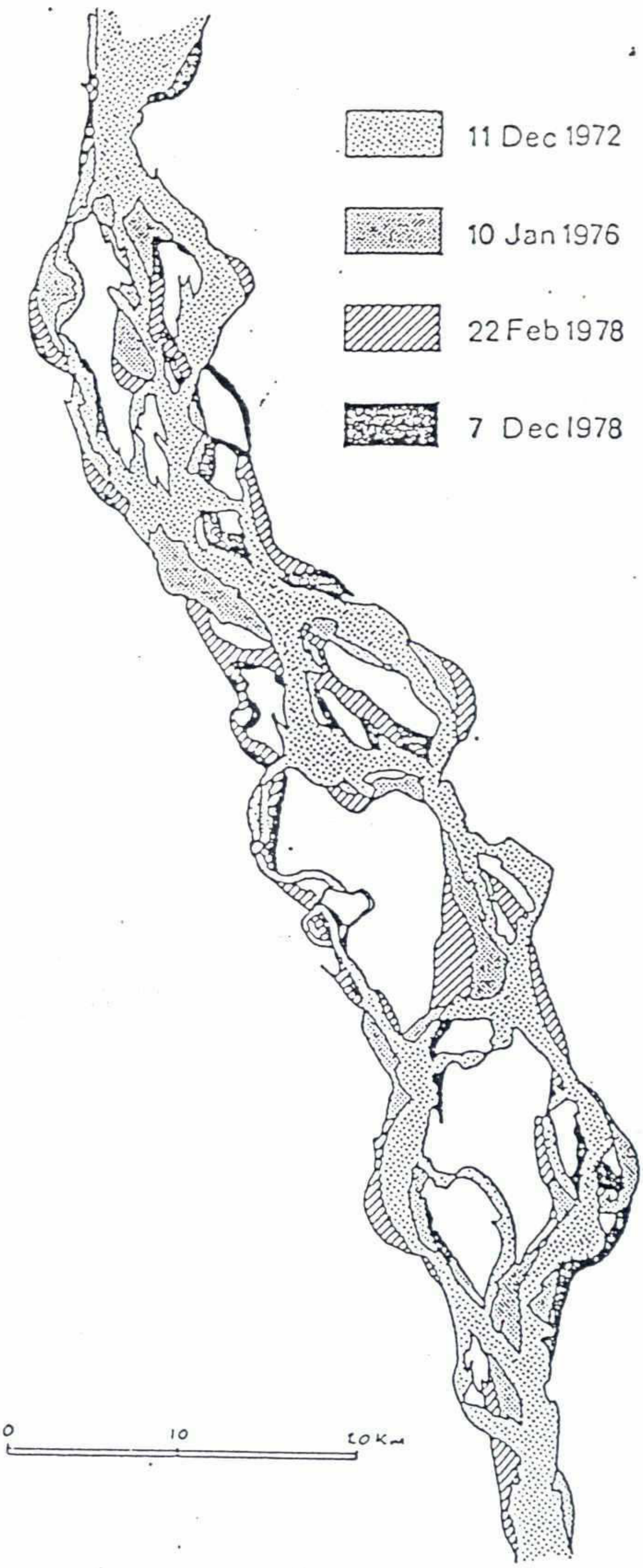

FIGURE C-3.33 CHANNEL PATTERN JAMUNA RIVER UPSTREAM OF SIRAJGANJ (BRISTOW, 1985).

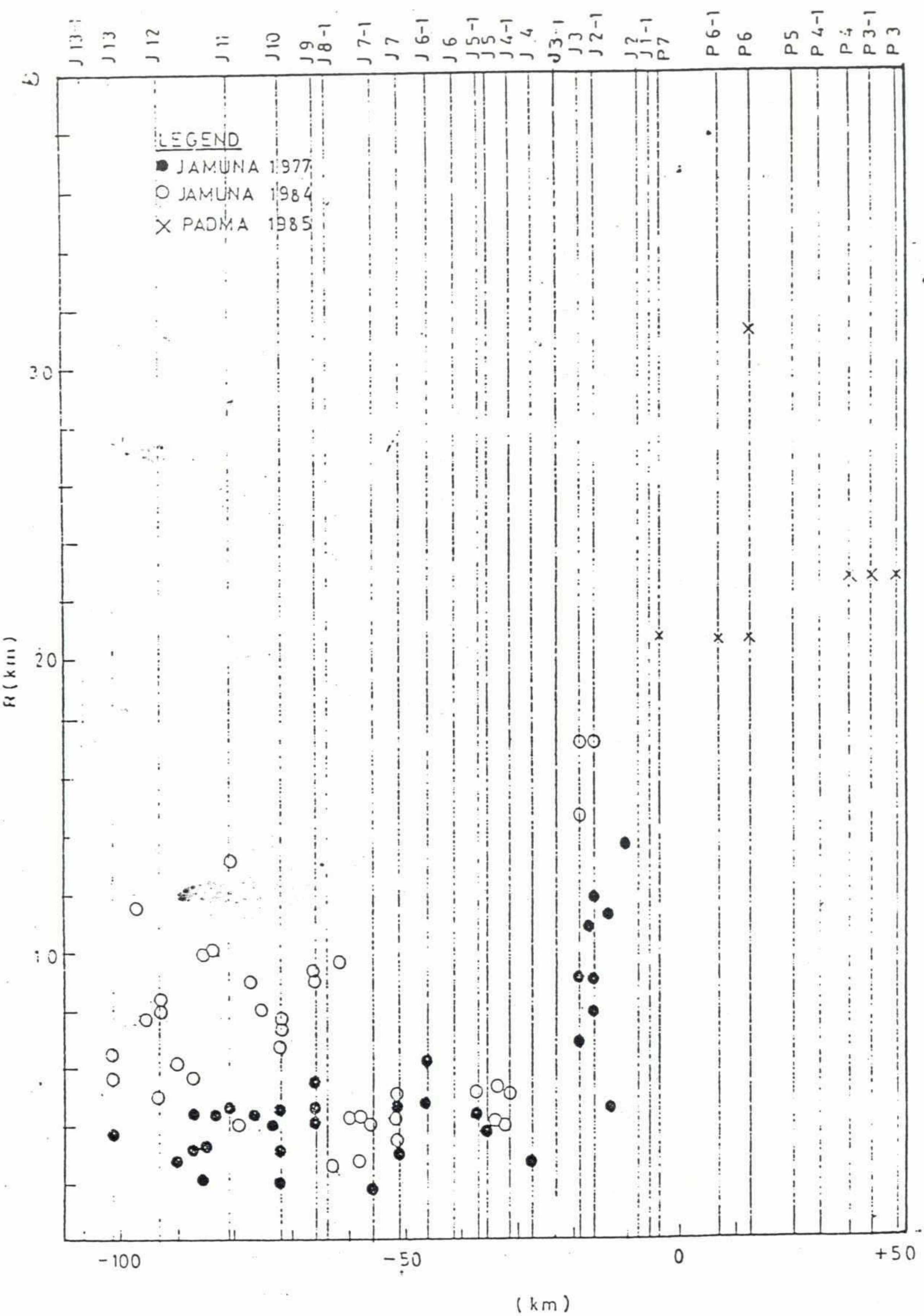

FIG. C-3.34 CHANNEL CURVATURE VERSUS CHAINAGE

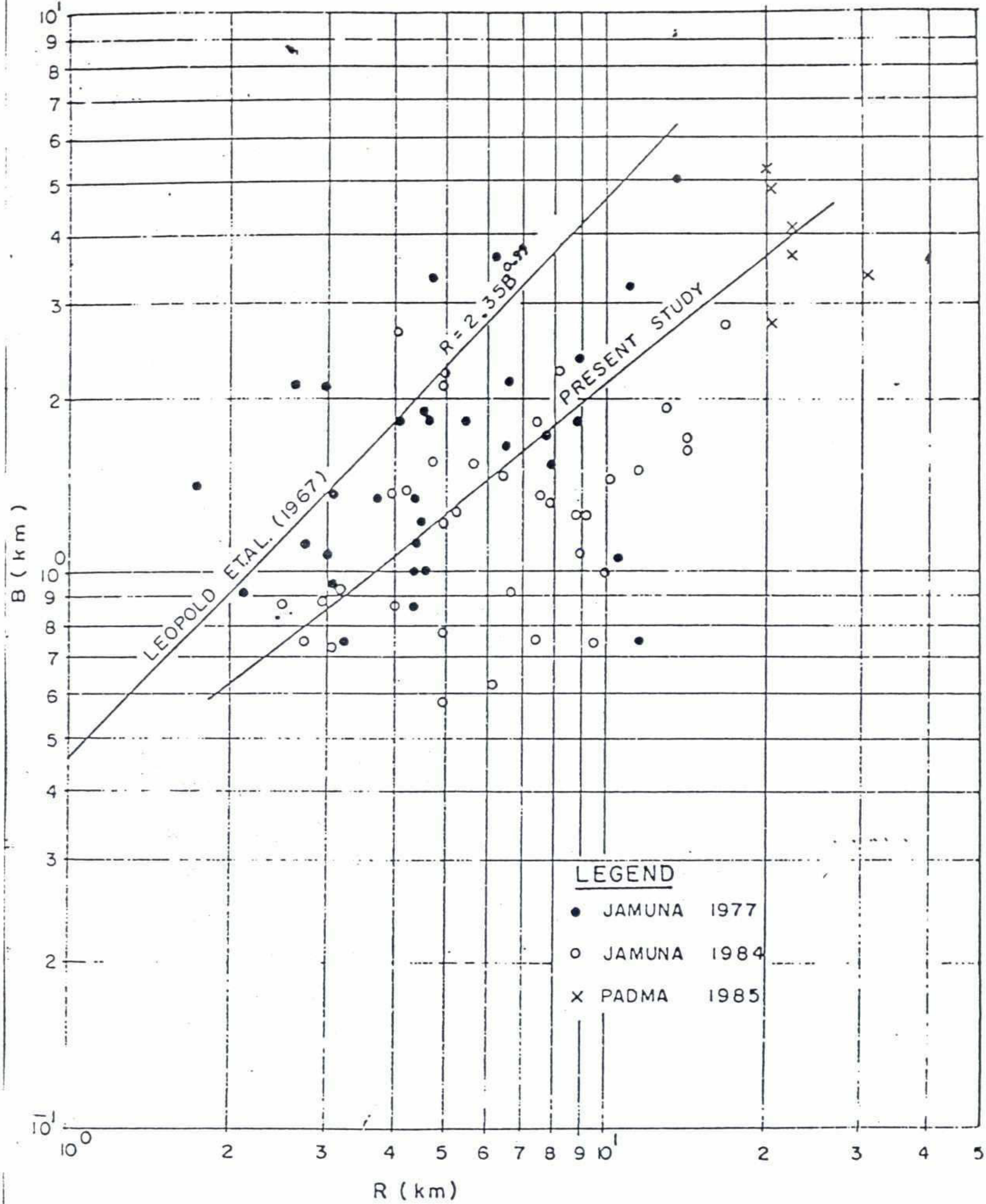

FIGURE C-3·35 WIDTH VERSUS CURVATURE FOR THE JAMUNA & PADMA RIVERS

588

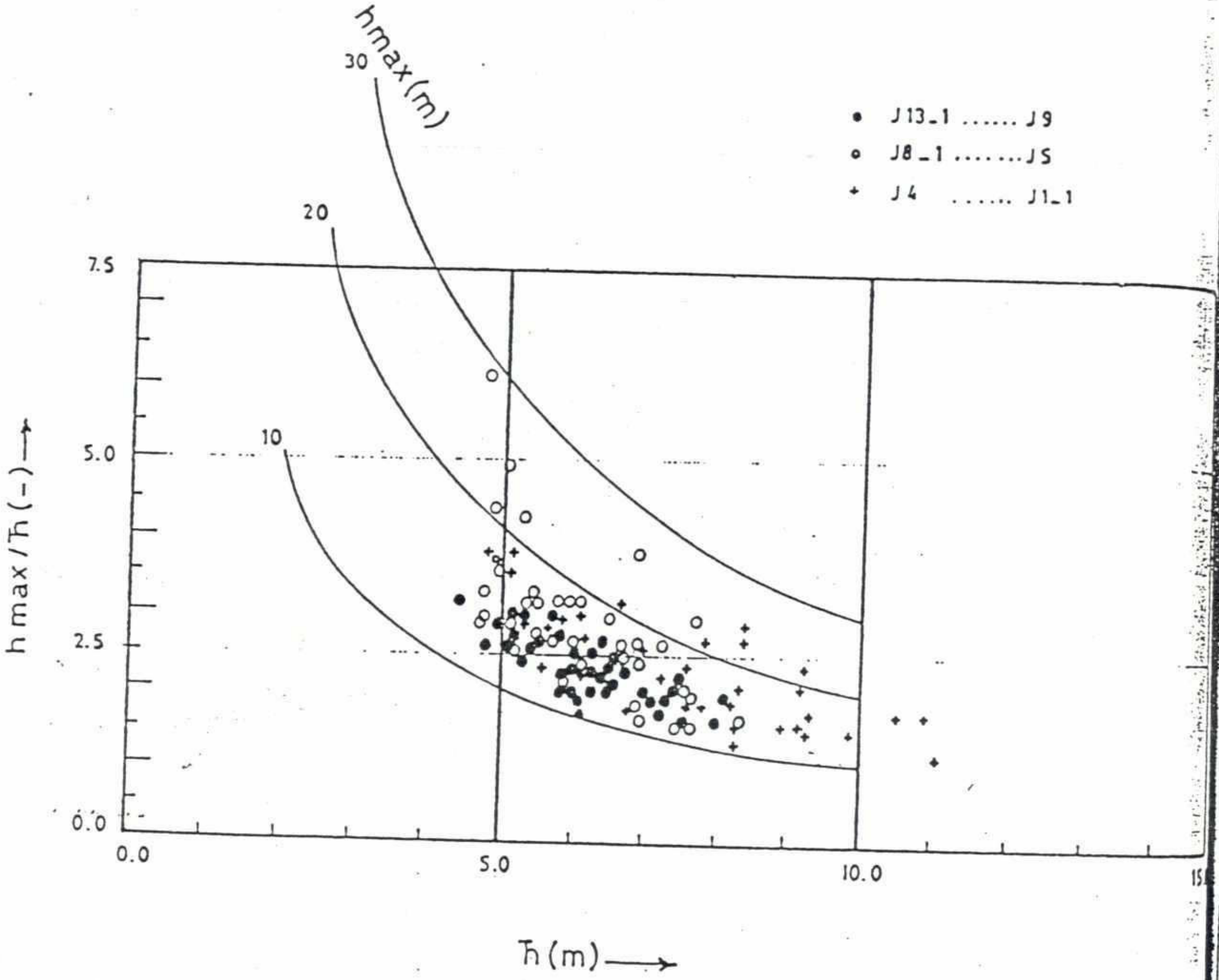

FIGURE C_3.36 RATIO OF hmax/h̄ versus h from BWDB— Soundings

283

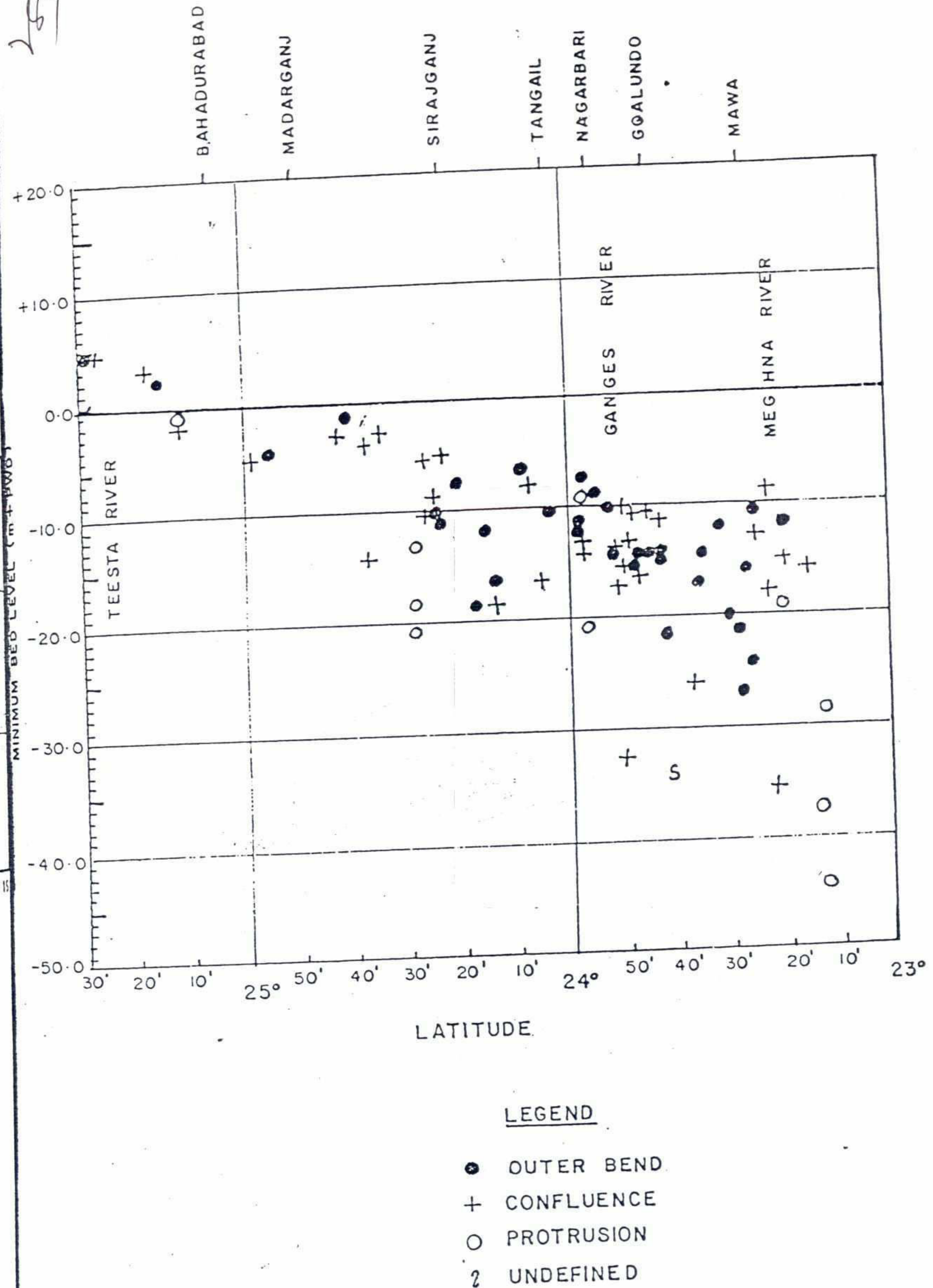

FIGURE C-3·37 MINIMUM BED LEVELS IDENTIFIED ON BIWTA SOUNDING CHARTS

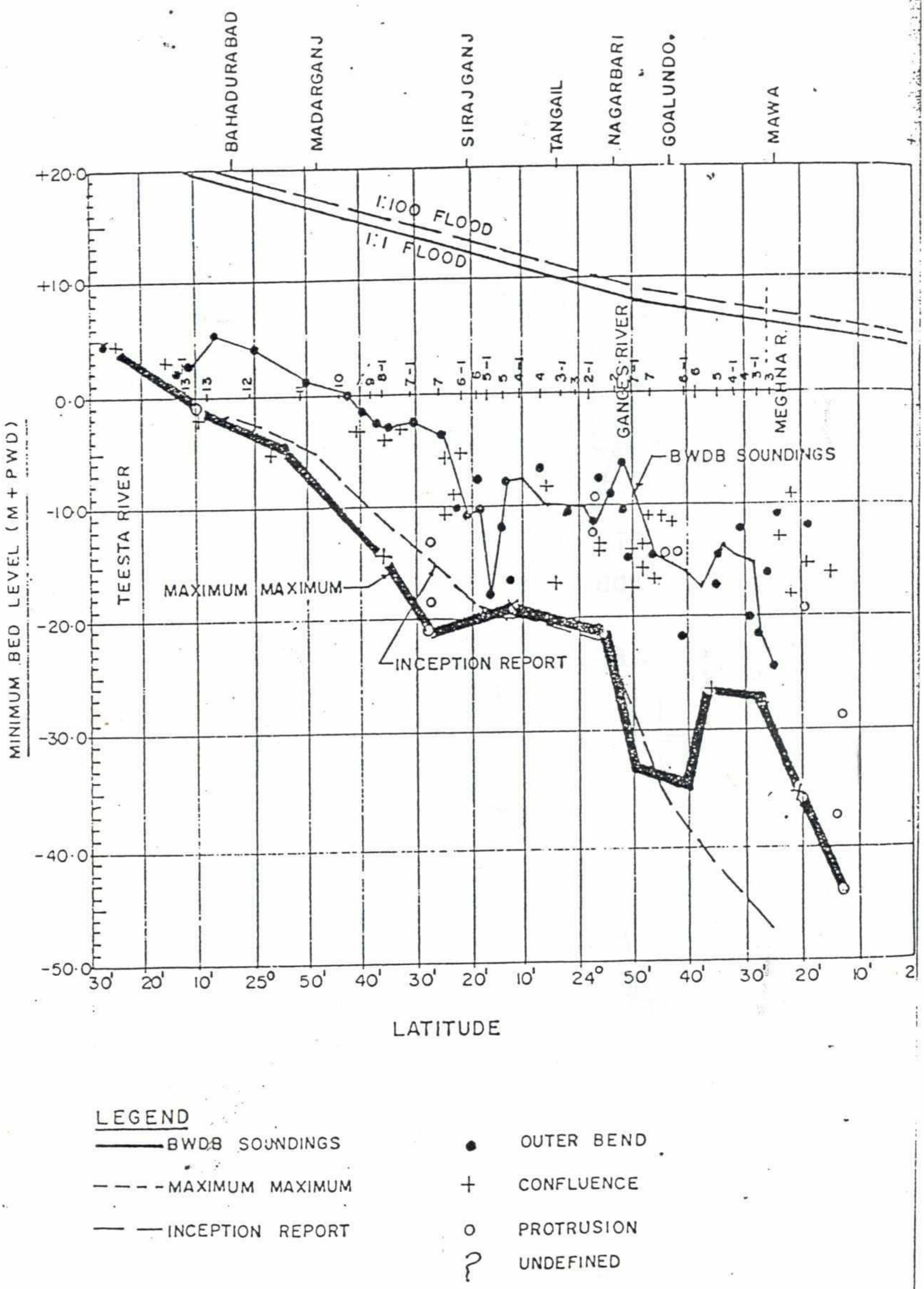

FIGURE C-3·38 MINIMUM BED LEVELS FROM DIFFERENT SOURCES

258

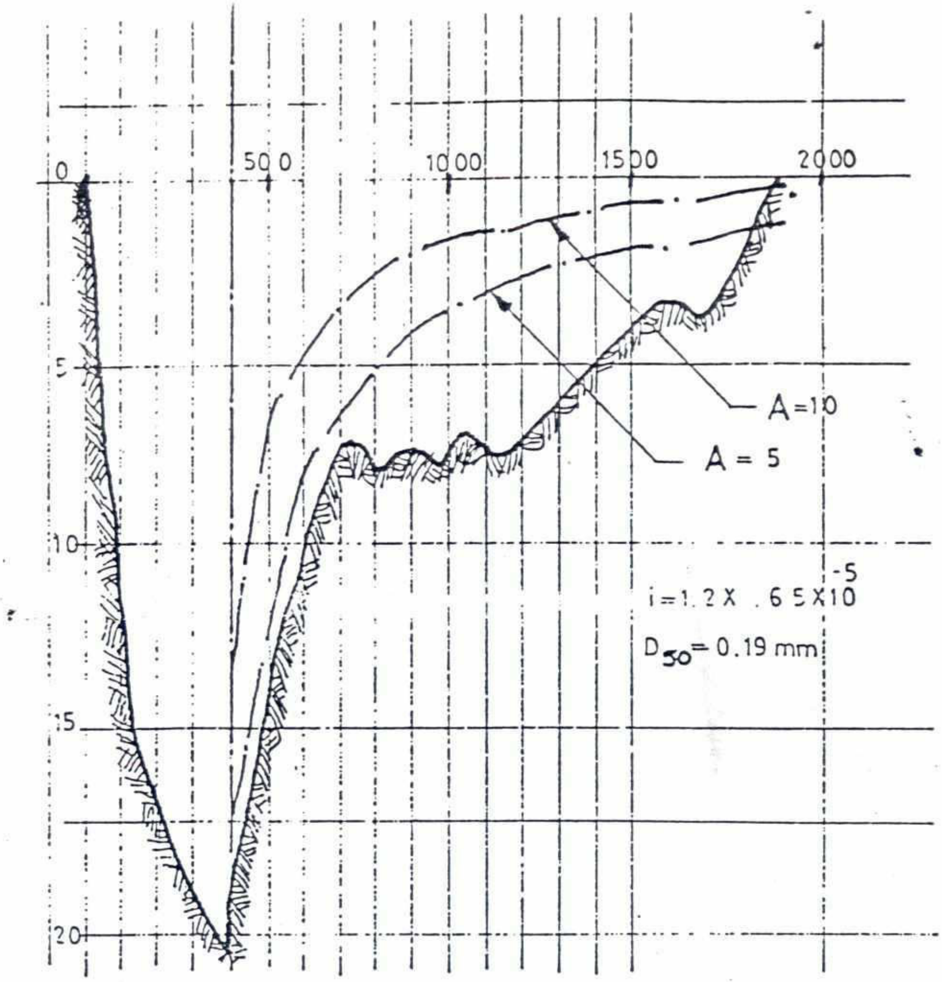

(a) BWDB CROSS-SECTION J5-1, 1977

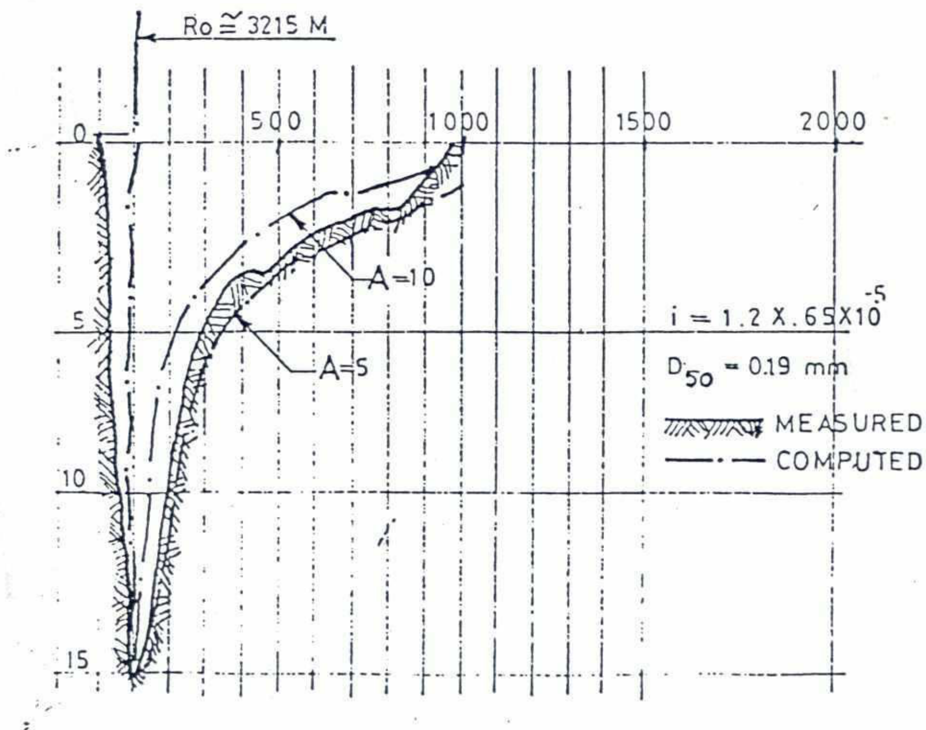

(b) BWDB - CROSS SECTION J-4, 1977

FIG. C-3.39 COMPARISON OF MEASURED AND COMPUTED BEND PROFILES

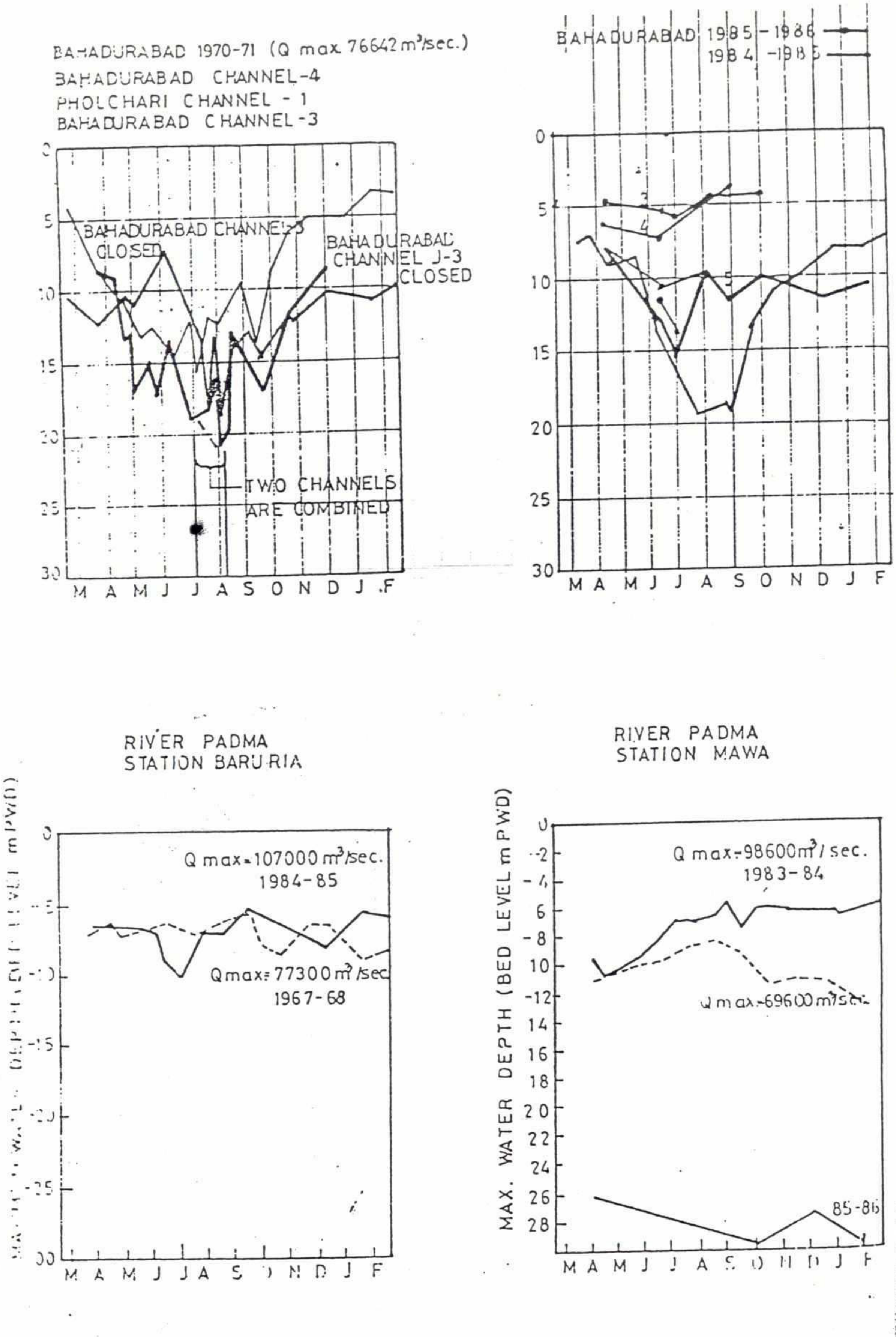

FIG. C-3.40 BED LEVEL CHANGES IN MAIN CHANNELS USED FOR DISCHARGED MEASUREMENTS

700

GOVERNMENT OF BANGLADESH

UNITED NATIONS DEVELOPMENT PROGRAMME / WORLD BANK

JAMUNA BRIDGE PROJECT

PHASE II STUDY FEASIBILITY REPORT

VOLUME II

ANNEX A: HYDROLOGY
ANNEX B: RIVER MORPHOLOGY
ANNEX D: RIVER TRAINING WORKS
ANNEX I: RISK ANALYSIS

Rendel Palmer & Tritton

nedeco

Bangladesh Consultants Ltd

AUGUST 1989

ANNEX B

River Morphology

B.3 Scour

From : RPT/Nedeco/BCL (1989), Jamuna Bridge Project, Phase II Study, Feasibility report

B.3 Scour

B.3.1 Introduction

In this chapter maximum scour depths in the Jamuna River will be discussed. In principle there are two possible approaches to this problem of maximum scour. The first one is to collect all available data on scour depths which have been measured during low, intermediate and (sometimes) average flood conditions and to extrapolate these data to extreme flood conditions. This approach is essentially followed in Section B.3.9. A second approach is to split up the total scour into the contributing elements (like bend or confluence scour, bedforms and local scour) and to extrapolate each of them seperately to flood conditions. The total scour in that case can be computed from the different contributions, taking into account any correlations, where appropriate. This is also done in Section B.3.9; the different contributions to scour, however, are discussed in the following sections.

B.3.2 Regime equations for Jamuna channels

Regime equations have originally been developed for stable canals on the Indian subcontinent. Lacey (1930,1947) derived the following equations for the wetted perimeter p and the hydraulic radius R of a stable channel:

$$p = 2.67\, Q^{1/2} \qquad \text{(B.3.1)}$$

$$R = 0.47 \left(\frac{Q}{f}\right)^{1/3} \qquad \text{(B.3.2)}$$

where Q = bankfull discharge and f = silt factor, defined via:

$$f = 1.59\, D_{50}^{\,1/2} \qquad \text{(B.3.3)}$$

where D_{50} = diameter of the bed sediment in mm. All other parameters are expressed in imperial units. Simons and Albertson (1963) extended the regime equations to include the effect of the soil properties of the banks. For canals with sandbanks and sandbeds they found:

$p = 3.3\ Q^{0.512}$ (B.3.4)

pointing at slightly larger widths for channels with sandy banks. Some others, e.g. Stevens (1986), have shown that the above equations hold for small sediment charges only. For larger charges the width may be larger.

It is of interest to attempt to compare the characteristics of the individual channels of the braiding Jamuna River to these regime equations. This was done for bankfull discharge (44,000 m^3/s). When it is assumed that the roughness and the energy slope of each channel in a cross-section is about the same, the total discharge in a cross-section can be distributed over the channels according to their conveyance. Next, width B and average depth $\bar{h}$ of the individual channels can be plotted against their discharge. The result is presented in Figure B.3.1. The plotted data can be described by the following relations:

$\bar{h} = 0.23\ Q^{0.32}$ (B.3.5)

$B = 16.1\ Q^{0.53}$ (B.3.6)

Both relations are in S.I - units. The Lacey equations, expressed in these units and assumming $p = B$ and $R = \bar{h}$ for these very wide channels, read:

$\bar{h} = 0.47\ (\frac{Q}{f})^{1/3}$ (B.3.7)

$B = 4.81\ Q^{1/2}$ (B.3.8)

As $D_{50} = 0.2$ mm, $f = 1.13$, so Equation (B.3.7) can be written as:

$\bar{h} = 0.45\ Q^{1/3}$ (B.3.9)

Comparison of the Equations (B.3.8) and (B.3.9) to the Jamuna Equations (B.3.5) and (B.3.6) yields the following conclusions:

- the exponent of the discharge is approximately the same in both comparable equations;
- the Jamuna channels are substantially wider and shallower than the stable channels of Lacey; also the relatively small increase of the width

indicated by Simons & Albertson (1963) is irrelevant for the Jamuna channels.

Apparently large sediment loads (in the Jamuna River up to 10,000 ppm for the total load, wash load included) result in very wide, shallow channels. The width/depth ratio of the Jamuna River is about 750, which is extremely high.

Furthermore, the following remarks are made:

(i) The substantial scatter in Figure B.3.1 is, at least partly, due to the channel direction not being perpendicular to the cross-section. However, other factors will play a role as well.

(ii) Lacey proposed a third equation for the slope of a stable channel. Introducing the relevant figures in this equation results in a slope which is 20% smaller than the actual slope of the Jamuna River.

Average depths and widths can also be derived for lower stages. For this, and also for the previous analysis, it is assumed that the cross-sections sounded during low-flow conditions do not substantially differ from cross-sections for higher stages (see Figure B.3.2). Under this assumption the following average at-a-station relationships are obtained:

$$\bar{h} = 0.56\ Q^{0.23} \qquad (B.3.10)$$

$$B = 18.9\ Q^{0.51} \qquad (B.3.11)$$

The relationship for the width is remarkably similar to the one for bankfull discharge only (Equation (B.3.6)). Apparently the Jamuna channels can to some extent be considered as regime channels for lower stages also, possibly indicating that morphological processes in the Jamuna River are relatively fast.

B.3.3 General scour

General scour is the lowering of the bedlevel owing to changes and developments in the catchment area. As already mentioned in Phase I report, Appendix C.8, the general scour may be influenced by the following factors.

- Construction of embankments, reducing the flood plain width and causing higher peak flows downstream,
- Increasing soil erosion in Nepal and possibly other parts of the catchment result in more sediment supply to the rivers contributing to the Brahmaputra/Jamuna discharge,
- Construction of dams will reduce the sediment load of the rivers downstream and also cause a general damping of seasonal water level fluctuation (not major floods), and
- Other natural causes may be instrumental in a change of river slope.

The Consultants are setting up a large-scale one-dimensional mathematical model for water flow and morphology based on the RIVMOR program. The RIVMOR program was also used for the constriction scour computations, but for the general scour model a different schematisation of the Jamuna River is being made. Almost 1000 km of the Jamuna/Brahmaputra will be schematisized in the model, from Dibrugarh in India to the confluence of the Jamuna with the Ganges River. The effect of a change of water or sediment discharge of the major tributaries of the Brahmaputra/Jamuna on the average bed level will be studied during the detailed design phase.
As only a very rough schematisation of the Brahmaputra/Jamuna river is possible with a one-dimensional model, the result of this study cannot be an exact prediction of the average bed level of the Jamuna River. However, the model is expected to give the general tendencies of the bed level as anticipated for the future. For the Jamuna Bridge study this is considered to be sufficient, as general scour will only have a small contribution in the total scour to be expected near the river training work and bridge piers.
For the time being, the Consultants assume 1 m as a fair estimate for general scour.

B.3.4 Bend scour

B.3.4.1 Introduction

Usually, in alluvial channel bends, the bed level in the outer bend is lower than in the inner bend. Consequently, the depth increases when going from the inner to the outer bend. The large depth in the outer bend, know as bend scour, was expected to give a considerable contribution to the maximum scour in the Jamuna River also. Already in Phase I Consultants realized that use of existing prediction techniques taking into account the possible occurence of overshoot (point bar formation) and suspended load (which in this case would result according to some prediction methods in an increase of the (axisymmetric) equilibrium depth with 450% compared to the case of bed load only) would provide estimates of the maximum outer bend scour far larger than any results from field measurements available. Most of these field observations, however, were done during low flow conditions, so this was the very reason that measurements of bend scour were included in the hydrographic survey in 1987. This was done to assess the maximum scour depth in outer bends in the Jamuna River during floods. The special hydrographic survey carried out in 1987 was intended to address the following two issues:

- How representative are low flow data for the conditions during (extreme) floods? (See also the absence of an incrase in observed scour depths in the Figures B.3.12 ... B.3.13 with increasing stage).
- Is it possible to derive predictors for bend scour, confluence scour and bedforms in the Jamuna River, and to use these predictors to derive refined design criteria?

In the following sections first the present knowledge on bend scour is summarized, and next the results of the field measurements are interpreted on basis of this summary.

As is shown Consultants had to lean heavily on field data and this was done because time-dependent bend scour in channels that are near transition to braiding, with suspended transport being the dominant mode of transport and under flood conditions when also the chars are flooded, is an extremely complicated and difficult subject that cannot be predicted theoretically with the present understanding available to explain the observations made in the field and to use this understanding to make a fair prediction of maximum bend scour during extreme flood conditions.

B.3.4.2 Theoretical considerations regarding bend profiles

In an alluvial channel bend with dominant bed load, the cross-sectional profile can be described by (Struiksma et al (1985)):

$$\frac{h}{h_c} = \left[1 + 0.5\ A\ 0.85\ \sqrt{\theta}\ (1 - R/R_c)\right]^{-2} \qquad (B.3.12)$$

in which h = water depth (m), R = radius of curvature, A is a factor (usually between 5 and 10) indicating the influence of the transverse bed slope on the bed load sediment transport, and θ = Shields parameter (-). The index c refers to the channel axis (see also Phase 1 report, Appendix C.3).

The above equation (B.3.12) is only applicable for a number of limiting conditions, notably:

(i) "equilibrium" profile, that occurs only at a considerable distance downstream of the beginning of the bend.

(ii) sufficient time has elapsed for the bend scour to develop fully.

(iii) suspended load is negligible.

These three limiting conditions and their implication are discussed hereafter in more detail.

Re (i) Equilibrium profile

The above equation (B.3.12) relates to the downstream parts of a long bend with constant radius only.

When the radius of curvature changes, the new equilibrium profile is reached after some distance only. The adaptation process depends on a typical wavelength and damping length of the considered alluvial channel. The longer the damping and wavelength, the longer the distance required before the equilibrium profile is obtained. The damping length L_D determines the magnitude of the overshoot phenomenon (see Figure B.3.3). The wavelength L_p is given by:

$$\frac{2\pi}{L_p} = \frac{1}{2} \left\{ \frac{b+1}{\lambda_s \lambda_w} - \frac{1}{\lambda_s^2} - \frac{b-3}{2\lambda_w^2} \right\}^{\frac{1}{2}} \qquad (B.3.13)$$

and the damping length L_D by:

$$L_D = \frac{4\, \lambda_w \lambda_s}{2\lambda_w - (b-3)\lambda_s} \qquad (B.3.14)$$

in which b = power in transport formula ($s \sim u^b$), $\lambda_s = \frac{1}{2\pi} h \left(\frac{B}{h}\right)^2 f(\theta)$, $\lambda_w = \frac{C^2 h}{2g}$, B = channel width (m), h = average channel depth (m), θ = Shields parameter (-), C = Chézy coefficient ($m^{\frac{1}{2}}/s$), g = acceleration of gravity (m/s^2).

It can be shown (see Struiksma & Klaassen, 1988) that for values of λ_s/λ_w higher than a criterion dependent of b, the solution is out of the periodic range. In that case, the individual channel is braiding and may show several smaller channels within its bed.

Re (ii) Time scale

The time-dependent adaptation of the bend profile can be characterized by a time scale. A change of discharge results in an adapted bend profile that gradually reaches the new equilibrium slope. The formula for the time scale of the cross-section adaptation reads (Klaassen, 1988):

$$T = \frac{B^2\ 0.85\ \sqrt{\theta}}{\pi^2\ s} \qquad (B.3.14)$$

in which B = width of the channel (m) and s = sediment transport per unit width (m^2/s).

B.3.4.3 Measured bend profiles in the Jamuna River

The methodology used by Consultants was to do hydrographic measurements in a number of selected reaches. Measurements were repeated to observe the scour during the flood season and subsequent period, although the difficult conditions in Bangladesh in 1987 resulted in a reduction of the actual number of observations.
The results of the repeated measurements of bend scour are provided below:

River reach	Data	Maximum bend scour (m + PWD)
Pechkaholo	17 Aug 1987	- 1.5
	21/22 Nov 1987	+ 0.3
Bhuapur	24/25 Aug 1987	- 2.4
	23 Oct 1987	- 2.1
Pingna	26/27 Sept 1987	0.9
	29/30 Oct 1987	0.9
Dinghapara (two bends)	11/13 Nov 1987	+ 5.5/+ 1.8

For the stages during those respective dates reference is made to Figure B.3.3a.

Some examples of comparisons of the measured cross-section profiles with the theoretical bend profile are given in Figure B.3.4. It was observed, that the maximum outer bend scour in the surveyed bends always appeared at the downstream end of an identified channel bend and that the maximum scour was always less than the theoretical equilibrium scour.

B.3.4.4 Discussions of results

When the adaptation wavelengths of the channels in which bend scour was observed are computed, it appears that they are more than twice as large as the length of the analyzed channel bends (wavelength is about 20 km). To compute the wavelength and damping length, the value of b is computed by using the Meyer-Peter & Müller formula for bedload transport, yielding $b \approx 3.5$. Bend scour is mainly governed by bedload transport and, therefore, this is justified. Taking a value of $b = 5$ (Engelund & Hansen formula) gives a solution out of the periodic range. Apparently the individual channels of the Jamuna River are on the treshold between meandering and braiding. The damping length is also very large (more than 50 km), implying, that the overshoot, causing a maximum scour more severe than the equilibrium profile, could be important for longer channel bends (more than ± 0.25 x wave length).

The amount of overshoot is determined by the change of radius of curvature. In alluvial channels these changes are usually rather smooth, reducing the overshoot phenomenon. For the Jamuna the overshoot phenomenon is therefore considered to be negligible.

Channel bends in the Jamuna River are too short to reach the equilibrium bend profile. For the design of the guide bunds and river training works, however, the equilibrium bend scour should be taken into account, as it is possible that the bridge works will allow longer bends to develop.

From the results of the field surveys (see the above Table) it can be concluded that bend scour measured during flood conditions is not much larger than during lower flow conditions (in retrospect the measurements in Pechkahola are not so representative, considering the unfavourable direction of this bend compared to the valley slope direction). The implication of the above is that a considerable increase in bend scour depth will not occur during design floods either. This is in line with the large time-scale predicted using Equation (B.3.14a). This equation yields a time scale of over 30 years, when the transport is computed with Equation (B-5.7), Appendix B-5. Consultants are convined of the applicability of this time-scale. This is based on their extensive experience with mathematical model recently applied by Consultants in which this time-lag was simulated shows that even during extreme flood conditions an increase of a few metres only has to be expected.

It is emphasized, that consultants did not state that THE morphological time scale of the Jamuna is thirty years. Morphological timescales can be defined for all kinds of morphological processes (see Klaassen, 1988).
Here a timescale for the adaptation of the cross-sectional frofile is discussed. For this time scale the width of the channel is very important, as the transverse sediment transport is very small in comparison with the longitudinal sediment transport.

The rapid change of the cross section over the years, and in particular the location of the individual channels, is not governed by this time scale. These channel processes are caused by severe local bank erosion and adaptation of the cross sections in longitudinal direction. The time scale related to these processes is hard to define, but it is probably very short as the longitudinal sediment transport is very high and the bank erosion can be as much as five hundred meters during one flood season locally. The effect of this enormous bank erosion on the channel pattern and the cross section profile may be substantial.

The conclusion must be that the large time scale for the development of the band profile is not in contradiction with the rapid changes of the channel pattern.

During flood conditions suspended sediment load is very important in the Jamuna River. These high suspended sediment load may or may not lead to substantially increased band scour. An increase may be expected looking at the condition in one cross-section, but the "smooting" effect of suspended load in the longitudinal direction may lead to a decrease. Inclusion of suspended load into the derivation of a prediction technique would result in a different value for e.g. the coefficient A to match the observed bend scour profiles, so the ultimate result would not become substantially larger.

130

B.3.4.5 Predictor for bend scour

Based on the observations in the field, both during low flow and during floods (in 1987), Consultants have derived a predictor for bend scour in the Jamuna River. This predictor corresponds to Equation (B.3-12) with A = 10. For the computation of n the value of θ and h_a during the average discharge of about 20,000 m^3/s are used.

During the year 1987 a relatively large flood (corresponding to a 1:10 year flood) occurred (see also Figure B.3.3a). According to Section A.4 of Volume II the difference in stage between the 1:10 and the 1:100 year flood is about 0.8 m. This implies that the design flood was approached during 1987. This does not imply, however, that the design conditions for bend scour were approached during the 1987, because also other factors like channel widths and radius of curvature should be critical. This also explains the scatter in the Figure B.3.12 (and B.3.13). The above underlines the need for a probabilistic design procedure.

With the planform of the Jamuna River near the proposed bridge site and planned training works in mind it is unlikely that a large channel with relatively small radius of curvature will attack the guide bunds. The scale model tests support this opinion. During flood conditions the river constriction will prevent the development of large channels with small radius of curvature near the guide bunds.

B.3.5 Confluence scour

During the Phase I study it was found that in the Jamuna River confluence scour seems to be dominant over bend scour. Only local protrusions produce deeper scour holes. For the bridge piers confluence scour may be the major contribution to the total scour. In the literature little information can be found on confluence scour. A review of literature in which the phenomenon is mentioned, is given by Ashmore & Parker (1983). Only in the last decade attempts have been made to look more closely at the phenomenon of confluence scour, aiming at identifying the mechanisms responsible for this phenomenon and to arrive at methods to predict the maximum depth and location of this type of scour. Until now, attention was given to gravel bed rivers with coarse

220

material only. During the present study it was attempted to expand the method of Ashmore & Parker (1983) to large sandbed rivers.

In the present study data obtained from field measurements in the Jamuna River in Bangladesh, are being used. The hydrograph of the Jamuna River is fairly constant (see e.g. Coleman, 1969). From April to July the discharge rises gradually. The actual flood season is from July through September, during which the discharge varies around a fairly constant value. From October onwards the discharge decreases. So, different from many gravel-bed rivers, long periods are present in which the variation in discharge is relatively small. Because sailing on the Jamuna River is quite common, also during flood conditions, it is possible to obtain soundings of confluence scour patterns which must represent approximate equilibrium conditions.

Two sets of field measurements are used in the present study, viz:

(i) Historical data

Since the late sixties regular soundings have been done by the Bangladesh Inland Water Transport Authority (BIWTA). These measurements are done to identify the best navigation routes, using echo sounder equipment in combination with a Decca positioning system. Measurements have been done mostly during low flow conditions, but some sounding maps relating to flood conditions are also available.

(ii) Special field survey

In the period July - November 1987 a special hydrographic survey was carried out to measure scour depths (and bedforms, see Klaassen, Vermeer & Uddin (1988)) in the Jamuna River. Scour depths were measured on different sites (see Figure B.1.1) and at different dates. Also these measurements were carried out by BIWTA. In addition to the Decca system, also a Trisponder positioning system (with an accuracy of 1 m) was used. Due to excessive flooding in Bangladesh during the measuring period the measuring programme had to be reduced, but still some data on confluence scour were collected. Results are presented on similar sounding maps as prepared by BIWTA for navigation purposes.

The method of analysis of the field data is similar to Ashmore & Parker (1983). They proposed the following relation for confluence scour:

$$\frac{h_s}{\overline{h}} = f\,(F_o,\ \overline{i}_w,\ \theta,\ \varepsilon) \tag{B.3.15}$$

where

h_s = maximum (confluence) scour depth (m)

$\overline{h}$ = average depth of the upstream anabranches, defined via $\overline{h} = (h_1 + h_2)/2$ (m)

F_o = densimetric Froude number, defined via $F_o = u_o/(\Delta g\ \overline{D}_g)^{.5}$ (-)

u_o = average anabranche velocity (m/s)

$\overline{D}_g$ = average mean grain size of the upstream anabranches (m)

Δ = relative density, defined via $\Delta = (\rho_s - \rho)/\rho$ (-)

ρ_s = specific density of sediment (kg/m^3)

ρ = specific density of water (kg/m^3)

i_w = average anabranch downstream water surface slope

Θ = angle of incidence of anabranches of confluence (°)

ε = $(Q_L - Q_R)/\frac{1}{2}\,Q_T$ (-)

Q_L, Q_R, Q_T = discharge in left and right anabranche and total discharge downstream of confluence.

236

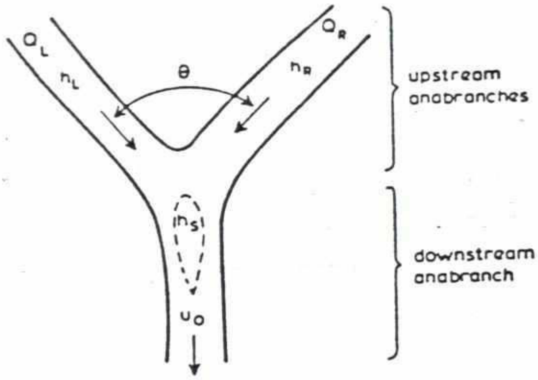

Ashmore and Parker analysed in total 118 points, including Mosley (1981) and their own field observations and results from laboratory studies. They found that the influence of F_0 and $\bar{i}_w$ on $h_s/\bar{h}$ is very weak. Not discriminating for the values of ε and thus including all data in the analysis, the following relationship between $h_s/\bar{h}$ and θ was obtained (see Figure B.3.5):

$$\frac{h_s}{\bar{h}} = 2.235 + 0.0308\ \theta \qquad \text{(B.3.16)}$$

Considering only points with $\varepsilon < 0.75$ (so confluences for which $Q_1/Q_2 < 2.20$ where the indices 1 and 2 refer to the anabranches with the largest (1) and smallest (2) discharge, respectively), then a relationship steeper than Equation (2) was found. For $\varepsilon > 0.75$ the slope of the regression line for $h_s/\bar{h}$ versus θ was indistinguishable from zero at the 95% significance level.

A similar analysis was carried out for the field data from the Jamuna River. The depths of the upstream anabranches (h_R, h_L) were determined by averaging the observed average depth of at least four cross-sections directly upstream from the confluence. The inclusion of more cross-sections did not yield substantially different average depths. The deepest confluence scour depth in the downstream anabranch, h_s, was also taken from the sounding maps. The plotted depths are related to the S(tandard) L(ow) W(ater), so the figures on the maps were corrected considering the water levels during the period in which the

238

soundings were done. The angle of incidence was obtained from the sounding maps, too. Some inaccuracy is inherent, because most upstream anabranches are not straight. In the Jamuna River also more complex confluences are present, where a short distance downstream of the confluence a third anabranch joins the river. Here a more complex scour pattern occurs and these confluences are discarded from the analysis.

For each confluence values of $\bar{h} = \frac{1}{2}(h_R + h_L)$, h_S and θ were obtained. Computed values of $h_S/\bar{h}$ are plotted against θ in Figure B.3.5. Although there may be an increase in $h_S/\bar{h}$ for increasing θ, this increase is obscured by the larger scatter.

As a second step of the analysis, an attempt was made to discriminate according to the value of ε. The parameter ε is a measure for the distribution of the total discharge over the two upstream anabranches. When Q_1 and Q_2 are the larger and the smaller discharge, respectively, then the relationship between ε and Q_1/Q_2 is as indicated below:

ε	0.00	0.25	0.50	0.75	1.00	1.50	2.0
Q_1/Q_2	1.00	1.25	1.67	2.20	3.00	7	∞

To establish the value of ε the value of Q_L and Q_R should be known, but these discharges were not measured simultaneously with the soundings. Here use is made of "at-a-station relationships" that were derived for the Jamuna River (see Section B.3.2 and Klaassen & Vermeer, 1988a). The proposed relationship between the average depth of an individual channel of the Jamuna and the discharge it carries, reads:

$$\bar{h} = 0.56\, Q^{0.23} \tag{B.3.10}$$

This relation can also be used for estimating the discharge in a channel once the average depth is known. The relation reads for that case:

$$Q = 12.44(\bar{h})^{4.35} \tag{B.3.17}$$

Using Equation (B.3.17) an estimate of the discharges in all confluencing anabranches was obtained. Next the value of ε was computed for each confluence.

The result is plotted in Figure (B.3.7), where in total six classes for ε were differentiated. For the results of the special survey in 1987 and the historical data, different symbols have been used. A figure is added to each point, indicating the estimated discharge in 10^3 m^3/s of the anabranch with the largest depth.

From inspection of Figure B.3.7 the following conclusions can be drawn:

(i) For small values of ε (for $\varepsilon < 0.25$ and to a smaller extent for $0.25 \leq \varepsilon < 0.50$) an increase of the ratio $h_s/\overline{h}$ with increasing θ is found, with a much smaller scatter than present in Figure B.3.5.

(ii) For larger values of ε, especially for $\varepsilon > 1.00$, no relationship between $h_s/\overline{h}$ and θ is found.

In Figure B.3.6 all data for $\varepsilon < 0.50$ (in total 18 points out of 78 data obtained) are presented. A linear regression line was determined through these 18 points, which reads:

$$\frac{h_s}{\overline{h}} = 1.292 + 0.037\ \theta \qquad (B.3.18)$$

The correlation coefficient is around 0.72, implying a significant result. The above relationship is supposed to provide a fair estimate of confluence scour in the Jamuna River.

For the estimation of confluence scour two major parameters are important, viz. $\overline{h}$ and θ. In Section B.3.2 sufficient information on $\overline{h}$ is provided. The probability of occurrence of θ can be derived from the same set of field data. For all data with $\varepsilon < 0.50$ an estimate of the probability of occurence is indicated below:

$20° < \theta < 30°$	:	$3/18 = 0.17$
$30° < \theta < 40°$	:	$3/18 = 0.17$
$40° < \theta < 50°$	:	$4/18 = 0.22$
$50° < \theta < 60°$	:	$2/18 = 0.11$
$60° < \theta < 70°$	:	$5/18 = 0.28$
$70° < \theta < 80°$	:	$1/18 = 0.06$

Broadly speaking, $\theta > 70°$ only in exceptional case, and between 20° and 70° θ is approximately evenly distributed.

Considering the discussion presented above, it can be stated that the Jamuna field data that are processed in the present study, provide a fair relationship between the dimensionless scour depth and the angle of incidence of the anabranches. The general character of this relationship is the same as derived by Ashmore & Parker (1983) for gravel-bed rivers, notably an increase in dimensionless scour depth for increasing angle of incidence. Confluence scour depths found here, are smaller than observed in gravel-bed rivers. There are some indications that this is caused by suspended load becoming the dominant mode of transport for higher stages in the Jamuna River. For a more detailed discussion of the present study in confluence scour reference is made to Klaassen & Vermeer (1988b).

B.3.6 Bedforms, resistance to flow and sediment transport

B.3.6.1 Introduction

Bedforms, resistance to flow and sediment transport are closely related. Bedforms at the interface between river bed and water, increase the resistance to flow considerably. They also have a close relation with sediment transport rates and consequently on the celerity of morphological processes like degradation and bank erosion. Bedforms are also of direct importance for the design of the bridge and the river training works.
Only limited information on bedforms (especially during floods) in the Jamuna River was available. Therefore, a special hydrographic survey was carried out during the 1987 flood season.
The results of this survey are discussed in Section 3.6.2. The analysis considering resistance to flow is given in Appendix B-5.

B.3.6.2 Bedform dimensions

Data on bedforms in the Jamuna River were first published by Coleman (1969). Based on an extensive study he distinguished the following bedforms:

- 'ripples': typical height 0.2 - 0.5 m (probably not relevant for the present study),
- 'mega ripples': typical height 1.0 m, typical celerity 120 m/day,
- 'dunes': typical height 5 m, typical celerity 60 m/day, and
- 'sand waves': typical height 10 m, typical celerity 200 m/day.

239

More recently Bristow (1985) presented some data on bedform heights observed during low flow conditions. Although it was possible to measure three times, for high flow conditions only limited data on bedform dimensions in the Jamuna River are available. Therefore, special measurements were carried out for the present study.

During flood conditions in 1986 and 1987, bedform dimensions were measured in the Jamuna River. This was done for two reasons:

- to study the relation between bedform dimensions and flow characteristics of the Jamuna River and, in particular, to check whether a reduction of bedform height occurs during flood conditions; and
- to determine a lowest bed level, owing to passing bedform dimensions and local scour for the design of the river training works and for the piers of the Jamuna Bridge.

The hydrographic survey in 1987 was carried out between July and November. At some locations two measurements were done during this period. This means, that the change of the bedform dimensions could be analysed as a function of the stage of the flood season. In Table (B.3.1) the soundings used for the bedform analysis are given. The water levels on the dates of the soundings are given, too. The maximum water level was reached in the second half of August. During the last measurements the water level had already dropped 4 m compared to this maximum flood level.

The following observations can be made when studying the bedform data:

i) During the measurements obtained in July and August, relatively large dunes were abundantly present according to all soundings, some of them having small dunes superimposed on them, (see Figure B.3.8.a)

ii) In the following month (September), so after the peak discharge in the second half of August, the large dunes are not reduced in height and their lengths have not increased. However, the small, superimposed dunes have disappeared (see Figure B.3.8.b)

iii) In the second half of October and in November the large dunes have disappeared as well as flat bed situations although some can still be observed on nearly all soundings (see Figure B.3.8.c)

So, when the peak discharge is reached, large dunes, having average height $H \cong 3.0$ m and average length $L \cong 200$ m (based on the sounding near Belkuchi on the 22 August 1987) are still present, with small dunes superimposed with average height $H \equiv 1.1$ m, and average length $L \equiv 24$ m. This seems in contradiction with the observation that resistance to flow of the Jamuna River is very low during the peak discharge. The washing out of the smaller superimposed dunes and the large dunes takes place in a later stage of the flood season only.

The reason for the present study of bedforms is the determination of scour depth, related to bedforms. The trough of the bedform is below the average bed level. Therefore, the dune height was investigated in relation with the water depth. A graph was made to investigate the dune height versus water depth relation (see Figure B.3.9). Maximum dune heights of 6 m were observed. This is not in line with observations by Coleman (1969) who discovered bedform heights up to 15 m. It seems possible that Coleman interpretated confluence scour erroneously as bedforms.

The relation $H/\bar{h}$ versus $\bar{h}$ was also investigated ($\bar{h}$ = average waterdepth). For H the average dune heights of reaches with approximately equal dune heights were taken. It appears, that the $H/\bar{h}$ ratio can be up to about 0.35 (see Figure B.3.10), but no relation with the water depth was found. Dune height prediction models like the ones provided by Yalin (1964) and Allen (1968) seem not applicable for the Jamuna River, particularly so for larger waterdepths. As a reduction of the $H/\bar{h}$ ratio for increasing waterdepth could not be shown, a maximum dune height of $H = (0.25 \pm 0.10)h$ should be taken into account for the maximum scour depth related to bedforms.

Finally the ratio $L/\bar{h}$ versus $\bar{h}$ was investigated. This ratio was always smaller than 20 and usually between 5 and 10 for waterdepths varying from 9 to 17 m. For the $L/\bar{h}$ ratio a dependence of the average depth can not be shown either.

B.3.7 Constriction scour

Further on the computations to predict constriction scour in the Jamuna River during Phase I of the study (see Phase I, final report, Appendix C.5.3) some additional computations were carried out to assess the influence of the bridge span on constriction scour and backwater.
These computations are treated in detail in Appendix B-5. Here, the results are given for a bridge length of 4600 meter.

- maximum constriction scour: 3.1 meter.
- maximum backwater : 0.3 meter.

These results apply for a long lasting (25 days), 1:100 year peak discharge (91,000 m^3/s).

B.3.8 Local scour

Local scour has been extensively considered in Phase I (see Appendices C.6 and C.7 of Annex C of the Phase I report). During the special hydrographic survey carried out in July - November 1987 also some local scour data were obtained, in particular near Sirajganj. Initially it was intended to collect also data on the local scour around some of the piers of the EW-connector near Aricha, but it appeared that none of the piers was located in a deep channel so any measurement of local scour near these piers would have been of limited interest only. For the scour around piers the Phase I assumption of 1.6 x b ± 10%, in which b is the diameter of a pile, still holds. In this respect it is of interest to cite the results obtained by Sutherland (1986), who studied experimentally the interaction between confluence scour and local scour around a pier. Sutherland found that there is no interaction, so both effects should be summed up (as was already done in the Phase I approach).
During the special hydrographic survey some measurements were done near the town protection of Sirajganj and near Bhuapur along the Eastern bank of the Jamuna River.
The results (deepest scour levels expressed in m + PWD) are listed below:
- Bhuapur 24 - 25 August 1987 - 8.0 m
- Sirajganj 3 - 19 September 1987 - 25.3 m
- Bhuapur 23 - 24 October 1987 - 6.1 m.

In addition results of measurements by BWDB are available. These are plotted in Figure D.10 of Annex D.
Furthermore, some data were obtained from BIWTA sounding charts. These are plotted in Figure B.3.14. It follows from this figure that maximum scour is about 32 m below LLW, corresponding to about 6.7 m + PWD. So according to the BIWTA soundings the lowest bed level is about - 25 m + PWD. This is in line with the observation on 3 - 19 September 1987 during the special hydrographic survey. The value of - 24.4 m + PWD has been accepted, for the time being (see Annex D, Section 3.1.3). This is well below the values predicted in Appendix C.7 in the Phase I report.

20

B.3.9 Total scour

In the preceding sections of this Annex the various causes contributing to the total scour near guide bunds and groynes and around the bridge piers, have been analyzed. In this section they are combined to arrive at a prediction of the total scour during a 1:100 year flood event.
In addition to this, the available data on maximum scour depths in the Jamuna River are plotted in such a way that direct extrapolation to extreme floods is possible. The results of both methods are compared and based on this comparison design scour depths are decided upon.

In general the maximum scour depth is made up of the following contributions (see also Phase I report, Appendix C.8):

- general scour;
- natural fluctuations due to non-uniformity of main channels and flood plain;
- constriction scour;
- three dimensional effects: bend scour or confluence scour;
- bedform scour;
- local scour.

After this, maximum scour at bridge piers and along guide bunds and groynes is considered separately.

The most critical conditions will occur when a bridge pier, or rather: a series of bridge piers, is located in an outer bend or in the deepest point of a confluence scour pattern. The various contributions to the local scour together with indications on both average values and standard deviations are briefly discussed hereafter.

(1) General scour

For the time being, until results from the mathematical model for general scour become available, it is assumed that owing to large-scale processes like deforestation, embankments, etc. a general scour of 1 m should be taken into account (see Section B.3.3).

(2) Non-uniformity

Not specifically taken into account. It included in the BWDB cross-sections and thus in the scatter around the regime equations for the Jamuna River.

(3) Constriction scour

According to the computations with a mathematical model, the following allowance should be made for constriction scour.

span of bridge (m)	constriction scour (m) for 1:100 year flood
5300	1.2
4600	3.1
3500	4.1

Remark: schematization for the bridge length of 4600 m was different from those for the other bridge lengths (see Appendix B-5).

(4) Three-dimensional effects

First confluence scour is considered. From the tentative design graph the following equation can be derived for the average value:

$$\frac{h_s}{\bar{h}} = 1.292 + 0.037\,\theta$$

The fluctuations in the computed value are due to fluctuations in the prediction and fluctuations in the angle of incidence θ. According to Figure B.3.6 fluctuations in $h_s/\bar{h}$ are ± 1. The average value of θ is about 50° with fluctuations ± 25°.

To compute either possible maximum confluence or bend scour, the average depths of the channels should be known. Use is made of the regime equations derived in Section B.3.2. For confluence scour it is assumed that the discharge is divided equally over two channels, so each carries about 45,500 m³/s. During bankfull stage each of them carries only about 22,000 m³/s, yielding an average depth of about 6 m. The difference in stage between Q = 44,000 m³/s and Q = 91,000 m³/s is about 2 m, so for the average depth of the two anabranches a value of about 8 m is taken. This results in an average confluence scour (for θ = 50°) of about 25 m.

For bend scour a maximum scour of 19 m is assumed.

(5) Bedforms

Extensive measurements of bedforms in the Jamuna River have been analyzed and the extreme values of 15 m quoted by Coleman (1969) were not confirmed. For the time being the following predictive method for average bedform heights can be used

$$\overline{H} = (0.25 \pm 0.10)\ \overline{h}$$

Further to the detailed analysis in the Phase I report, it was found during the analysis of the results of the special survey in 1987 that maximum scour depth can be 1.0 * $\overline{H}$ below the average bed level. Finally, it should be emphisized that in the deepest outer bends and in confluences, bedforms seem to vanish. So the extreme possibility of maximum confluence or bend scour and bedforms need not be taken into account.

(6) Local scour

The expression for local scour around bridge piers in the Phase I report, viz:

$$h_{scour} = (1.6 \pm 0.16)\ b$$

where b = bridge pier diameter, still remains unchallenged. According to Sutherland (1986) local and confluence scour do occur simultaneously and they do not affect each other. The same is probably true for local and bend scour.

For the estimation of maximum scour around bridge piers, the following values are obtained:

- confluence scour: $h_{max} = 1 + 0 + 3 + 25 + 0 + 1.6 \times 2.5 = 33$ m
- bend scour: $h_{max} = 1 + 0 + 3 + 19 + 0 + 1.6 \times 2.5 = 27$ m.

For the scour along guide-bunds and groyns such an analysis can not be made, because local scour is dominant over all other contributions. This local scour is determined, to a large extent, by the geometry of the structures envisaged.

Finally, the observed scour depths are processed in this section. That is done in two ways; (1) a plot of scour depth versus chainage, and (2) a plot of confluence scour, bend scour and local scour versus the Sirajganj water level.

The results are provided in Figures B.3.11 through B.3.14. From an inspection of these figures it is concluded that i) confluence scour is dominant over bend scour, ii) there is hardly any increase in confluence scour with the stage, and iii) a fair estimate of maximum confluence scour is 24 m below LLW. The difference between LLW and 1:100 year flood is about 7 m, so confluence scour level at Sirajganj will not be below + 15 m + PWD -31 m = -16 m + PWD. For local scour deeper scour are found, notably -32 m below LLW, meaning -25 m + PWD.

Location	Data	Water level at Sirajganj	$\bar{h}$	Large Dunes			Small Superimposed			Remarks
				$\bar{H}$	$\bar{L}$	$\bar{\alpha}$	$\bar{H}$	$\bar{L}$	$\bar{\alpha}$	
Nagarbari	27-07-87	13.48	10.8	2.8	80	11	N.A.	N.A.	N.A.	
Nagarbari	20-11-87	9.30	-	N.A.	N.A.	N.A.	N.A.	N.A.	N.A.	flat bed predominant
Belkuchi	22-08-87	14.00	18.1	3.0	220	32	1.1	24	10	
Belkuchi	17-11-87	9.46	-	1.2	75	30	N.A.	N.A.	N.A.	flat bed predominant
Sirajganj	11-09-87	13.82	11.7	2.4	70	10	N.A.	N.A.	N.A.	
Sirajgang	11-10-87	12.33	12.7	2.4	50	7	N.A.	N.A.	N.A.	flat bed predominant

α = slope of the dune lee side

Table B.3.1 Bedforms of the Jamuna River

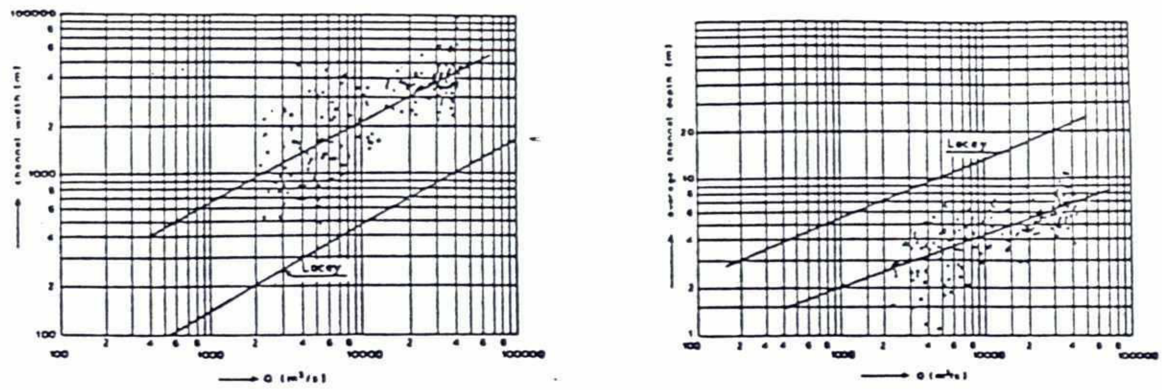

(a) width versus discharge

(b) average depth versus discharge

Figure B-3.1 Regime relationships of Jamuna River channels at bankfull stage

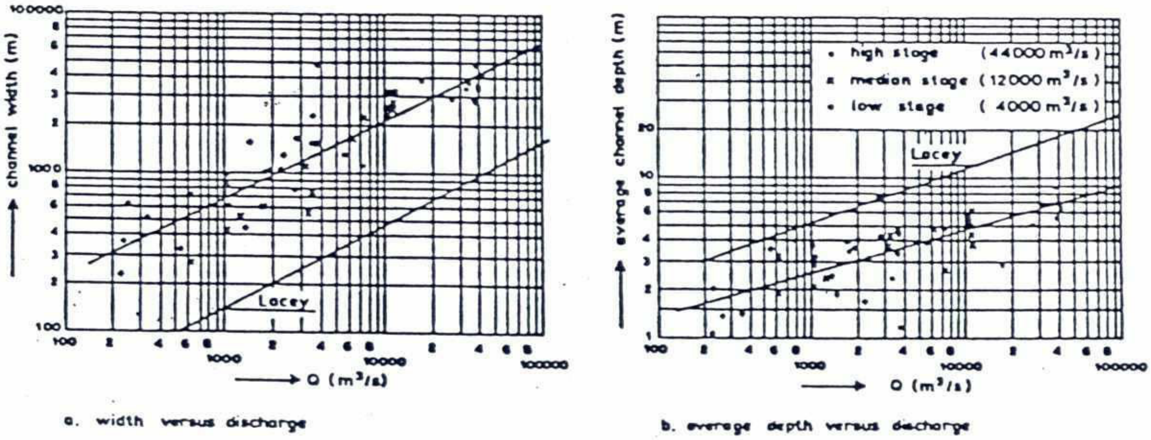

(a) width versus discharge

(b) average depth versus discharge

Figure B-3.2 Average at-a-station relationships Jamuna River channels

79

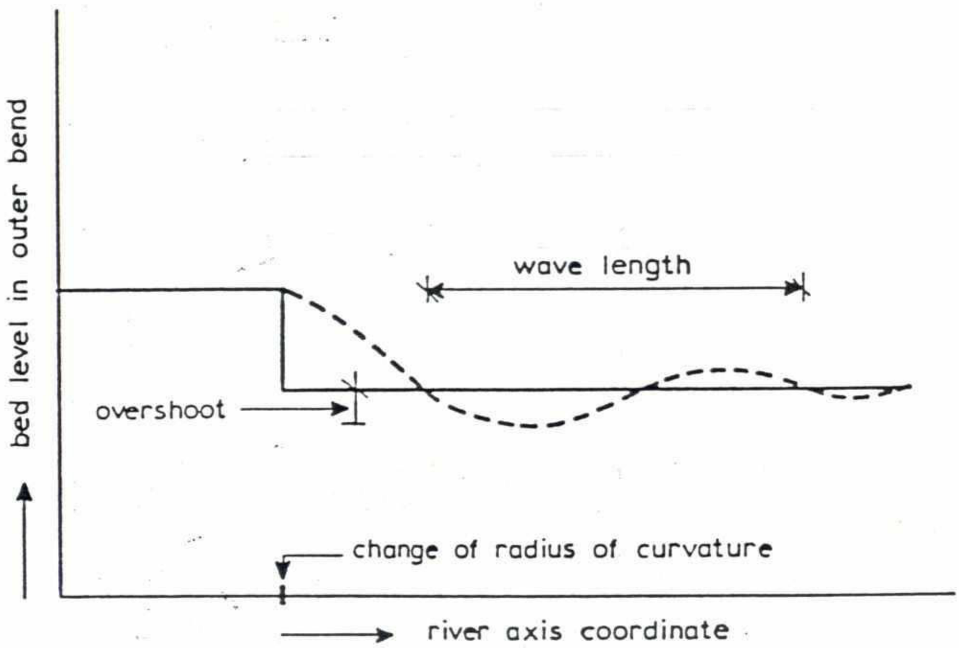

ADAPTATION OF BEND PROFILE		
RPT / NEDECO / BCL	Q 553	FIG. B.3.3

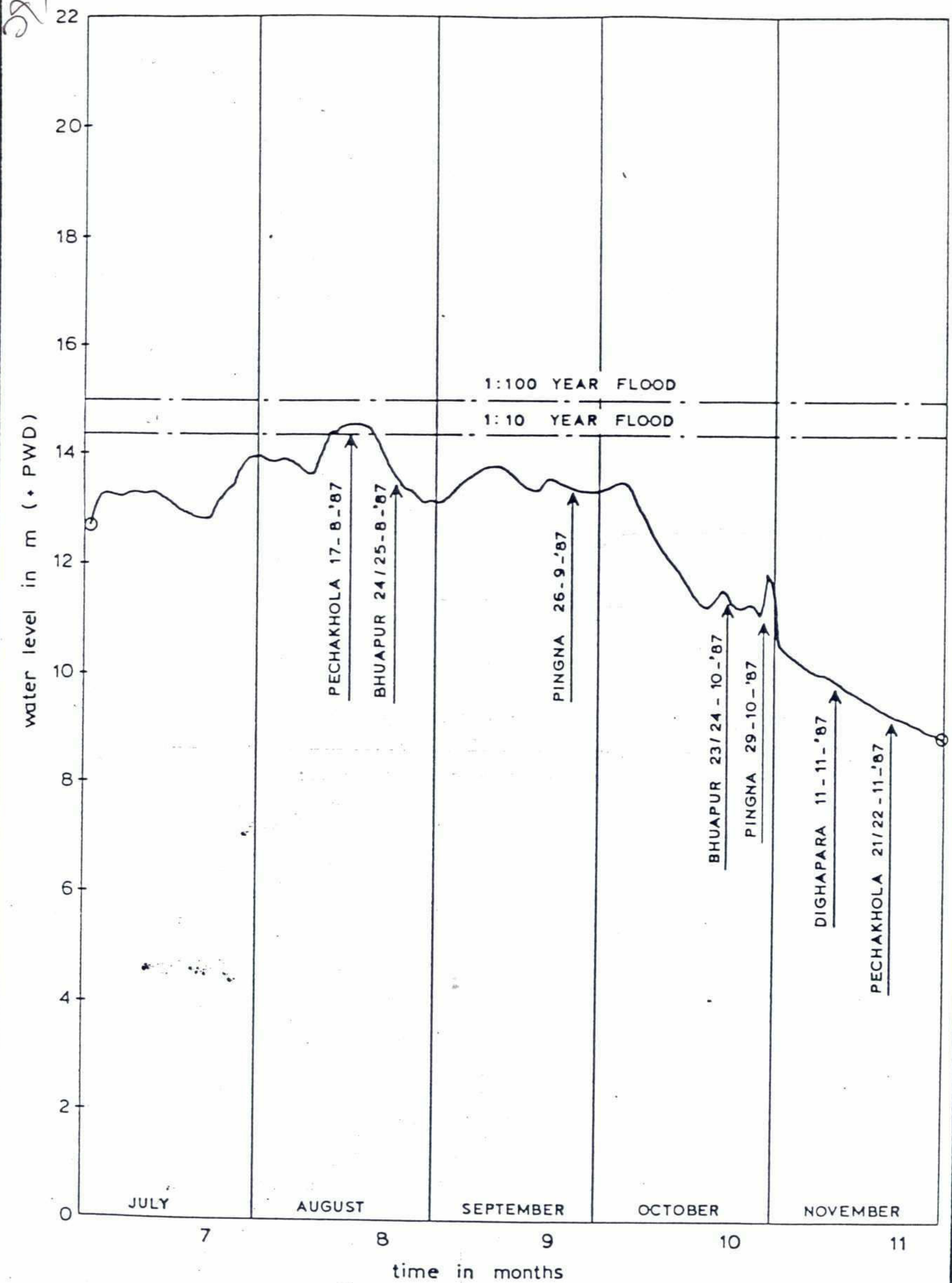

DAILY WATER LEVEL AT SERAJGANJ FROM 1-07-87 TO 30-11-87	JAMUNA PROJECT	
RPT/(DELFT HYDRAULICS) NEDECO/BCL	Q 553	FIG. B 3.3a

299

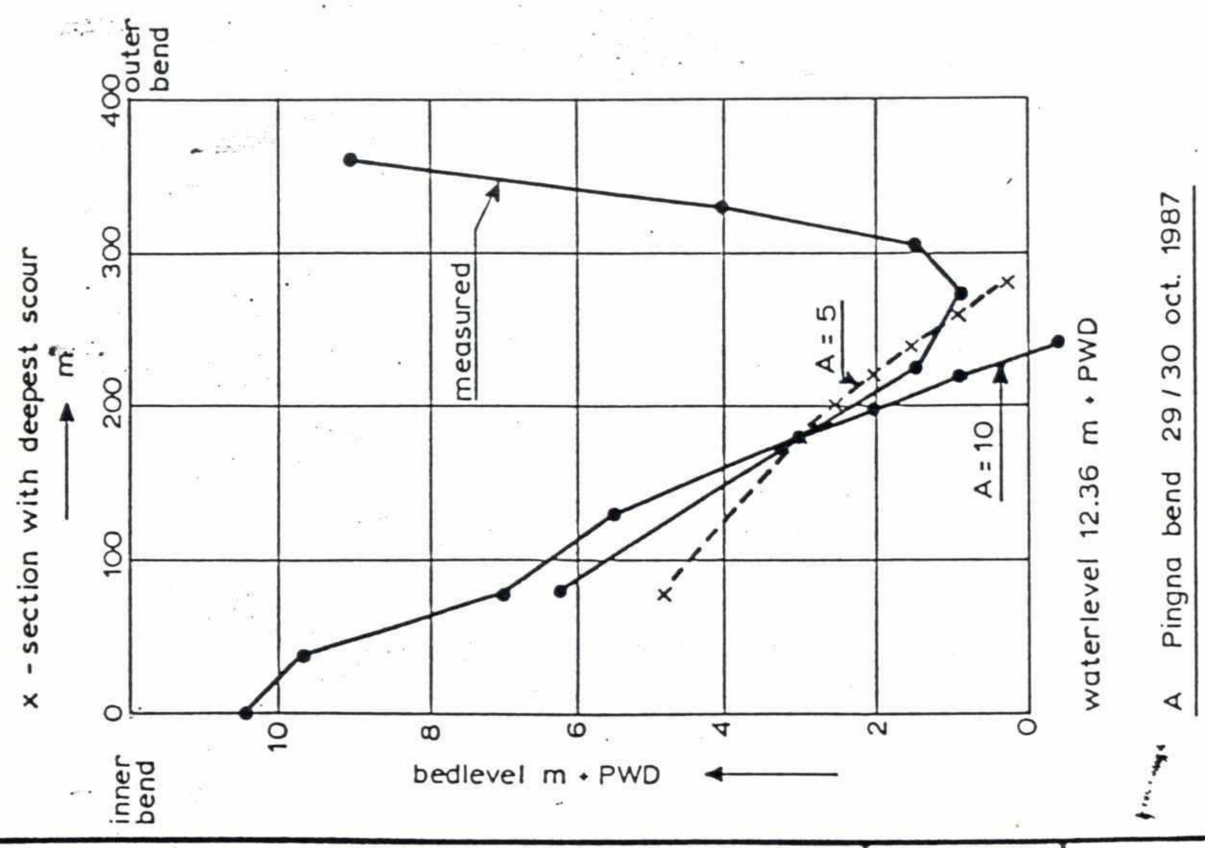

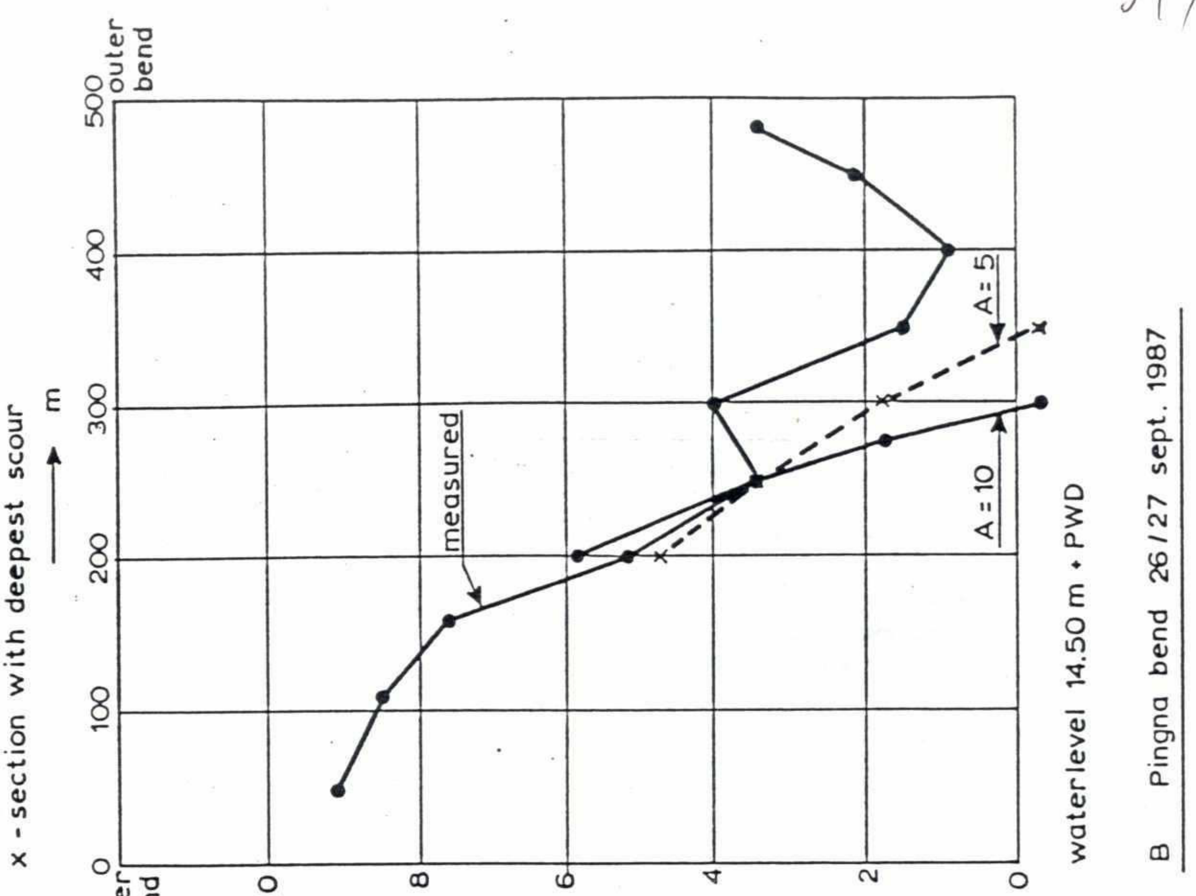

BEND PROFILE AT PINGNA COMPARED WITH THEORETICAL BEND PROFILE FOR DIFFERENT VALUES OF FACTOR A		
RPT / NEDECO / BCL	Q 553	FIG. B. 3.4

28

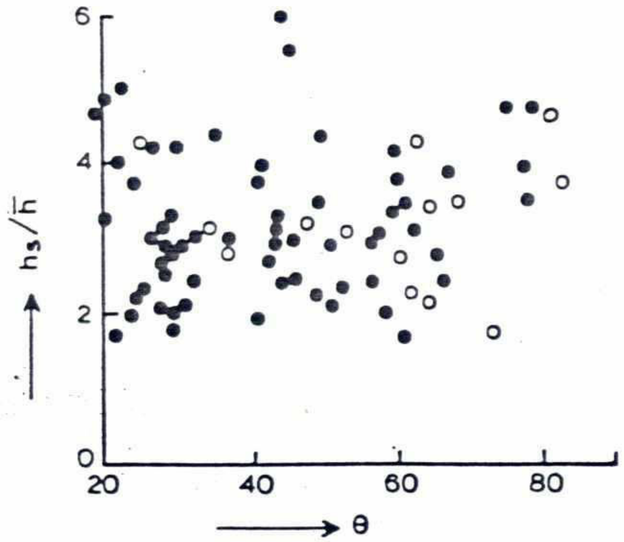

LEGEND

- • historical data
- o special survey '87

Figure B.3.5 Confluence scour Jamuna River, all data

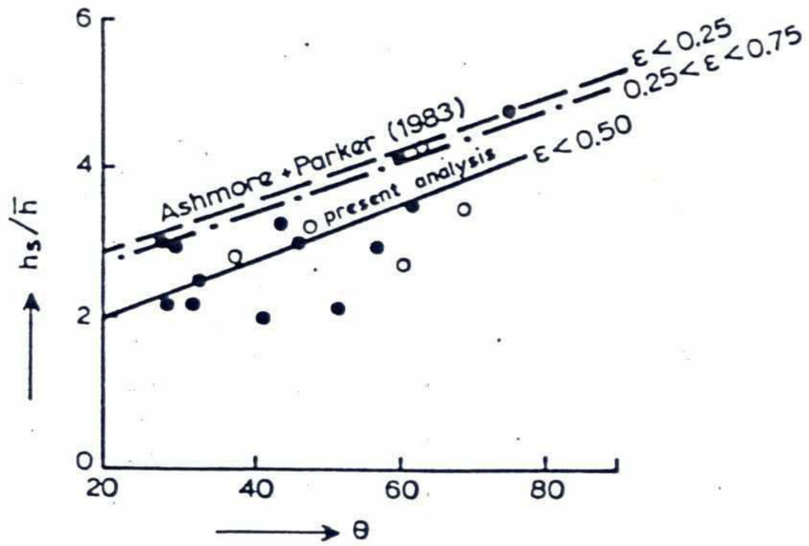

LEGEND

- • historical data
- o special survey '87

Figure B.3.6 Tentative design curve confluence scour Jamuna River

RPT / NEDECO / BCL	Q 553	FIG. B.3.5/B.3.6

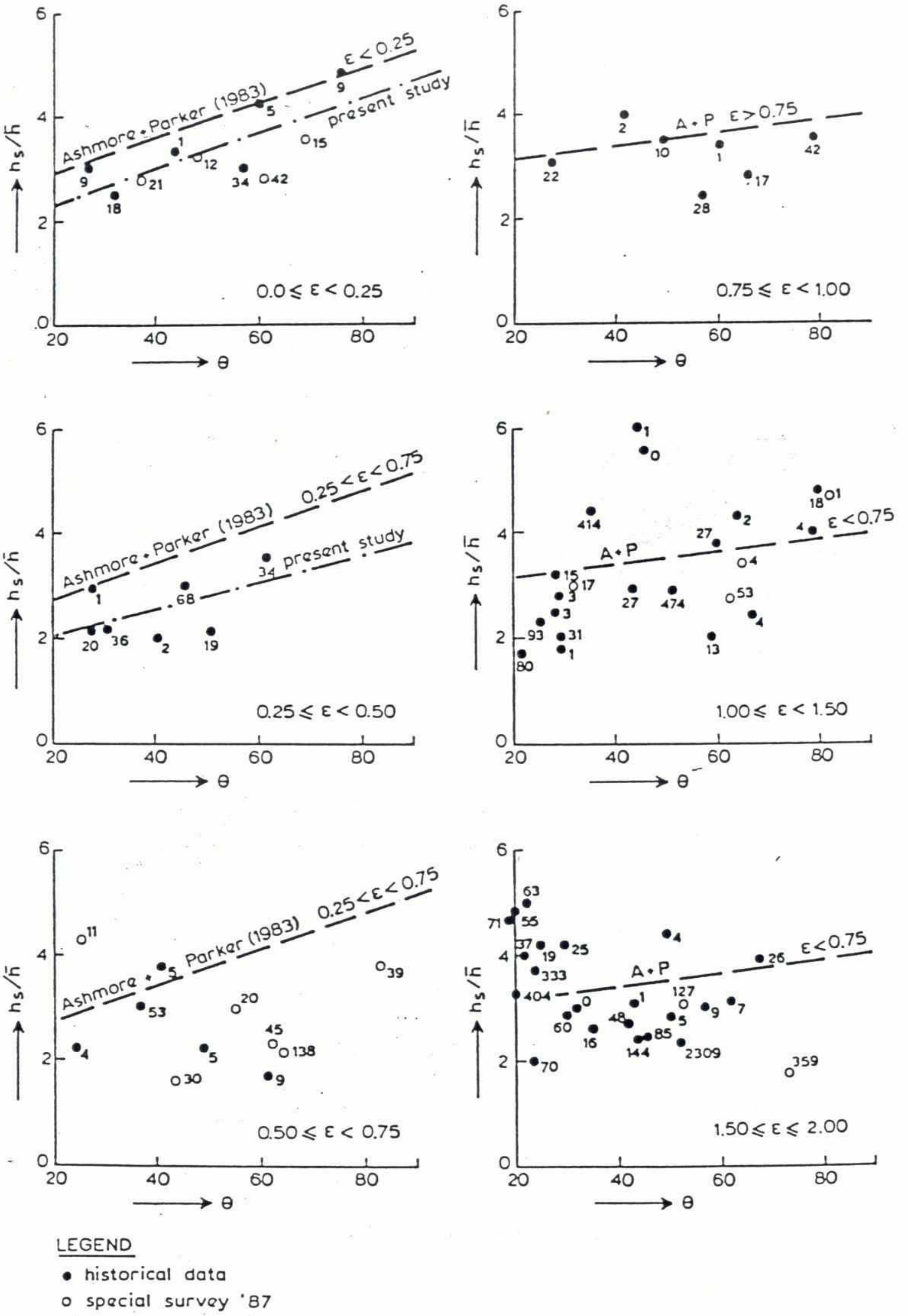

CONFLUENCE SCOUR JAMUNA RIVER, SEPARATED ACCORDING TO RATIO OF DISCHARGE OF CONFLUENCING CHANNELS

RPT / NEDECO / BCL

Q 553

FIG. B.3.7

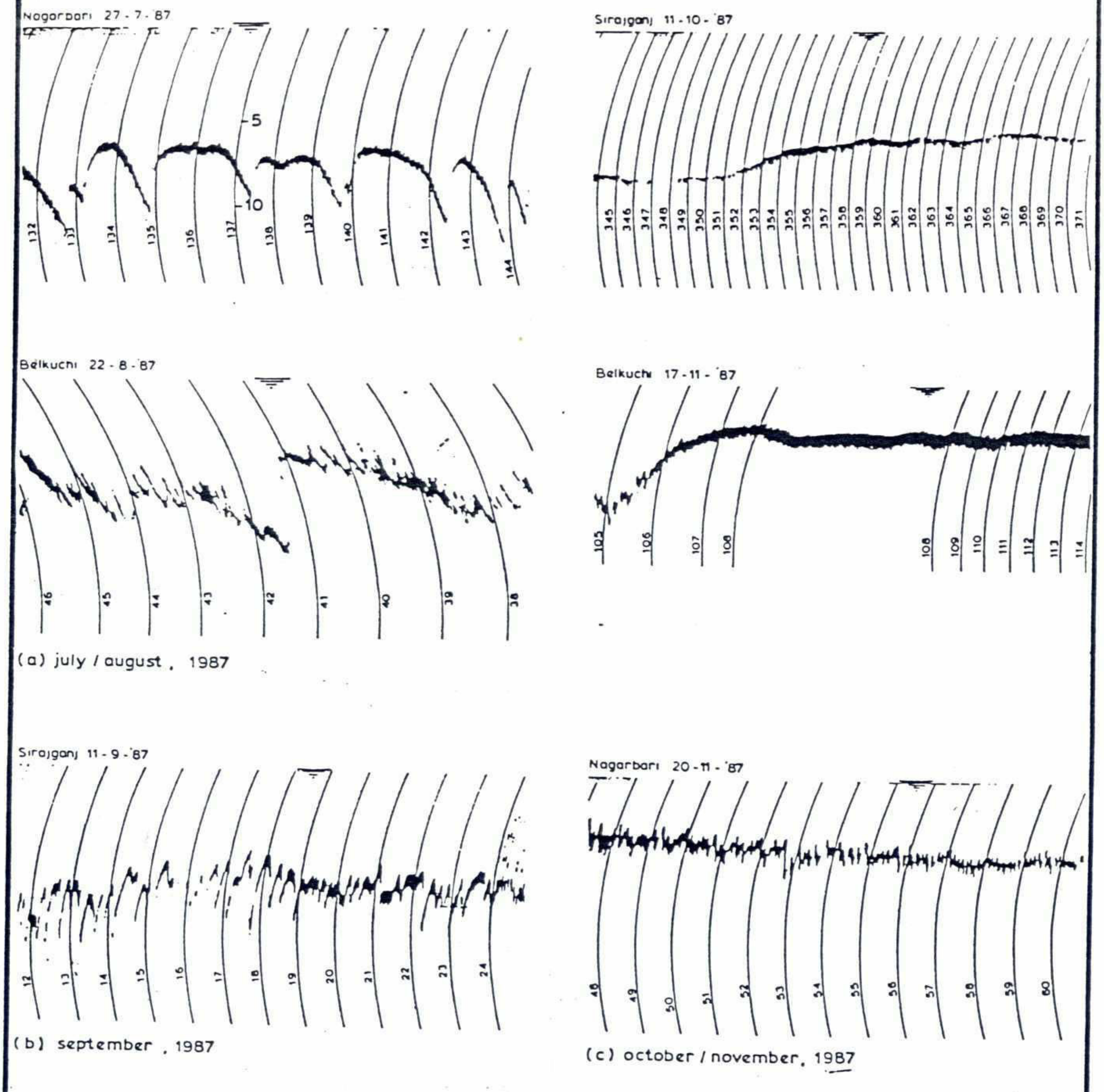

BEDFORMS IN THE JAMUNA RIVER OBSERVED DURING SPECIAL FIELD SURVEY IN 1987 (VERTICAL SCALA ± 1 : 500)		
RPT / NEDECO / BCL	Q 553	FIG. B.3.8

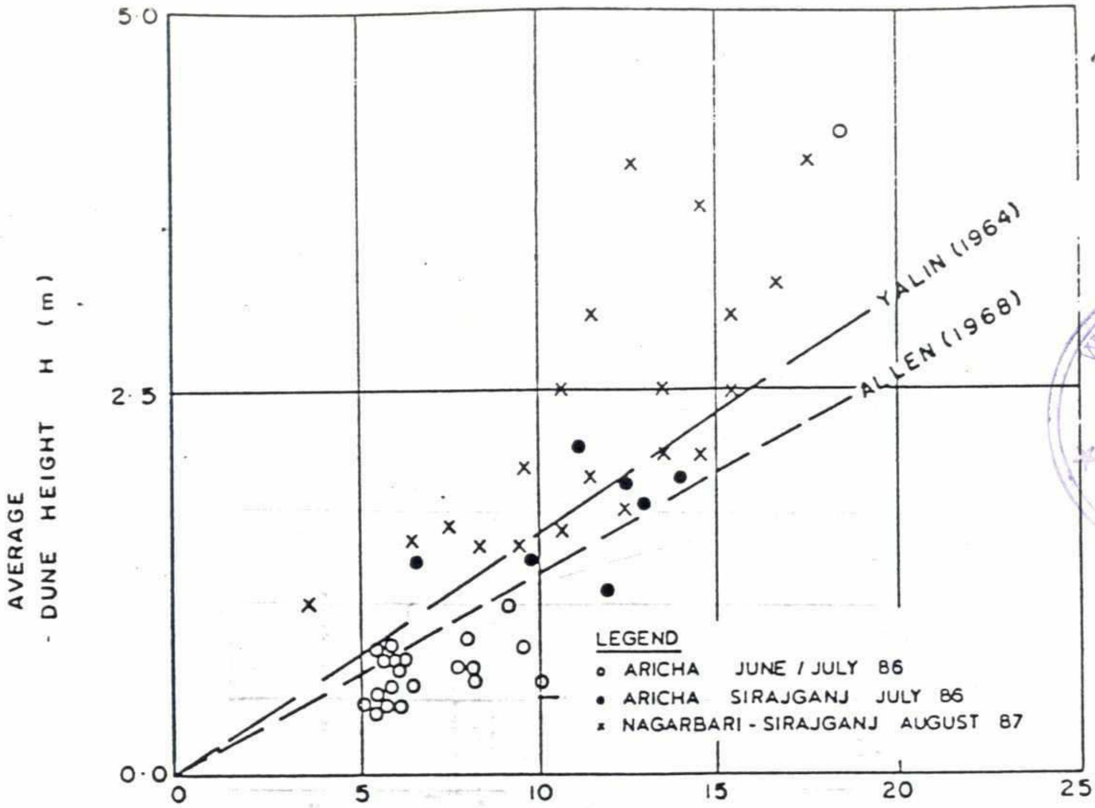

Figure B.3.9 Average dune height versus waterdepth

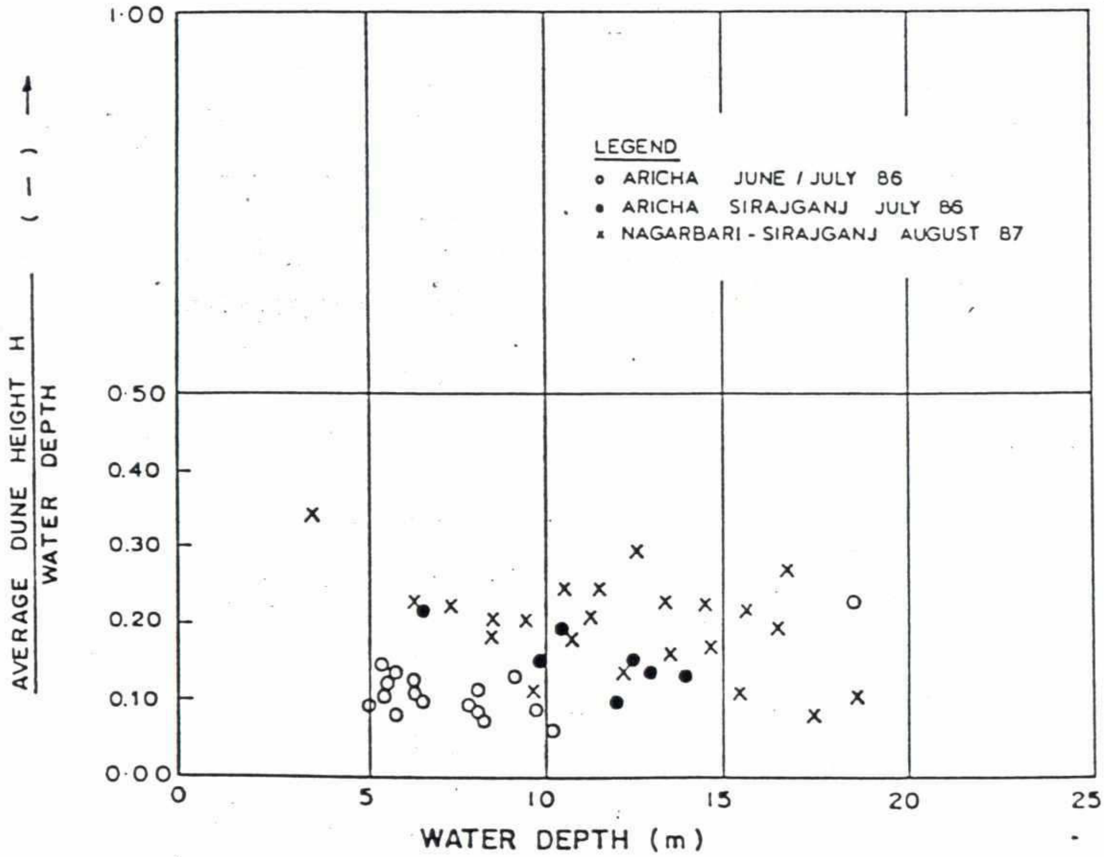

Figure B.3.10 Relative dune height versus waterdepth

RPT / NEDECO / BCL	Q 553	FIG. B.3.9/ B.3.10

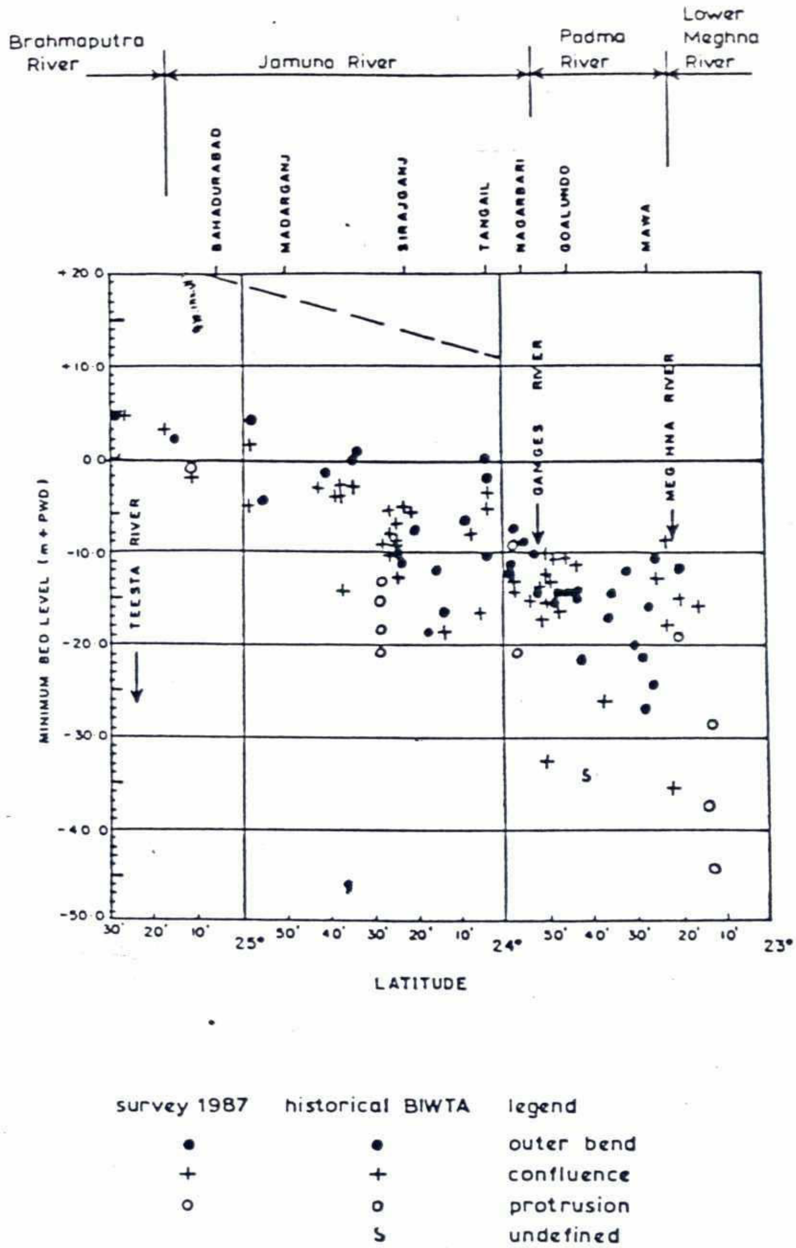

MAXIMUM DEPTHS OBSERVED IN THE JAMUNA RIVER OBTAINED FROM HISTORICAL BIWTA SOUNDING MAPS AND FROM SPECIAL SURVEY IN 1987		
RPT / NEDECO / BCL	Q 553	FIG. B.3.11

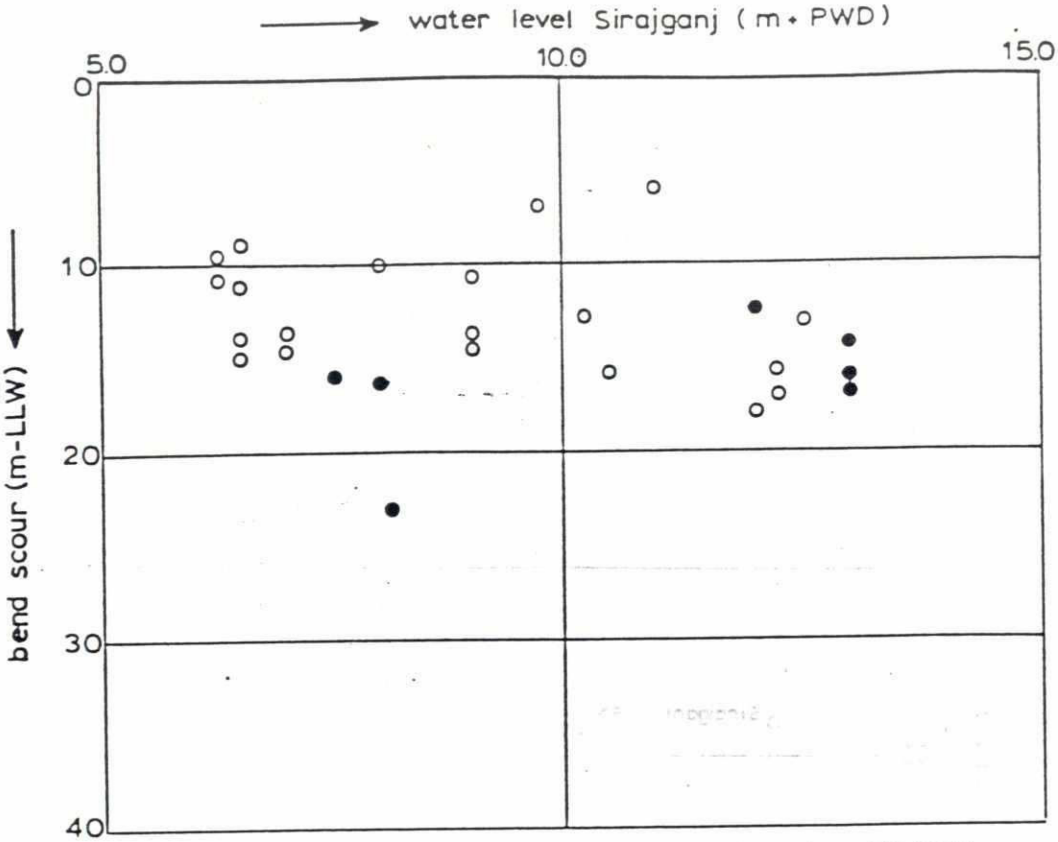

Figure B.312 Observed maximum bend scour depths BIWTA maps

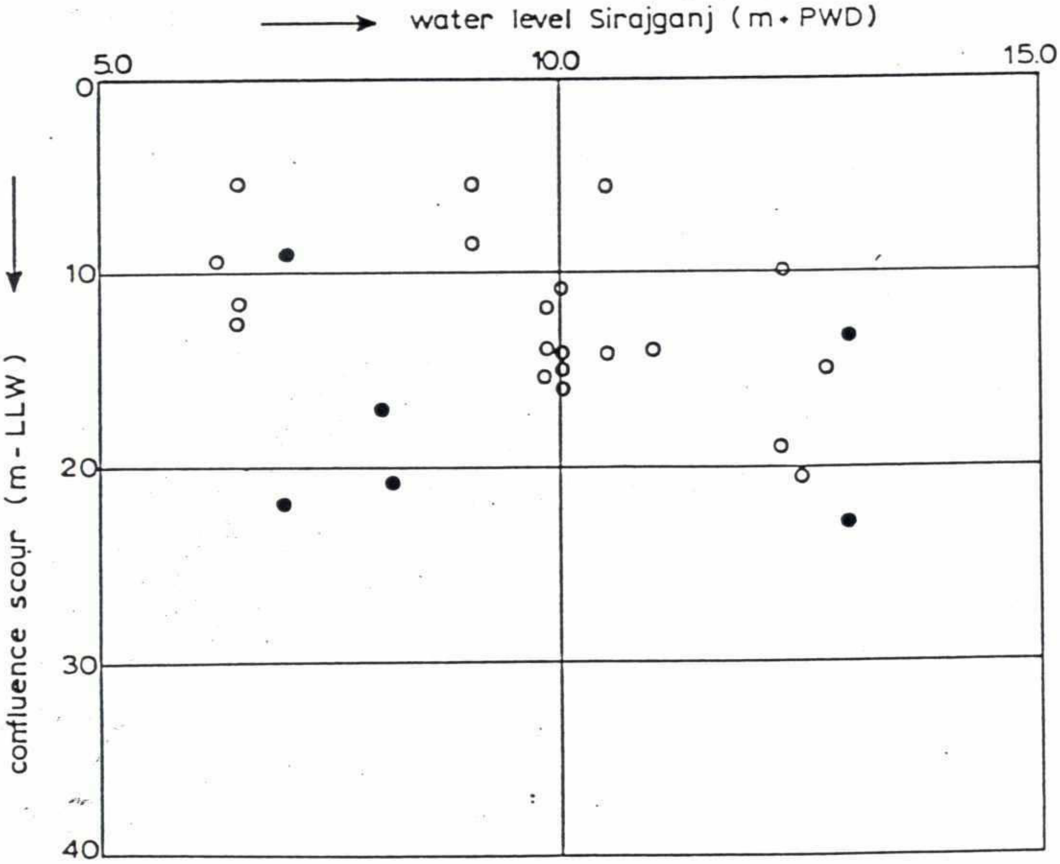

Figure B.3.13 Observed maximum confluence scour depths BIWTA maps

RPT / NEDECO / BCL	Q 553	FIG. B.3.12/ B.3.13

158

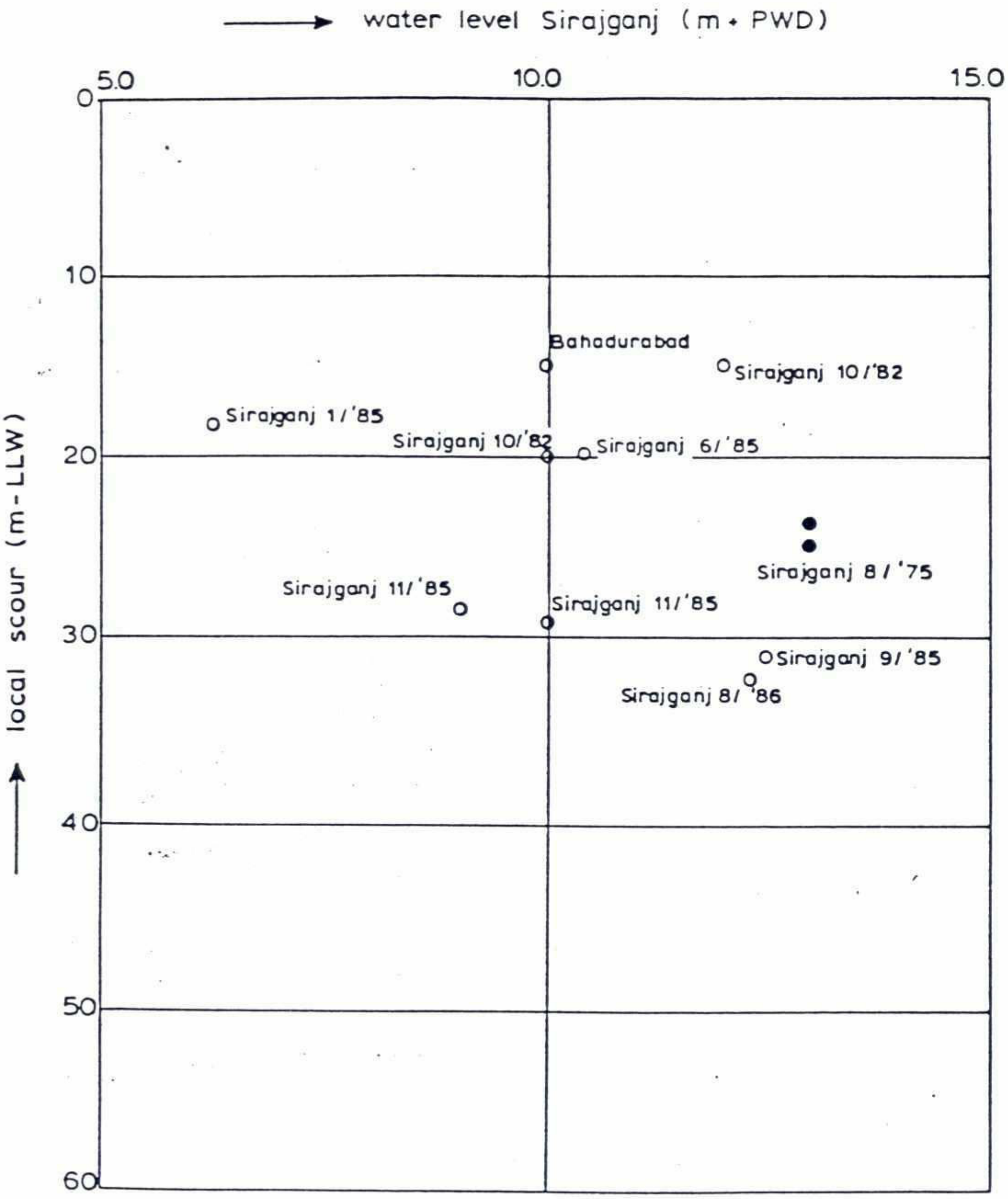

OBSERVED LOCAL SCOUR DEPTH ON BIWTA - MAPS		
RPT / NEDECO / BCL	Q 553	FIG. B.3.14

ANNEX B

River Morphology

Appendix B-1 References

787

APPENDIX B-1

REFERENCES

- ALLEN, J.R.L. (1960), Current ripples, Amsterdam, North Holland Publ. Cy.
- ASHMORE, P. & PARKER, G. (1983), Confluence scour in coarse braided streams, Water Resources Research, Vol. 19, no. 2, pp. 392-402
- BRISTOW, C. (1985), Brahmaputra River: Channel Migration and Deposition (paper prepared for Conference on Fluvial Sedimentology, preprint sent as private communication to W.K. Cross).
- COLEMAN, N.L. (1969), Brahmaputra River: channel processes and sedimentation, sedimentary Geology, Vol. 3, pp. 129-239
- ENGELUND, F. and HANSEN, E. (1967), A monograph on sediment transport in alluvial streams, Teknisk Vorlag, Kopenhagen, Danemark
- HICKING, E.J. & NANSON, G.J. (1983), Lateral migration rates of river bends, Journ. of Hydraulic Engng., Vol. 110, pp. 1557 - 1567
- HOWARD, A.D., KEETH, M.E. & VINCENT, C.L. (1970), Topological and geometrical properties of braided streams, Water Resources Research, Vol. 6, No. 6, pp. 1674-1688
- IECO (International Engineering Company) (1969), Bank-line movement of the Brahmaputra - Jamuna River, Prepared for East Pakistan Water and Power Development Board
- JOHANNESSEN, H. & PARKER, G. (1985), Computer-simulated migration of meandering rivers in Minnesota, Univ. of Minnesota, St. Authony Falls Hydr. Lab., Rep. no. 242
- KLAASSEN, G.J. & VERMEER, K. (1988a), Channel characteristics of the braiding Jamuna River, Bangladesh, Proc. Intern. Symp. on River Regime, Wallingford, U.K.

189

REFERENCES (continued)

- KLAASSEN, G.J., VERMEER, K. & UDDIN, N. (1988), Sedimentological processes in the Jamuna (Lower Brahmaputra) River, Bangladesh, Proc. Intern. Conf. on Fluvial Hydraulics, Budapest, Hungary

- KLAASSEN, G.J. & VERMEER, K. (1988b), Confluence scour in large braided rivers with fine bed material, Proc. Intern. Conf. Fluvial Hydraulics, Budapest, Hungary

- KLAASSEN, G.J., OGINK, H.J.M. & RIJN, L.C. van (1986), DHL-research on bed-forms, resistance to flow and sediment transport, 3rd Int. Symp. on River Sedimentation, Jackson (MS), U.S.A.

- LACEY, G. (1958), Flow in alluvial channels with sandy mobile bed, Proc. Instr. Civ. Engers, Vol. 9, Mp. 145-164

- LACEY, G. (1930), Stable channels in alluvium, Minutes of Proc. Instn. of Civ. Eng., Vol. 229, pp. 259-292

- LACEY, G. (1947), A general theory of flow in alluvial, Journal supplement, Instn. of Civ. Eng., no. 8, papaer 5518, pp. 425-451

- LEOPOLD, L.B., WOLMAN, M.G. & MILLER, J.P. (1964), Fluvial processes in geomorphology, San Francisco, W.H. Freemand and Cy.

- MEYER-PETER, E. and MÜLLER, R., (1948), Formulas for bed load transport, Rep. 2nd Meeting IAHR, Stockholm, Sweden

- MOSLEY, M.P. (1976), An experimental study of channel confluences, Journ. Geol., Vol. 84, pp. 535-562

- NAZIM, U. (1985), Hydraulic parameters of the flow and riverbed routing of the Lower Brahmaputra/Jamuna River, Moscow Hydrotechnical Engineering Institute, Ph. D. Thesis (in Sussian).

REFERENCES (continued)

- RIJN, L.C. van (1984), Sediment transport, part I, II, and III, Journal of Hydraulic Engineering ASCE, Vol. 110, pp. 1431-1456 + 1613-1641 + 1733-1754.
- ROQUE, N. (1983), Application of remote sensing technology for detecting fluvial changes of the Ganges and Brahmaputra-Jamuna river courses in Bangladesh, Albequerque (New Mexico), Univ. of Mexico/Dhaka, SPARSSO
- RPT/NEDECO/BCL (1987), Jamuna Bridge Appraisal Study, Phase I, London, Final Report (prepared for UNDP/World Bank and JMBA)
- STEVENS, M.A. (1986), Width of straight alluvial channels, Journ. Hydr. Engng., ASCE, Vol. 112, no. HY 9, pp.
- STEVENS, M.A. & SIMONS, D.B. (1973), Manning's roughness coefficient for the Padna River, Proc. 15 IAHR Congress, Istanbul, Turkey, paper A.2.
- SIMONS, D.B. and ALBERTSON, M.L., (1960), Uniform water conveyance channels in alluvial material, Journ. Hydr. Div. ASCE, Vol. 86, no Hy 5, pp. 33-71
- STRUIKSMA, N., OLESEN, K., FLOKSTRA, C. & VRIEND, H.J. de (1985), Bed deformation in curved alluvial channels, Journal of Hydraulic Research, Vol. 23, No. 1, Mp. 57-79
- STRUIKSMA, N. & KLAASSEN, G.J. (1988), On the threshold between meandering and braiding. Paper submitted for River Regime Conference, Wallingford, U.K.
- SUTHERLAND, A.J. (1986), Scouring in channel confluences, Proc, 9th Australasian Fluid Mechs. Conf. Auckland, New Zealand, pp. 260-263
- ULLAH, M.H. (1987), Computer modelling of river channel changes in alluvial conditon. First Interim Report: Analytical study of channel changes of the Brahmaputra, Dhaka, Bangladesh University of Engng. and Technology, Institute of Flood Control and Drainage Research.

REFERENCES (continued)

- YALIN, M.S. (1964), Geometrical properties of sand waves, Proc. ASCE, Vol. 90, no. Hy5, pp. 105-169.

~~MD~~

ANNEX B

River Morphology

Appendix B-2 Table of Jamuna River BWDB cross-sections analysed

	66/67	67/68	68/69	69/70	-	76/77	77/78	78/79	-	80/81	81/82	-	84/85	85/86
J2-1	n.a.	19/2	5/5	29/11		4/4	27/12	8/12		10/1	13/1		n.a.	1/4
J4	12/3	n.a.	23/2	7/1		9/6	24/1	28/12		16/3	27/1		2/1	19/4
J5	30/1	16/2	27/1	23/1		10/11	17/4	7/1		11/3	5/2		7/1	1/5
J5-1	n.a.	17/1	13/1	30/1		21/11	11/4	13/1		24/2	9/2		n.a.	7/5
J6	23/1	24/12	10/1	3/3		26/11	3/4	18/1		4/2	12/2		12/1	13/5
J6-1	n.a.	8/12	24/11	18/3		10/12	28/3	24/1		15/1	5/12		-	23/11/86
J8	14/2	1/2	13/5	4/6		6/1	10/3	18/2		16/11	11/1		26/1	19/5
J11	n.a.	16/12	11/4	3/5		25/2	31/1	6/4		8/3	7/2		10/2	22/4
J12	25/12	n.a.	16/3	13/3		n.a.	13/1	16/4		2/4	7/12		15/2	4/5
J13-1	12/12	26/2	4/2	24/1		9/4	1/1	1/5		n.a.	1/2		n.a.	16/5
J16	24/10	12/11	22/11	10/11		20/10	27/11	27/5		15/2	26/1		3/7	25/7

Appendix B-2 Table of Jamuna River BWDB cross-sections analyzed

ANNEX B

River Morphology

Appendix B-4 Location and dates of special hydrographic surveys (1987) m6

APPENDIX B-4

LOCATION AND DATES OF SPECIAL HYDROGRAPHIC SURVEYS (1987)

Date	Location	Type of survey/ phenomenon surveyed
18/24-07 & 25/29-11	"1"&"2" Aricha	Confluence scour
27-07, 20-11	Nagarbari	Bedforms & dune tracking
17-08, 20/22-11	Pechakhola	Bend scour
22-08, 16-11	Belkuchi South	Bedforms & dune tracking
10-09, 11-10	Project area	Overall survey
11-09, 11-10	Sirajganj	Bedforms & dune tracking
31-08, 09/10-10 & 13-10	"1"&"2" Sirajganj	Confluence scour
24/25-08, 23/24-10	Bhuapur	Bend scour and bedforms
03/19-09	Sirajganj	Local scour near town protection works
26/27-09, 29/30-10	Pingna	Bend scour
22/25-09, 26/27-10	Kazipur South	Confluence scour
11/13-11	"1"&"2" Dighapara	Bend scour
09-11	Chandpara	Bedforms & dune tracking

VD8

ANNEX B

River Morphology

Appendix B-5 Constriction scour, backwater calculations and resistance to flow

APPENDIX B-5

B-5 Constriction scour, backwater calculations and resistance to flow

B-5.1 Introduction

Apart from the RIVMOR computations carried out to predict constriction scour and backwater effects near Jamuna Bridge (see Phase I, final report, Appendix C.5.3), some additional situations were computed.
For one schematization of main channel and flood plain, two different bridge lengths were taken. The results relating to scour and backwater are compared in Appendix B-5.2. A computation with schematization adapted to the final location and length of the bridge, was carried out on well. These computations are in Appendix B-5.3.
In Appendix B-5.4 the resistance to flow of the Jamuna river during flood conditions is discussed. This is important as far as the backwater effects are concerned. In Appendix B-5.5 sediment transport in the Jamuna River is treated. Sediment transport rate determines the time scale of morphological processes and is therefore important for constriction scour.

B-5.2 Effect of bridge length on constriction scour and backwater

In order to asses the effect of the bridge length on the constriction scour and backwater, computations were carried out for two bridge lengths with the same schematization of main channel and flood plain (char). This schematization can be summarized as follows (see also Figure B-5.1):

- the cross-section is supposed to consist of a main channel representing the sum of the deeper channels and a more shallow part representing the chars;
- the total width of main channels and chars in 4500 m for each, so the total river width is 9000 m;
- the difference in level between main channel bed and char is assumed to be 6.7 m.
- the slope of the main channel and char equals 7.10^{-5} ;
- the Chézy coefficient of main channel and chars was 67 $m^{\frac{1}{2}}/s$ and 50 $m^{\frac{1}{2}}/s$ respectively;
- the sediment transport is computed using the Engelund/Hansen formula;
- the bed material size is 0.18 mm;

- the total reach included in the model is 100 km, where the bridge is assumed to be located at 50 km;
- the geometry of the constriction is as indicated in Figure B.5.1.

The following boundary conditions were applied:
upstream boundary (km 0):
- bed level constant, implying that the actual sediment transport corresponds to the sediment transport capacity,
- discharge corresponding to a normal year and to an extreme year (see Table B-5.1)
- discharge rapidly increasing from bankfull to 1 : 100 year flood. A maximum rise of the water level of 3 m in 10 days was assumed.

downstream boundary (km 100):
- water level from a rating curve where it is assumed that normal depth is present, so:

$h_d < 6.7$ m $\qquad Q_t = B_d h_d C_d \sqrt{h_d i}$

$h_d > 6.7$ m $\qquad Q_t = B_d h_d C_d \sqrt{h_d i} + B_s h_s C_s \sqrt{h_s i}$

where $h_d = h_s + 6.7$ m

- no changes in the rating curve over time.

Initially, the bed level in the model was straight for all computations. A grid size of 500 m was applied and a maximum time step of 5 days. This time step is automatically reduced by RIVMOR in case numerical instability would occur.

Four cases were computed:

T1 : bridge length of 5300 m, 4 normal + 1 extreme year
T2 : bridge length of 3500 m, 4 normal + 1 extreme year
T3 : bridge length of 5300 m, fast rise of water level to 1 : 100 year flood
T4 : bridge length of 3500 m, fast rise of water level to 1 : 100 year flood

2209

In Figure B-5.2 the resulting bed levels of T1 and T2 are given. In the case of a bridge length of 5300 m a maximum contriction scour at the bridge site of about 0.8 m is observed in the year with high maximum discharge. For a further constriction to 3500 m a maximum constriction scour of 3.0 m was computed. This severe scour is caused by the reduction of the main channel width in T2, while in T1 only the char width (with less flow) was constricted. In Figure B-5.3 the water level 3 km upstream of the bridge (where the constriction starts) is given. For T1 only a very limited rise of the maximum water level is observed, less than 0.1 m. For T2 the backwater effects are more noticeable, a maximum increase of 0.3 m is noticed. For T2 a considerable lowering of the water level during low flow is computed (± 0.3 m). This is caused by the scour hole at the bridge site, which is reducing the resistance to flow. T3 and T4 were computed to predict the worst condition scour that may occur. The discharge increases from 40,000 m³/s, which is about bankfull, to 91.000 m³/s, which is the 1 : 100 year discharge, in 14.5 days. This corresponds approximately with a rise of water level of 3 m in 10 days. This was the maximum rise of water level observed in the available hydrographs. The top discharge was maintained for 25 days.
In Figure B-5.4 the resulting bed levels of T3 and T4 are given. For a bridge length of 5300 m a maximum scour at the bridge site of 1.2 m is reached after 25 days of maximum flood. For a bridge length of 3500 m the maximum scour is 4.1 m. Maximum backwater is 0.1 m for the 5300 m bridge and 0.3 m for the 3500 m bridge. See Figure B-5.5.

From the present computations it is concluded, that a river constriction which includes a reduction of the main channel, leads to considerable more constriction scour and backwater effects, than a reduction of char width only.

B-5.3 <u>Constriction scour for proposed situation</u>

Additional computations were carried out with the constriction scour model when the approximate final location and length of the bridge was decided. This resulted in an adaption of the schematized cross-section:

- the width of the main channel was 3400 m and the width of chars was 8900 m, so the total river width was 12300 m,
- bridge length was 4600 m.

See Figure B-5.6.
The same computations were carried out for this situation as described in Appendix B-5.2. The resulting bed levels are given in Figure B-5.7. For the extreme year hydrograph a maximum scour of 1.7 m was found. For the extreme 1 : 100 year discharge the maximum scour was 3.1 m after 25 days of maximum flood.
The backwater effects are presented in Figure B-5.8. For the extreme year hydrograph the backwater effects are less than 0.2 m. For the extreme 1:100 year discharge the maximum backwater effect was 0.3 m.
In the computations the backwater effect is noticeable over a considerable reach. Even at the upstream boundary (50 km upstream of the bridge) about 10% of the maximum backwater is present. It is not possible to draw the same conclusion for the prototype at this moment, as the schematization in the mathematical model is fairly rough.

B-5.4 Resistance to flow

In this Appendix, the resistance to flow of the Jamuna River is determined in two ways, using historical data on the Jamuna River:
- via discharge measurements (local average water depth and flow velocity in combination with measured slope over a larger distance) and,
- via average at-a-station-relationships between average depth and discharge, and between channel width and discharge.

For the first method, the resistance to flow, as represented by the Chézy coefficient:

$$C = Q/B\ (h)^{3/2}\ i^{\ 1/2}, \qquad \text{(B-5.1)}$$

in which Q = discharge [m^3/s], B = stream width [m], $\bar{h}$ = average depth [m], i = slope [-], is computed, using data presented by Uddin (1985). The data were derived from BWDB (Bangladesh Water Development Board) discharge measurements. The results for station Sirajganj are given in Figure B-5.9. From these data it is concluded that Chézy values vary between 40 $m^{\frac{1}{2}}/s$ for low flow and 100 $m^{\frac{1}{2}}/s$ for flood conditions. The very high Chézy values for flood conditions indicate a transition to flat bed for high discharge. However, during the (very high) flood of 1987 a flat bed situation was only observed some two

Resistance to flow of the Jamuna River for low-flow conditions is comparable to other rivers, while for flood conditions a rather low resistance to flow was observed. This is in line with the conclusions of Stevens & Simons (1973) for the Padma River. Dune heights appear to be larger than current prediction models indicate, especially for larger water depths. During flood conditions, resistance to flow owing to particle roughness, seems to be in the same order of magnitude as the form roughness, the bedforms having such gentle lee side slopes that they hardly contribute to form roughness.

Sediment transport on the Jamuna River is quite large, particularly at high discharge. The Engelund/Hansen transport formula multiplied by 2, gives a fair prediction of the bed material transport in the Jamuna River.

200

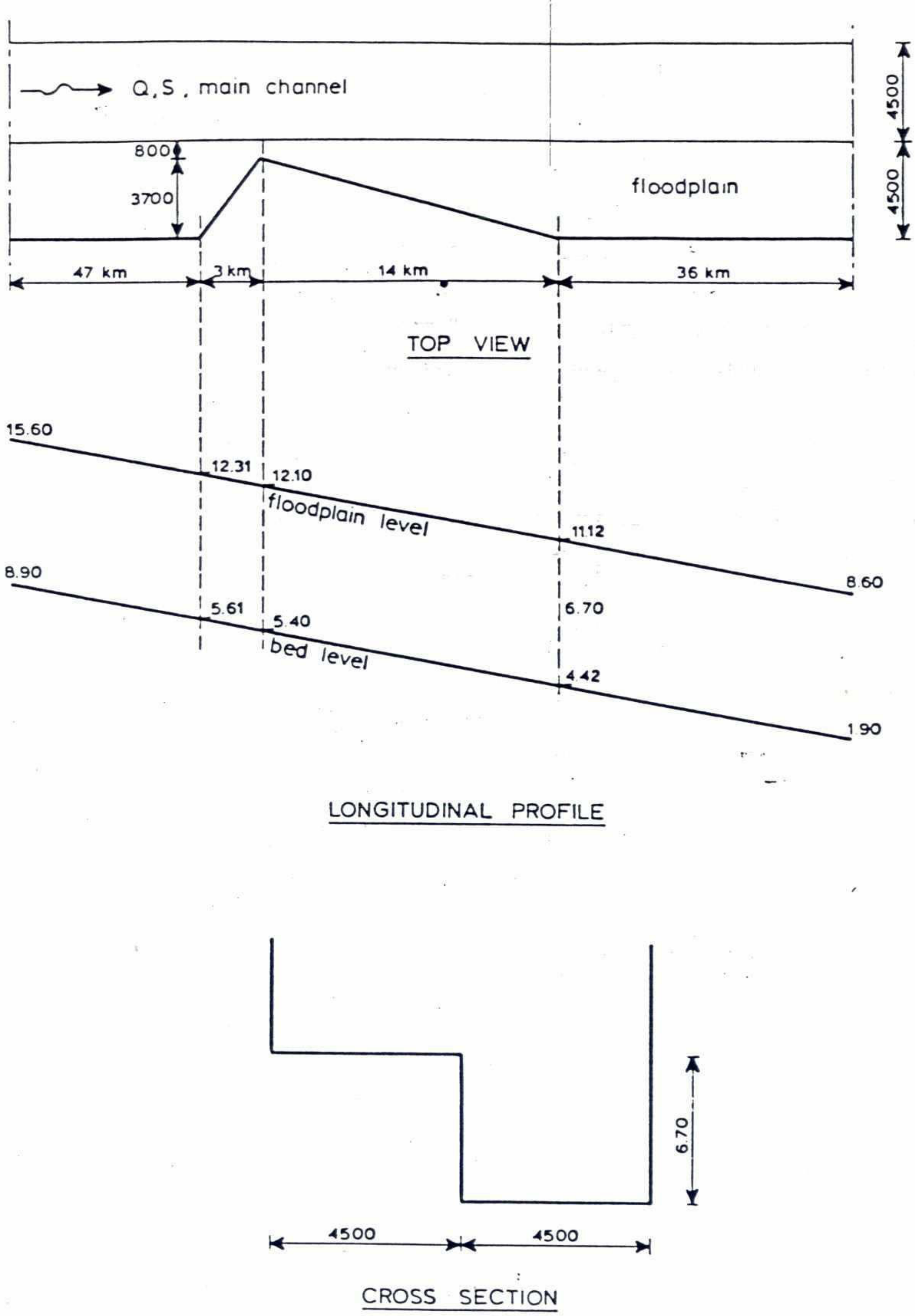

measures in metres

SCHEMATISATION FOR CONSTRICTION SCOUR COMPUTATIONS		
RPT / NEDECO / BCL	Q 553	FIG. B-5.1

20P

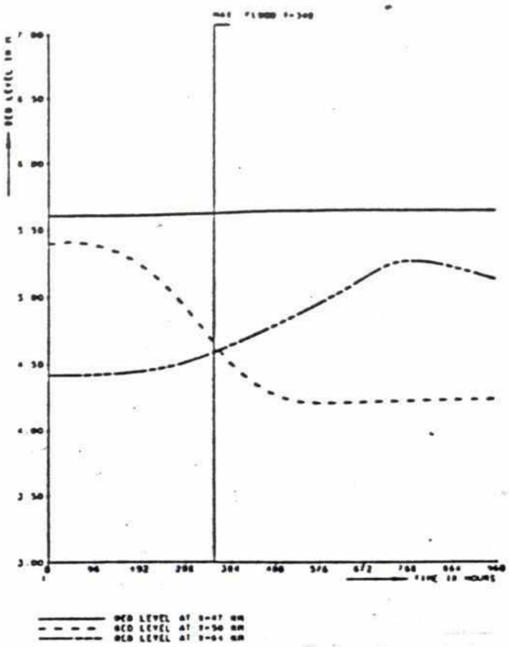

a. scour at beginning of constriction, bridge site and end of constriction as function of time, extreme discharge

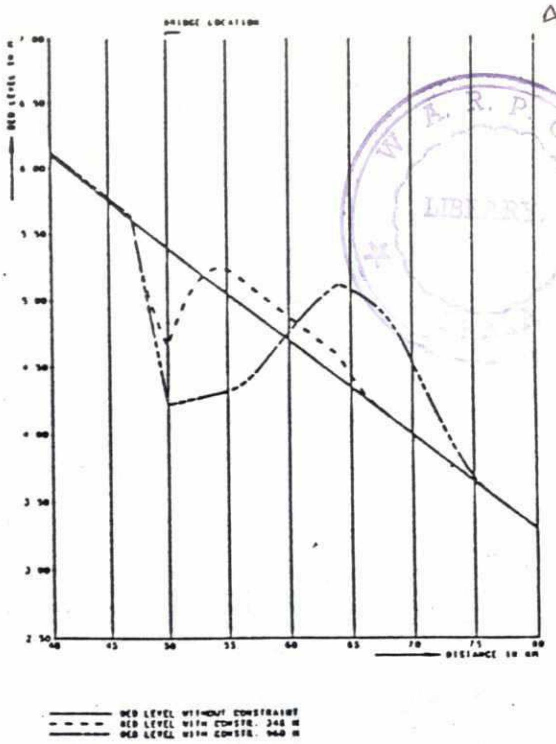

b. constriction scour as function of place, extreme discharge

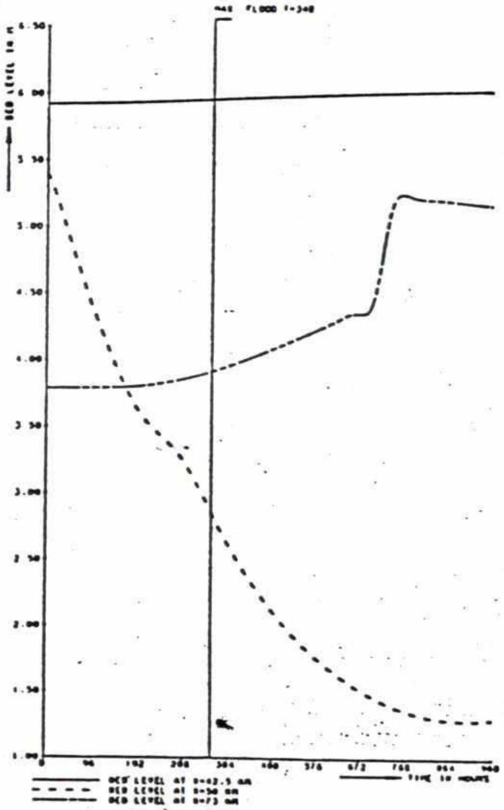

c. scour at beginning of constriction, bridge site and end of constriction as function of time, extreme discharge

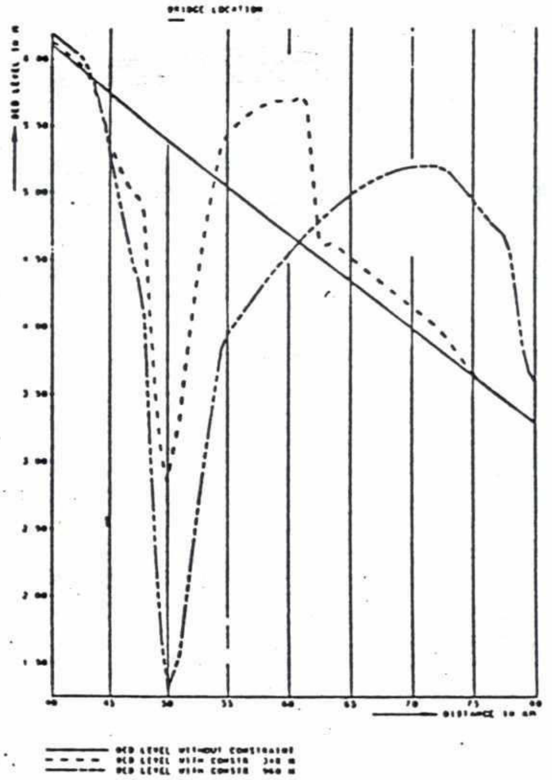

d. constriction scour as function of place, extreme discharge

CONSTRICTION SCOUR IN THE JAMUNA RIVER FOR A BRIDGE LENGTH OF RESP. 5300 m AND 3500 m, EXTREME DISCHARGE 1:100 YEAR FLOOD		
RPT / NEDECO / BCL	Q 553	FIG. B-5.4

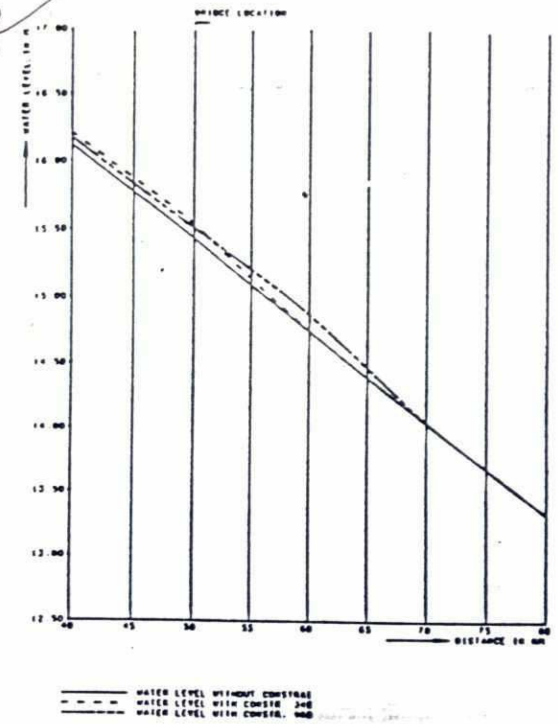

a. backwater as function of place, bridge lengt 5300 m

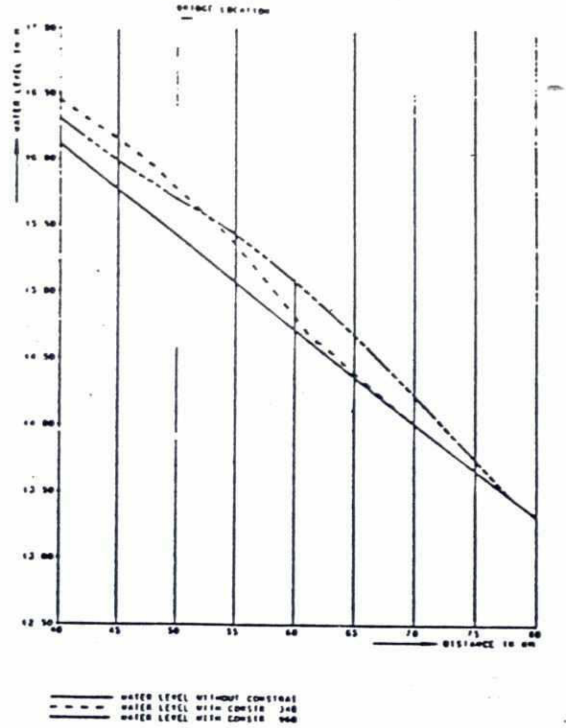

b. backwater as function of place, bridge length 3500 m

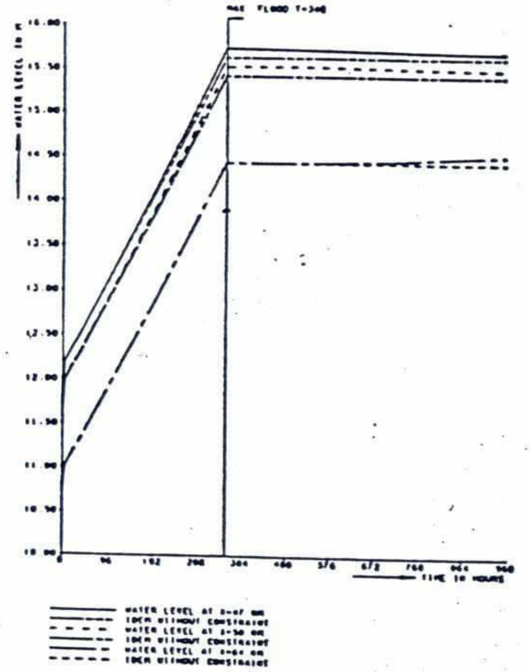

c. backwater at beginning of constriction, bridge site and end of constriction as function of time, bridge length 5300 m

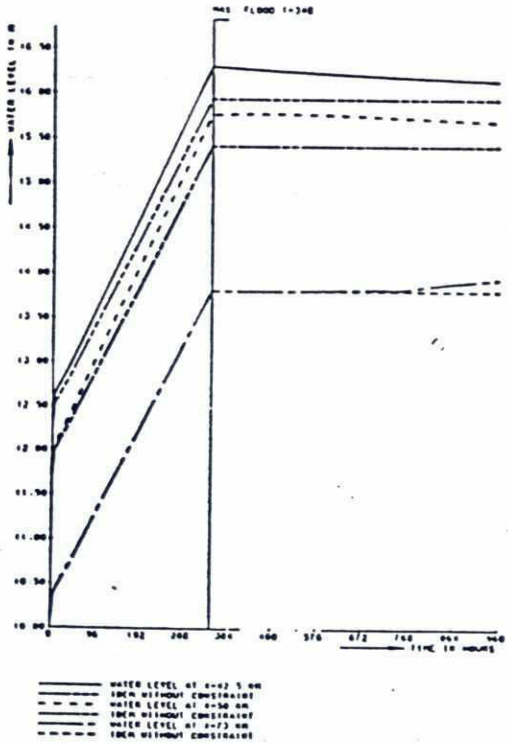

d. backwater at beginning of constriction, bridge site and end of constriction as function of time, bridge length 3500 m

BACKWATER IN THE JAMUNA RIVER FOR A BRIDGE LENGTH OF 5300 m AND 3500 m, EXTREME DISCHARGE 1:100 YEAR FLOOD

RPT / NEDECO / BCL

Q 553

FIG. B-5.5

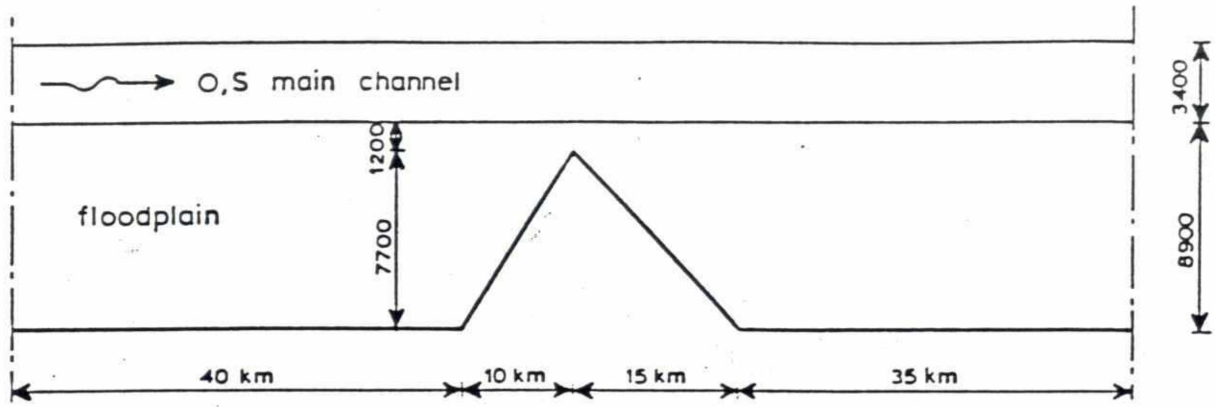

TOP VIEW

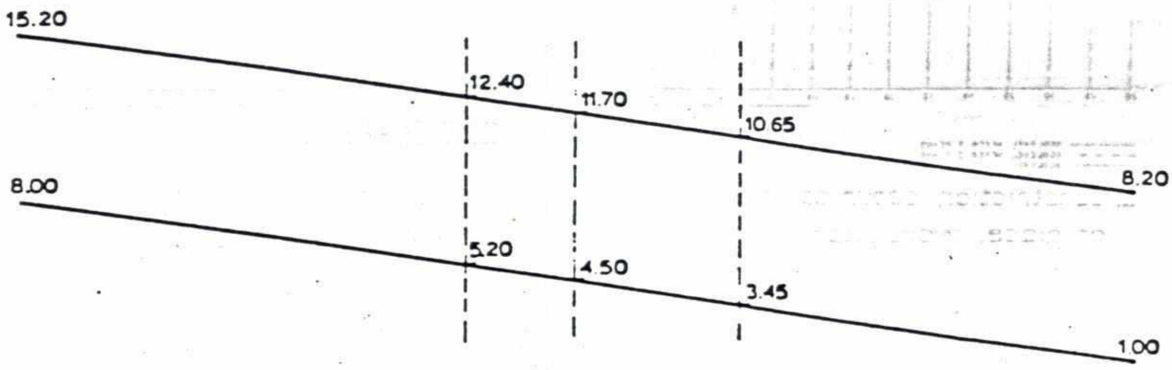

LONGITUDINAL PROFILE

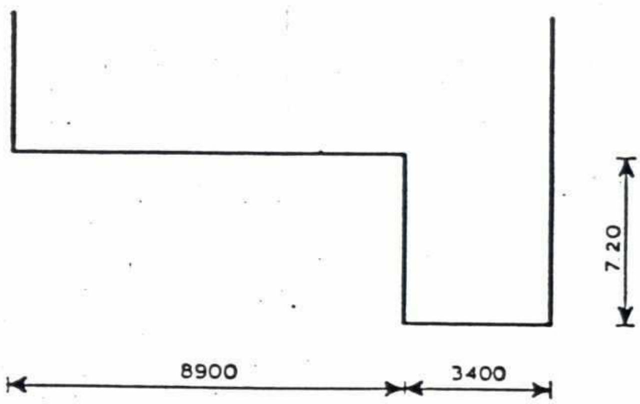

CROSS SECTION

measures in metres

SCHEMATISATION FOR CONSTRICTION SCOUR COMPUTATIONS FOR PROPOSED BRIDGE LOCATION		
RPT / NEDECO / BCL	Q 553	FIG. B-5.6

208

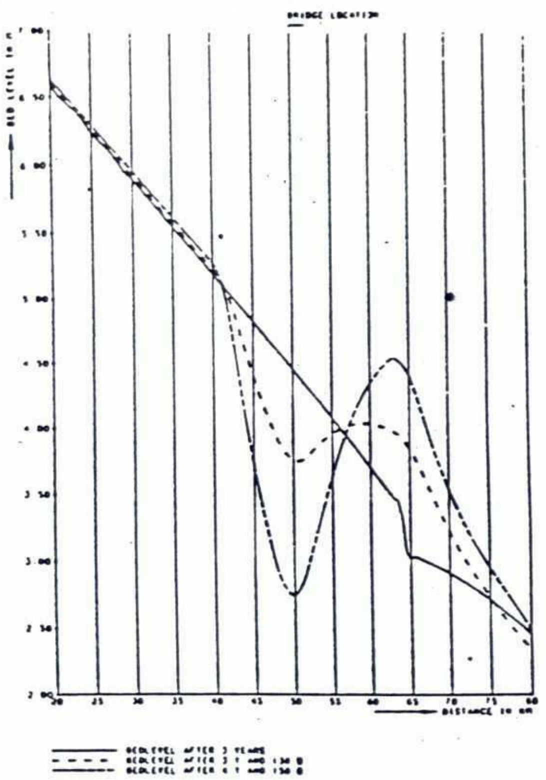

a. constriction scour as function of place, hydrograph

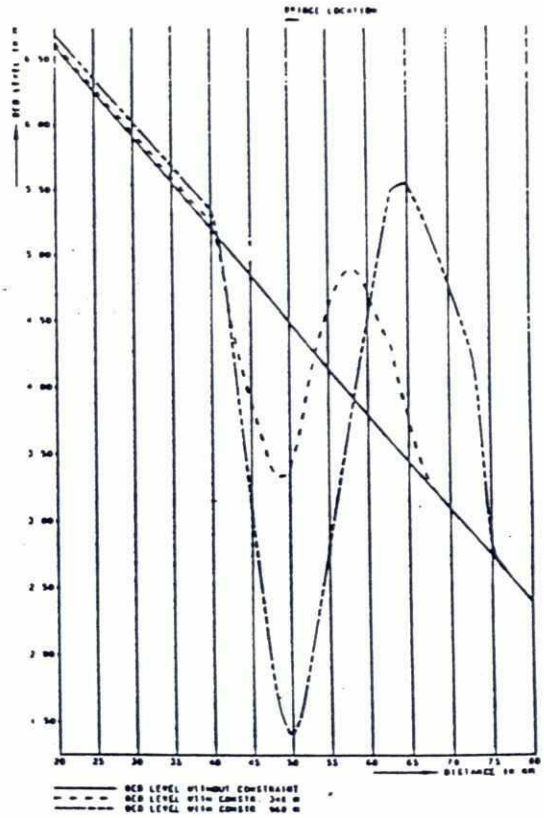

b. constriction scour as function of place, extreme discharge

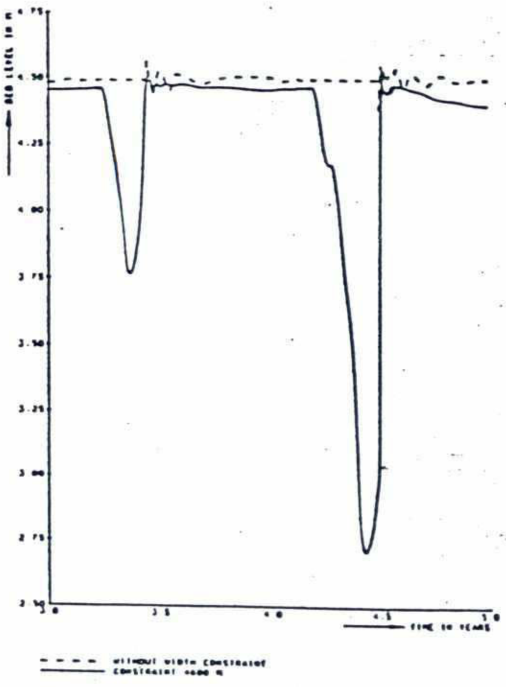

c. constriction scour as function of time at Jamuna Bridge, hydrograph

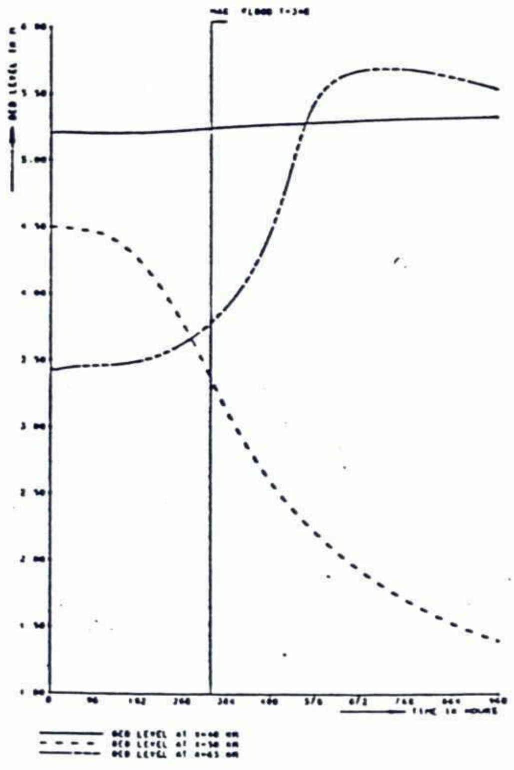

d. scour at begiming of constriction, bridge site and end of constriction as function of time, extreme discharge

CONSTRICTION SCOUR IN THE JAMUNA RIVER FOR A BRIDGE LENGTH OF 4600 m		
RPT / NEDECO / BCL	Q 553	FIG. B-5.7

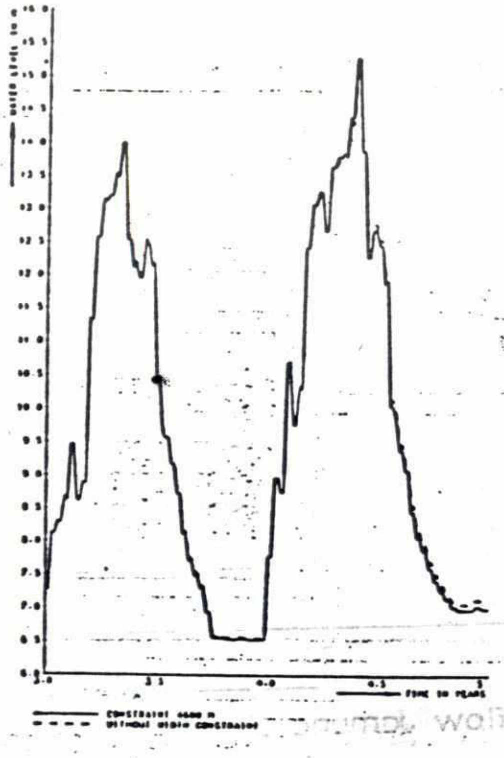

a. backwater at Jamuna Bridge due to constraint, hydrograph

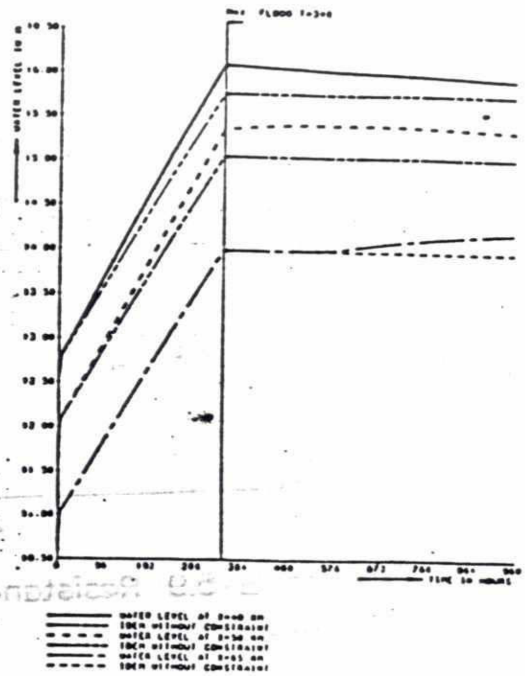

b. backwater near Jamuna Bridge, extreme discharge

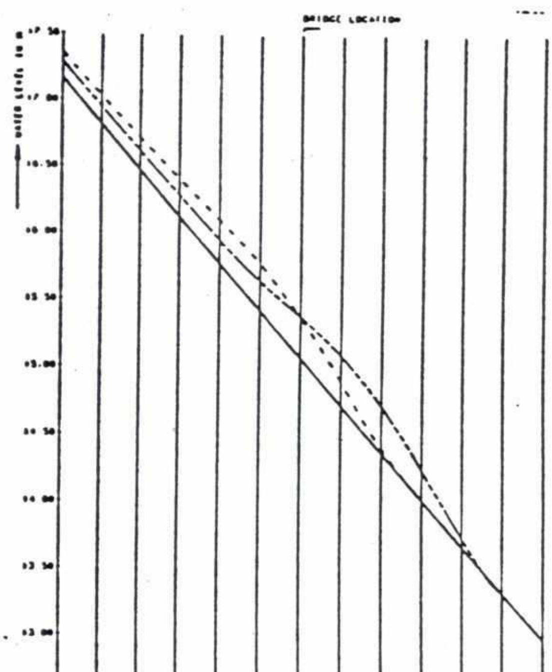

c. backwater on Jamuna River, extreme discharge

BACKWATER IN JAMUNA RIVER FOR A BRIDGE LENGTH OF 4600 m		
RPT / NEDECO / BCL	Q 553	FIG. B-5.8

207

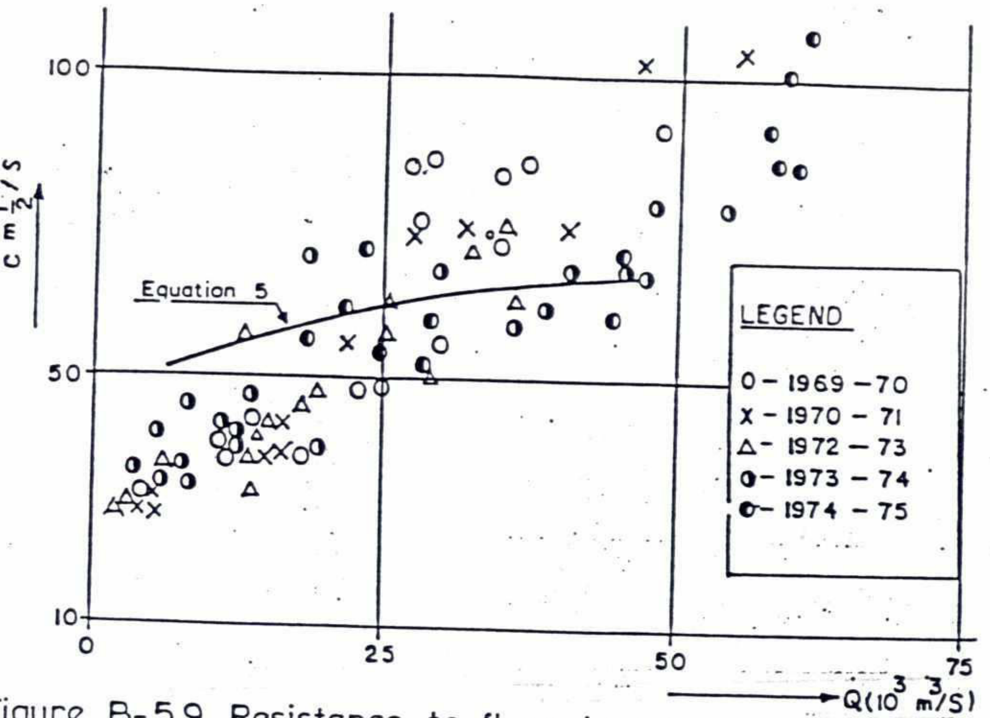

Figure B-5.9 Resistance to flow Jamuna River at Sirajganj

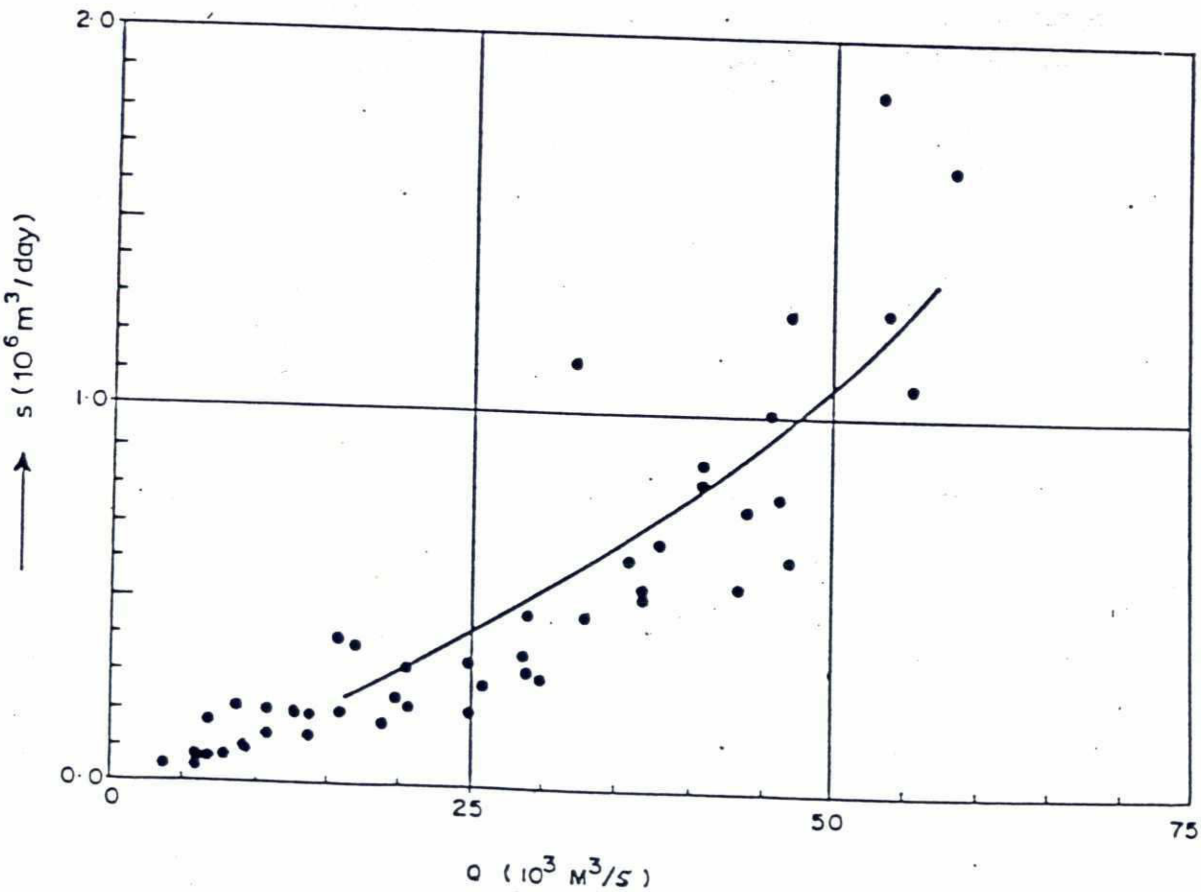

Figure B-5.10 Measured suspended bed material load in Jamuna River at Bahadurabad (1968-1970)

209

ANNEX B

River Morphology

Appendix B-6 Figures cross/section data

207

APPENDIX B-6

Figures cross-section data

In the following pages, some plots are given of the analyzed cross-section. An inventarisation of all the analyzed cross-sections is given in Appendix B-2. The plots give an impression of the stability of the individual channels of the Jamuna River.
Each figure consists of four cross-section plots for different years and one plot in which the relative conveyance of the plotted years is given. For cross-sections J6 and J12 no figures are given as it was not possible to select four years for which the reference monuments are in the same location. The figures support the opinion, that individual channel of the Jamuna are very mobile in horizontal direction. However, the outer limits of the combined channels remained more or less in the same location, indicating horizontal stability for the Jamuna River as a whole.

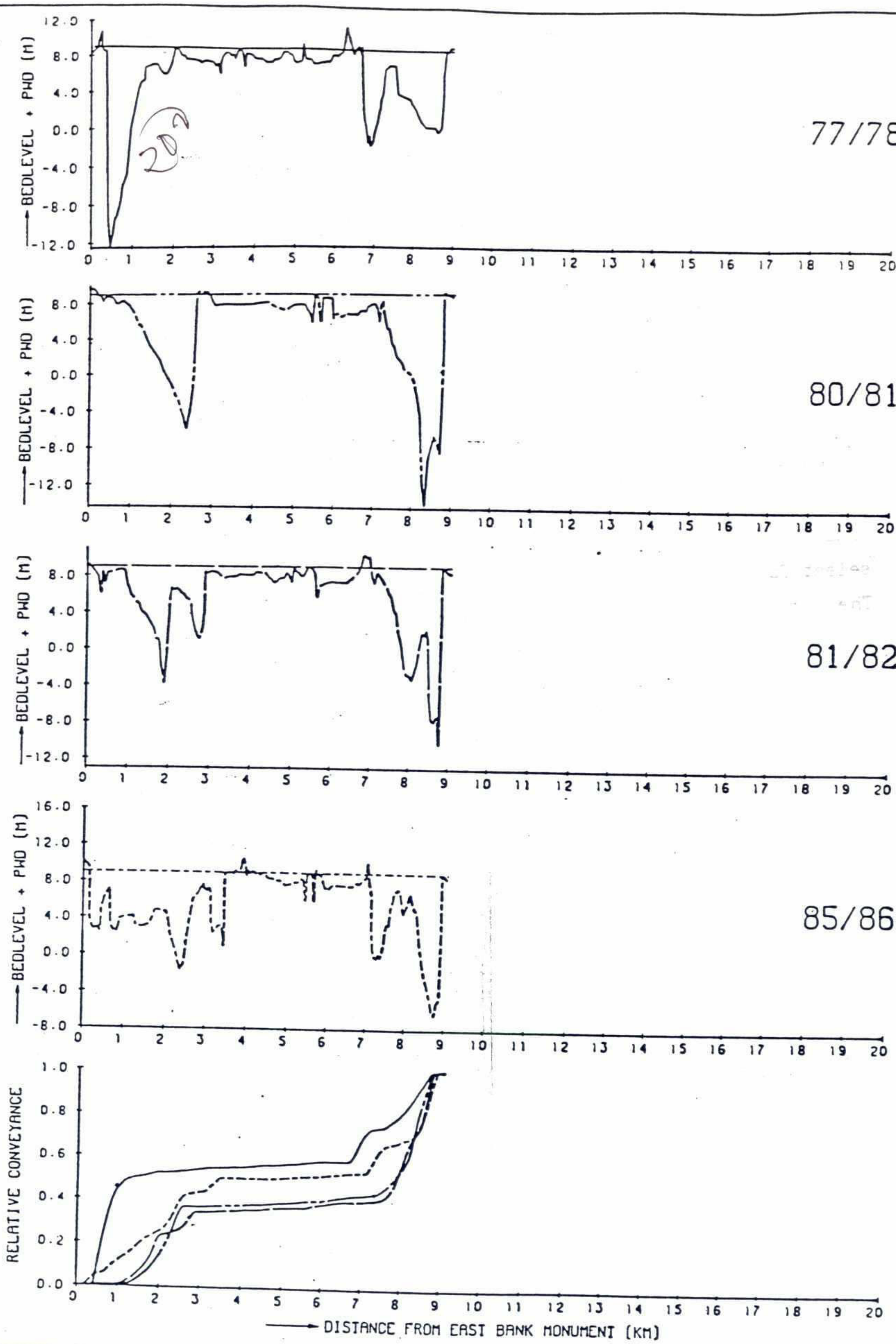

CROSS SECTIONS JAMUNA RIVER BANGLADESH (77/78-80/81-81/82-85/86)	J2-1	
RPT - NEDECO - BCL	Q 0553	FIG. B-6.1

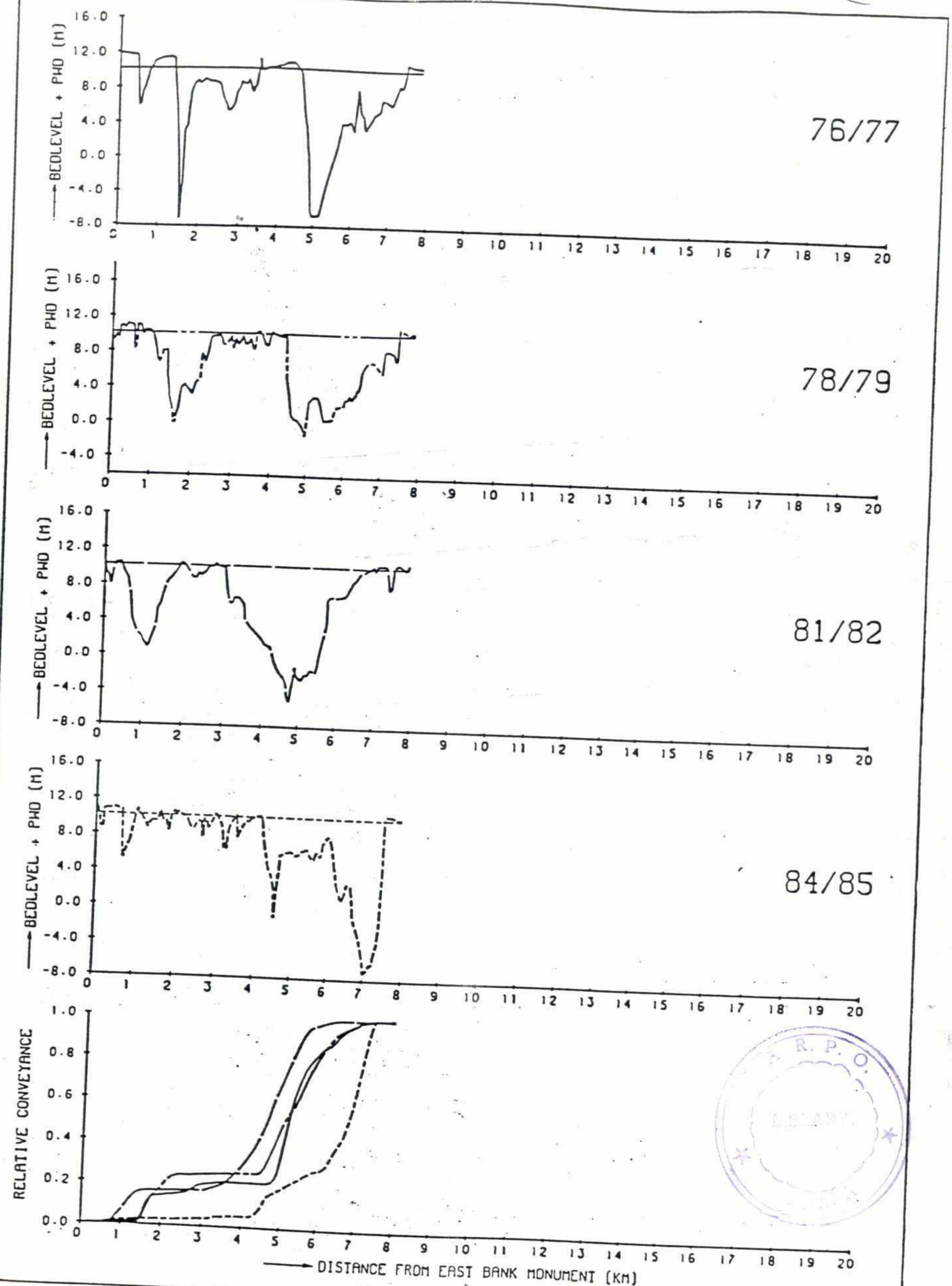

CROSS SECTIONS JAMUNA RIVER BANGLADESH (76/77-78/79-81/82-84/85)	J4	
RPT - NEDECO - BCL	Q 0553	FIG.B-6.2

222

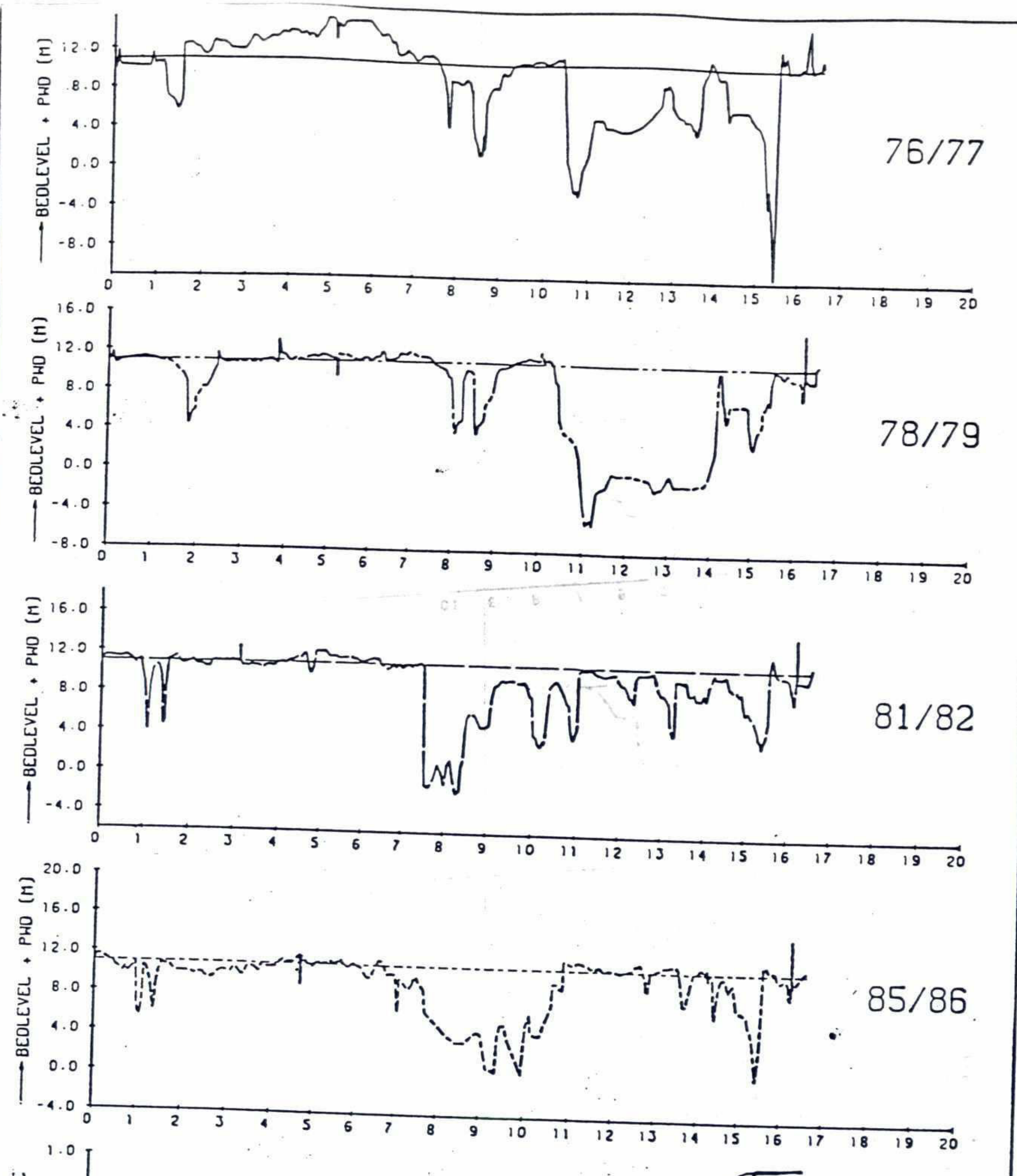

CROSS SECTIONS JAMUNA RIVER BANGLADESH (76/77-78/79-81/82-85/86)	J5	
RPT - NEDECO - BCL	Q 0553	FIG. B-6.3

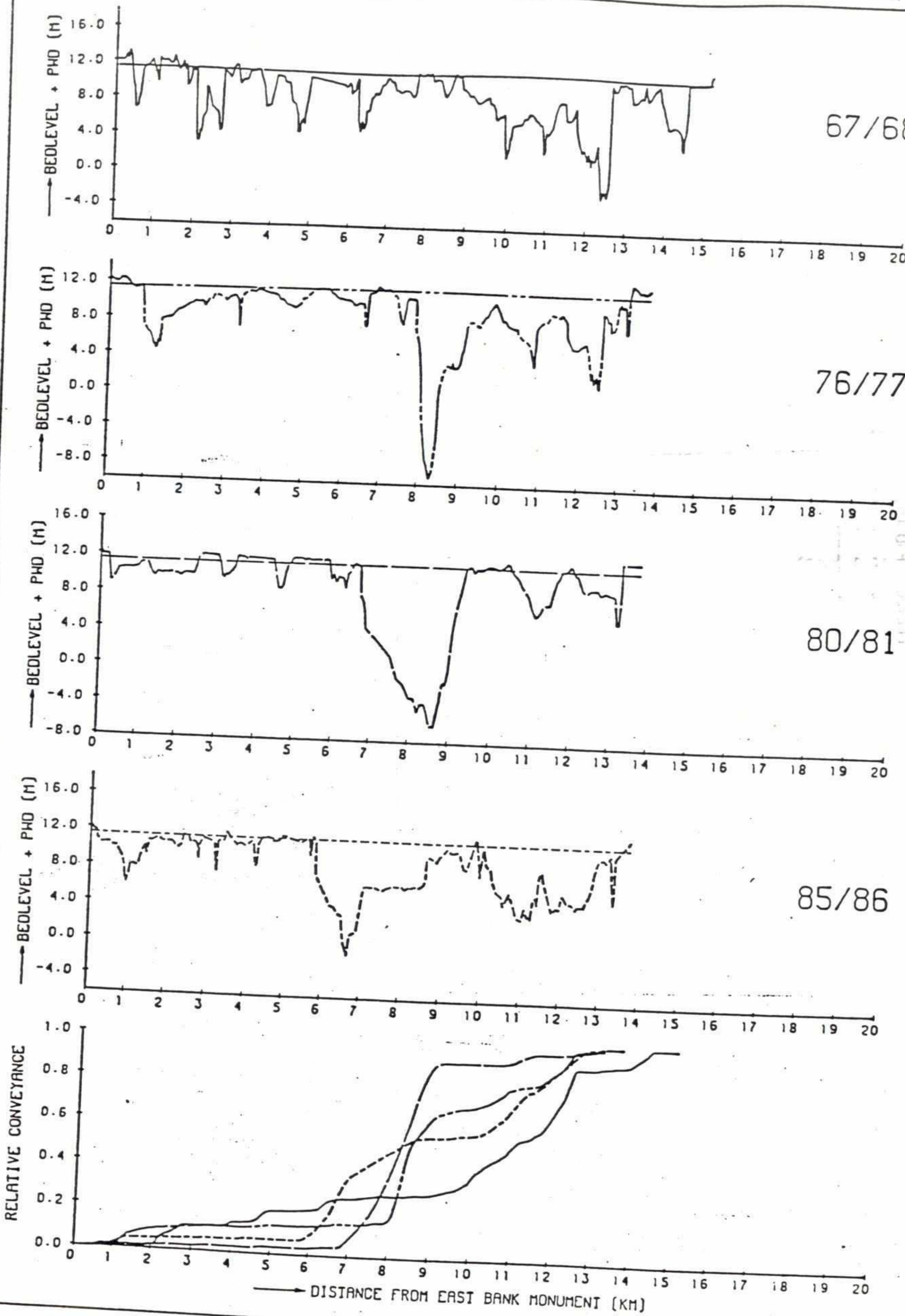

CROSS SECTIONS JAMUNA RIVER BANGLADESH (67/68-76/77-80/81-85/86)	J5-1	
RPT - NEDECO - BCL	Q 0553	FIG. B-6.4

P2G

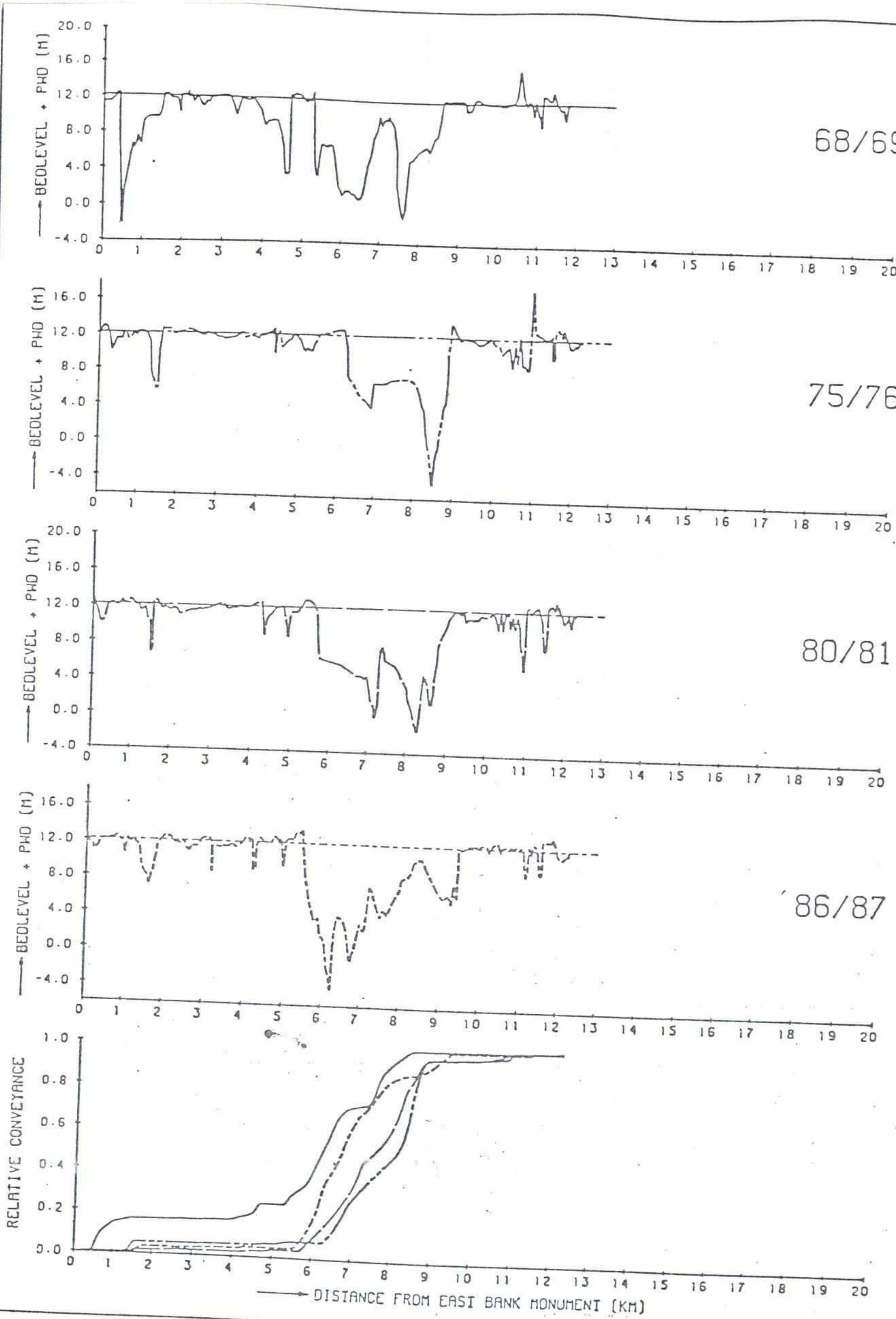

CROSS SECTIONS JAMUNA RIVER BANGLADESH (68/69-75/76-80/81-86/87)	J6-1	
RPT - NEDECO - BCL	Q 0553	FIG. B-6.5

228

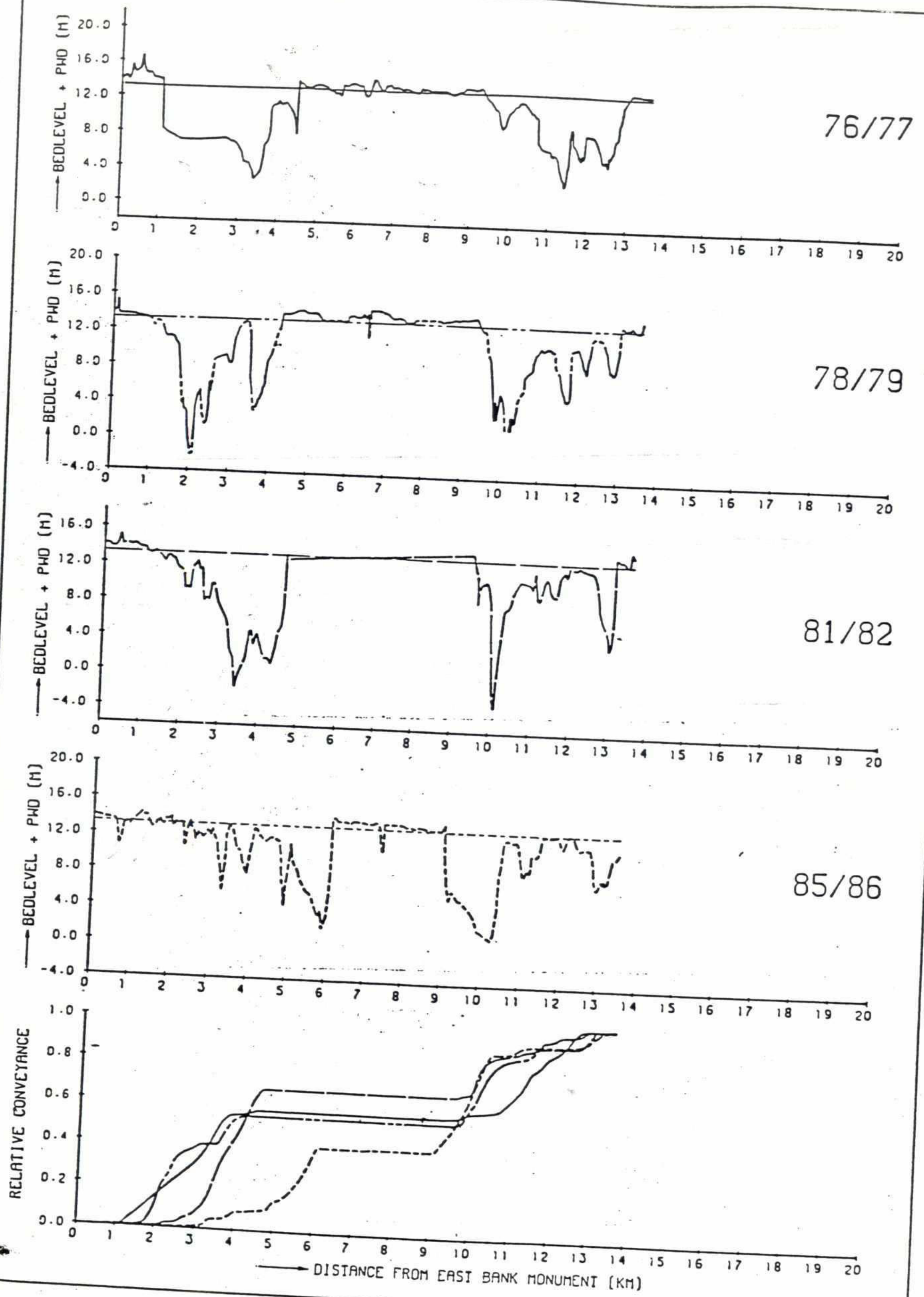

CROSS SECTIONS JAMUNA RIVER BANGLADESH (76/77-78/79-81/82-85/86)	J8	
RPT - NEDECO - BCL	Q 0553	FIG. B-6.6

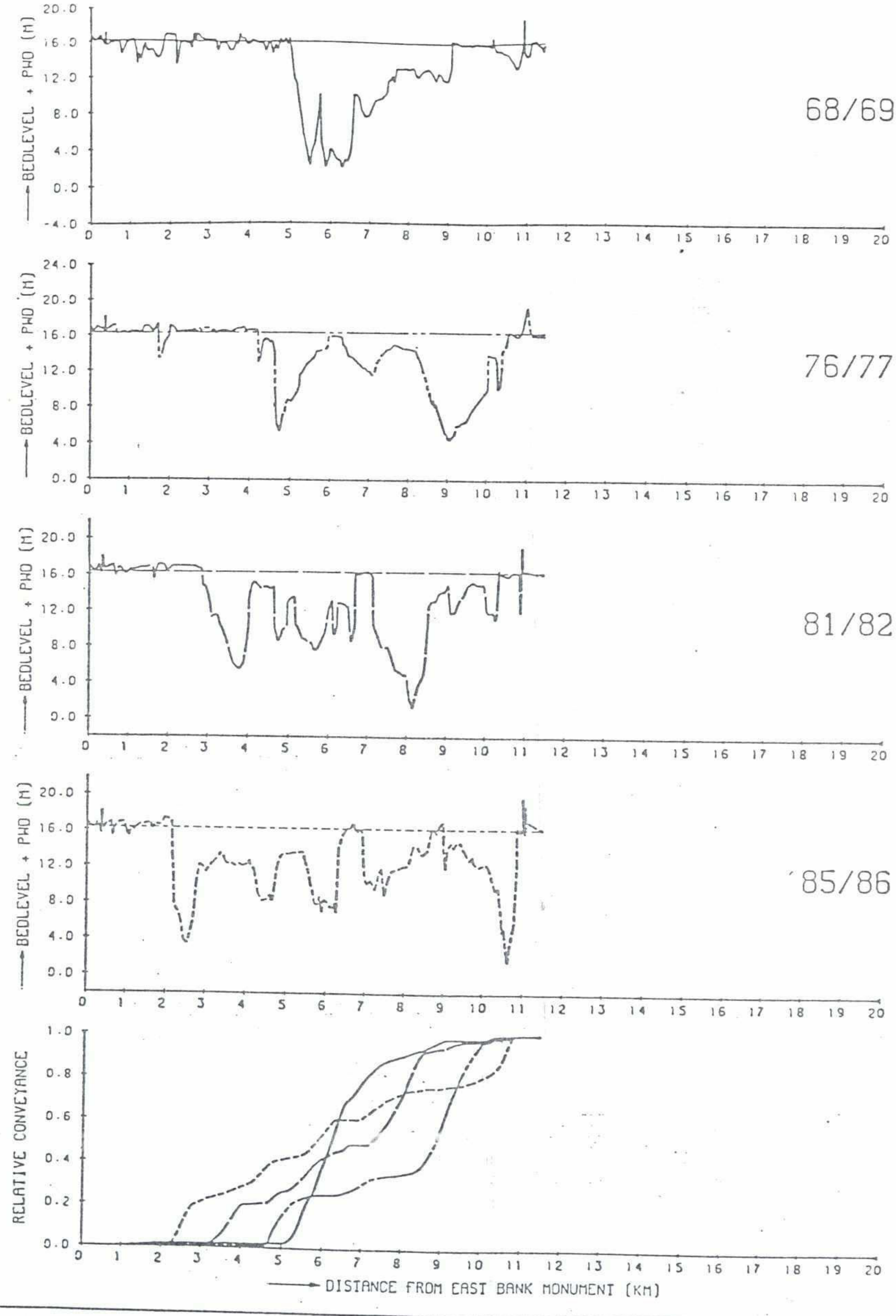

CROSS SECTIONS JAMUNA RIVER BANGLADESH (68/69-76/77-81/82-85/86)	J11	
RPT - NEDECO - BCL	Q 0553	FIG. B-6.7

227

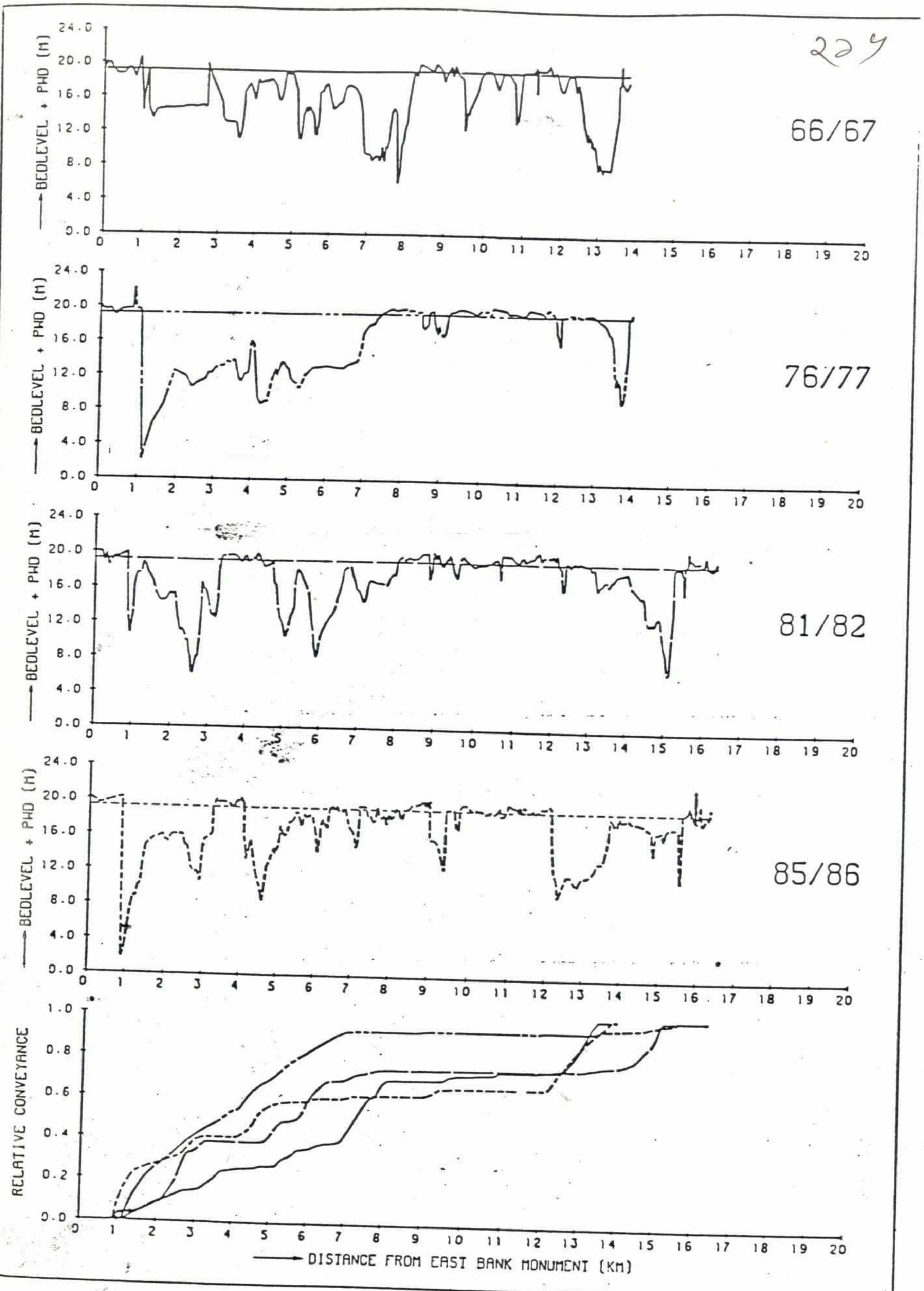

CROSS SECTIONS JAMUNA RIVER BANGLADESH (66/67-76/77-81/82-85/86)	J13-1	
RPT - NEDECO - BCL	Q 0553	FIG. B-68

228

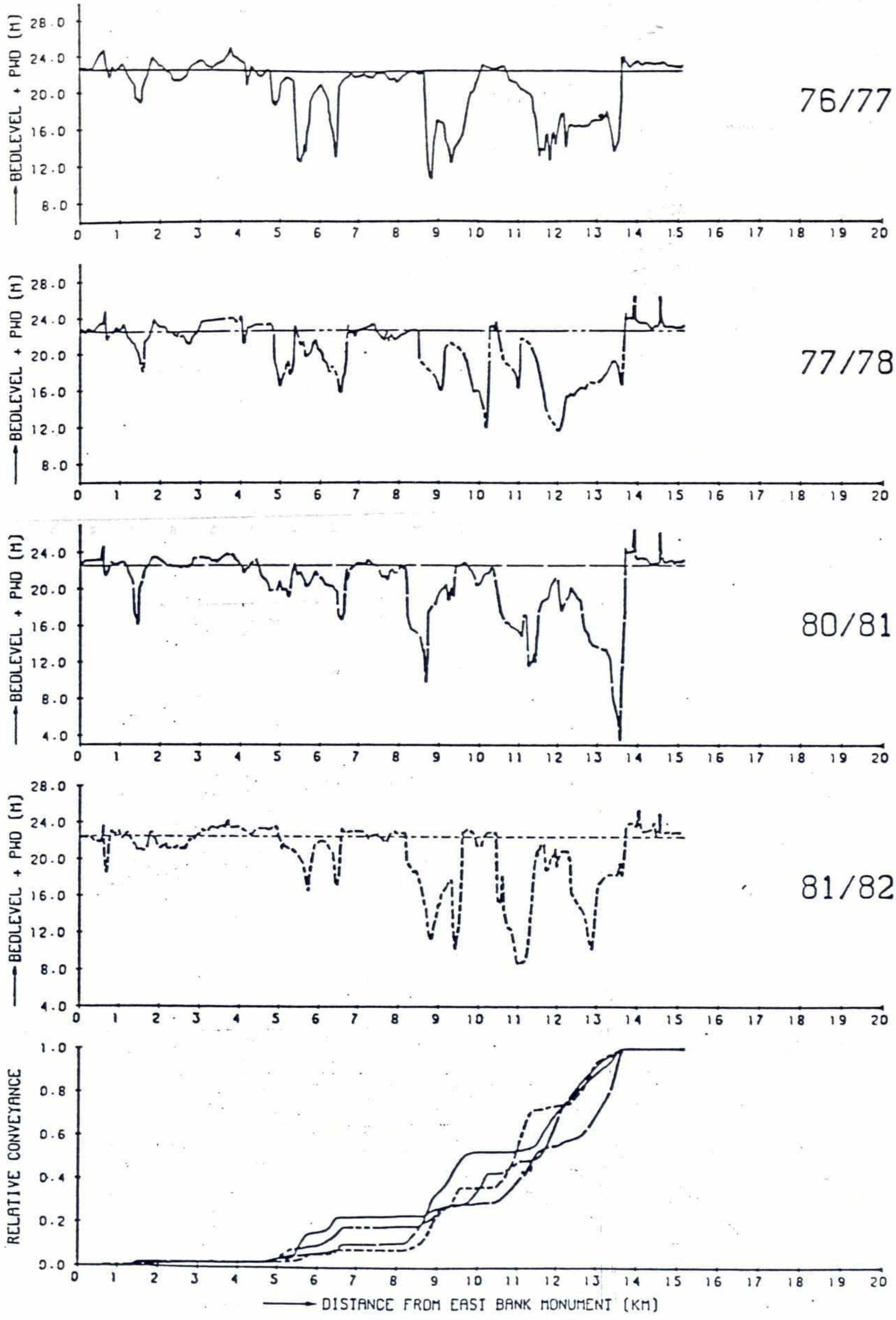

CROSS SECTIONS JAMUNA RIVER BANGLADESH (76/77-77/78-80/81-81/82)	J16
RPT - NEDECO - BCL	Q 0553 FIG. B-6.9

207

ANNEX B

River Morphology

Appendix B-7 Remote sensing studies